Author:
Holder, James

Title:
Enhancing the Strength of Conventional Glass Ionomer Cements Using Nanomaterials

Enhancing the Strength of Conventional Glass Ionomer Cements using Nanomaterials

James Adam Holder

A dissertation submitted to the University of Bristol in accordance with the requirements for award of the degree of Doctor of Philosophy in the Faculty of Health Sciences.

Bristol Dental School

December 2018

[Word Count: 72589]

Abstract

Glass Ionomer Cements (GICs) are a dental restorative material with a variety of uses. They exhibit fluoride release, biocompatibility, adhesion to tooth structure and tooth coloured aesthetics making them useful for anterior restorations. However, they suffer from low strength in comparison to other restorative materials available and, due to the phasing down of dental amalgam, there is a need for strong alternatives. Nanostructures can be used to strengthen or reinforce materials, one mechanism being the absorption of energy via crack propagation in a failing material. Synthesised hydroxyapatite nanofibers (HANFs) and commercially available halloysite nanotubes (HNTs) were selected as potential reinforcing agents due to their biocompatibility, reported strength enhancing properties and anticipated chemical interactions with the GIC. HANFs were found to be vulnerable to the low pH that occurs during the setting reaction of the GIC and may have been dissolved, destroying their fibrous morphology. HNTs were more acid resistant but exhibited large amounts of agglomeration and thus required milling to disperse them throughout the GIC. Substituting 5% HNTs into a commercial GIC increased the compressive strength by over 30% creating a commercially potentially viable route to GIC reinforcement. Other important clinical properties such as handling properties, wear resistance, fluoride release, hardness and diametral tensile strength were also investigated.

Acknowledgements

I would like to thank my supervisor Michele Barbour for all her patience and reassurance over the years, particularly in the first couple when results did not go my way. My thanks go to the other academics and professionals who assisted me in various tasks, information and techniques: Sian, James Puryer, Jeroen, Joachim, Lindsay and Xu to name a few. My appreciation and respect to Graham Mayoh for his support (financial and moral) and giving me this incredible opportunity, I hope I can now give back to Kemdent as much as they have given to me. My friends and colleagues at Kemdent, particularly Tony, Justin and Brian who have pushed me to strive for more and developed my career over the years. Over the years at the University I have had the privilege to work with some incredible people including Sarah, Peter, Laura, Alex, Helena (and her bible), Candice and our little Roo Roo. To my family (Dad, Anna, Jenni, Jack, Andrew, Ceri (and all his kids), Luke, Mum) who have supported and encouraged me, particularly my late Nans, who never got to see me finish this, I hope I've made you proud. Finally, to Katherine (Miss Read Miss Read!), you have been my rock over the years and have supported me to the end, I'm sorry this project has sometimes taken priority in my life, thank you for understanding and loving me regardless, this is dedicated to you.

Is it Christmas yet?

Author’s Declaration

I declare that the work in this dissertation was carried out in accordance with the requirements of the University's Regulations and Code of Practice for Research Degree Programmes and that it has not been submitted for any other academic award. Except where indicated by specific reference in the text, the work is the candidate's own work. Work done in collaboration with, or with the assistance of, others, is indicated as such. Any views expressed in the dissertation are those of the author.

SIGNED: ..... DATE: .....

Table of Contents

List of Figures

List of Tables

List of Abbreviations

ADA	American Dental Association
ADA-MMT	12-amino-dodecanoicacid-montmorillonite
ANOVA	Analysis of Variance
ART	Atraumatic Restorative Treatment
BBT	2,5-bis(2-benzoxazolyl)
BFS	Biaxial Flexural Strength
Bis-GMA	Bis-phenol-A-diglycidyl dimethacrylate
CDTA	1,2-cyclohexane diaminetetraacetic acid
CER	Clinical Evaluation Report
CNTs	Carbon Nanotubes
CS	Compressive Strength
DLS	Dynamic Light Scattering
DMFT	Decay Missing Filled Teeth
DTS	Diametral Tensile Strength
FA	Fluorapatite
FDA	Food and Drugs Administration
FM	Flexural Modulus

FS	Flexural Strength
FT	Fracture Toughness
FTIR	Fourier Transform Infrared Spectroscopy
GIC	Glass Ionomer Cement
HA	Hydroxyapatite
HEMA	Hydroxyethylmethacrylate
HNT	Halloysite nanotube
ICDAS	International Caries Detection and Assessment System
IMS	Industrial Methylated Spirit
ISO	International Organisation for Standardisation
LED	Light Emitting Diode
MDD	Medical Device Directive
MDR	Medical Device Regulations
MHRA	Medical Health Regulatory Authority
MID	Minimal Intervention Dentistry
MMGIC	Metal Modified Glass Ionomer Cement
NF	Nanofibre
NP	Nanoparticle

PAA	Polyacrylic Acid
PEG	Polyethylene Glycol
PMMA	Polymethylmethacrylate
PVC	Polyvinyl Chloride
PVPA	Polyvinyl Phosphonic Acid
QC	Quality Control
QMS	Quality Management System
RMGIC	Resin Modified Glass Ionomer Cement
SBS	Shear Bond Strength
SDS	Safety Data Sheet
SEM	Scanning Electron Microscopy
TEGDMA	Triethylene Glycol Dimethacrylate
TEM	Transmission Electron Microscopy
TISAB	Total Ionic Strength Adjustment Buffer
UDMA	Urethane Dimethacrylate
VHN	Vickers Hardness Number
XRD	X-Ray Diffraction
ZOE	Zinc Oxide Eugenol

Chapter 1 Introduction

1.1 Dental Caries: Overview

Dental caries, commonly known as tooth decay, is one of the most prevalent diseases, and all age groups are susceptible to the disease[1]. A 2010 study found around 35% of people of all ages combined experienced untreated caries in permanent teeth worldwide, equivalent to 3.9 billion people[2]. The incidence in England is declining overall; while 46% of patients exhibited some caries in 1998, only 28% had caries in 2009[3]. The 2009 adult dental health survey found that 31% of adults in England, Scotland, Wales and Northern Ireland had tooth decay, whether restored or not, classified using the decay missing filled teeth (DMFT) index, with an average 2.7 carious teeth per adult. The age group with the highest percentage of dental decay was 25-36-year olds (36%)[4]. Public Health England reported 23.3% of children aged 5 had experienced dental decay and the average number of teeth that were decayed, missing or filled was 3.4 (at age five, children normally have 20 primary teeth as adult teeth begin to erupt from the age of six). The average number of DMFT in the whole sample (including the 76.7% who were decay free) was 0.8[5]. Middle income areas of the globe such as eastern Europe, northern parts of South America and southern Asia were shown to have the highest level of DMFT in 12-year olds between 1994 – 2014 (Figure 1.1).

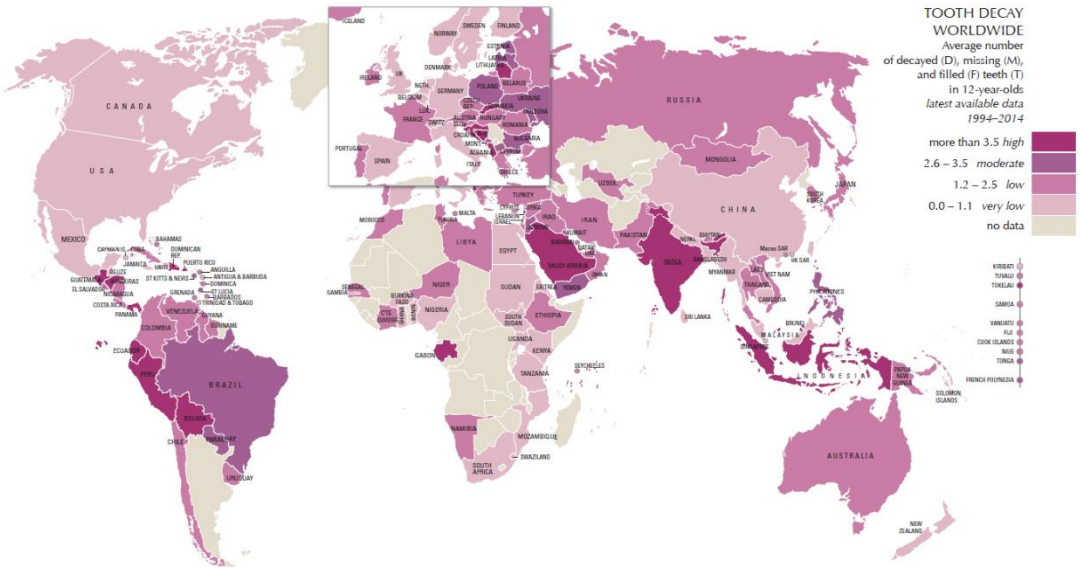

Figure 1.1 - The Global Distribution of DMFT per individual in 12-year olds averaged from 1994 – 2014. Darker areas represent a higher average number of 12-year olds affected. Lower income areas exhibit lower levels of tooth decay, however, the majority of this goes untreated. Highest levels of combined DMFT are seen in middle-income countries[6].

1.1.1 Pathogenesis of Caries

Willoughby D. Miller first introduced the chemicobacterial theory of dental caries in 1890 building on then recent findings by Louis Pasteur regarding the transfer of microorganisms[7]. Teeth become colonised by bacteria which over time co-aggregate and proliferate in the warm, moist, nutrient-rich oral environment, forming biofilms known as dental plaque. Some plaque bacteria such as *Streptococcus mutans* and *Streptococcus sobrinus* metabolise fermentable carbohydrates from the host's diet and produce acids as metabolic by-products. The hydroxyapatite (HA) of which the enamel and dentine are primarily composed is sparingly soluble in acids, so the acids produced

by the bacteria cause a slow dissolution of the mineral component of these tissues[8]. The acids produced move through the dental plaque and into the porous structure of the enamel or exposed dentine, releasing hydrogen ions which attack the calcium - phosphate bond, liberating free ions. These ions diffuse into the surrounding solution in a process called demineralisation and thus reduce the amount of tooth structure present, leading to porosity and then destruction of the tooth surface[9]. Poor oral hygiene, low salivary flow, compromised immune system activity and diet are all contributory factors in caries, while other more complex factors such as socioeconomic status, education and lifestyle choices also contribute to the likelihood of caries being present[10]. Caries diagnosis is usually done by visual examination sometimes with the use of low technology dental tools or probes, however by the time caries can be seen by the unaided eye (Figure 1.2), it is often substantially developed and requires treatment[11-14].

Figure 1.2 - Clinically apparent dental caries. Images provided by Dr James Puryer BDS DPDS MFDS RCS(Eng) MDFTEd MSc FHEA, University of Bristol.

1.1.2 Prevention of Caries

Demineralisation and remineralisation both occur concurrently in the mouth, and a carious lesion is the result of a net demineralisation even when remineralisation also occurs[15]. This 'balance' (Figure 1.3 and Figure 1.4) at the tooth-pellicle-plaque-saliva interface can shift over time favouring caries progression or arrest.

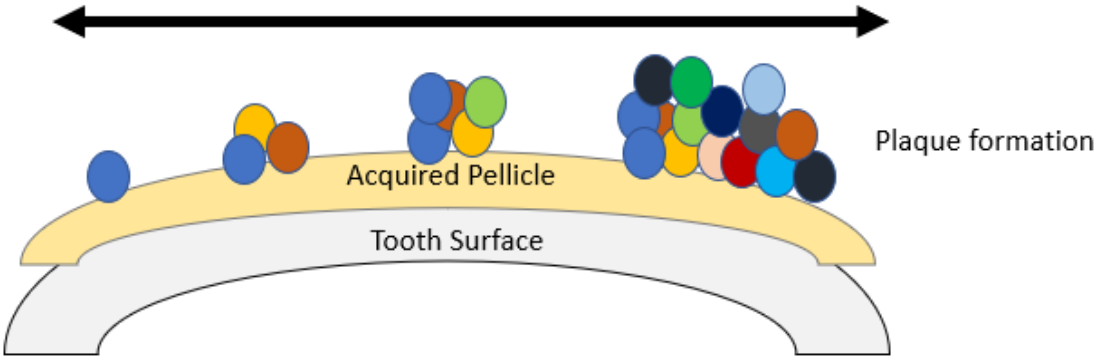

Figure 1.3 - Tooth pellicle plaque interface. Plaque forms on the surface of the saliva pellicle and acids migrate through this to the tooth surface. The process is a reversible balance which can progress to the right or left.

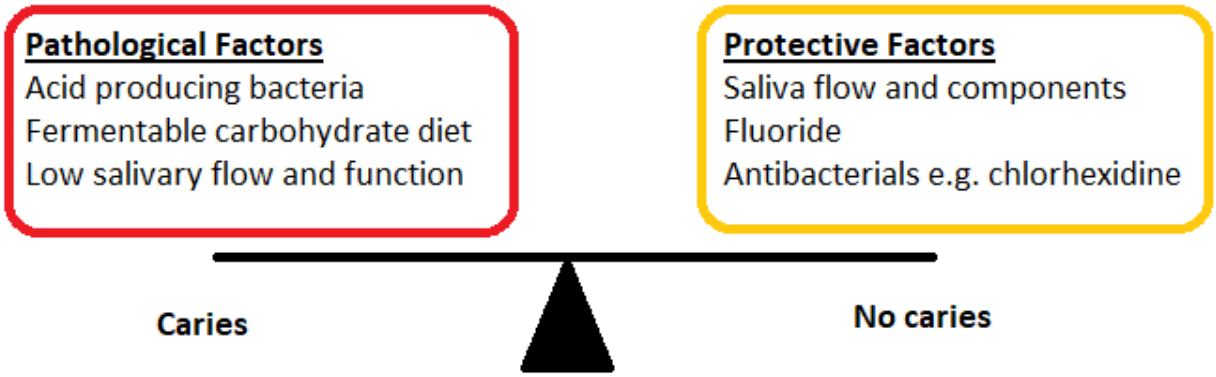

Figure 1.4 - The caries balance. If the balance tips in favour of demineralisation then is likely to develop; increased demineralising protective factors reduce the likelihood of caries formation. Illustration adapted from Featherstone[16]

Saliva is a natural buffer, neutralising the oral pH, and is the first defence against caries. Acidosis, medicines or illnesses that reduce saliva production increase the risk of caries developing[17]. Preventative measures such as tooth brushing are important in removing the dental plaque through physical abrasion. Another effective self-administrative preventative method is fluoride. Fluoride may be delivered in many ways, in mains water supplies in some areas, in oral care products such as toothpastes, or at an elevated concentration in professionally applied fluoride varnishes[18-22]. Exposure of HA to fluoride can result in the formation of fluorapatite (FA) which is more resistant to acid attack and less porous than HA, as well as reservoirs of calcium fluoride that can release fluoride at a later time[23]. Public water fluoridation began in the United States (US) in 1945 as a dental caries preventative measure and in 2014 around 74% of all US citizens received fluoridated water[24] costing an average of $1.06

per person per year[25] ranging from concentrations between 0.7 – 1.2ppm[26]. The move was a great success, particularly in primary dentition[27] and various national surveys reported a substantial decrease in dental caries among children aged 12 – 17 years from 90.4% in 1971 - 1974 to 67% in 1988 - 1991[28-31]. In the United Kingdom (UK), around 10% of the UK population receives fluoridated water[32] with the following water companies currently fluoridating their water: Anglian Water Services Ltd., Northumbrian Water Ltd., South Staffordshire Water PLC, Severn Trent PLC and United Utilities Water PLC. However, water fluoridation in the UK has been controversial, with some communities showing some opposition to introducing it. In 2014, Public Health England were forced to abandon water fluoridation for Southampton and south-west Hampshire over council objections and mass protests lasting several years[5,33] and in 2016 water fluoridation was agreed to be implemented in Hull despite protests and demonstrations[34]. In November 2004, Scotland abandoned plans to add fluoride to drinking water following a public consultation[35] and many other nations around the world have either ceased their fluoridation programmes or have never implemented any, despite an overwhelming number of studies concluding the safety and effectivity in reducing DMFT[36-40].

1.1.3 Classification of Carious Lesions

Early research found that restoration of lesions alone was ineffective against the treatment of caries and cavity preparations must be designed with the anticipation of recurrent caries, particularly with root lesions[41]. Up to date clinical practice requires an

assessment of the carious tissue using a variety of systems, one of which is the international caries detection and assessment system (ICDAS) using categories of 0 – 6 in ascending severity, as described in

Table 1.1. In addition, radiographic assessment is recommended to aid the diagnosis of the caries depth and progression, particularly with posterior teeth. These are often combined to create an in-depth analysis and classification of the lesion, summarised in Table 1.2.

Table 1.1 - ICDAS categories and definitions used in modern dentistry for characterisation of carious tissue[42]

Code	Description
0	Sound
1	First visual change in enamel (seen only after prolonged drying or restricted to the confinements of a pit or fissure)
2	Distinct visual change in enamel
3	Localised enamel breakdown (without clinical visual signs of dentinal involvement)
4	Underlying dark shadow from dentine
5	Distinct cavity with visible dentine
6	Extensive distinct cavity with visible dentine

Table 1.2 – Radiographic and Clinical Combinational Coding System for Carious Lesions[43].

Definitions of the categories are found in Table 1.3.

Clinical Category	Radiographical Category				
	R_0	**R_{1-2}**	**R_3**	**RB**	**RC**
C_{SOUND}	$Sound_{CR}$	$Initial_{CR}$	$Initial_{CR}$	$Moderate_{CR}$	$Extensive_{CR}$
$C_{INITIAL}$	$Initial_{CR}$	$Initial_{CR}$	$Initial_{CR}$ OR $Moderate_{CR}$	$Moderate_{CR}$	$Extensive_{CR}$
$C_{MODERATE}$	$Moderate_{CR}$	$Moderate_{CR}$	$Moderate_{CR}$	$Moderate_{CR}$	$Extensive_{CR}$
$C_{EXTENSIVE}$	$Extensive_{CR}$	$Extensive_{CR}$	$Extensive_{CR}$	$Extensive_{CR}$	$Extensive_{CR}$

Table 1.3 - Definitions of the clinical and radiographic categories used in Table 1.2

Category	Definition
$Sound_{CR}$	No evidence of visible caries (no or questionable change in enamel translucency) when viewed clean and after prolonged air-drying (5 seconds). No radiolucency (R_0)
$Initial_{CR}$	First or distinct visual changes in enamel seen as a carious opacity or visible discolouration (white spot lesion and/or brown carious discolouration) not consistent with clinical appearance of sound enamel and which show no evidence of surface breakdown or underlying dentine shadowing. Radiolucency in the outer ½ of the enamel (R_1) and enamel-dentine junction (R_2) or outer 1/3 of the dentine (R_3)
$Moderate_{CR}$	A white or brown spot lesion with localised enamel breakdown, without visible dentine exposure or an underlying dentine shadow which obviously originated on the surface being evaluated. No radiolucency (R_0), radiolucency in the outer ½ of the enamel (R_1) and enamel-dentine junction (R_2) or outer 1/3 of the dentine (R_3) or middle 1/3 of dentine (RB)
$Extensive_{CR}$	A distinct cavity in opaque or discoloured enamel with visible dentine. No radiolucency (R_0), radiolucency in the outer ½ of the enamel (R_1) and enamel-dentine junction (R_2) or outer 1/3 of the dentine (R_3) or middle 1/3 of dentine (RB) or inner 1/3 of dentine or pulp (RC)

1.1.4 Restoration of Carious Lesions

When a carious lesion has been diagnosed it may require intervention. Extraction of the tooth is only performed as a last resort and has largely been replaced by restorative options to maintain tooth tissue and teeth for longer, according to the principles of minimally invasive dentistry[44]. In some instances, a material can be applied directly to the prepared tooth surface or cavity and in others an intermediate material is required to cause the material to adhere, or bond, to the tooth. Those materials with an inherent affinity for tooth tissue, avoiding the need for a "bonding agent", are sometimes preferred in situations where a simpler or faster technique is required. There are many important properties that can affect the likely clinical outcome, and these are discussed below, in detail for the glass ionomer cement (GIC), the main subject of this thesis, and briefly for alternative materials.

1.1.5 Minimal Intervention Dentistry

By early 1990 the minimal intervention dentistry (MID) approach was established as a way of managing dental caries without unnecessary destruction of health tooth tissue. The principle of MID is early detection, ongoing prevention and retaining as much sound dentition as possible. MID encompassed the following strategies:

1. Early caries detection and assessment of caries risk with validated instruments
2. Remineralisation of demineralised enamel and dentine
3. Optimal caries prevention methods
4. Tailor-made recalls

5. Minimally invasive operative interventions
6. Repair over replacement of restorations[45]

1.2 Restorative Dental Materials

Restorative materials can be divided into two groups: direct and indirect. Direct materials are manipulated at chairside and placed directly into the cavity still in their pliable or plastic form, whereas indirect materials are prepared elsewhere, for instance in a dental laboratory or milling machine, and are placed in the mouth in their finished or near-finished state. Direct restorative materials include composites, compomers, GICs and amalgam. Indirect restorative materials include ceramics and alloys other than amalgam[46].

1.2.1 Glass Ionomer Cements (GICs)

GICs (also known as glass polyalkenoate cements) were initially developed in 1968 in London at the Laboratory of the Government Chemist by Brian Kent and Alan Wilson, replacing the dental silicate cements that were in use prior to that time[47]. It wasn't until 1975 that a marketable example of the GIC came about as DeTreys ASPA by the Amalgamated Dental Company, but these were initially unsuccessful due to their prolonged setting time[48]. Further developments were made over the course of several years including the addition of (+)-tartaric acid forming a chelating bridge between calcium ions thus increasing the speed of the setting reaction dramatically[49]. Soon after, resin modified GICs (RMGICs) were developed and led to production of brands

such as Vitrebond (3M, Minnesota, USA)[50]. A common GIC used today, the high viscosity GIC, gained recognition through the release of Fuji IX (GC Corp, Tokyo, Japan) and developed into faster setting, stronger restoratives such as Ketac Molar (3M) and Chemfil Molar (Dentsply Sirona, Pennsylvania, USA). Further development of GICs have included paste-paste mixes. Products such as Ketac Nano (3M) introduced in 2007 used two cartridges, a 'clicker' dispenses the correct amount of each component which are then mixed together[50]. More recent developments of GICs involve replacing the standard fluoroaluminosilicate glass with more bioactive glasses. The Glass Carbomer® (GCP Dental, Ridderkerk, Netherlands), recently undergoing clinical assessments, contains a bioactive component in the form of HA and FA as well as a higher silica concentration within the acid-washed glass component as well as a silicone oil[51]. These are designed to retard the setting reaction and therefore a higher powder to liquid ratio can be used, showing increased flexural properties (Glass Carbomer 117.4 MPa vs Fuji IX 34.9 MPa)[52]. However, the setting of these require the use of a heat lamp at 60°C to speed up the reaction[53]. Long term clinical studies of Glass Carbomer have yet to be published but early findings indicate little additional benefit over resin sealants[54].

1.2.1.1 Composition

Modern conventional GICs are often referred to as acid-base cements and usually consist of a two-part system of a basic glass fluoroaluminosilicate powder and an aqueous acidic polyacrylic acid (PAA) liquid. Anhydrous PAA (Figure 1.5) can alternatively be included in the powder component leaving the liquid component as

the water required to initiate the reaction. The glass also often contains various inorganic components such as barium and strontium for radiopacity. Anhydrous acids such as tartaric acid (Figure 1.5) are added to form calcium tartrate enhancing the trivalent setting reaction and thus creating a faster setting cement[55]. Polyvinyl phosphonic acid (PVPA) has also been included in Kemdent's GIC Diamond Carve™ (Kemdent, Swindon, UK) with the intention of conferring increased moisture tolerance and rapid setting[56,57]. The fluoroaluminosilicate glass powder and PAA liquid are mixed together in a specific ratio to form a paste which sets through an acid-base reaction. The acid reacts with the glass releasing Ca^{2+} and Al^{3+} ions which crosslink with the polyacid chains to harden over the course of a few minutes[58]. As the cement matures, fluoride ions migrate out of the matrix into any surrounding solution such as saliva[59]. Additional trivalent crosslinking occurs more slowly to set the cement further, increasing the tolerance of water, strength, hardness and various other properties[60]. It is thought the resultant glass then finishes with silanol (Si-O-Si) surface groups through the hydrolysis from bound water[61].

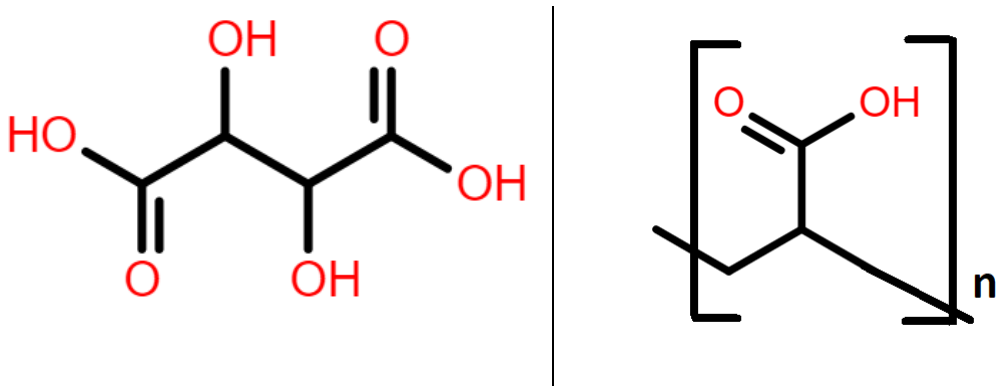

Figure 1.5 - Tartaric Acid (Left) and Acrylic Acid Monomer (Right), components of modern day GICs

1.2.1.2 Properties

GICs have found their place in clinical dentistry because of their chemical adhesion to dentine and enamel without the use of bonding agents[62,63], and the fact that they can store and release fluoride which means they are therefore often used in patients thought susceptible to secondary caries[64,65]. Biocompatibility is considered to be very good[66,67] and aesthetics are more acceptable than amalgam but not as good as composites[68]. Another favourable property, related to the adhesion, is the ease of use[69-71] allowing fast treatment in anxious patients. These properties are discussed in more detail in section 1.6, and mechanical properties of GICs are discussed in section 1.4.

1.2.1.3 Applications

GICs have a wide range of uses, these include:

- Abrasion and erosion lesions
- Class III lesions involving exposed root dentine
- Occlusal lesions on deciduous dentition
- Temporary anterior restorations
- Temporary posterior restorations
- Repair of crown margins
- Cavity bases under composites, amalgams and ceramics
- Cavity liners

- Blocking out undercuts
- Cementation of crowns, bridges, inlays and onlays[72]

Contraindications of GICs include:

- Class II restorations involving the marginal ridge
- Class IV restorations
- Teeth with large loss of labial or buccal enamel
- Cusps
- Area subjected to large masticatory loads[73]

Clinically GICs can be divided into three main classes and have the following indications:

- Type I: Luting and bonding cements
- Type II: Restorative cements
- Type III: Liners or base cements

There are two sub-divisions of Type II cements, depending on the importance of appearance (either aesthetic or reinforced cement)[51]. As more developments in GICs came to market, more modern-day classifications include three further types:

- Type IV: Fissure Sealants
- Type V: Orthodontic Cements
- Type VI: Core Build Up[74]

These are discussed in further detail in the following sections.

1.2.1.3.1 Luting

Luting cements, such as Diamond Micro Luting Cement (Figure 1.6) are low viscosity 'spreadable' adhesives, their properties and indications include[51] cementation of crowns, bridges, inlays, onlays and orthodontic appliances. They use a powder: liquid ratio (around 1.5 – 4:1), leading to only moderate strength, but are usually slower setting with some early resistance to water and are usually radiopaque.

Figure 1.6 – Kemdent's Diamond Micro Luting Cement Hand Mix. A lower viscosity GIC with an extended working time for use with crowns, bridges and various orthodontic appliances

1.2.1.3.2 Restorative

Conventional GICs fall into two categories[51]:

Type II (i): For anterior repairs where appearance is considered a priority:

- Use high powder: liquid ratio (at least 3:1, and up to 6.8:1).
- Have a good colour match and translucency
- Often need protection from moisture for at least 24 h with varnish or petroleum jelly
- Are usually radiopaque

Type II (ii): For use where appearance is not important (posterior restoration or repairs):

- Use high powder: liquid ratio (around 3:1 or 4:1)
- Fast setting and some moisture resistance
- Radiopaque

Due to their low compressive strength, conventional GICs are usually not indicated for load bearing restorations.

1.2.1.3.3 Liners

There are various cavity liners available, including calcium hydroxide, zinc oxide eugenol (ZOE) and zinc-phosphate cements, all of which were in use well before the invention of the GIC[75]. These materials protect the pulp against irritation such as chemical stimuli from resins or thermal stimuli from amalgam or exothermic setting cements. ZOE and calcium hydroxide cements have been shown to exhibit antibacterial activity against common endodontic bacteria when tested *in vitro*[76,77] which may prove useful in their role as liners in previously carious cavities.

Conventional GICs are often used as liners and provide benefits such as radiopacity and fluoride release. These type III cements can be summarised as[51,78]:

- Lining or base cements
- Low powder: liquid ratio for liners (around 1.5:1) allowing better adaptation to the cavity walls.
- High powder: liquid ratio for bases (3:1 to around 7:1), where the base acts as a dentine substitute in the "open sandwich" technique with a composite resin.

1.2.1.3.4 Fissure Sealants

Dental fissure sealants are another use of dental cements and are applied to the fissures in the posterior teeth to prevent the adhesion of plaque producing bacteria, known as pit and fissure caries, in these potentially hard to reach sites[79]. They have been recognised as an effective means of preventing pit and fissure caries in children[80,81]. The American Dental Association (ADA) recommend the use of sealants in permanent molars with both sound occlusal surfaces and non-cavitated occlusal carious lesions in children and adolescents[82]. These are generally categorised into four types: resin based sealants (composites), polyacid modified sealants (compomers), RMGIC sealants and GIC (usually high viscosity GICs) sealants[83], none of which have been found to be superior to the others clinically[84,85] (however, due to relevance to the project, only GIC sealants are discussed here).

GICs were proposed in 1974 as useful fissure sealants because they adhere to tooth tissue without the need of bonding agents or acid etching[86]. Due to the hydrophilic

nature of GICs they can absorb any residual moisture at the bottom of the fissure, still retaining this bond[51] and their dimensional stability thus creating a close marginal seal make them a useful clinical tool for caries prevention[87].

1.2.1.3.5 Core Build-Up

Some materials require special techniques for use in large restorations. Composites, for example, require incremental placement, each increment requiring light curing. Some more modern examples will allow up to 5 mm 'bulk fill' such as Filtek™ One Bulk Fill (3M). If the remaining tooth contains exposed pulp, the use of a core build-up material such as a composite may be inappropriate. Therefore, a combination of sealers, core build-up and restoratives maybe required, or in the case of some indirect restoration, luting agents may also be used. Materials such as compomers, composites, amalgams and GICs (Figure 1.7) have been used as core materials, although most are not specifically developed for this purpose. GICs, as self-adhesive, chemical curing, fluoride releasing materials have found occasional use as core materials[88].

Figure 1.7 - Rarely are materials specific to core build-up indications only. Those that are may be coloured, such as Diamond Core (Kemdent), to distinguish it from surrounding restoratives

1.2.1.3.6 Primary Dentition

A recent 10-year study investigating the survival rate of class II restorations found a significantly lower rate of survival in children, particularly those prone to secondary caries[89]. A review of over 12000 restorations in primary dentition found a failure rate of 12.5% across a range of restorative materials; 36.5% of these were directly caused from secondary caries. The study also found that faster and less technique sensitive restorative techniques such as conventional GICs, RMGICs and compomers were clinically more likely to survive when used in similar indications to composites[90]. The release of fluoride is considered an important factor in the choice of restorative material, because of the high occurrence of secondary caries[91], despite its clinical

effects being the subject of ongoing discussion[9,64,92,93]; this is discussed in detail in section 1.6.2.

Table 1.4 - Comparison of the various materials used as fissure sealants, core build-up and primary restorations

	Fissure Sealants	Core Build-Up	Primary Dentition
Uses	Fissures in the posterior teeth to prevent the adhesion of plaque producing bacteria, known as pit and fissure caries[79]	Core or base of the restorative before 'capped' with the main external restorative such as a ceramic crown[94]	Restorations in primary dentition
Indications	permanent molars with both sound occlusal surfaces and non-cavitated occlusal carious lesions in children and adolescents[82]	Where a large section of the tooth has been damaged or lost due to disease or trauma, thus the remaining tooth cannot support a restorative itself[95]	Those prone to secondary caries or classed as a high caries risk
Types	resin based sealants (composites), polyacid modified sealants (compomers), RMGIC sealants and GIC (usually high viscosity GICs) sealants[83]	GICs, compomers, composites and amalgam	GICs, compomers and RMGICs[90]

1.2.1.3.7 Atraumatic Restorative Treatment

Atraumatic restorative treatment (ART) is a technique covering the fifth point of the MID approach. ART uses hand tools only for excavation of cavities rather than metal/polymer and ceramic burs and employs either a preventative sealant or a repairing restorative[96]. One intention of ART is the alleviation of anxiety in patients; it is common for dental anxiety to develop at a young age which may lead to avoiding professional care in later life[97]. Hand instruments appear to cause less dental anxiety, discomfort and pain when treating children[98] and the outcomes can compete with the survival rate of other restoratives including amalgam and composite materials[97]. GICs have particular use in ART technique (due to their simplistic nature of mixing and chemical curing) and are especially useful in dentistry within developing countries where electric hand pieces and other equipment can be expensive or unavailable[99].

1.2.1.4 Presentation of Glass Ionomer Cements

Two presentational forms of conventional GICs are used by manufacturers today: a hand mixed form and the encapsulated GIC.

1.2.1.4.1 Hand Mix Glass Ionomer Cements

Typically, these are provided in a two-part system consisting of a blend of fluoroaluminosilicate glass powder mixed with dry acids and a PAA solution (shown in

Figure 1.8). Various other forms are available such as replacing the PAA liquid with water and adding the acrylic polymer in an anhydrous form into the powder component. The two-part systems are often packaged with plastic spoons where a level scoop of the spoon measured out a precise amount of powder which is then mixed with several 'drops' of GIC liquid. These are ideal for use with ART as they use hand instruments to dispense, mix and place the cement. They give the user the flexibility on the amount of cement mixed for indications such as bulk placement or small luting applications. Hand mixed GICs require skill to mix effectively to create a homogenous mix, additionally, the scoops and dropper bottles are often uncalibrated leading to irregular results[100].

Figure 1.8 - Kemdent's Diamond Carve™ GIC consisting of a fluoroaluminosilicate based powder and a PAA-water liquid mixed in a 4:1 ratio by hand

1.2.1.4.2 Encapsulated Glass Ionomer Cements

These contain the powder component inside a plastic capsule (such as those shown in Figure 1.9), attached to which is a small pouch of the PAA liquid, the capsule is 'activated' by breaking this pouch before agitating mechanically to mix the two. This reduces the effects of poor mixing such as consistency, incorrect ratios and quick setting cements and can be dispensed easily through a nozzle as part of the capsule. However, due to the aggressive nature of the mixing at high speeds, this method can incorporate porosity into low viscosity GICs[101] which has been shown to reduce the strength of the restoration[102,103] and are unsuitable for ART due to the requirement of mechanical mixing equipment[100].

Figure 1.9 - Kemdent's Diamond Rapid Set Capsules. Encapsulated GIC containing pre-dosed powder and liquid

1.2.1.5 Limitations

GICs can be pigmented to various shades using iron oxides to match tooth colour and develop translucency to mimic the tooth enamel and create a better match to the tooth itself[104] but are not as aesthetically similar to natural tooth tissue as composites[105]. Another limitation of GICs is their comparatively low strength, especially compared to alternative materials such as amalgam. Low strength limits their use to non-load bearing and anterior restorations of specific class[106]. In addition, GICs are often used as a base in conjunction with another higher strength restoration such as amalgams or composites[51].

It has been reported that GIC restorations currently require the most incidences of re-intervention than any other restorative in England and Wales[107]. It can be hypothesised this may be due to GICs having lower wear, compressive and tensile strength than many alternative restoratives (discussed in detail in section 1.4). Additionally, GICs have been reported to have a high level of use in primary dentition, particularly patients with a high risk of caries[108,109] which may have a significant effect on the longevity of dentition and restorations[110], as well as dentine lesions. This appears to be presented as a serious limitation of GICs and their longevity, such as only a 28% survival rate over a 15-year period, however, this may be considered by some clinicians as excellent considering the indications, uses of GICs and their mechanical limitations.

1.2.2 Amalgam

Metal based fillings were first used clinically as a dental restorative in 1528 by Johannes Stockerus[111]. In 1818 when mercury (later silver-mercury coins) was added to the metal alloy mix to create a soft mouldable material the material became popular as amalgam, a filling containing bismuth, lead and tin, heated and poured directly into the cavity at 68°C[111]. In 1883 the Crawcour family's abuse of dentistry using cheap coin silver amalgam left many patients with impure and poor fillings which reduced the profession's confidence in the material. As a result, the amalgam war between 1840 and 1855 broke out and in 1841 the American Society of Dental Surgeons ruled the material "hurtful both to teeth and every part of the mouth" and condemned the use of amalgam as malpractice. As amalgam was studied further and more evidence came to light of its effectiveness as a restorative material the society suffered from backlash and was disbanded 1856, later replaced by the ADA[112,113]. 70% of dental restorations undertaken were amalgam rising to 80% in the 1950s compared with only 24% in 2018[114,115]. The American Dental Association and the US Food and Drugs Administration (FDA) fully endorse the use of amalgam as "a valuable, viable and safe choice for dental patients"[116,117] however the use of dental amalgam is to be phased down through the Minamata agreement due to its mercury content (see section 1.2.2.5).

1.2.2.1 Composition

Dental amalgam alloy powder consists of 40 – 70% silver, 12–30% tin and 12–24% copper and which is then mixed approximately 50:50 with elemental mercury. These are generally referred to as non-gamma 2 dental amalgams due to the absence of a highly corrosion-prone gamma 2 phase, owing to the concentration of copper[118]. Examples of dental amalgam capsules available commercially include Tytin™ (Kerr Dental, California USA), Cavex Non-Gamma 2 (Cavex, Haarlem, Netherlands) and Amalcap Plus (Ivoclar Vivadent, Schaan, Lichtenstein).

1.2.2.2 Properties

Dental amalgams have high wear resistance, good moisture tolerance and are inexpensive compared to other dental restoratives. They have a compressive strength of between 400 - 500 MPa and a diametral tensile strength 30 - 50 MPa[119,120] and are used in load bearing restorations. They are hard but brittle materials and have a Vickers Hardness number (VHN) around 90 (dentine and enamel VHN are 62 and 313 respectively)[121]. Properties relating to mechanical properties discussed throughout the chapter are discussed further in 1.4. Specifically, brittle materials are discussed in detail in section 1.4.4. Compressive strength is discussed in section 1.4.1.2, tensile strength in section 1.4.1.1 and VHN in section 1.4.10.

1.2.2.3 Application

Due to amalgam's higher compressive strength than other restoratives, the material is ideal as a bulk filling material in posterior restorations[90]. The material has been shown to resist masticatory impact and bite as well as repeated brushing[122]. Amalgam's strength rivals that of enamel and this along with several other properties (high wear, hardness etc.) means restorations using the material can often last several years[123].

1.2.2.4 Limitations

Amalgam is silver-grey (shown in Figure 1.10) which means it is limited to use in posterior teeth. It is unsuitable for thin profile restorations due to the poor tensile properties therefore these are limited to bulk placements[124,125]. Flow of amalgam can lead to marginal breakdown[72] and creep [126]. Amalgams are known to corrode in the oral environment producing metal oxides which produce a protective seal around the restoration[127]; however, excessive corrosion of the material can significantly reduce the strength and wear resistance of the material by forming pits as the precipitates are washed away by the saliva[128]. Amalgam does not chemically bond to tooth surface and the use of retentive cavity designs are required, which involves the loss of healthy tooth structure[72].

Figure 1.10 - Dental amalgam posterior restoration. Image provided by Dr James Puryer BDS DPDS MFDS RCS(Eng) MDFTEd MSc FHEA, University of Bristol.

1.2.2.5 Minamata Agreement

The use of dental amalgams is to be phased down as set out in the Minamata Agreement due to the environmental impact of mercury. The agreement, signed by 128 nations and effective from August 2017, aims to "reduce the mining, export and import, transport and waste management of various products and materials containing mercury"[129]. Dental amalgam is the second largest use of mercury in the European Union[130] but despite a number of challenges, the UK ratified the agreement recently in March 2018. Annex A Part II of the Minamata Agreement states that a minimum of two of the following nine measures shall be taken by member signatories[131]:

1. "Setting national objectives aiming at dental caries prevention and health promotion, thereby minimizing the need for dental restoration;

2. Setting national objectives aiming at minimizing its use;
3. Promoting the use of cost–effective and clinically effective mercury-free alternatives for dental restoration;
4. Promoting research and development of quality mercury-free materials for dental restoration;
5. Encouraging representative professional organizations and dental schools to educate and train dental professionals and students on the use of mercury-free dental restoration alternatives and on promoting best management practices;
6. Discouraging insurance policies and programmes that favour dental amalgam use over mercury-free dental restoration;
7. Encouraging insurance policies and programmes that favour the use of quality alternatives to dental amalgam for dental restoration;
8. Restricting the use of dental amalgam to its encapsulated form;
9. Promoting the use of best environmental practices in dental facilities to reduce releases of mercury and mercury compounds to water and land".

The move has received mixed support from dentists and the use of amalgam separators is favoured by many,[132] but nevertheless the need for alternative materials is unequivocal.

1.2.3 Composite

Composite materials for restorative dentistry were first developed in the late 1950s and early 1960s where epoxy resins were mixed with filler particles[133]. This led to

epoxy light curable resin composites being introduced in the 1970s creating a restorative material with a 'command set'[134].

1.2.3.1 Composition

Dental composites consist of a polymerisable resin matrix, glass fillers acting to reinforce the material, and silane coupling agents[135]. The polymerisable resin matrix typically contains resin monomers such as bis-phenol-A-diglycidyl dimethacrylate (Bis-GMA) (Figure 1.11), urethane dimethacrylate (UDMA) and/or triethylene glycol dimethacrylate (TEGDMA). Polymerization of the resin matrix can be chemically initiated in "self-cure" composites, light activated, or a combination of both with various inorganic materials such as glass fillers are used as reinforcing components and make up the bulk of the material[51]. Composites may also incorporate barium and/or strontium, which add radiopacity to aid radiological monitoring of the composite in *vivo*[136].

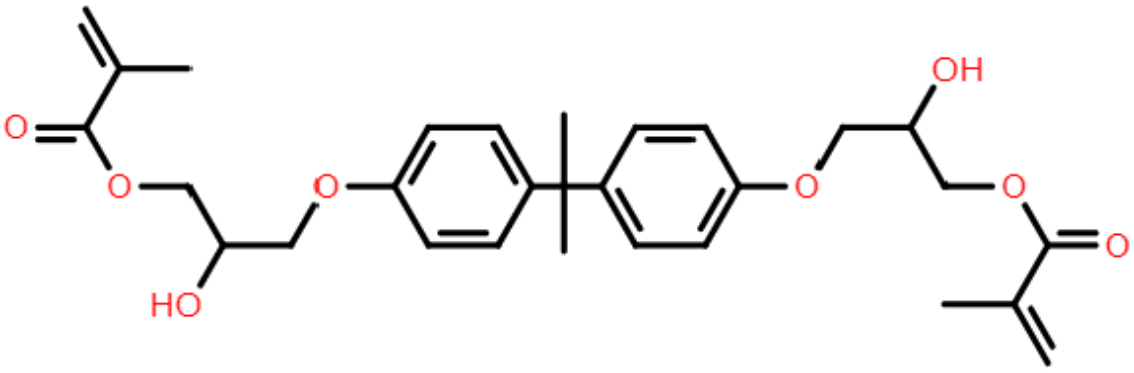

Figure 1.11 - Bis-GMA resin used in composite restoratives

The now outdated Lutz and Philips Classification[137] was common use for grouping composite types, however, hybrid composites are most prevalent on the market and used by clinicians nowadays due to their wide use in most classes of restoration.

1.2.3.2 Properties

These composites have good aesthetic properties due to the translucency of the partially polymerised resin matrix and thus provide a better match to natural tissue than amalgam and GICs[138]. The compressive and diametral tensile strength of these (around 200 MPa after 24 h) approach those of amalgam and generally exceed those of GICs (section 1.4.1.2.3)[120]. Clinically, composites have good longevity with over 99% surviving up to 3.5 years in patients with severe tooth wear[139]. Composites are not as widely used in primary dentition and a survey in 2017 found that 75% of anterior restorations were placed in patients between 35 and 65 years old[140]. In the Netherlands, an extensive study of over 75,000 patients found an annual failure rate of less than 5% up to 10 years with 56% of the anterior and posterior restorations remaining[89]. Composites have also been shown to rival the longevity of dental amalgam[141].

1.2.3.3 Applications

Modern composites have a variety of uses in most classes of restoration. Composites are the most widely used materials for restorations of anterior teeth[142] and are now

routinely used in conservative occlusal and proximal preparations on posterior teeth as well[143].

1.2.3.4 Limitations

Restorations using composites are technique sensitive and not following exacting procedures can lead to porosity, poor bonding, and inadequate degree of conversion [144]. Some patients exhibit sensitivity to the resins used in the composite which can cause post-operative sensitivity[145,146]. Modern composites require bonding agents and acid etching to create an adequate bond between restoration and tooth[147]. The materials exhibit polymerisation shrinkage of typically ~2-3% due to the polymerisation reaction which if not adequately compensated for can cause marginal gaps[148,149], potentially leading to secondary caries[150].

1.2.4 Resin Modified Glass Ionomer Cements

RMGICs were developed to overcome the dissolution and wear resistance of conventional GICs. Similarly, to conventional GICs, RMGICs use an acid-base reaction to form its set cement. However, these also incorporate light polymerising resins which are either added directly or grafted onto the polyalkenoate chain creating a more resistant 'command cure' GIC[151]. The compressive strength is documented to be higher than conventional GICs but lower than composite and amalgam[120,152,153].

1.2.4.1 Composition

RMGICs are presented as either a powder-liquid system containing a fluoroaluminosilicate glass and a resin containing PAA-based liquid, or as a pre-dosed capsule. The liquid component containing resins and initiators such as hydroxyethylmethacrylate (HEMA) (Figure 1.12) or bis-GMA but can also include other copolymers and photo-initiators[154].

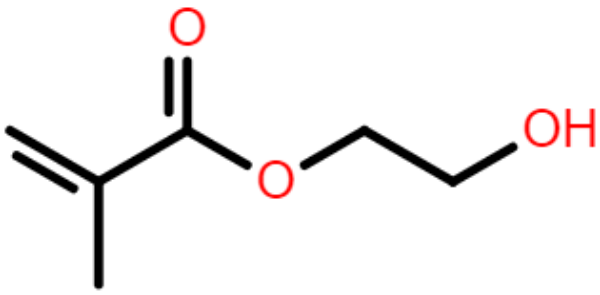

Figure 1.12 - Structure of HEMA resin used in RMGICs. Due to GICs being water-based materials, a highly hydrophilic resin such as HEMA is ideal[155]

The glass powder and acids (such as PAA and tartaric) used are often the same as those found in conventional GICs. Because the glass is in a lower concentration of the overall cement to make way for resins, properties associated with the glass components, such as fluoride release, were initially poorer than conventional GICs [156]. However, as the materials have developed more modern RMGICs have shown to have similar fluoride release levels to conventional GICs[157,158].

1.2.4.2 Properties

These materials exhibit similar levels of bonding to both oral tissue such as dentine and enamel in addition to other resin-based restoratives such as composites if used correctly (around 12 MPa)[159,160]. RMGICs release fluoride and exhibit moisture tolerance unlike many conventional GICs which often require a rubber dam to protect the early setting restorative. These restoratives set when exposed to blue light from a light curing unit creating a command cure GIC[72,161]. Due to the addition of resins, these materials have superior wear resistance and acid stability to GICs when used in anterior and posterior restorations[140,162] and similar aesthetics to GICs when polished[138].

1.2.4.3 Applications

Originally, RMGICs were popular as bases and liners under composites, amalgams and ceramics before eventually becoming restoratives alone[50,163]. These materials have similar indications to those of conventional GICs and are useful in class I, II, III and V restorations and as pit and fissure sealants due to their aesthetic properties[164].

1.2.4.4 Limitations

Incorporation of the resin in place of glass led to decreased levels of fluoride release and increased levels of thermal expansion which may “cause interfacial stress development, which has been implicated as one of the etiological factors in marginal deterioration and microleakage”[92,165,166].

1.2.5 Compomer

Introduced to the market in 1993[167], compomers are composites which have been modified using polyacids and contain a small percentage of fluoroaluminosilicate glass[168]. In a similar way to a RMGIC, these materials are a hybrid between a GIC and composite, although they are more closely related to the latter and are regularly described as polyacid-modified composite resins[169]. RMGICs differ in that they are GICs modified with resins and are mostly made of fluoroaluminosilicate glass, whereas compomers are composites modified with glass and polyacids where the bulk of the material are silane resins, creating a range of materials varying in both resin and glass concentration[170].

1.2.5.1 Composition

Compomers contain both fluoride-containing glass as a filler and resins which can either can act as initiators of the reaction or as polymers. To provide the acid-base reaction to release fluoride, an additional carboxyl source is provided in the form of dimethacrylate monomers, often UDMA. Additionally, to aid the diffusion of water into the matrix and further assist the flux of fluoride, hydrophilic resins such as glycerol dimethacrylate are used[170,171].

1.2.5.2 Properties

While these materials possess both glass and resinous components, it is mainly the light curing polymerisation reaction that controls the setting of the material while the glass remains as a fluoride releasing filler[172]. They provide tooth coloured aesthetics and have greater wear resistance and strength to the conventional GICs[173]. Clinically, compomers have been reported to last several years with a higher survival rate than conventional GICs in a range of applications[174,175]

1.2.5.3 Applications

The substitution of the resin component for glass brings the indications of these devices closer to that of conventional and RMGICs. They have similar applications to composites and have been used in class II[176,177] and V cavities[178] as well as fissure sealants and even bonding agents in orthodontics[179]. Additionally, they can be used in proximal, cervical and abrasion erosion lesions[180] and long-term restorations in primary and permanent dentition with long term clinical success of more than 5 years[181]. Coloured compomers available with glitter have been developed in the last decade, particularly aimed at children[177] and have shown to be clinically effective in primary dentition for at least 24 months[181,182].

1.2.5.4 Limitations

Compomers have some of the limitations associated with both composites and conventional GICs. Due to the higher resin content, the bonding to enamel and dentine

lower compared to higher glass containing restoratives and thus bonding agents are occasionally required[183] and these extra steps require additional time. Additionally, they exhibit similar polymerisation shrinkage to that of composites of up to 7%[184] and have increased water sorption due to the addition of hydrophilic resins[158]. This water sorption can lead to marginal discolouration which may interfere with aesthetics, particularly in anterior restorations[185]. While their mechanical properties do exceed those of conventional GICs, they are inferior to those of composites and RMGICs and are therefore not recommended for load bearing restorations but mainly deciduous teeth[186,187].

1.3 Indirect Dental Restorative Materials

As previously described, indirect restorative materials generally required two or more visits to complete. These materials often involved a dental technician or specialised laboratory to create and are thus multi-step processes and are therefore more expensive[188]. Due to the time and cost of these, they are often the second choice as a restorative method where a direct restoration is an option[46].

1.4 Mechanical Properties of Glass Ionomer Cements

1.4.1 Strength

Strength is defined as the capacity of an object or substance to withstand force or pressure. Strength of a GIC can be assessed using a range of methods such as biaxial

flexural strength (BFS), flexural strength (FS), shear bond strength (SBS) and fracture toughness (FT)[189,190] although the main parameters tested are compressive strength (CS) and diametral tensile strength (DTS) because of the similarity to the stresses the materials undergo during mastication and the brittleness of the material[191], that is, brittle materials such as conventional GICs are mostly exposed to compressive and (indirectly) tensile stresses in their use as restoratives.

1.4.1.1 Tensile Strength

1.4.1.1.1 Concept

When a material is subjected to a tensile load, tensile stresses occur, and the tensile strength of a material is its resistance to that tensile stress. Ductile and elastic materials such as rubbers, plastics and silicones exhibit a high tensile strength and can be pulled and stretched without permanently deforming. However, brittle materials such as concrete have low tensile strength and exhibit little elastic or plastic deformation before failure. Brittle and ductile materials are discussed in detail in section 1.4.4.

1.4.1.1.2 Measurement

Tensile testing usually involves applying a tensile force or “pulling” the material along a uniaxial direction at a constant rate and monitoring deformation until failure. Usually, grips attached to a tensiometer hold the material in place and the stress-strain applied

measured through a load cell (Figure 1.13). Tensile stresses are directly proportional to the force applied to the material. Higher forces applied created greater stresses while lower forces create less stress. Stress can be defined as the force applied per the cross-sectional area of the material (see Equation 1)[72]. As the stress is applied, deformations in the material occur and the material deforms as the displacement of force occurs creating a strain within the material. This displacement in the material length is measured and used to create a stress-strain graph.

Equation 1 - Calculation of the stress of a material where σ = stress, F = the tensile force and A = the cross-sectional area

$$\sigma = \frac{F}{A}$$

Figure 1.13 - Grips attached to a tensiometer measuring the tensile strength of a piece of dental modelling wax

1.4.1.1.3 Within Glass Ionomer Cements

GICs are brittle materials, particularly conventional GICs that do not contain any resins. Therefore, they exhibit little strain when a load is applied and fracture abruptly with little elastic and virtually no plastic deformation. Because of this, it is difficult to measure tensile strength of GICs using the conventional method, thus it is measured indirectly using the DTS method (Figure 1.13). It is the internal tensile forces within a cement when compressed that can be measured to calculate the tensile strength across a high surface area specimen. These are usually thin disc shaped to maximise the tensile stresses within the specimen over the compressive forces.

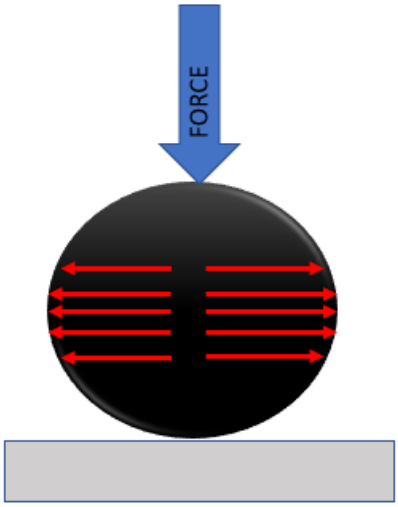

Figure 1.14 - Internal tensile stresses within a specimen when a compressive load is applied to measure indirect tensile strength DTS. This test results in a clean fracture down the centre of the specimen. The red arrows show the internal forces exerted on the specimen under compression.

1.4.1.2 Compressive Strength

1.4.1.2.1 Concept

CS of a material is its resistance to stresses induced by normal loading and is suitable for brittle materials which exhibit little or no plastic deformation. During compression, friction occurs between the test specimen and the compression platforms which is not consistent across the entire specimen. The maximum frictional force is contained at the edges of the specimen, while the centre has the minimal amount of force. Specimens presenting some form of plasticity can undergo barrelling due to the inconsistent frictional forces across the surface area[192,193]. It is thought the minimum compressive strength necessary to resist the masticatory forces in the posterior teeth

would be 125 MPa, or 100 MPa for primary dentition[194]. Studies assessing the bite force of humans found these to be in the region of 285 N (average man) and 254 N (average woman)[195] with around 25% of that being utilised during chewing[196].

1.4.1.2.2 Measurement

Testing compressive strength involves compressing a material uniaxially using two plano-parallel platforms until failure. This is usually measured using a compression unit where the compression platform is attached to a load cell which measures the load applied until break. The failure is usually sudden and very little energy is absorbed by the material before failure.

1.4.1.2.3 Within Glass Ionomer Cements

CS of a conventional GICs is relatively poor compared to other restorative materials such as composites and amalgams (Table 1.5) and is a limitation of the applications of the material.

Table 1.5 - Summary of DTS and CS of dental restoratives

Restorative	Typical DTS (MPa)	Typical CS (MPa)
Conventional GIC	6 - 12[153,197,198]	80 - 170[199,200,193]
Composites	30 - 50[120,201,202]	130-220[120,152,201]
Amalgam	30 – 54[120,202,203]	250 - 486[120,202,119]

1.4.2 Failure Mechanisms of Glass Ionomer Cements

Restorative materials, undergo three types of stress in regular use, these are:

1. Tension – stresses resulting from a pulling motion
2. Compression – stresses resulting from a pressing motion
3. Shear – stresses resulting from a lateral force parallel to its surface

1.4.2.1 Macroscopic Failure

Macroscale failures are visible fractures or flaws in the material structure and can be explained by several theories including the maximum stress theory (section 1.4.3). When the load or energy capacity of the material is exceeded, macroscopic failure

occurs. Fractures of GICs are an example of macroscopic failures as compressive forces (such as chewing) on the material cause the cement to fracture and fail[204]. Once macroscopic failure of a material has been seen, such as with GICs, either repair or replacement of that material is required[90].

1.4.2.2 Microscopic Failure

Microscopic failure is failure not visible to the naked eye. Atomic level stresses between planes of crystals, glasses and lattices can lead to microscopic failures and a combination of microscopic failures may lead to a macroscopic failure, such as cracking. Because of this, microscopic failures are difficult to observe in the clinic and even more difficult to predict, it is therefore vital that correct clinical technique is followed to reduce the risk of failure[90] and improve the longevity of the material[205].

1.4.3 Maximum Principle Stress Theory

Developed by Rankine in 1850, the theory states "the failure of a material or component will take place when the maximum value of stress exceeds the limiting failure of stress"[206]. This theory applies to tensile and compressive stresses only. It is at this maximum stress point (also known as the ultimate stress limit) that brittle materials fail and do not exhibit any further strain. However, within ductile materials, further strain can occur before the material fails, even though the maximum stress limit (also known as the yield stress) has been reached. In brittle materials, a crack will start at the point where the ultimate stress limit is reached. The theory is generally

used more successfully in brittle materials to ductile as the latter exhibit extensive shear behaviour (which are assumed to be absent in this theory)[207,208].

1.4.4 Brittle and Ductile Materials

Ductile materials show a region of linear elasticity, a yield point and ductility past the point of what is considered failure. During failure, ductile materials undergo 'necking' where the width of the material is reduced, and it becomes elongated, the fracture appears as an irregular shaped break with a 45° angle to the direction of the pull in a cup and cone shape.

Brittle materials exhibit a sharp linear elastic region and fracture suddenly with no evidence of elasticity. No necking is seen during a brittle material failure mechanism and the break will be at 90° to the direction of the pull (when under normal tension). Materials such as acrylic used in dentures can be considered as brittle plastics produce greater levels of strain per stress applied, while they often break rapidly with little plastic deformation[72] (Figure 1.15).

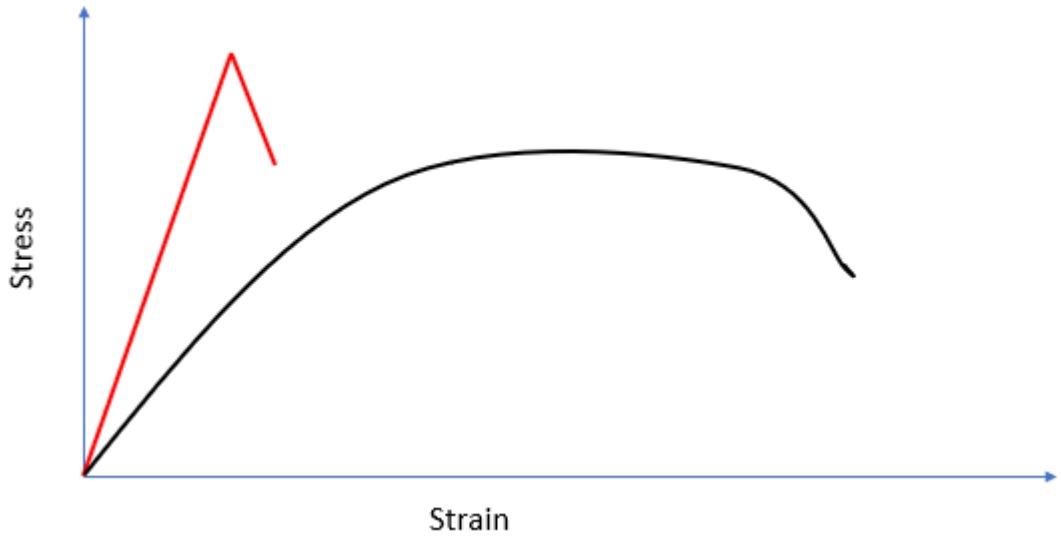

Figure 1.15 - Stress Strain Curves of Brittle (red) and Ductile (black) failures. Brittle materials show no ductility or plasticity whereas ductile materials go through an elastic phase and exceed the yield point before reaching fracture

1.4.5 Flexural Strength and Flexural Modulus

FS is mostly quoted in relation to resin-based restorative materials, including RMGICs, and is one of the prerequisites of International Standard (ISO) 9917-2 for these materials. BFS is more commonly investigated in GICs. Flexural properties of materials are usually only assessed in ductile and elastic materials because they can absorb high levels of stress and exhibit yielding rather than immediate fracture[209]. Testing is usually conducted using three- or four-point bending tests which flex the material under increasing and constant loading until failure, an example of a three-point bend test is shown in Figure 1.16.

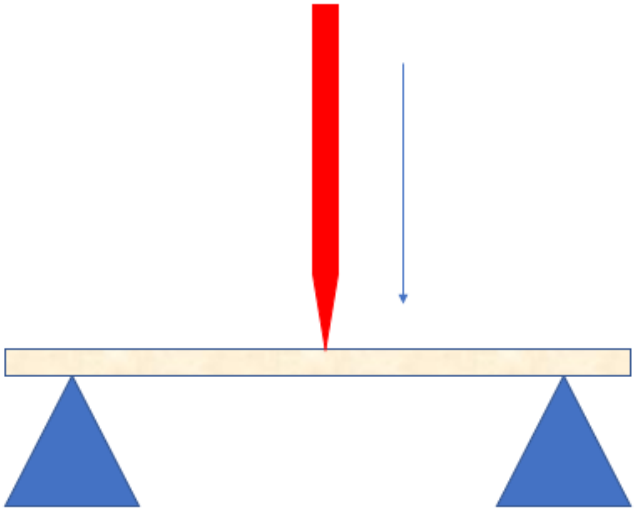

Figure 1.16 - FS testing using a three-point bending test. The bar shaped specimen is balanced on two supports while a third point compresses the material at the centre point

In a similar way to FT, this technique involves creating bar shaped samples (usually 2 x 2 x 25 mm) which are balanced on two platforms with a load applied centrally until fracture (Figure 1.16). The procedure is often described as a three-point bending test due to the three points of contact with the material during testing. The test produces a bending motion and evaluates how able the material is to resist flexure owing to processes such as mastication[210,211]. Brittle materials such as conventional GICs exhibit very limited flexural properties and these types of tests are rarely conducted. When flexural stresses are measured in restorative materials, these are usually resin based cements such as RMGICs, compomers and composites as the resin component increases the flexural properties[210,212].

1.4.6 Fatigue

In most cases, materials experience stresses which vary over time. These stresses may be mechanical, chemical, biological or a combination of these. In the example of a dental restoration, the material is exposed to higher stress during masticatory processes and lower stresses while the individual is asleep. This continued and irregular stress exertion on the material can lead to fatigue where failure can occur significantly below the maximum stress due to the accumulation of microscopic failures, which may lead for instance to crack propagation[213]. Thus, a material may be strong enough to withstand loads placed on it when initially put to use but this does not mean it will always be able to withstand these loads[72]. Fatigue is tested by applying numerous stresses well below the materials limit in a number of 'cycles' until failure, the maximum cycles applied before failure can then be used to calculate the materials endurance limit[214]. When testing a material, it is important to take into account the environment in which it is being used, as this can often have a profound effect on the endurance of the device[72]. GICs have been found to be inferior in fatigue testing than many other restoratives including RMGICs and composites[215]

1.4.7 Shear Stress

Shear stress was founded on the early work by Tresca who recognised that metals plastically deform through shear processes thus, opposite to normal stress, shear stress acts parallel to the cross-section of the material[216]. Once the elastic range of the

material is exhausted the metal utilise dislocation slip systems to accommodate the excess energy absorbed.

1.4.8 Crack Propagation

Fractures occur within the material and reach the surface of the material to dissipate the energy contained, known as crack propagation[216]. Fatigue has been shown to be a significant contributor to crack propagation as small stresses cause the material to internally fracture[217]. In 1921 Alan Griffin published investigations of brittle solids, demonstrating that "crack growth can occur if the energy required to form an additional crack with size can just be delivered by the system"[218]. At the tip of any crack, a stress field occurs, resonating out from the crack in a shearing motion causing cleavage within the material structure[219]. As previously mentioned, only three types of stress are exerted on materials, tension, compression and shear. Tension is solely responsible for crack propagation, while compression will only close cracks further[208]. GICs, as brittle materials, exhibit crack propagation through the cement matrix, often moving around bulkier glass particles. Crack growth often occurs parallel to the surface of the restoration and originate at weakened sections of the cement, such as a pore. Tension caused through desiccation of the setting GIC can be a significant factor in early crack propagation and is common in GICs[220]. Shear force has been reported to increase crack width and reduce crack spacing within brittle materials, such as GICs[221].

1.4.9 Fracture Toughness

The FT of a material is its resilience to propagation of a pre-formed crack. This is tested by introducing a crack into the material and applying a load, usually compressive, (in a similar method to FS) and measuring the stress required for the crack to grow and the material to ultimately fail[72]. Ductile materials have superior fracture toughness to brittle materials as crack propagation can only occur within a ductile material when load is applied. For denture base polymers, an incision of 3 mm is made into a bar shaped specimen measuring 39 x 8 x 4 mm and a compressive load applied to the surface opposite the crack[222] (shown in figure Figure 1.17). This is a commonly used standardised method where the deflection of the material vs the force applied is used to calculate FT. Cracks and pores are a common occurrence in GICs throughout the structure[101,223] and have shown to weaken the structure[102]. As previously mentioned in section 1.4.8, cracks propagate when tensile stresses are applied, in GICs, stresses such as desiccation, mastication or expansion can cause these already existing cracks to macroscopically fail[224].

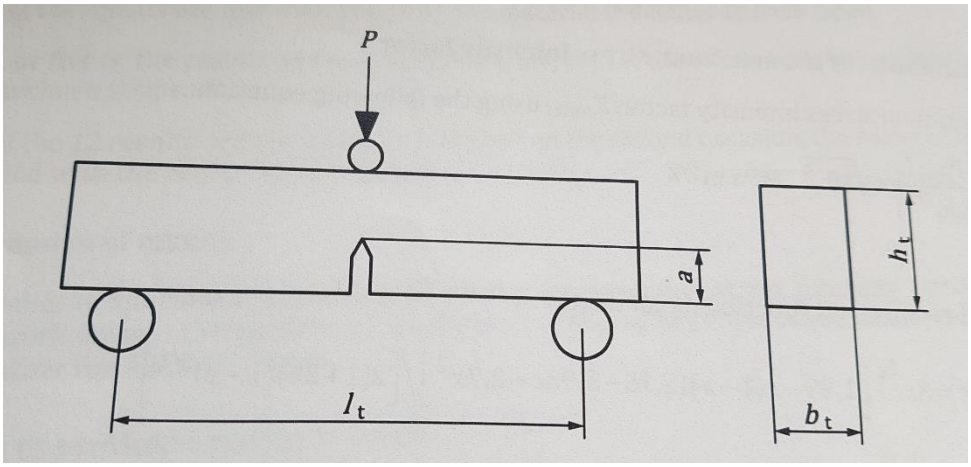

Figure 1.17 - FT with a modified bending test set up for denture base polymers. Where P = load, a = pre-crack depth, Lt = distance between the supports of the material, bt = the breadth of the material, ht = the height of the material[222]

1.4.10 Hardness

Hardness is the resistance of a material to localised deformation and is correlated with the wear resistance of a material against applied forces such as occlusal loading[225,226]. Hardness can be tested in several different ways, one of the most widely known being the Mohs scale ranging from soft talc at 1 to hard diamond at 10[227]. Hardness tests are considered simple and use inexpensive equipment as well as being relatively non-destructive compared to other strength testing methods[216]. Modern tests use indentation as a quantitative way of measuring hardness, once the indent is applied, the penetration depth is calculated from the lateral extent of the indent and the known geometry of the indenter. Several different hardness tests are available and have subtle variations[121].

1. Vickers – a small diamond tipped pyramidal indenter is pressed onto a surface under a known load for a pre-set period. The indent appears under a microscope as a diamond shape which is then measured laterally[228]. This method has been well used since the 1950s[229] due to the low cost, easy sample preparation and small amount of material require making the test simple and convenient[230]. Vickers tests are particularly useful in hard, brittle materials such as ceramics and conventional GICs and was chosen because of this, in addition to its ease of use.
2. Knoop – uses a similar method to Vickers, this is preferred for thinner profile specimens and produces a shallower but wider indent using a rhomboid shape indenter.
3. Rockwell – a very common and simple test to perform with the option of several different indenters, loads and scales. Indenters such as conical diamond tipped for exceptionally hard materials can be used; however, steel balls of various diameters are more common. A minor load is applied to enhance test accuracy followed by a major load of 3 or 10 kg and up to 150 Kg respectively. Because of this, test specimens are usually required to be a considerable size, particularly for repeated measurements.
4. Brinell – in a similar way to Rockwell testing, this test uses spherical steel or tungsten carbide balls as indenters. Loads generally range between 500 – 3000 Kg for metals which are applied for a specified time in increasing weight. Once an impression is made, the diameter of the load is measured and converted using a standardised table.

Other less commonly used methods are also available such as ultrasonic microhardness, dynamic, durometer and scratch hardness tests[231].

1.4.11 Bond Strength

SBS is often evaluated for GICs because of their use as either luting agents, or as restorations which need to adhere to the tooth surface for several years[232]. The test is conducted on GICs and bonding/luting agents by fixing these onto burred and polished flat surfaces of tooth specimens before being clamped into place and pulled apart until dislocation[233,234]. Typical values for tensile bond strengths varied from 4.90 to 11.36 MPa on enamel and from 2.52 to 5.55 MPa on dentine for conventional GICs[199,235,236] and 10 – 23 MPa for resin-based adhesives[237]. Because of this, adhesive failure of GICs is clinically rare[238] and only occurs when the bond to enamel is less than 3.5 MPa[239]. Usually, the only form of bond failure that occurs clinically is cohesive failure within the GIC.

Table 1.6 - Comparison of shear bond strength values of various dental restoratives on dentine. All restoratives were prepared with or without the use of etching/conditioning/bonding agents as recommended by the manufacturer's instructions for use[240].

Composite (MPa)	Compomer (MPa)	RMGIC (MPa)	GIC (MPa)
18.16	11.96	9.71	3.81

1.5 Strength Reinforcement

To make materials stronger and more resistant to fatigue and failure has been an aspiration for millennia. Increasing the strength of a material can be achieved by physically or chemically altering the structure or by the addition of reinforcing materials.

During the initial design of the GIC, it was concluded that the highest powder to liquid ratio creates the best setting rate, CS, hardness and moisture tolerance, but these became difficult to mix so the advantages of this should be weighed against the clinical usability of the cements[241]. Further approaches that have been explored to increase the strength of glass ionomer cements include adjusting the GIC liquid-powder ratio, adding or modifying glass fillers, increasing mixing time[242], compaction and using spherical instead of irregular shaped particles. These and other approaches to increasing strength in GICs are discussed in depth in section 1.5.1. More recently, nanomaterials have been explored as a way of reinforcing materials; this is discussed in section 1.7.1.1.

In metals, work hardening causes dislocations within the material structure and consequently further internal stress, an increase in the dislocation density (the number of dislocations within a given volume) increases the yield strength of the metal[243]. As previously discussed with amalgam, adding stronger metals, known as alloying, is another popular method of modifying the strength of a metal. The addition of different sized and higher atomic weighted metal creates an irregular lattice which can interfere

with failure modes such as crack propagation[244]. In polymers, increasing the molecular weight of the monomer has been shown to enhance strength as well as further covalent cross linking and bridging by the addition of disulfides[209].

1.5.1 Strength Developments in GICs

GICs have been modified numerous times since their initial development in the 1960s. Metal, zinc, glass, calcium phosphates, fibres and particles have all had reasonable success in increasing strength[51]. One of the most recent developments has been incorporating amino acids into GICs for enhanced strength, various amino acids have been studied giving good increases in flexural strength but few changes in compressive or DTS[245] although studies with proline addition resulted in increases of 27% and 94% for CS and DTS respectively[246]. The proline was thought to have increased the spacing linking the PAA backbone and reducing steric hindrance and increasing the mobility of the carboxylic acid groups. However, these amino acids are complex to manufacture involving several hazardous substances with low yields (around 60%). Other developments include the addition materials such as metals like zirconia, titanium and zinc, or glasses and various forms of calcium, all with varying amounts of failings or success in enhancing the GICs mechanical properties as will be described in the following sections.

1.5.1.1 Metal Modified GICs

One approach to improve the mechanical properties of GIC were the 'cermets' or metal-modified GICs (MMGICs), originally particles of a silver alloy were added into the powder component eventually developing into sintering these fine particles onto the glass itself[50], while theoretically these were expected to be stronger they did not perform better clinically over several studies[247-249] and evidence also suggested fluoride release was reduced slightly as a result of the silver inclusion[50]. In subsequent research a stainless steel modified GIC was developed, providing a 50 and 60% increase in CS and DTS respectively compared with two commercially available MMGICs with favourable working/setting times and low solubility, however the cement exhibited a grey colour thus reducing the GICs aesthetic appeal and limiting its use[250]. Silver has not been abandoned, a recent study using 0.5% silver nanoparticles (NP) (6 nm in diameter) increased the CS of a GIC by 32% although the author fails to comment on any changes to aesthetics which was seen in the previous generation[251]. Titanium has also been investigated; 5% TiO_2 nano-powder was supplemented into FX-II GIC (Shofu Dental, California, USA). This saw improvements to the FS (15.1 ± 2.9 MPa to 21.4 ± 5.0 MPa) and VHN (54.3 ± 9.0 MPa to 63.8 ± 4.1 MPa). The authors also studied CS but published surprisingly low values (control 5.6 ± 2.3 MPa, 5% TiO_2 nano-powder 8.6 ± 1.5 MPa) despite using a standard ISO method and citing the minimum requirements of at least 100 MPa required to resist primary masticatory forces[252]. In another study, Michael Swain et al. used 3% TiO_2 NPs and generated a significant increase in FT, FS, CS and VHN in Kavitan® Plus GIC (Kerr Dental), the increases are summarised in Table 1.7[200]. However, as more NPs were added, the setting time

decreased, this was attributed to the NPs taking part and strengthening the acid-base reaction, although they do not elaborate on how this is done, if this is the case, it would be strongly be related to the causation of the increases in strength, although at higher concentrations of NPs, the setting time further decreased but the strength did not. The authors further note a decrease in setting time being clinically advantageous as it reduces the risk of dehydration or excessive water contamination of the setting GIC. No comment is made on the changes in working time, but a reduced setting time may often indicate more rapid hardening when being mixed, which may not be clinically advantageous. A different group also used 3% TiO_2 nanoparticles (10 – 20 nm diameter) in Fuji IX and found a significant increase in CS from 140.03 (± 9.08) MPa to 172.55 (± 14.88) MPa[253]. Furthermore, a group in China using TiO_2 NPs increased CS by 18.9%, bond strength by 51% and reduced wear by 5%[254]. TiO_2 is a commonly used white pigment in food, personal care products, paints etc. due to it brightness and high refractive index[255], despite these successes in increasing mechanical properties none of these studies comment on the changes to colour and translucency of the cement as a result of the pigment. Additionally, TiO_2 NPs has some demonstrated some concentration-based toxicity to the central nervous system[256,257], the respiratory system[258], the liver[259] and gametes[260].

Table 1.7 - Increase in mechanical properties using TiO_2 NPs. The standard deviations are shown in the parenthesis. Data adapted from[200]

	FT (MPa $m^{1/2}$)	FS (MPa)	CS (MPa)	VHN	Setting Time (s)
Control	0.69 (0.03)	13.57 (2.52)	149.06 (7.91)	46.3 (4.36)	268 (11.51)
3% TiO_2 NPs	1.29 (0.05)	23.17 (2.77)	176.27 (8.35)	48.34 (4.92)	217 (10.36)

A newer product containing ceramic, Amalgomer CR (Advanced Healthcare Ltd., Tonbridge, UK) claims CS exceeding 300 MPa[261]. The product was first introduced around 2005 in a zirconia alloy when it was claimed the aesthetics and hardness were superior to a conventional GIC[197,262]. Clinically, after 1-year Amalgomer CR had a clinical success rate of 97.4% and 94.2% for class I and II restorations in children ages 4 – 9 (n = 100) respectively, compared to 94.9% and 88.5% for Fuji IX[263]. Fluoride release was not compromised either, in one study Amalgomer CR was found to be superior to Fuji II (GC), Fuji IX, Beautifil II (Shofu Dental), Dyract extra (Dentsply Sirona), and Coltene Synergy (Coltene, Altstätten, Switzerland) over a 15 day period, although it should be noted that some of these were not conventional GICs[264]. Bond strength (6.38 MPa) was also found to be superior to others tested (5.39 MPa Miracle Mix (GC) and 4.84 MPa Ketac Molar (n = 30))[234]. However, Wang and Darvell found the inclusion of zirconia increased moisture sensitivity and deteriorated the cement in artificial saliva[265], however with good clinical practice, these risks are significantly reduced.

Zinc reinforced high viscosity GICs came onto the market as the product ChemFil Rock (Dentsply Sirona) in 2011[266] as a material requiring no cavity conditioning or surface

coating. The manufacturer quotes at least a 25% increase in hardness and strength through the incorporation of zinc into the fluoroaluminosilicate glass itself[267]. An independent study by Ilie found increased flexural properties due to the reduced visible defects, however, contrary to the manufacturer's recommendations, the use of a resin coat had a significant positive effect[266]. Other independent studies using this product have given mixed results, while some reported significantly higher CS and DTS compared to hand mixed high viscosity GICs[268] other properties such as fracture toughness and surface hardness did not stand out[269]. Against other restoratives such as RMGICs, ChemFil Rock CS over 24 h was still significantly lower (244 ± 13.0 MPa vs 156 ± 21.8 MPa respectively)[270]. Even more recent studies using zinc oxide NPs supplemented GIC have still yet to find any increases in mechanical properties[271,272].

1.5.1.2 Glass Fibre GICs

The incorporation of glass fibres into GICs has also been studied with some promising results. The fibres often have a similar chemical composition to the glass used in the GIC. A study using micron scale glass fibres with 1 mm length and 10 µm thickness incorporated by addition to a conventional GIC at 3 and 5% w/w provided a significant increase in the highest addition for DTS (7.49 to 11.86 MPa), VHN (38.6 to 53.2), FT (0.194 to 0.585 $MPa.m^{1/2}$), FS (15.02 to 28.76 MPa) and flexural modulus (FM) (0.679 to 1.192 GPa)[273]. Lohbauer and co-workers added smaller fibres 430 µm long and 26 µm thick in much higher 20% concentrations giving much higher FT and energy release rates (up to 440% more for the latter) but fails to test any DTS or CS of these[274,275].

Micron scale hollow fibres have shown increases in FT of up to 200%[276] Kobayashi added aluminosilicate based fibres of varying aspect ratios into a conventional GIC and concluded the smallest in terms of length and diameter gave the best increase in strength at 1.8 times higher for DTS and 4.5 times higher for FS[277], however the creation of these fibres involve heating materials to extreme temperatures, spinning and passing through an electromagnetic sifter, a costly and very specialised manufacturing process. A recent 2018 study reported on additions made to Fuji IX using glass fibres of around 10 µm in diameter and 10 – 500 µm in length over a range of percentages[278]. A 25% addition of the glass fibres gave an increase in FS (26 MPa to 48 MPa), FM (1 GPa to 3.7 GPa) and DTS (8 MPa to 17 MPa). Fracture surface scanning electron microscopy (SEM) images showed good interaction between the fibre and the surrounding GIC matrix and fracture occurred at fibre pull out sections of the cement. Due to this interaction, the authors note the load is successfully absorbed by the stronger glass fibre giving it a reinforcing ability. On the other hand, a study using bioactive glass within a GIC and compomer had a negative effect on the CS of the materials of around 54%, possibly due to the active glass acting as loose filler instead of forming part of the cement matrix[279,280].

1.5.1.3 Calcium Salts and Related Materials

Calcium salts have been investigated as a material to enhance the mechanical properties of a GIC.

A novel study found an increase in compressive strength from 52.45 ± 1.8 MPa to 71.43 ± 16.7 MPa with the inclusion of 5% chicken egg shells[281] which has also been shown to increase strength in acrylic resins[282], composites[283] and concrete in construction[284]. The eggshells are a natural source of calcium carbonate[285] and considered to be an environmentally beneficial way of reusing the 190,000 tonnes of eggshell waste in the US[286] for developments in materials.

FA has been considered due to its biological presence in dental enamel. 3% FA NPs (70 nm) were added w/w to a GIC giving an increased compressive strength (46.10 ± 3.39 MPa v 102.61 ± 4.00 MPa)[287] which coinciding with similar increases found by Moshaverinia et al. who also saw significant increases in DTS and BFS[198]. The study noted that HA and to a lesser extent FA are soluble in acidic solutions[288] and the release of calcium from this increased the acid-base reaction thus creating a stronger cement.

Micro HA from a commercially available source was added to a RMGIC and zirconia reinforced GIC and its hardness measured. Additions of 5 and 15% significantly increased the hardness from 46.70 ± 1.66 MPa to 56.46 ± 3.33 MPa and 53.63 ± 1.48 MPa respectively for the zirconia and from 54.95 ± 4.35 MPa to 71.28 ± 0.91 MPa and 67.26 ± 2.57 MPa respectively for the RMGIC[289]. The authors attributed this to an increased ion migration and formation of HA within the GIC strengthening the matrix, however as higher concentrations were added, a decrease in hardness was seen which was attributed to a decreased density of the GIC. Similarly, Rasheed and Mohammed synthetically created HA and added this to a GIC in 10, 15, 20, 25 and 30% w/w[290]. Increased DTS and hardness were seen amongst all additions, optimising at 20% in

particularly. This was explained by the finer particle size amongst the GIC which led to a stronger cement, however as the additions increased, significant changes in the powder to liquid ratio may have had detrimental effect on the mixing. The authors did not provide data regarding the particle size of the HA or provide a comparison against these increased powder volumes without the HA; therefore it cannot be concluded the increased mechanical properties were solely due to the HA.

Work has advanced in using HA to the synthesis and introduction of nano HA particles and fibres, these are discussed in detail in section 1.7.2.

Calcium phosphates, including HA, are sparingly soluble in solution, particularly under acidic conditions, and it is not clear whether the HA withstands the acidic conditions that prevail during GIC setting[291-293]. As previously discussed, the mechanism by which caries forms is through the process of hydroxyapatite dissolution when exposed to acids. Moshaverina noted that HA and to a lesser extent FA exhibits some level of solubility in acidic solutions and within a setting GIC, the polyacid can extract calcium from the apatite surface when mixed with the powder[198]. The solubility of HA is accelerated at a pH of less than 2.05[294], like those seen in the early stages of the GIC setting reaction and even at a pH around 4.5 some surface solubility can be measured[295]. Work in 2004 suggests the older studies may have overestimated the solubility of HA[292] however studies previously mentioned indicate some success in using HA to enhance the mechanical properties of restorative materials[71,289,296,297].

1.6 Other properties of GICs

1.6.1 Biocompatibility

Biocompatibility is defined as "the ability of a biomaterial to perform its desired function with respect to a medical therapy, without eliciting any undesirable local or systemic effects in the recipient or beneficiary of that therapy, but generating the most appropriate beneficial cellular or tissue response in that specific situation, and optimising the clinically relevant performance of that therapy"[298]. Medical devices, such as GICs, have a requirement to exhibit acceptable levels of safety, biocompatibility and the risks of these should be outweighed by the benefits[299-301]. Modern GICs, as a class IIa medical device, are usually assessed for biocompatibility using the ISO 10993 series[299]. These measure a range of properties, such as genotoxicity[302], cytotoxicity[303] and sensitization[304] using various cell cultures *in vitro*. A RMGIC has been shown to possess reduced biocompatibility and toxicity within several studies, suggesting a negative biological effect from the inclusion of resins[305-308], although the effect reduces over time[309]. GICs however have shown good biocompatibility after 24 h, 7 days[310], 14 days[311] and up to 60 days[312].

1.6.2 Fluoride Release and Secondary Caries

It is well documented that GICs release fluoride ions in solution[157,158,313-315]. An initial relatively higher concentration release of fluoride is usually seen during the initial 24-48 h of most of the fluoride releasing restoratives[65] (Figure 1.18). Additionally, these materials can recharge from additional fluoride such as mouthrinses[316], although

recent evidence indicates this effect is only evident in new GICs and as they age, their ability to release this fluoride is significantly reduced[104,316,317]. The complete removal of caries from cavities is difficult and it has been claimed up to 50 – 60% of dental restorations go on to develop further caries[318]. The release of fluoride has been shown to be antibacterial against plaque bacteria such as *Streptococcus mutans*[252,319-321], but these studies are laboratory based, making them poorly representative of the oral environment. The suggested reason for this in the oral environment is likely due to the formation of FA[322]. This may be down to several specific mechanism, fluoride ions are known to affect the growth and metabolism of oral bacteria by altering the membrane permeability to protons, leading to acidification of the cell cytoplasm and ultimately cell death. It may also bind to the enzymes in the cells often found in plaque, thus reducing their acid producing metabolism of carbohydrates. Other factors such as the difference in ion charge between the fluoride and proton ion substituted in FA for HA and stereochemistry of the FA molecule may also play a part[323]. Furthermore, it has been argued the antibacterial properties of a GIC comes from the low pH of the setting cement[324] or more likely a combination of the two[325]. A common reason for failure in dental restorations has been attributed to secondary caries[205,326-328] but while GICs fluoride release has been shown to prevent secondary caries in vitro[329], little evidence is present clinically[330,331]. Fluoride can induce caries lesion remineralisation under some circumstances, such under neutral pH and availability of free fluoride and apatite[332-334] however GICs as antimicrobial materials they may be capable of preventing the initial adhesion of bacteria through the creation of more acid resistant FA from HA[335].

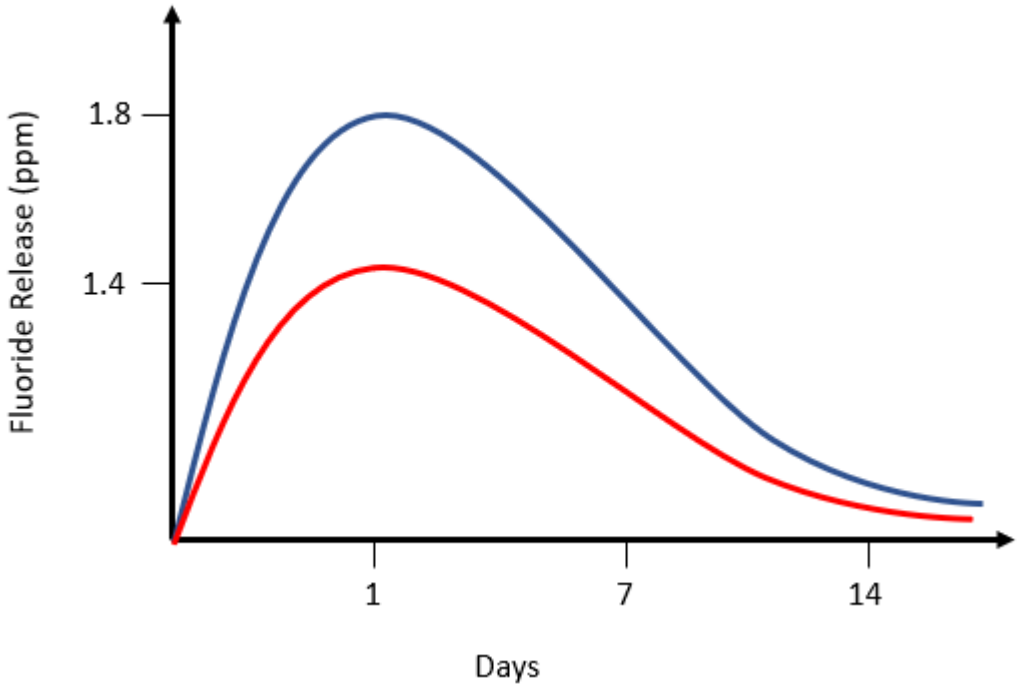

Figure 1.18 - Typical fluoride release pattern from a GIC showing the fluoride release (ppm) from the GIC (blue) and release to the same GIC in days after brushing with 1000 ppm fluoride toothpaste (red)[336]. Fluoride is released rapidly within the first 24 h, followed by a slower release up to 7 days before a further reduction in the rate of release past 7 days.

1.6.3 Aesthetics

Aesthetics are one of the most important aspects dentists consider when choosing a direct restorative material, particularly with anterior restorations[337]. Translucent materials match the surrounding tooth colour better as they allow light to travel through the material, thus the refractive index is generally used as a means of measuring how aesthetic the material is likely to be[105]. GICs are tooth coloured materials, matched using a blend of various iron oxide pigments during manufacturing. As the GIC matures, the colour develops, usually over the course of a 7-day period[104].

1.6.4 Adhesion to Tooth Structure

Adhesion of GICs to tooth structure and bond strength testing has been the subject of extensive study[338-340]. When the tooth surface is prepared and freshly cut a smear layer of 1-2 µm thick coats the dentine[341]. Removing this layer, usually with an acidic gel which dissolves the material, creates an optimal bond between the GIC and allows the GIC to penetrate the tubules providing opportunities for mechanical as well as chemical bonding[58]. This process is described as total etch or conditioning depending on the material used and is widely used in clinics[342]. As mentioned in section 1.4.10, the bond strength of GICs is higher to enamel than dentine, suggesting the main interaction is between the HA rather than the collagen matrix. As the cement is placed onto the surface, wetting is vital to produce initial hydrogen bonding between the GIC and tooth structure which are then gradually replaced by ionic bonding between the calcium ions in the tooth and the carboxylate groups within the cement[343]. PAA, like many acids, has been shown to strongly bond to HA and is likely to extract phosphate ions from the HA structure to bond directly to the calcium in the HA structure[63,344]. This process is known as true chemical bonding and is considered the main mechanism of bonding for GICs to tooth structure[58].

1.7 Nanoparticles and Nanofibres

The term nanomaterial refers to “A natural, incidental or manufactured material containing particles, in an unbound state or as an aggregate or as an agglomerate and

where, for 50% or more of the particles in the number size distribution, one or more external dimensions is in the size range 1 nm–100 nm"[345,346].

1.7.1 Uses in Materials

1.7.1.1 Enhancing Strength in Materials

NPs and nanofibres (NFs) have been investigated widely as a means of reinforcing various materials. Fibres are seen to have a strong resilience to applied forces allowing stresses to be received by them without permanent deformation, this essentially absorbs the energy from a crack as it propagates or deflects the crack itself [347]. It is also thought that these materials change the microstructure of the cement and fill in small voids due to porosity in the material[348,349] which was evident in indentation testing[350]. Fibres have shown to give good strength increases in various composites[351], brackets[352], acrylics[353] and concrete[354] both within and outside of dentistry.

1.7.1.2 Incorporation into Restorative Materials

The reinforcing effects of microscale glass fibres inhibiting crack propagation in a GIC leading to an enhanced strength was described in section 1.7.1.1. This was enhanced using smaller micro and nano sized fibres through a large and varied number of studies as early as 1982[273-275,277], it is therefore thought NFs and NPs could have a greater effect. Silica and alumina fibres/particles have been studied extensively but synthetic methods for these are often complex involving poorly scalable sol-gel and

electrospinning[355-359]. Calcium phosphate in its various forms have been the subject of incorporation into GICs; for example, Moshaverinia incorporated hydroxyapatite nanoparticles (HANPs) and fluorapatite nanoparticles (FANPs) of around 50 nm into Fuji II and found an increase in DTS (approx. 75%) and CS (approx. 15%) although these too were obtained through a sol-gel method[198,360]. Another study substituted the GIC powder with nano calcium deficient hydroxyapatite in RMGICs through an unusual microwave synthesis. The results showed a small increase in the CS of the material although higher levels of solubility were exhibited which in turn led to a later decrease in its CS[361]. It is important that these materials interact positively with the PAA containing GIC liquid and not hinder the reaction, in order to interact with the cement matrix some dissolution or surface interaction would be likely and expected, as seen with the glass particles in the GIC.

1.7.2 Hydroxyapatite Nanofibres and Nanoparticles

HA has a structure and composition very similar to human bone[362] and has had clinical success as a bone cement, often in combination with polymethylmethacrylate (PMMA) with acceptable strength, biocompatibility and osseointegration[363-368]. Other biological uses included hearing reconstruction[369], managing bone necrosis[370], nasal repairs[371] and as previously discussed, dental cements. The use of HA in current biomaterials makes it a promising option as a biocompatible high aspect ratio fibre for reinforcement. For example, nano HA needles were added to Fuji II LC (GC) in 1, 2, 5, 7 and 10% concentrations by weight and subjected to wear testing through a

toothbrushing simulation using a toothpaste slurry[297]. Increases in wear resistance was found in all groups, particularly in 2 and 5% additions. The mechanism was attributed to an increase in calcium release as the HA interacts with the acidic setting GIC which increased cross linking within the structure[372]. Higher concentrations failed to have the same level of reinforcement due to the change in viscosity of the drier mix, thus poor dispersion may have contributed. Porous spherical HA (20 – 30 nm in diameter) was added to Fuji IX increasing the FS from 18 MPa to 33 MPa but had no increase in CS[294]. The authors then went on to use Fuji III (GC) (a strontium substituted GIC), reducing the glass component and replacing with 25% commercially available spherical HA particles with a diameter of 10 – 20 nm. Surprisingly, they found an increase in fluoride release, despite the fact the fluoride releasing glass was at a lower concentration than the control. An increase in CS was seen from around 110 MPa to 135 MPa, since calcium has demonstrated to enhance the formation of the GIC matrix[373] it was concluded that only materials which take part in the reaction assist the increase in CS and demonstrated this by comparison against cellulose acetate fibres which showed a significant reduction in CS. HA is also relatively easy to produce and readily available commercially. A synthetic method creating fibres of around 100 nm diameter and 60 – 80 µm in length were added to dental composites of up to 10% attributed to a 22% increase in BFS[374]. The calcium nitrate and sodium dihydrogen phosphate dehydrate act as the calcium and phosphate source while the roles of the gelatine and urea is thought to be involved in maintaining and directing the HA crystal structure and the latter additionally breaking down and having a buffering effect on the basic solution[375].

Consequently, due to its biocompatibility and promising CS and DTS enhancing results HA in GICs presents as an opportunity for strength developments.

1.7.3 Halloysites and Clays

Nanoclays are layered silicates with nanometric thickness of clay within the layers, often tubes with a diameter of 50–200 nm. Montmorillonite (MMT) clays in GICs have been studied by Dowling and Fleming using ChemFil® Superior (Dentsply Sirona)[376,377] building on previous work in the early 1990s showing a reinforcing effect on polymers[378-380]. They found a decrease in compressive strengths for all additions of clays, however, when the clay was changed to 12-amino-dodecanoicacid-montmorillonite (ADA-MMT) a significant increase was seen for 0.5% (133 ± 20 MPa) and 1% (128 ± 22 MPa) compared with the control (105 ± 22 MPa). The increase was attributed to the stereochemistry of the larger ADA-MMT molecule causing greater d-spacing between the layers of GIC, giving the PAA more opportunity to react. This work focused on making additions to the powder component of the GIC system but it was found that the dispersion of the material is important in achieving optimal results and the clay is unlikely to interfere with the setting reaction[381] and has been shown to disperse well within a PAA based solution such as the GIC liquid due to the hydrophilic nature of the material[382]. MMT has been successfully grafted onto PAA and incorporated into a GIC (0.2% w/w) and created a significant increase in bonding strength as the surface PAA on the modified clay was more freely available to bond to the HA within the dentin[383]. 1% MMT mixed into the GIC liquid had a significant

increase in CS from 120 ± 19 MPa to 137 ± 16 MPa after 1 week of storage but no differences were seen compared to their respective control in any other concentrations or time periods[384]. The clay was substituted for the water component in the GIC liquid which led to reduced setting and working times in 2 and 3% substitutions but significant increases in CS.

Halloysite nanotubes (HNTs) are hollow aluminosilicate tubules with an alumina inner lumen between 15 – 25 nm and an outer silica lumen of between 40 - 50 nm[385,386] with lengths typically up to 1 – 2 µm. Barr conducted early research using the material focused on the use of the material as acid-base stable clays for use in the gastrointestinal tract although their size and morphology wasn't discussed results showed promise as good absorbers of toxins such as atropine[387-389]. The absorption studies weren't taken further until work using halloysites as a surface catalyst for hydrazine was published with a more in depth look at the surface chemistry of the material[390,391]. The differences in charge between the inner and outer lumens lead to various useful properties as a nanomaterial such as a drug or protein carrier[392-394], fixing and removing water metal pollutants [395,396], ammonia [397,398], anticorrosive coatings [399], dyes [400], CO_2 [401,402], as well as incorporating into composites[403-405]. HNTs have found various potential medical applications, including topical creams by loading slow release glycerine into the hallow tubes[406], antiseptic loaded sprays[407], wound dressings loaded with Vancomycin[408] and drug doped tablets consisting of around 55% HNT[409,410], however to date none of these have been commercialised.

HNTs have shown promising results in dental materials, for example, they were incorporated into resins in 5, 10 and 20% concentrations leading to an increase in

shear bond strength (control 28.5 ± 1.6 MPa vs 5% HNT 34.8 ± 1.6 MPa) in dental adhesives[411]. HNT have been shown to reinforce adhesive resins by enhancing modulus of elasticity of the adhesive, decreasing polymerization shrinkage, improving stress distribution[412]. HNTs in concentrations of up to 30% in an adhesive dentine bonding agent gave a significant increase in bond strength (control 21.8 ± 5.9 MPa v 30% HNT 30.5 ± 6.5 MPa) and increased hardness from 48 to 58 but led to an increase in adhesive failure and reduction in the cure depth of the material from 85% to 75%[413]. The two studies agree that nanofillers increase bonding strength of adhesive cements and SEM images showed significant resin infiltration into dentinal tubules and resin tag formation. It is suggested the hydrophilic nature of the HNTs assist in bringing the resin further into the dentin tubules.

Various strength improvements have been found through incorporation of HNTs, one study developed on the well-established surface chemistry of HNTs using a composite material with polypropylene with an addition of 2,5-bis(2-benzoxazolyl) (BBT) presenting an increased tensile strength of 22%, an increased FS of 33% and an increased FM of 59%, little increase was seen without the HNTs present (BBT only). The authors attributed this to the interaction and electron transfer between the BBT and HNTs as the electron acceptor due to its anionic potential, this alongside melt shearing created a higher crystalline BBT fibril[414]. Incorporation of halloysites into a soft elastomer gave an increase in the Young's Modulus with a 20% addition (from 0.82 MPa to 1.51 MPa), Ultimate Tensile Strength (from 0.6 MPa to 1.58 MPa) and strain before break (from 110% to 226%) created similar mechanical properties to connective tissue[415].

High Impact polystyrene was doped with varying concentrations of HNTs using a surfactant as a way to disperse the material throughout the polymer, results showed a 300% increase impact strength[416]. Moreover, a chitosan HNT composite material showed some good increases in strength up to a 7.5% HNT concentration with 134% increase in tensile strength and 65% increase in tensile strength although this maybe down to the HNT chitosan interactions[417]. A study added up to 2.5% HNTs into resin based dental adhesives saw good increases in mechanical properties, however further addition did not enhance the strength which was attributed to the agglomeration and undispersed HNTs within the resin weakening and counteracting the strengthening properties initially seen[418].

HNTs have been shown to be stable in a range of pH conditions from 2 – 11, however, at low pH the HNTs become unstable and are prone to agglomerate due to greater van der Waals forces[419]. This effect has been estimated to decrease the mechanical properties of the HNTs due to a change in the structure of the materials by a decrease in the wall thickness from protonation/oxidation[385]. Contrary to this, it was found when the internal diameter of the HNTs fell below 50 nm, the elastic modulus was found to increase to 460 GPa as the thinner walls contained less structural defects than thicker structures and an increased surface tension[420] Another study directly measured the experimental Young's Modulus and was found to be 130 ± 24 GPa and could even be bent to 90° without fracture[421]. HNTs have seen numerous applications in composite materials, exhibiting increased mechanical properties, thermal stability and flame retardancy[422-426]. In many studies, it was found that good dispersion of the filler is vital for exhibiting these properties[427,428]

Due to the widespread interest in using HNTs to augment mechanical properties, the cytotoxicity and biocompatibility has been questioned and been evaluated against human cervical and breast cancer cell lines[429]. The study used halloysites fluorescently labelled to view the uptake of the nanotubes into the cells with varying concentrations between 1 μg/ml to 1 mg/ml and found growth inhibition of the cell lines on a concentration dependant manner when assessed at 24, 48 and 72-h intervals. In all cases, % cell viability was shown to be lower at 24 h up to 50 μg/ml compared to the 72-h period although this was not seen at concentrations up to 1000 μg/ml with a maximum and minimum cell viability of around 75% (48 h) and around 40% (24 and 72 h) respectively for cervical cancer cell lines and a maximum and minimum around 40% (24 h) and around 5% (72 h) for breast cancer cell lines. The authors cited asbestos as a warning to how small fibrous materials can exhibit high levels of toxicity but notes the differences between these and HNTs, particularly regarding the length of the fibres. It was considered materials below 1 micron do not exhibit such levels of toxicity as they are more easily removed by cellular macrophages (HNTs vary from 50 to 5000 nm, with an external diameter of 20−200 nm and internal diameter of 10−70 nm). Equally the study showed safe use of the material up to 75 μg/ml (> 90% cell viability) which far exceeds the toxic limit of asbestos by nearly 1000 times. Additionally, it was found biocompatibility with a Polyvinyl acetate/Halloysite composite with mouse osteoblasts alongside fibroblast attachment and growth up to a 7.5% concentration[430]. An earlier discussed paper also conducted a cytotoxicity study based on ISO 10993 involving mouse fibroblasts and found to be well under the limit for toxicity up to 10% concentrations in the composite material[415] and addition to an electrospun

nanofibrous poly(lactic-co-glycolic acid) composite material also showed good biocompatibility[431].

Since the 1970s, HNTs have been used as a filler in paper and paint, as well as ceramics due to its exceptional whiteness[432]. Since then, they have found use in animal feed for piglets and chickens to remove mycotoxins[433]. HNTs are an environmental protection agency (EPA) 4A listed material (minimal risk inert material) and generally recognised as safe (officially termed GRAS) by the Food and Drugs Administration (FDA)[434,435]. In 2016 a study found HNTs to be one of the biologically safest clay compared to silica, graphene, kaolin, bentonite and montmorillonite[436].

HNTs are relatively cheap and abundant materials, at around $4/kg compared to carbon nanotubes (CNTs) at around $500/kg with global supply exceeding thousands of tonnes per year available in USA, Australia and New Zealand[437-439].

1.8 Research Gap

With the Minamata agreement phasing down dental amalgam and the need to find restorative alternatives there remains a significant gap in research particularly associated with GICs. To date, no commercial GICs can be used for many of the indications associated with dental amalgam. Developments to increase various strength properties of GICs have been undertaken since their initial development. These are discussed in section 1.5 including developments to create the 'cermets' and other metal modified GICs, zinc oxide modified GICs, high-viscosity GICs and amino-acid modified GICs. Using other additives such as glass fibres, HA particles and other

calcium phosphates have also been discussed, all with varying degrees of success and failure. Many of these have not led to strength improvements being significant enough as an amalgam replacement. Additionally, other properties such as fluoride release and aesthetics have also been reported to have been compromised. Research into reinforcement of composite materials is abundant, as discussed in this chapter, however GICs benefit from many advantageous properties composites often lack. It is therefore important to develop these restorative materials and provide clinicians with a GIC restorative which can be used for a wider range of clinical indications.

1.9 Aims of the Project

The aim of the project was to increase the compressive and tensile strength of the GIC because of the high number of restorative failures due to fracture. A study assessing GICs used as a base found 57.8% of failures were due to fracture[440]. A study by Burke found that while GICs can exhibit good longevity for some years, the primary reason for failure was fracture[441]. GICs CS and DTS are relatively low compared to alternatives available, but these cements also have numerous other desirable properties making them more attractive to the clinician over amalgam or composite materials. Increasing the CS and DTS without jeopardising other properties such as hardness, wear resistance, fluoride release (discussed in 1.6.2) and the handling properties is pivotal to the project objectives. The hypothesis relating to the HANFs and HNTs within GICs are as follows:

Hypothesis (H_1): The substitution of HANFs in GICs significantly increases the CS

Null hypothesis (H_0): The substitution of HANFs in GICs does not significantly increase the CS

Or in the instance of the HNTs:

Hypothesis (H_1): The substitution of HNTs in GICs significantly increases the CS

Null hypothesis (H_0): The substitution of HNTs into GICs does not significantly increase the CS

1.10 Thesis Structure

This thesis is separated into 6 chapters. Chapter 2 describes methods and techniques used during the experimental and results gathering during the project. Chapters 3 – 5 describe the three main sections of experimental work carried out, including the synthesis and substitution of hydroxyapatite nanofibres (HANF) into a conventional GIC and the substitution of halloysite nanotubes (HNTs) into a conventional GIC. The final experimental chapter looks at other properties of the HNT substituted GIC such as wear, fluoride release and hardness. Chapter 6 explores future opportunities arising from the project, including additional experiments and research required, industrial scale up and regulatory requirements relating to commercialisation. The appendix includes papers which were co-authored and posters/abstracts from conferences. All references can be found at the end of the thesis before the appendix.

Chapter 2 Methods and Techniques

2.1 Preparation of GIC Powder

All GIC powders were prepared using Diamond Carve™ base materials at Kemdent using the process of ball milling. All controls used in studies were Diamond Carve™ shade A3 lot 24623 unless otherwise stated. Ball milling uses mechanical grinding through impact and attrition to grind particles into smaller particles using solid balls, usually of ceramic or steel. Materials are loaded into a hollow cylindrical unit along with the balls, placed onto its side on rollers and spun for a timed period (Figure 2.1). This type of milling is generally known as tumbling milling and has been popular in the cements, pigments and pharmaceutical industry since the early 19th century where the majority of developmental work occurred in Germany[442]. The first industrial use for this type of ball milling was the grinding of clinker for the cement industry[443] and it has since developed in grinding ores for metal extraction. These mills later developed into tube mills (where the length of the mill equated to more than twice the diameter of the mill) then to conical mills, a cone shaped mill which containing larger balls and smaller balls at opposite ends of the cone and as the powder was ground to smaller particle sizes, it shifted through the cone naturally[442].

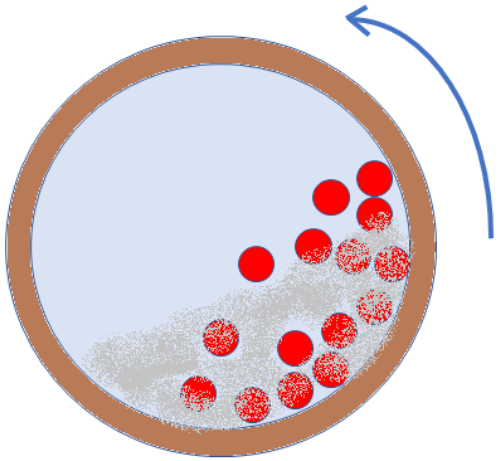

Figure 2.1 – Cross-sectional representation of a tumbling ball milling used to create the GIC Powder. The mill here is rotating in an anticlockwise direction causing the ceramic balls (in red) to impact and grind the powder inside.

All manufacturing, testing and packing was undertaken by the thesis author using established standard operating procedures in place at Associated Dental Products Ltd.

Fluoroaluminosilicate glass was pre-milled at 350 rpm for up to 96 h before sieving through a sub 50 µm mesh to obtain the base powder. The glass powder was then mixed with dried tartaric, polyacrylic and polyvinyl phosphonic acids and added to a ceramic ball mill measuring 240 mm x 220 mm (17 L capacity) filled with ceramic balls of various diameters and milled for 4 h at 350 rpm. The ratios and suppliers of these materials are commercially sensitive and not part of the development of the project, these are therefore not included. The control powder (commercial Diamond Carve™ Shade A3 lot 24623) was tested in-house before being released by assessing the rheology of the setting profile and colour of the final cement when mixed with the GIC liquid according to the instructions for use. The resultant powders were sealed into

plastic bags containing anhydrous silica sachets to retain an anhydrous environment and preserve the powder. Control powders were kept for a maximum of 36 months.

Modified GIC powders were created using either a mixing method or an IKA milling method.

For mixing, a percentage (either 1, 2, 3, 5, 10 or 15%) substituted GIC powder was added to its corresponding material (either HANF or HNTs) and shook vigorously by hand for 10 seconds in a sealed "universal" plastic container measuring 120 mm in length and 25 mm in diameter. These were further mixed on a tube roller (Cole-Parmer, Staffordshire, UK) at 33 rpm for 30 minutes.

For IKA milling, all powders were initially mixed in a tube on a tube roller according to the method described, then 100 (51.9 g) steel balls measuring 5 mm in diameter were added to a 5% HNT substituted GIC powder in a BMT-50-S-M tube (Figure 4.3) and milled at 3000 rpm for 20 minutes using an Ultra-Turrax® tube drive (IKA, Staufen im Breisgau, Germany). The resultant powder was separated from the balls and stored in the sealed tube until use. Powders were milled for 2, 4, 8, 10 and 20 minutes.

2.2 Preparation of GIC Liquid

GIC liquids were also prepared at Kemdent by an addition of dried tartaric acid to a diluted PAA solution. Mixing of the liquid was done by incorporating the dried components into the PAA solution into a plastic container, once combined the solution was mixed by vertically tumbling the container at a speed of 30 rpm for 4 h. A sample of the solution was tested in-house by assessing the rheology of the setting profile by

mixing with a control cement powder (commercial Diamond Carve™ A3 lot 24623) according to the manufacturer's instructions for use. The liquid was stored between 20 - 25°C away from sunlight in a translucent plastic bottle and kept for a maximum of 24 months.

2.3 Cement Preparation

Cements were prepared by mixing the powder and liquid in a ratio of 4:1 by mass except for studies using lower GIC liquid contents where stated in the chapter text[444]. The powder was agitated in the bottle to loosen it and was then mixed by adding one half of the total powder initially by a 'fold and swirl' technique where the powder is folded into the liquid, followed by the circular mixing motion with a stainless-steel spatula on a glass plate. Once the first half of the powder had been added, the second half was incorporated using the same method resulting in a final cement paste. The maximum mixing time did not exceed 60 seconds and all cements were hand mixed in the same way by the same person at a room temperature maintained between 15 - 25°C. The combined cement was then placed into the relevant moulds for either DTS, CS, wear, hardness or fluoride testing to slight excess placed on top of a small sheet of acetate lining a circular steel disc. This was covered with another acetate sheet and steel disc before firmly clamping. The entire unit was stored at 37°C for 15 minutes before removing the mould and 'finishing' the end surfaces using wet 120 grit silicon carbide paper (Kemet International Ltd, Kent, UK). Specimens were then removed from the moulds and placed into a universal polyethylene tube plugged with damp tissue to

maintain a 100% relative humidity chamber and sealed before storing at 37°C for 24 ± 1 h ensuring the cement did not come into direct contact with the tissue. 100% humidity was used to create an atmosphere similar to that in the oral environment.

2.4 Compressive Strength Specimen Preparation and Testing

CS is a method of calculating the maximum force a material can withstand from compression before failure. The method requires a cylindrical specimen of a known volume crushed between two plates, with the top plate moving down onto the specimen held on a stationary bottom plate. The top plate is connected to a load cell which measures the force applied to it from the resistance of the cement according to Newton's third law[445]. Cements were prepared as described in section 2.3 and placed into stainless steel cylindrical moulds (Figure 2.4) of 4 mm ± 0.2 mm diameter and 6 mm ± 0.3 mm height stored at room temperature (20 - 25°C). They were placed between two steel discs lined with an acetate sheet to prevent the cements sticking to the discs. The resultant cements were compressed using an Instron universal testing machine model 3366 (Figure 2.2) using Bluehill® LE testing software (both Instron, Buckinghamshire, UK). Each sample diameter was measured three times and an average taken. A crosshead speed of 0.5 mm/min was used with a load cell of 10 kN (in line with the ISO and other studies[278,446]) and the samples compressed to failure. The maximum force of each sample was recorded and used to calculate the CS (in MPa) using Equation 2.

Equation 2 - Formula to calculate compressive strength

$$CS = \frac{4 \text{ x } Fmax}{\pi \text{ x } r^2}$$

Where Fmax is the maximum force applied at fracture, π is the mathematical constant equal to 3.14 and r is the average radius calculated from three measurements.

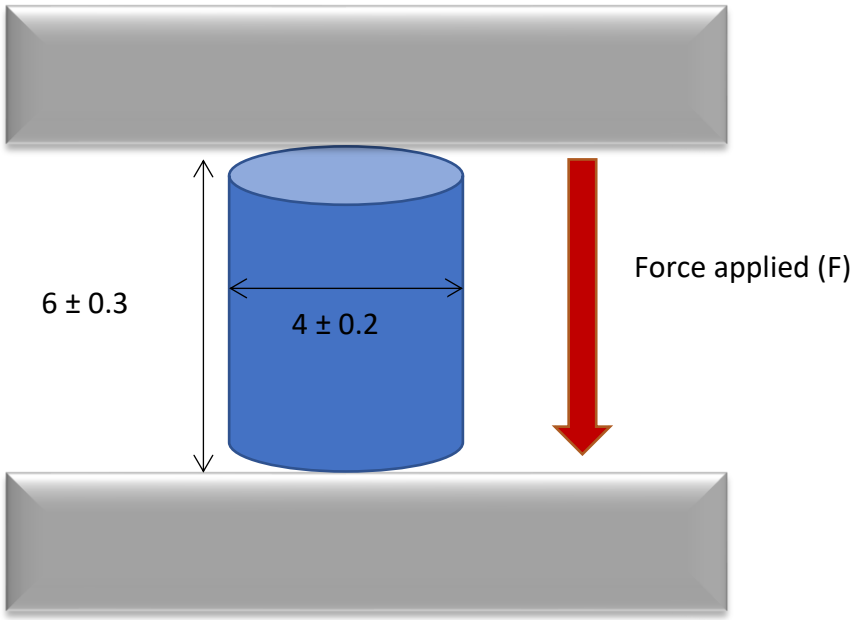

Figure 2.2 - CS specimen orientation and testing

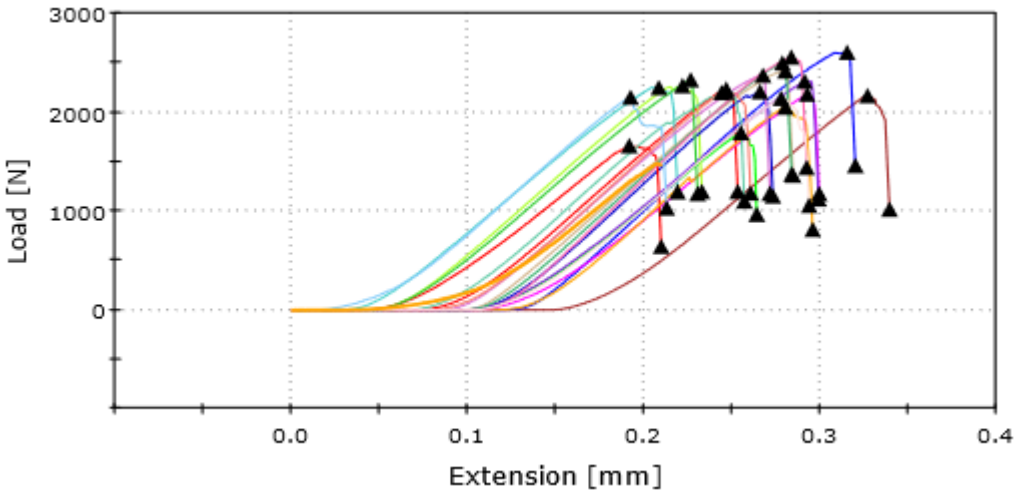

Figure 2.3 - Typical force displacement graph for CS testing. Forces up to 3000 N were exerted onto the GICs. Each curve is one individual specimen which was compressed to fracture.

2.5 Diametral Tensile Strength Specimen Preparation and Testing

DTS works in a similar principle to CS in that it uses compression to calculate the strength of a material. However, DTS measures the resistance of the material to tensile forces, which is much lower than the compressive resistance of a GIC. Cylindrical specimens of 6 mm ± 0.3 mm diameter and 4 mm ± 0.2 mm height made in steel moulds (Figure 2.4) were compressed to failure across the diameter (Figure 2.5) using an Instron universal testing machine at a crosshead speed of 0.5 mm/min using a load cell of 10 kN. Each sample diameter was measured three times and an average taken. The maximum force of each sample was recorded and used to calculate the DTS in MPa using Equation 3.

Equation 3 – Formula to Calculate Diametral Tensile Strength

$$\mathrm{DTS} = \frac{2\ \mathrm{Fmax}}{dh}$$

Where *Fmax* is the maximum force applied at fracture, *d* is the average diameter of the specimen calculated from three measurements and *h* is the height of the specimen.

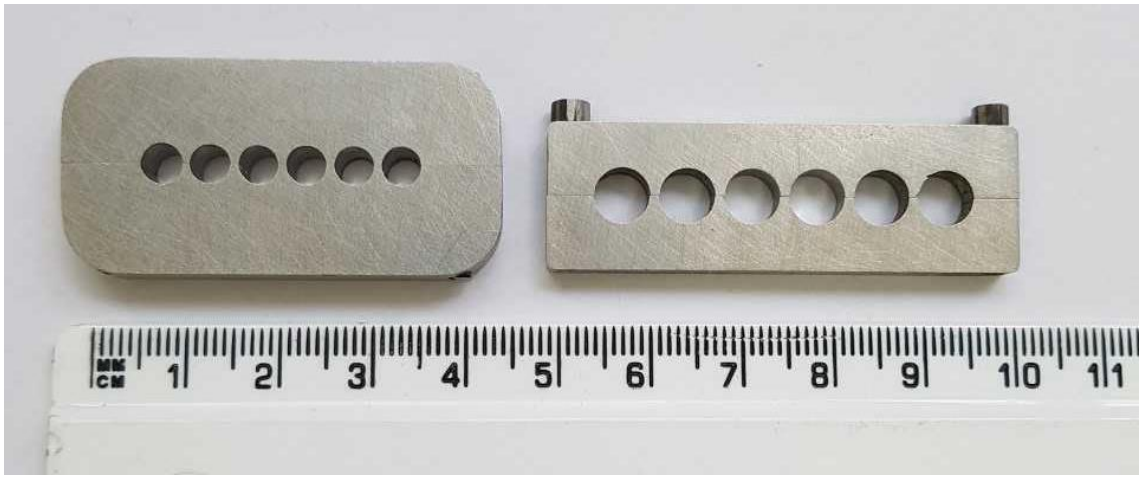

Figure 2.4 - CS (Left) and DTS (Right) specimen moulds after they have been prewashed and air blasted clean

Moulds were prewashed before each use by placing them into warm deionised water in an ultrasonic bath for 5 minutes, dried at 37°C for 1 h and air blasted prior to use. The moulds were visually inspected for any surface defects or remaining debris before use.

The specimen is placed onto its side and compressed as shown in Figure 2.5.

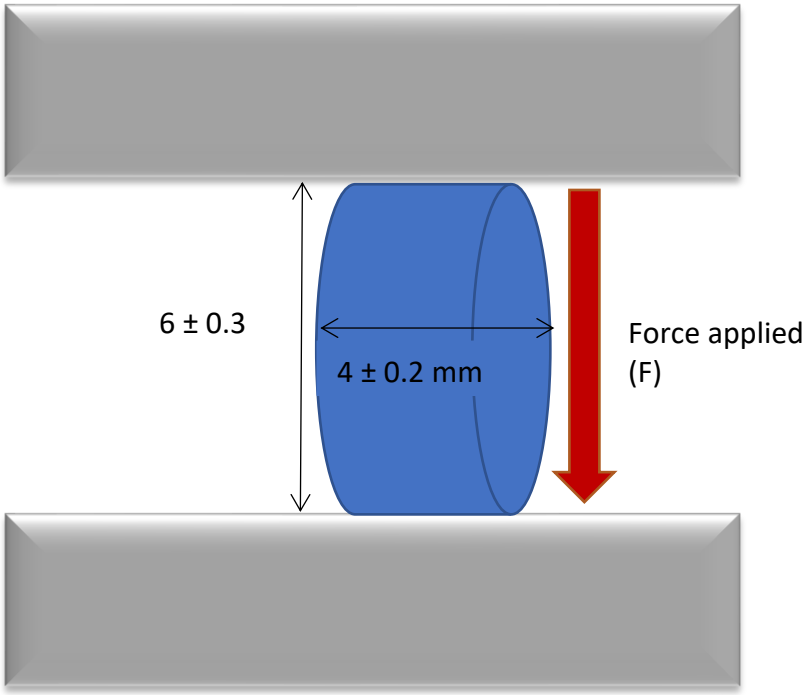

Figure 2.5 - DTS specimen orientation and testing

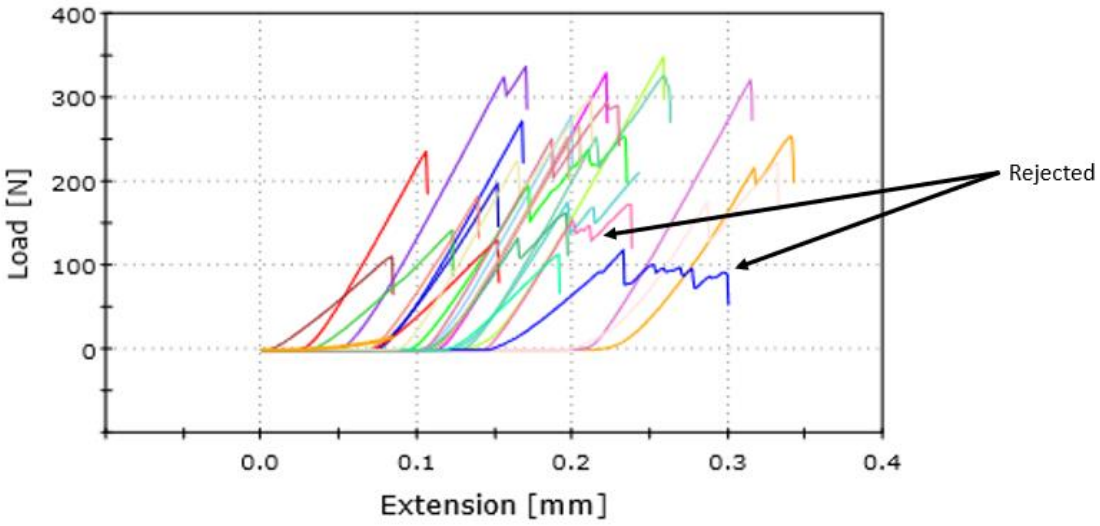

Figure 2.6 - Typical force displacement graph for DTS testing. Examples of rejected specimens due to their break behaviour are highlighted. Each curve is one individual specimen which was compressed to fracture

2.6 Synthesis of Hydroxyapatite Nanofibres using a Modified Reflux Condensation

Reflux condensation is used in many industrial and laboratory processes as a means of heating a solution while retaining the solvent through continuous condensation of the vapour given off. The reactants are placed into a round bottom flask, usually dissolved in a solvent, then connected to a condensation column (Figure 2.7). The column contains an inner and outer wall, between these a continuous flow of coolant (usually water) is circulated around the inner column walls countering the direction of the vapour, cooling the vapour and thus condensing this back into its liquid form. The condensed solvent falls back into the round bottom flask returning to the original mixture; therefore, no solvent is lost by evaporation. The round bottom flask can be heated by several ways, rarely is a flame ever used due to the uneven heating and potential volatility of solvents, reagents or resultant compounds within the mixture. Solutions requiring exceptionally high temperatures are usually placed into an oil or sand bath, however usually the flasks are contained in water baths or heating mantles. These offer the advantage of even and continual heating without exposure to a flame. Heating mantles usually incorporate a magnetic stirrer to ensure continuous mixing of the solution to optimise the reaction. However, the process is expensive to run, and lab-based set ups often involve running water through rubber tubing into the condensation column before disposing of it immediately down the drain via another set of tubing. In industry, reflux is generally used to separate mixtures of hydrocarbons or solvents by using condensing plates throughout the column. These systems cool the

columns using highly efficient recirculated coolants such as polyethylene glycol which are pumped back through cooling units in a continuous loop. To create an efficient and economically viable synthetic process, a Findenser™ (R. B. Radley & Co., Essex, UK) was used as a replacement to the condensation column (also Figure 2.7). The Findenser™ is a glass column with an internal glass compartment surrounded by an external 'finned' aluminium jacket. Between these two layers is a static permanent layer of water acting as a conducting heat transfer solution from the inner glass walls and the outer aluminium fins[447]. The overall result of this created a 'green' synthetic and reproducible method without the loss of any water through cooling the vapour.

Prism like nanorods have previously been created from commercially available HA powder through a relatively simple process involved dissolving the powder in an acidified solution and precipitating out new HA in at various temperatures over the course of a few days, the rods were in bundles of 10-20 nm in width and 100-200 nm in length[448]. Similarly to this a novel synthesis first created their own HA from a calcium and phosphate source, along with gelatine and urea they were able to create fibres of 100 nm diameter and 60 – 80 μm in length through a one pot simple synthesis, the advantage of this was that no extra steps were needed until filtration and the materials were dissolved into water and heated to 95°C for 72 h, a method replicated and modified here.

HANFs were made by dissolving calcium nitrate (0.02 mol/L), sodium dihydrogen phosphate dehydrate (0.02 mol/L), gelatine (0.4 g/L) and urea (0.04 mol/L) (Sigma, Gillingham, UK) in deionised water and heating to 95°C for 72 h (summarised in Figure 2.8). The resultant suspension was filtered through a Buchner funnel lined with nylon

0.45 µm filter membrane (GVS Group, Bologna, Italy), washed with 3 x 15 mL of deionised water and dried at 37°C for 24 h[374]. The resulting fibres were stored in a sealed glass jar in a desiccator until required. These were characterised by SEM, transmission electron microscopy (TEM), Fourier transform infrared spectroscopy (FTIR) (to ensure they were dry) and x-ray diffraction (XRD) spectroscopy. The synthetic method of HANF chosen gave approximately 0.5 – 1.0 g of product for a 250 mL solution.

Figure 2.7 - Reflux condensation set up to synthesise the HANFs. Image shows both the original method using a water fed cooling tube (left) and a 'greener' method using a Findenser™.

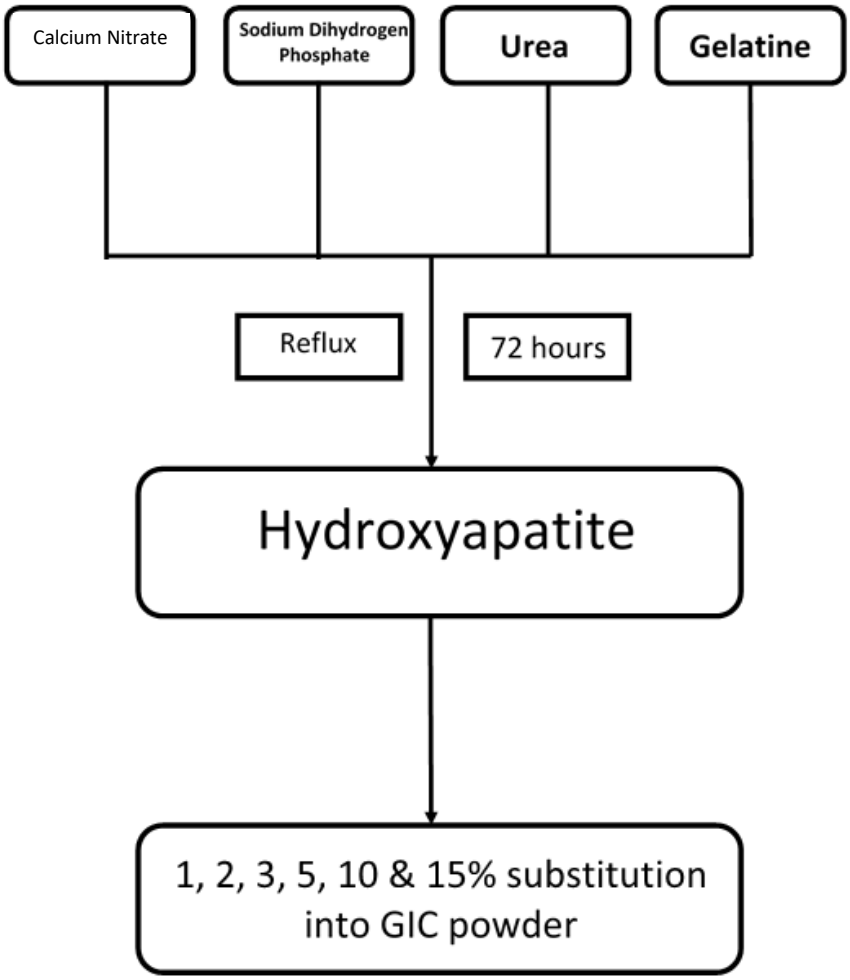

Figure 2.8 - Reflux Condensation Method

2.7 Acid Stability of HANFs

HA is known to be soluble at pH values as high as 5[449] gradually breaking down from the surface[450]. This process is seen in the dissolution of enamel through the acids produced by carbohydrate metabolising bacteria in dental plaque and has shown to dissolve a much wider range of calcium phosphate salts, including HA[451]. pH within GICs is well studied and has been shown to reach as low as around 1.5, rapidly rising to a pH of 4 within 15 minutes before slowly rising to a pH of 5-6 within a 24 h

period[78,452,453] therefore any additives to the cement powder or liquid would likely experience these conditions too. To simulate the initial and harshest conditions of the GIC setting pH, fibres were dipped into a pH 2 solution for 15 minutes to assess the acid stability on HANFs with and without polyethylene glycol (PEG), as well as HNTs. The powders were fixed onto a sticky pad used on an SEM stub and the excess shaken off until visibly fully covered, the stub was then clamped and lowered into a pH 2 dilute hydrochloric acid (HCl) solution covering one half of the powder-coated stub for 15 minutes to replicate the time that the GIC would be at this range of pH, shown pictorially in Figure 2.9. It was noted that while corrosion of the SEM stub may occur, this was not subjected to analysis and acted as a platform to hold the fibres. The solution was made using 0.1M HCl and diluting this with deionised water until pH 2 was achieved. pH readings were taken using a pH probe model EC620131 connected to an Orion 3-star benchtop pH meter (Thermo Fischer Scientific, Massachusetts, USA). The whole stub was then immersed into deionised water to quench the reaction, dried at 37°C for 24 h and imaged using optical microscopy and SEM.

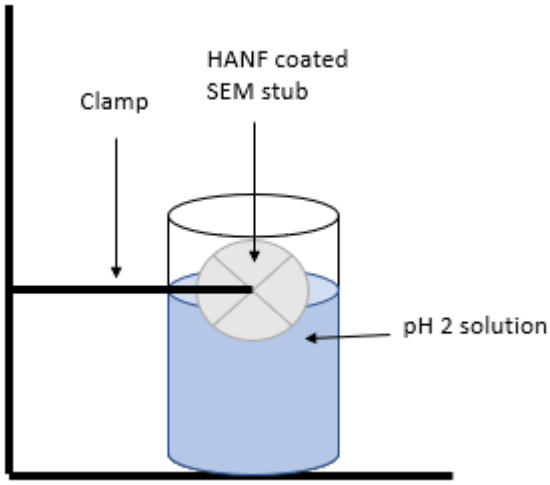

Figure 2.9 - Set up of acid dipping a SEM stub covered in the HANFs

2.8 Spectroscopy

2.8.1 Fourier Transform Infrared (FTIR) Spectroscopy

FTIR is a tool to help establish the chemical structure of a material and its molecules. An infrared source (usually a nickel-chromium wire) is directed through a collimator which directs the beams towards the interferometer consisting of a beam splitter, a fixed mirror and moving mirrors which reflect the beam back. The beam then further splits half of the radiation back to the source while the other half moves through the chamber where the sample is held[454], this is represented in Figure 2.10. Molecules vibrate or rotate when IR radiation is passed through them and the type of vibration is dependent on the expansion or contraction of the bond between individual parts of the molecule. Vibrations can occur in the form of 'stretching' (the change in bond length) or 'bending' (the change of the bond angle)[455]. These outputs from the bond vibrations are unique to each molecule, the resultant spectra can be analysed against

the known molecular bend or stretch at a wavelength. All FTIR was undertaken on a Spectrum 100 (Perkin Elmer, Massachusetts, USA) with a scan range between 400 – 4000 cm^{-1} with the average of three scans being used, bands were individually assigned using reference tables within a textbook[456] and other published spectra. The powder was placed onto a blanked stainless-steel disc, the detector was positioned to the correct height according to the indicator on the machine and scans were taken between 20 - 25°C.

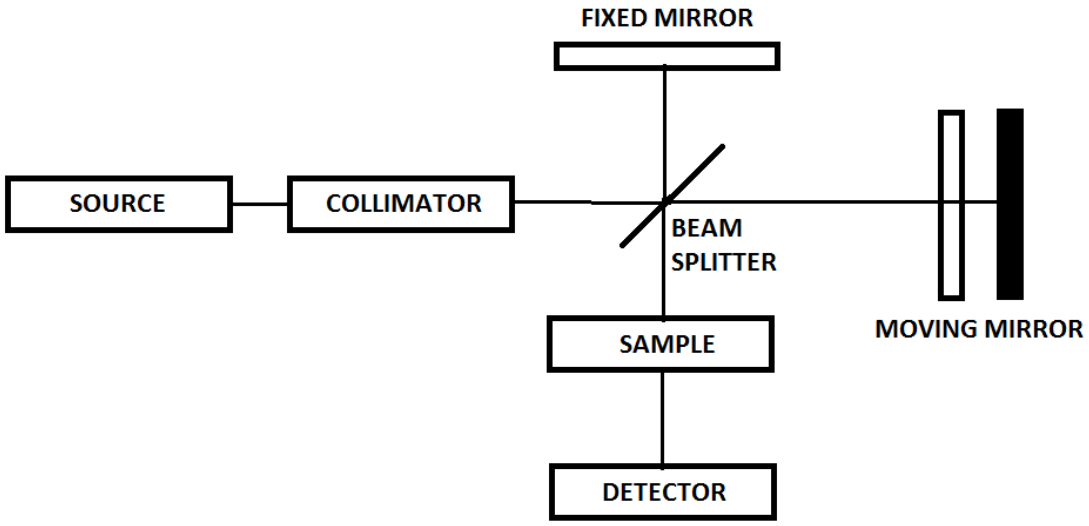

Figure 2.10 - A block diagram of a FTIR. The detector will often be linked to a computer or other visual output where the Fourier transformation takes place to convert the detector output into a visible spectrum.

2.8.2 X-Ray Diffraction Spectroscopy

Crystal structures of a material can be determined by passing x-rays of a comparable to interatomic distances through a sample and analysing how the beam is diffracted.

Powder XRD was used on samples collected on a plastic holder and x-rays projected (usually produced from a copper source) over a range of angles with respect to a detector on the opposite side of the sample. As the radiation hits the sample, the rays are scattered by the electrons of the atoms that make up the material. Some of the x-ray photons interfere coherently to give a 'reflection' on a detector according to the Bragg equation (Equation 4).

Equation 4 - The Bragg Equation describing the relationship between constructive diffraction and the interatomic distances of the lattice planes. Where λ is the x-ray wavelength, d_{hkL} is the interatomic spacing for a crystallographic plane and θ is the angle of incident radiation

$$\lambda = 2\mathrm{d}_{\mathrm{hkL}} \sin\theta$$

An XRD pattern produced is a plot of the reflected radiation intensity against the incident angle. Most common materials now have a 'fingerprint' spectrum stored in a database which can be used to identify the crystalline structure in question[457].

All XRD was carried out using a Bruker D8 Advanced Powder X-ray Diffractometer (Bruker Cooperation, Massachusetts, USA) with Cu Kα radiation (λ = 1.54 Å) at 2θ values 5-70 or 5-85 with a step size of 0.1°.

2.9 Microscopy

2.9.1 Optical Microscopy

Optical microscopy uses one or more lenses to magnify an image, generally using a halogen lamp or light emitting diode (LED) while some of the more basic models use natural light on a mirror. Most modern optical microscopes are designed as compound microscopes, these magnify an object in two steps, the first magnifies the actual image between the single and double focal points generating an image much larger than the original, but not as focussed. Finally, this image is picked up just in front of its focal point through a second lens, creating a parallel beam of rays which reaches the eye piece and subsequently the retina[458].

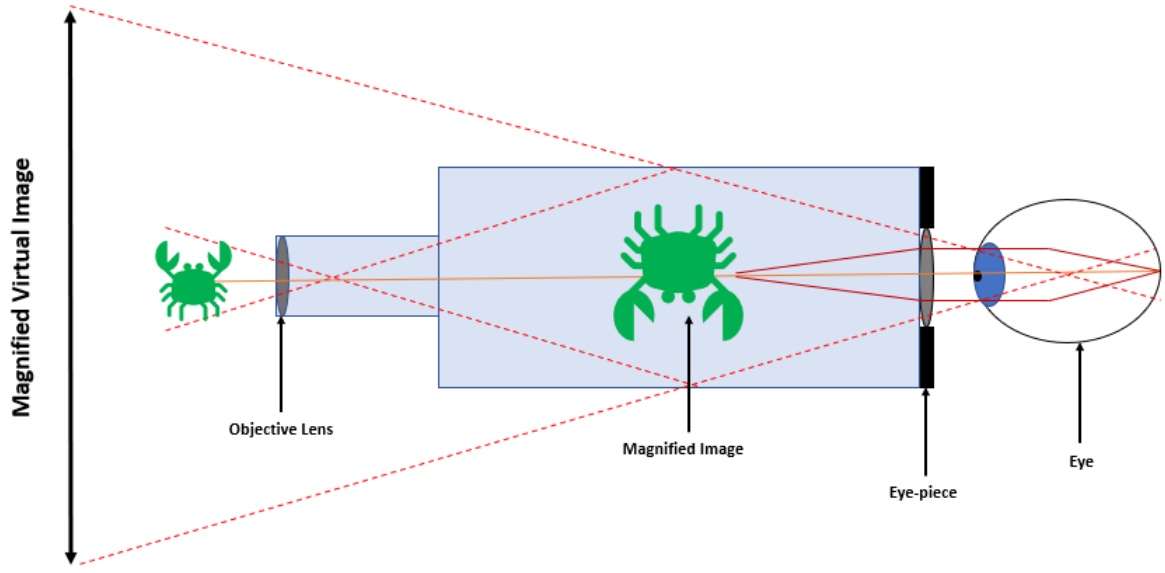

Figure 2.11 - Pictorial representation of how a compound optical microscope creates a magnified image. Image adapted from[458]

Optical microscopy was carried out using a Leica DMLB Type 020-519.502 (Leica Microsystems, Wetzlar, Germany) using x 4 magnification. For fluorescence microscopy a ColourView Lamp (Olympus Cooperation, Tokyo, Japan) was used with a wavelength filter of 520 nm. For these, HNTs were dyed using acridine orange, a dye traditionally used for cytology and tissue culture[459,460]. Presently, the dye is still well used in various applications such as labelling DNA[461], photodynamic therapy of cancer cells[462] and the detection of HIV[463] due to its effective fluorescent staining properties[464]. Details regarding the acridine orange dying methodology can be found in chapter 4 section 4.2.2.

2.9.2 Scanning Electron Microscopy

SEMs consists of a high-powered electron generating and accelerating system known as the electron gun, a high vacuum, a focussing and scanning system, a specimen stage, an electron detector/multiplier, amplifiers and a form of photograph or visual imaging (connected as shown in Figure 2.12). The electrons are generated by a primary cathode, usually made of a tungsten filament, which is then projected through a charged cylinder with a slightly more negative potential than the cathode to focus the electron beam. An anode plate, approximately 2 cm below the cathodic filament tip helps to generate a potential difference of between 1-50 kV thus creating an accelerating voltage to aim the electron beam at the specimen[465]. Unlike TEM, SEM electrons do not penetrate the specimen but cause electrons from the atomic surface to be released. These secondary electrons reach the detector and are translated into

an image[466]. In all specimens described/reported within this thesis, the specimens were thoroughly cleaned using compressed air and sputter coated with gold twice for 90 seconds before placed into the Phenom Pro SEM (Phenom World, Eindhoven, Netherlands). Optical images were analysed using x 2 magnification, other SEM magnifications used have been described in the image captions.

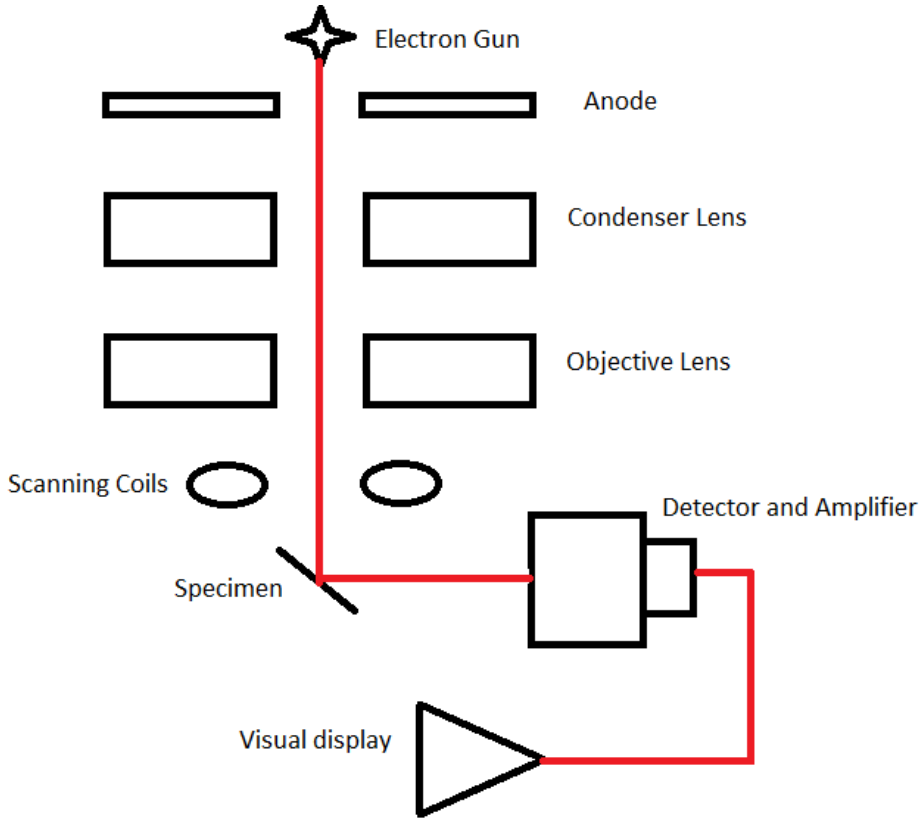

Figure 2.12 - Block diagram of a SEM. The red line shows the path of the electron beam as it is focused and accelerated through the lenses to the specimen

2.9.3 Transmission Electron Microscopy

Modern TEMs consist of three electromagnetic lenses: an objective lens, an intermediate lens and a projector lens (Figure 2.13). An electron beam, usually sourced from a tungsten filament, is projected and accelerated into the sample before passing through these three lenses in turn before the diffraction pattern appears as an image on a fluorescent screen[467]. The electrons ejected are accelerated by a 120 keV potential difference towards a hallow anode before entering a condenser system where the beam is de-magnified, and the diameter and convergence angle are controlled to create a higher resolution image. Lens aberrations like astigmatism are corrected by altering the magnetic field of the objective lens before the image is magnified 50-100 times using an array of various other projector lenses. Samples are placed onto a small copper grid coated with a thin carbon or polymer film; these produce a dense electron image on the phosphorus screen[457]. All TEM, except those of the HNTs provided by Durtec GMbH (Neubrandenburg, Germany), were performed on samples on a carbon coated copper-gold grid (Agar Scientific, Stansted, UK) using a JEOL JEM 1200 EX1 TEM (JEOL Ltd., Tokyo, Japan) machine.

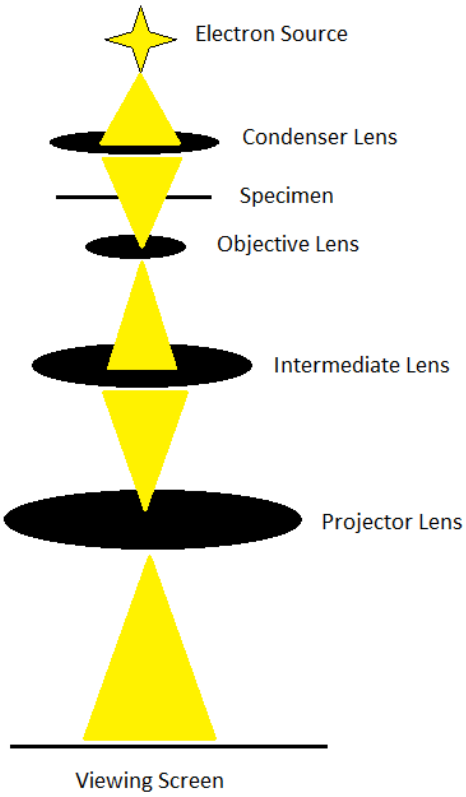

Figure 2.13 - Schematic of a TEM showing the electron beam (in yellow) as it projects and accelerates through the various lenses. A condenser lens in front of the electron source concentrates the initial beam towards the sample surface

2.10 Other Techniques

2.10.1 Working and Setting Times

The working and setting time of a GIC can be measured using the ISO 9917-1:2008 method which defines working time as the time from the start of mix when the cement can no longer become manipulated without having an adverse effect on its properties[446]. Additionally, the standard assesses setting time using a weighted indenter placed onto a block of setting cement, the setting time is reached when the

needle fails to make a complete circular indent under 2 x magnification[468]. Clinically, the working time is met when the cement becomes difficult to mix, while the setting time is when the restoration can be polished, carved or varnished. The differences between the technique sensitive ISO testing and clinical application have led others to use different methods of evaluation, including rheology, a technique used long before the creation of the standard[49,469]. The cement is mixed according to the technique described in section 2.3 and placed onto an ABB SE120 Wilson's Oscillating Rheometer (ABB, Zürich, Switzerland). The cement is placed onto two aluminium grooved plates separated by 1 mm (shown in Figure 2.14). The lower plate oscillates clockwise at a rate of 6 seconds per oscillation and as the cement sets, the oscillations of the bottom plate are reduced which is displayed graphically over time. A pen moves 95% of the length of the graph papers at t = 0 and the paper moves down at a rate of 1 cm per minute, the cement is considered set when the distance covered is 5% of t = 0. The working time is calculated by when the oscillation begins to reduce below 95%[470]. A typical output graph is shown in Figure 2.15.

Figure 2.14 - Aluminium plates of the Wilson's Oscillating Rheometer. The mixed cement is placed onto the grooved surface of the top plate (left) before securing onto the oscillating bottom plate (right)

Figure 2.15 - Example setting profile graph from a Wilsons Oscillating Rheometer

2.10.2 Fluoride Release of GICs with and without Halloysite Nanotubes

Fluoride is well known to be released from GICs when in an aqueous environment[64,313,314,471-473] and to detect ions such as fluoride in solution a fluoride ion-selective electrode was used. Ion-selective electrodes have been used since 1906 to detect hydrogen ions to calculate the pH of a solution. Since then various other electrodes have been developed to detect ions including cadmium, bromide, fluoride etc. and even gases such as nitrogen oxide, carbon dioxide and ammonia. They work on the principle of a galvanic cell containing a reference electrode, ion-selective membrane and voltmeter. The reference electrode contains a stable and constant potential while the ion-selective electrode measures the potential difference between

the high concentration solution and the low concentration electrode binding sites which can then be calculated through calibration of the metre against known concentration standards[474]. All solutions and equipment for fluoride testing were obtained from Thermo Fischer Scientific unless otherwise stated. Fluoride containing solutions were analysed using an Orion 96-09 ionplus® fluoride selective electrode connected to an Orion 4 Star pH/ISE benchtop digital unit. Solutions were mixed for a minimum of 5 minutes with Orion ionplus® Total Ionic Strength Adjustment Buffer (TISAB) II containing 1,2-cyclohexane diaminetetraacetic acid (CDTA) in a 1:1 ratio using a magnetic stirring bar before fluoride testing. The role of the buffer was to stabilise the pH and ionic strength of the solution as well as hydrolysing fluoride ion pairs to form all available free fluoride for detection. Before testing, the electrode was calibrated using diluted solutions of 1000 ppm fluoride standard solution lot 0652 (Hanna Instruments, Rhode Island, USA). All specimens analysed were identical to the size described for DTS testing (section 2.5) with a surface area of 132 mm^2. Cements were mixed and stored according to the method described in section 2.3 after which they were added to 20 ml of deionised water (stored at 37°C for 24 h prior) and stored at 37°C for 1, 2, 3, 7, 14, 21 and 28 days. The cement was removed at each time point and placed into 20 ml of fresh deionised water (also stored at 37°C for 24 h prior). After the final time point, the cement was removed from the deionised water and discarded. Solutions were stored at room temperature alongside all equipment for a minimum of 24 h before testing and all fluoride measurements (including calibration) were made on the same day by the same individual.

2.10.3 Wear Testing

Wear can be categorised in many ways such as abrasive, fatigue, mechanical or adhesive wear. Abrasive wear is achieved by friction onto a surface when the surface of one of the materials is harder than the surface of the other[475]. Wear resistance is an important property of most biomaterials and is a good indicator of resistance to everyday stresses. Various methods of wear testing have been documented, including hip simulation[476] according to ISO standards[477], rotational knee simulations[478], two body or three body wear[479], finger-simulated wear[480] and even computer simulated testing[481]. Historically, when testing wear, it is important that the method chosen correlates with the clinical situation[482]; for dental materials it is widely accepted to use toothbrushing as a form of wear[483-485] as this is the most abrasive force applied to a dental material in regular occurrence. For wear studies, an in-house tooth brushing machine using a linear motion arm connected to a motor was used. Cement specimens measuring 6 x 8 x 3.2 (± 0.1) mm were prepared according to the method described in section 2.3 in a silicone mould and covered across one half of the exposed surface using a polyvinyl chloride (PVC) tape (Figure 2.16) and immersed into a small bath containing 500 mL of 19.1 mM citric acid pH 3.3 solution made using the method described from Barbour et al.[486] by mixing citric acid powder (Sigma) with deionised water. These were then brushed with Colgate® medium extra clean toothbrush heads (Colgate Palmolive, New York, USA) affixed using Kemdent sticky (Figure 2.16) wax for a defined number of brush cycles. When the brushing had finished, the specimens were immediately immersed and rinsed in deionised water for 30 seconds before imaging to prevent any further acid erosion to the surface. All covering PVC tape was

removed and the cements were imaged within 1 h of testing using a Scantron Proscan 2000 non-contact profilometer (Scantron Industrial Products Ltd., Taunton, UK). Any specimens where the PVC tape had either been partially or fully lost or dislodged during the brushing process were discarded. All solutions of used or unused citric acid were also discarded after the test was complete. The method was initially created using deionised water and artificial saliva[314] but failed to produce any significant wear, therefore a harsher acidic environment was used, this data was reported in Table 5.2.

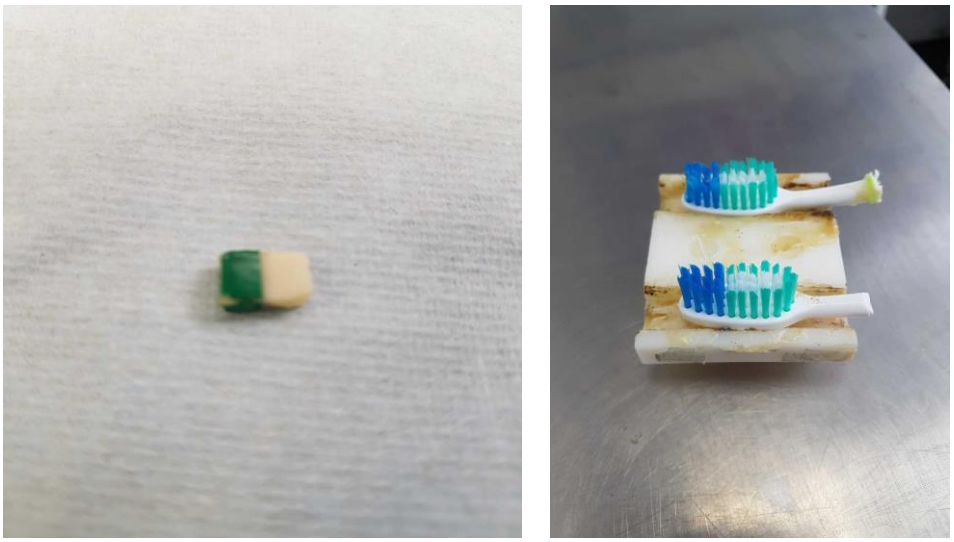

Figure 2.16 - GIC specimen prepared for wear testing (left). Half of the specimen is covered by green PVC adhesive tape to protect the surface against brushing. This provides an untouched control side to the specimen. Toothbrush heads are affixed into a PVC unit using sticky wax (right).

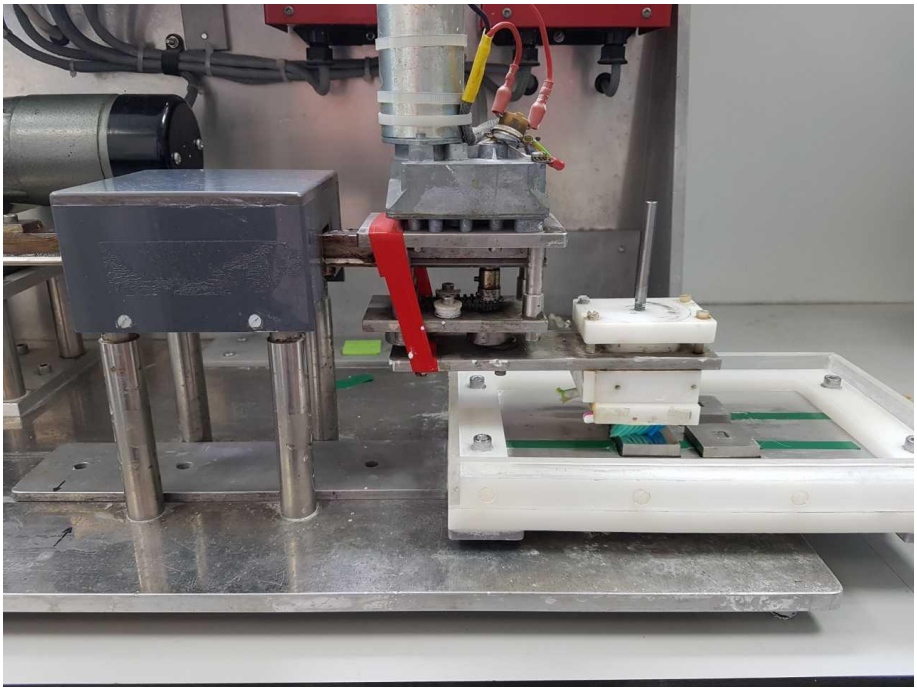

Figure 2.17 - Toothbrush machine set up. Specimens are held in steel moulds in a bath containing citric acid. Fixed brush heads are moved horizontally across the specimens for a known number of cycles

2.10.4 Optical Profilometry

Optical profilometry is a non-contact, non-destructive (to materials not sensitive to light) technique using a beam of light to measure the three-dimensional cross section of a material, most often used to measure differences in height[487]. Light emitted from a source is split, one half travels down towards the specimen while the other half travels down a reference path of known distance. The reflected light off the specimen and the reference light are collected at a detector after they recombine creating a phase difference and therefore interference pattern between them. These interference fringes can be measured and the difference in height calculated thus

creating a ‘map’ or image of the specimen topography. Optical profilometry was used to assess roughness and wear of specimens using a Proscan 2100 machine with a Scantron PSU module, the camera used was a S65/9.5 connected to a chromatic confocal sensor (CHR 150-L) (Scantron Industrial Products Ltd.). Before analysis, background light intensity readings were taken to subtract these from the final scan. Cross sections of 2.0 mm x 4.00 were analysed using a step size of 0.01 mm and the resultant scan (Figure 2.18) was analysed by comparing the height of the two corresponding sections in a two-step analysis using the Proscan 200 software.

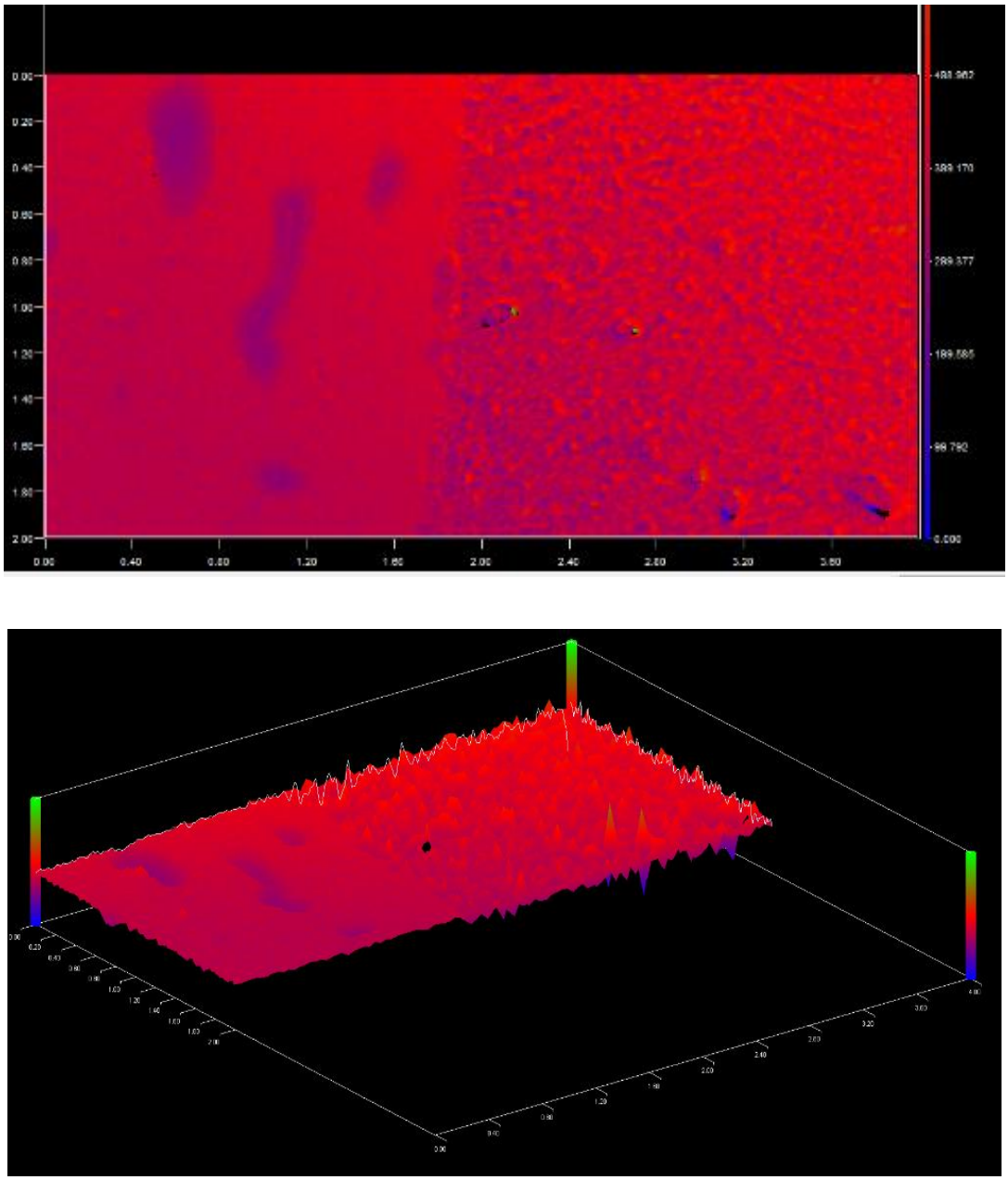

Figure 2.18 - Example non-contact profilometry scan showing a smooth covered area of the cement (left) and a rough uncovered area from brushing (right)

2.10.5 Hardness Testing

As discussed in chapter 1 section 1.4.10, hardness testing is a relatively simple and non-destructive technique. The information obtained shows a strong correlation to the

strength of the material[488] and can be tested several times on a larger specimen such as those used in the wear testing. Cement specimens measuring 6 x 8 x 3.2 (± 0.1) mm were prepared and stored according to the method and times described in section 2.3. These were fixed flat using stainless steel grips and tested for microhardness. Microhardness was tested using Duramin 1 indenter fitted with a Vickers diamond tip (Struers, Rotherham, UK). A force of 1.961 N was applied to the cement for 20 seconds at temperatures between 20 - 25°C and indentation measurements were made using a x 40 lens CCD camera (Toshiba-Teli Co., Tokyo, Japan) by measuring the cross-sectional lengths of the indentations. This force was chosen through trial and error using various loads on the equipment, 1.961 created the most uniform indentation. Once measured, the VHN was calculated automatically by the software within the unit. Two samples of each cement were made on three different days (6 samples of each group) and 10 indentation measurements were made randomly on each, five on each side of the cement, no specific distance was measured but an attempt was made to test most sections of the surface. Any indents made on a pore or surface imperfection on the cements were rejected and the test repeated.

2.10.6 Particle Size Distribution

It is rarely useful to measure the size of one particle in a sample as a means of estimating the size of particles in a batch, often a range of particle sizes are present. Simple methods such as sieve analysis is ideal for use with large samples and particle sizes greater than around 50 µm, the technique was historically used in soil

analysis[489,490]. The technique uses different mesh (aperture) sieves stacked on top one another in descending mesh size, these are then rapidly oscillated to move the powder through the tower of sieves. The resultant powders in each sieve is converted to a percentage of the overall mass giving a discrete data range of particle sizes[491]. As previously discussed, TEM and SEM methods are useful in assessing individual particle sizes, providing a visual and accurate measurement of the material but is often limited by depth of focus at smaller sizes due to the diffraction effect and are unable to practically give a range of sizes alone[492]. Other methods include light scattering techniques such as dynamic light scattering (DLS)[493] and electro-resistance methods such as Coulter counter technique[494]. Laser diffraction was developed in the 1970s[495,496] and works by detecting the scattered laser light in the forward direction after they hit a particle. This pattern of diffracted light is Fourier transformed, often by computer in modern systems, to calculate the diameter of the particle hit. The laser passes through a beam expander to generate a monochromatic, coherent, parallel beam having a diameter of a few mm which passes through the sample before being focussed by a Fourier lens onto a detector which measures the intensity of the original or remaining light beam and the intensities of the scattered light by the particles at different angles[497]. The light scattering technique laser diffraction (Figure 2.19) was used in all particle size distribution tests, these were undertaken under contract by Dr Xu Cao (Technical Manager, James Kent Group, Stoke-on-Trent, UK) using a Malvern Mastersizer 2000 (Malvern Instruments, Malvern, UK) on one powder sample extracted after 2, 4, 6, 8, 10 and 20 minutes of milling using the technique described in chapter 3 section 3.2.3.

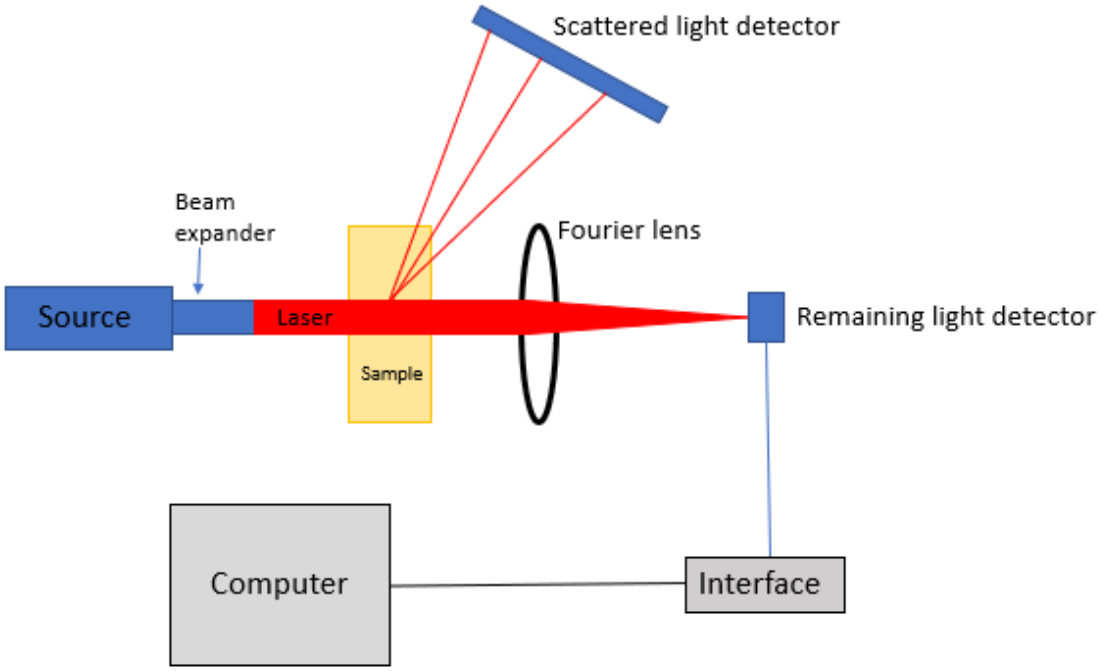

Figure 2.19 - Block diagram of a laser diffraction analyser. Laser light is passed through a sample and diffracted wave are compared against the residual light. Fourier transform is applied to convert the data into particle sizes

2.11 Statistical Analyses

Data was statistically analysed using Excel 2010 (Microsoft, New Mexico, USA) for any statistical difference using paired t-tests to analyse differences between each independent group vs the control. Groups statistically different from the control were marked with an Asterix. Data consisting of two groups only were analysed using a student t-test also using a significance level $p < 0.05$.

Chapter 3 Investigation of Hydroxyapatite Nanofibres as Reinforcing Agents for Glass Ionomer Cements: Synthesis, Analysis and Testing

3.1 Introduction

Previous studies indicated strength increases across various dental restorative materials with the addition of nano and micro fibrous materials[212,274,374,411]. Building on these observations, the HA was chosen as a potential material to increase the strength properties of the GIC. The rationale for the choice of HA, listed in order of importance, was based on:

- The fact that HA forms very high aspect ratio nanorods or fibres which, it is seen from earlier studies, are favourable particles for reinforcing related materials (chapter 1, section 1.5.1.3)
- The biocompatibility of HA (chapter 1, section 1.5.1.3)
- The relative ease of synthesis and the fact that this can be scaled for industrial manufacture (chapter 2, section 2.6)
- The inexpensive starting materials required
- The biocompatibility and biological ubiquity of the breakdown products should the HA degrade *in vivo*.

HANFs were synthesised using a modified reflux condensation method described in chapter 2 section 2.6 and analysed with various amendments to the method to determine their composition, size and shape. As a method of protecting the fibres from acid attack, HANFs were synthesised with and without PEG and assessed for their acid lability. It is well documented that GICs undergoes pH conditions of between 1 and 3 for approximately 10 minutes before neutralising over the course of several

weeks as the setting reaction continues[498-500]. Apatite fibres with a high aspect ratio and thus high surface area are more susceptible than particles/agglomerations to acid attack due to the greater number of exposed hydroxyl sites[501]. Due to these two factors, the effects of the low pH conditions on the hydroxyapatite was examined to assess the extent of acid mediated dissolution and the effect on the HANFs within the GIC. PEG 300 and PEG 600 (relating to the average molecular weight) were added in a 1% w/w concentration to the reaction vessel to create a protective coating as it has been reported to adhere to the surface of crystalline structures[502-504] in a similar process to many different types of cationic and anionic surfactants which can protect against this acid attack[505-507]. 1% concentrations were used as previous studies showed concentrations higher than this can adversely affect the morphology of the HA to form spherical particles[508]. The use of PEG as discussed previously creates a 'protective coating' of the fibres leading to some resistance to the proton attack[503,504]. PEG was chosen because of its wide commercial availability, low cost and low toxicity. In solution, PEG molecules become highly mobile with large exclusion zones free of charges which reduce the interaction between other constituents[509]. In aqueous solutions, the PEG-OH bond (Figure 3.1) is formed which can chelate free Ca^{2+} ions which then react with free phosphate in solution to form the hydroxyapatite (Figure 3.2)[508]. SEM was conducted on the resultant fibres and these were then incorporated into the cements via a 5% substitution before testing for their CS. As no concentration of HANFs increased the CS, 5% was chosen as a reasonably varied CS value from the commercial control to assess what effect PEG would have directly on the fibres. HANFs

with and without PEG coatings were incorporated into the GIC and the impact on CS and DTS parameters assessed.

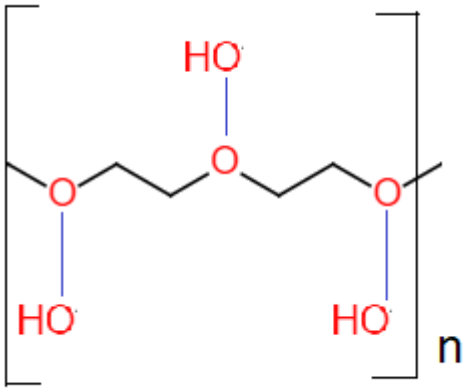

Figure 3.1 - PEG polymer in solution forming the PEG-OH bond represented by the blue bond lines

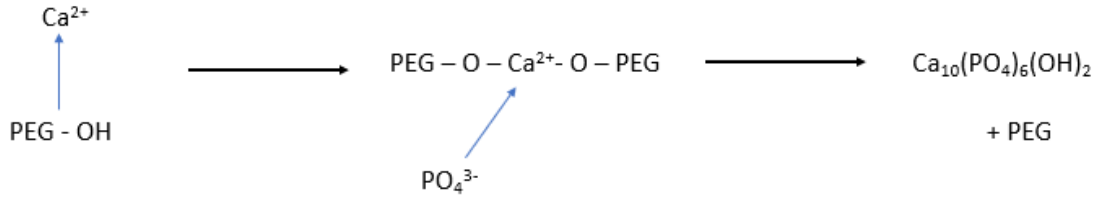

Figure 3.2 - PEG-OH creates an intermediate with the calcium ions to help form the HA

3.2 Materials and Methods

3.2.1 Synthesis of HANFs using a Modified Reflux Condensation

HANFs were synthesised using a reflux condensation reaction equipped with a Findenser™ and modifications to the synthesis made as previously described in chapter 2 section 2.6. Modifications were made to determine the effect on the morphology of the HA assessed using SEM. These included:

- Reflux time (24, 48 or 72 h)
- Effect of gelatine (presence or absence)
- Effect of urea (presence or absence)
- Effect of surfactant (1% w/w PEG 300 or PEG 600)

The PEG additions were made by dissolving the solutions (1% w/w) into the solvent before the other components were added. The solutions were otherwise processed in the method previously described in chapter 2 section 2.6. PEG was only used as an additive to all other materials present. When the effects of urea or gelatine (presence or absence) were assessed, PEG was not involved in the reaction mixture.

3.2.2 Analysis of HANFs

Powders manufactured using all the reagents and refluxed for 72 h were chemically analysed using FTIR and XRD as described in chapter 2 sections 2.8.1 and 2.8.2. FTIR was used as a method of chemically characterising the phosphate groups present within the HA structure and ensuring the drying process was effective. Dry powders

were scanned between wavelengths of 400 – 4000 cm^{-1}. SEM and TEM were used to determine the morphology of the HA from the reflux condensation. XRD was used to characterise the presence of HA because of the high crystallinity of the structure. Dry powders were scanned between a 2-theta angle range between 5 and 70 known to be within the fingerprint region for HA. A threshold value of 80 was used to filter non-specific peaks in order to differentiate between the signal and any background. SEM was used on all samples, while TEM was only used on the standard reflux synthesis powder as an additional method to characterise the morphology of the material taken further. TEM of other fibres was not undertaken because these were not used further, and full characterisation was not deemed necessary. To mimic the acidic conditions that prevail during setting of the GIC, the HANFs were immersed in a pH 2 solution of 1M HCl adjusted to the correct pH using deionised water. Fibres were affixed to the SEM stub using a carbon coated adhesive disc but otherwise processed according to the specific method for the analysis as describe in chapter 2 section 2.7. Stubs coated with the HANFs were immersed into the acidic solution covering roughly one third to one half of the disc, before thoroughly drying and imaging. PEG substituted HANFs were substituted in 5% w/w of the glass powder into the GIC powder. This concentration was chosen because it has the largest impact on CS and therefore easier to determine if PEG was successful, no other percentages were used. Cement specimens were then created and tested to determine their CS. Additionally, this new PEG substituted HANFs were fixed onto a SEM stub and the excess removed thoroughly until an even coverage was seen. This was then half/third immersed into a pH 2 solution for 15 minutes before imaging via optical microscopy and SEM.

3.2.3 Preparing and Testing GICs Incorporating HANFs

HANFs were incorporated into the GIC powder by adding the fibres to GICs containing a corresponding reduced proportion of the fluoroaluminosilicate glass component. Therefore, the mass: mass ratio of powder to liquid remained the same for all GICs, but the proportion of that powder which was HANF and fluoroaluminosilicate glass varied according to the substitution. The HANFs were substituted into the GIC powder by mass for the fluoroaluminosilicate glass component of the cement at 1, 2, 3, 5, 10 and 15% by mass. To combine the HANF with the glass, the two powders were mixed according to the method describe in chapter 2 section 2.1 by shaking vigorously. The powder was then mixed with the GIC liquid at the ratio according to the manufacturer's instructions using the method described in chapter 2 section 2.3 and stored at 37°C 100% relative humidity for 24 ± 1 h before testing.

3.2.3.1 Fracture Surface Analysis

Cement specimens cleanly broken from DTS testing using 5% HANF substituted GICs were selected and used for fracture surface analysis. Of the 40 specimens, 5 were selected as cleanly broken, where they had fracture down the central area of the specimen diameter with fewer than 3 visible fragments as a result of fracture. Specimens were filed flat on the opposite side to the facture using 1200 grit silica

carbide paper to create a smooth flat edge. These were then fixed onto SEM stub and processed using the same method described in section 2.9.2.

3.2.4 Statistical Analysis

Samples were analysed for their changes in CS and DTS according to the method described in chapter 2 section 2.11. More specific hypothesis are as follows:

H_1: Substitution of HANFs into a conventional GIC increases its CS

H_0: Substitution of HANFs into a conventional GIC does not increase its CS

3.3 Results

3.3.1 Analysis of HANFs

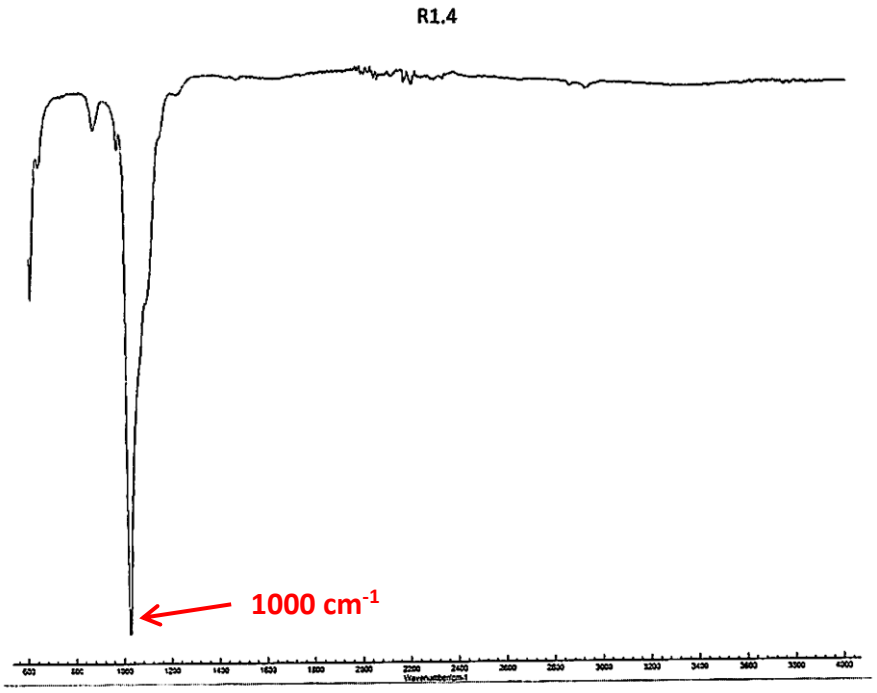

Figure 3.3 - FTIR of HANFs created using reflux condensation showing a sharp peak at 1000 cm^{-1} indicating the presence of phosphate. Scale bar ranges from 400 to 4000 cm^{-1}

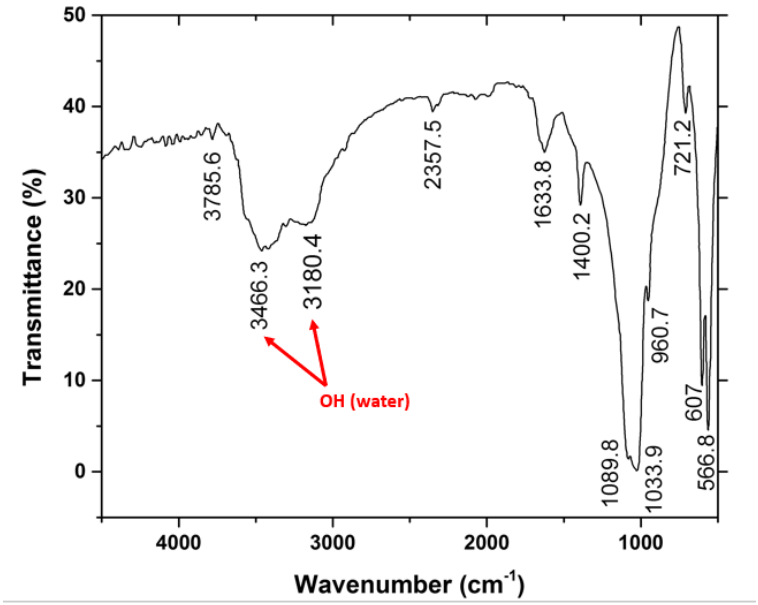

Figure 3.4 - Reference FTIR of wet HA. Bands highlighted at 3466 and 3180 cm^{-1} are characteristic of OH^- relating to water[510]

No peak characteristic of OH from water was seen in Figure 3.3, therefore the powder was dry and free from moisture. For comparison, Figure 3.4 showing HA with water contamination has been provided.

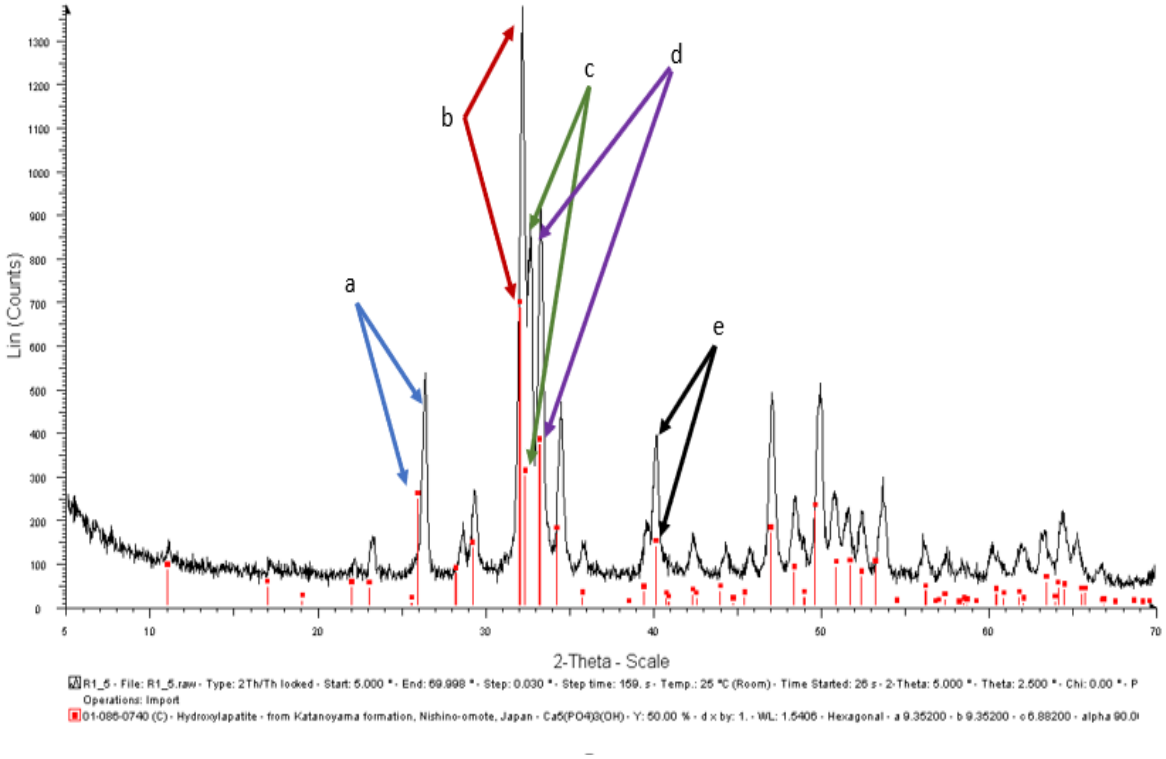

Figure 3.5 - XRD Spectroscopy of the HANFs against the library match for HA (red markers). Scan range 5 - 70. Areas of interest labelled at 26 (a), 32 (b), 32.5 (c), 33 (d) and 40 (e) are characteristic for HA and identical matches for the sample and the library reference. No background threshold was used as main characteristic peaks identified were not interfered with by background noise.

Red markers aligned with the peaks and intensities of the HANF XRD spectrum in Figure 3.5.

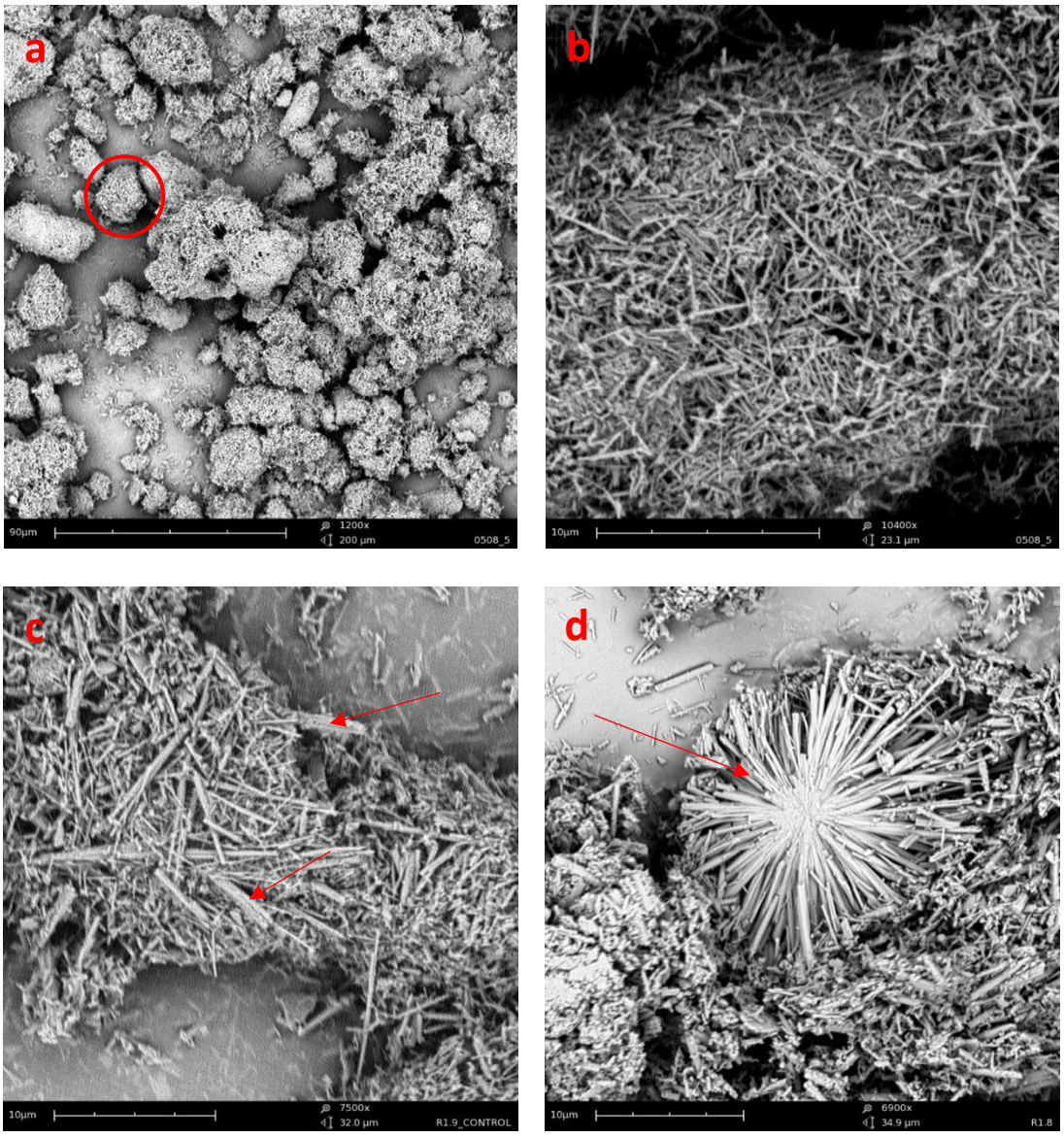

Figure 3.6 - SEM of the HANFs. Image (a) shows an even coverage of spherical bundles (scale bar 90 µm) where most agglomerates such as those highlighted in red were around 10 µm in diameter. These bundles consisted of rod-like fibrous material in various agglomerated forms, such as those highlighted (b – d, scale bar 10 µm).

Agglomeration of fibres were seen across the entire surface of the SEM stub shown in Figure 3.6.

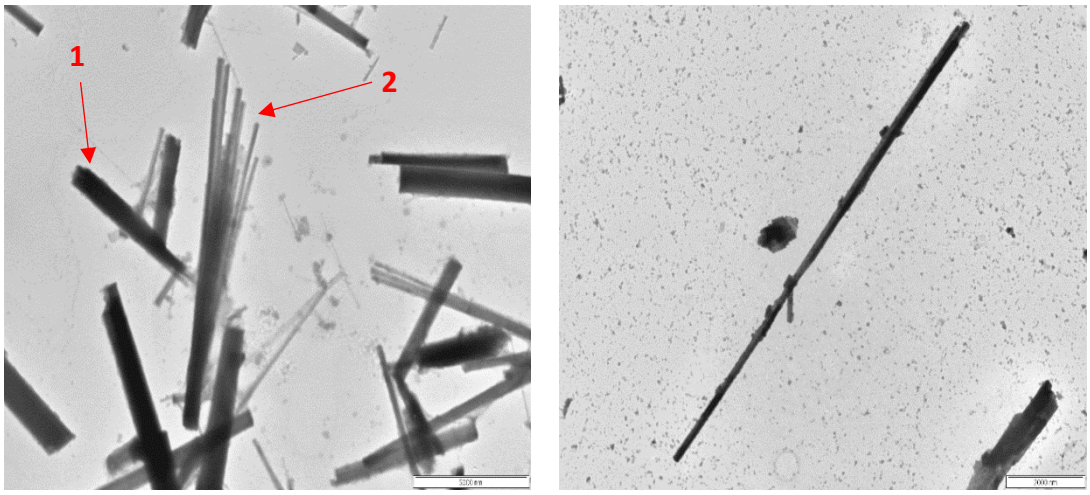

Figure 3.7 - TEM Images of the HANFs showing a rod-like morphology of up to 10 µm and a few nanometres wide. Scale bar 5000 nm (left) and 2000 nm (right). (1) are bundles of short fibres. (2) showing some splitting of these bundles into their individual fibres.

TEM in Figure 3.7 showed fibres became agglomerated across the length of the fibre giving the appearance of wider fibres which were several smaller fibres together.

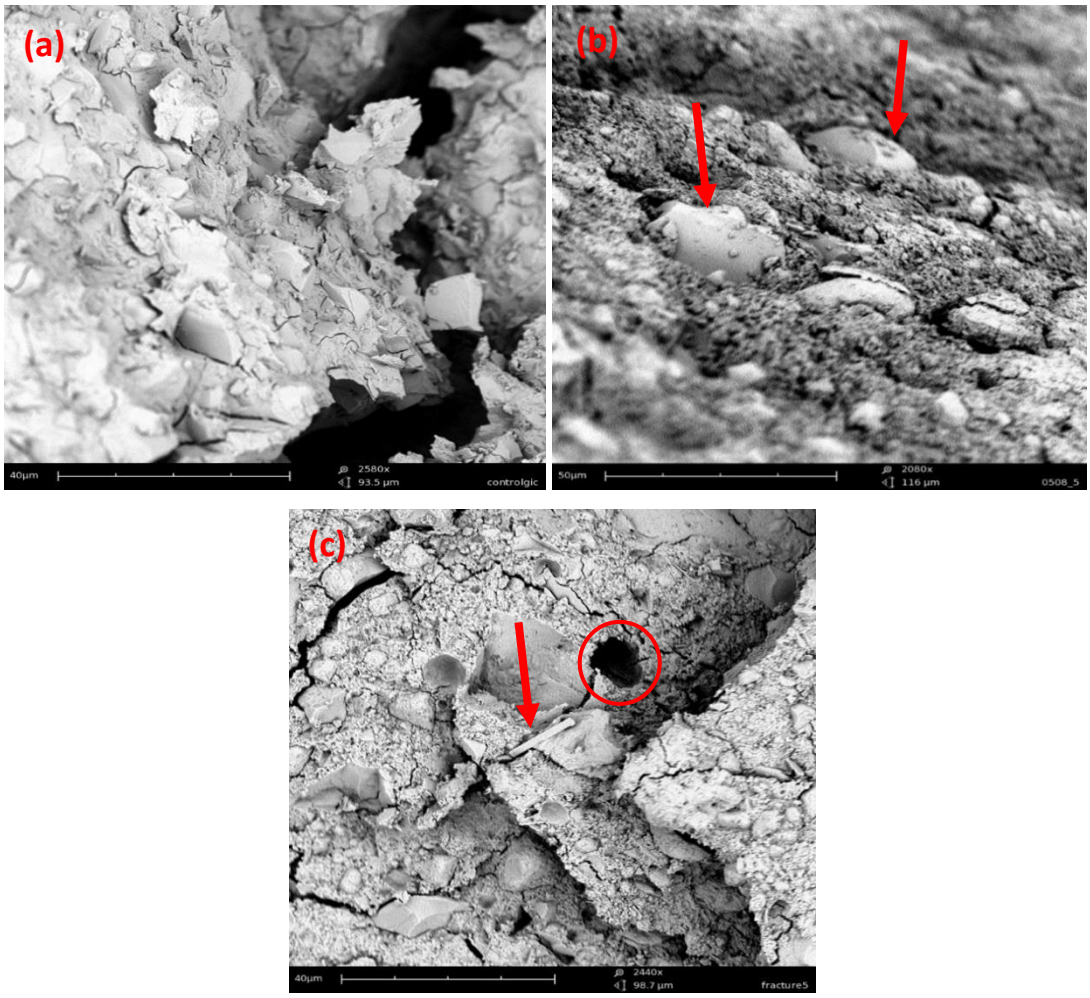

Figure 3.8 - SEM of the fracture surfaces of the GICs with 0% (a) (scale bar 10 µm), 3% HANFs (b) (scale bar 50 µm) highlighting large glass particles and 5% HANFs (c) (scale bar 10 µm) where a pore within the cement through desiccation has been identified. A fibre (highlighted) may have been found present in image (c) as this appears to match the morphology and size found in previous HANF images

Large glass particles were visible in the SEM (Figure 3.8) with occasional fragments. Pores, similar to that identified can be a source of weakness in the GIC structure and crack propagation. The fibre-like material highlighted matches the size and shape of HANFs and may have pulled out from the matrix, however this was inconclusive.

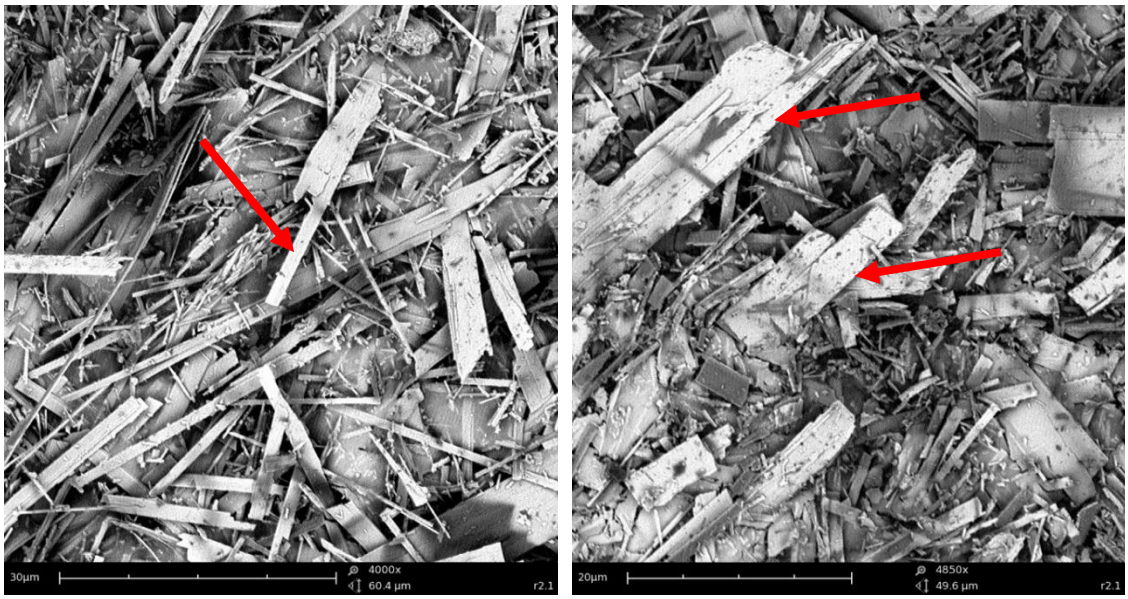

Figure 3.9 - 'HANFs' synthesised without gelatine gave a shard-like morphology, these are highlighted in the image. Scale bars are 30 µm (left) and 20 µm (right). Shards were irregular in width and length around 20 – 40 µm in length and around 5 µm in width

These shards were irregular in width and length with some areas exhibiting evidence of broken sections of shards from fragile fibres.

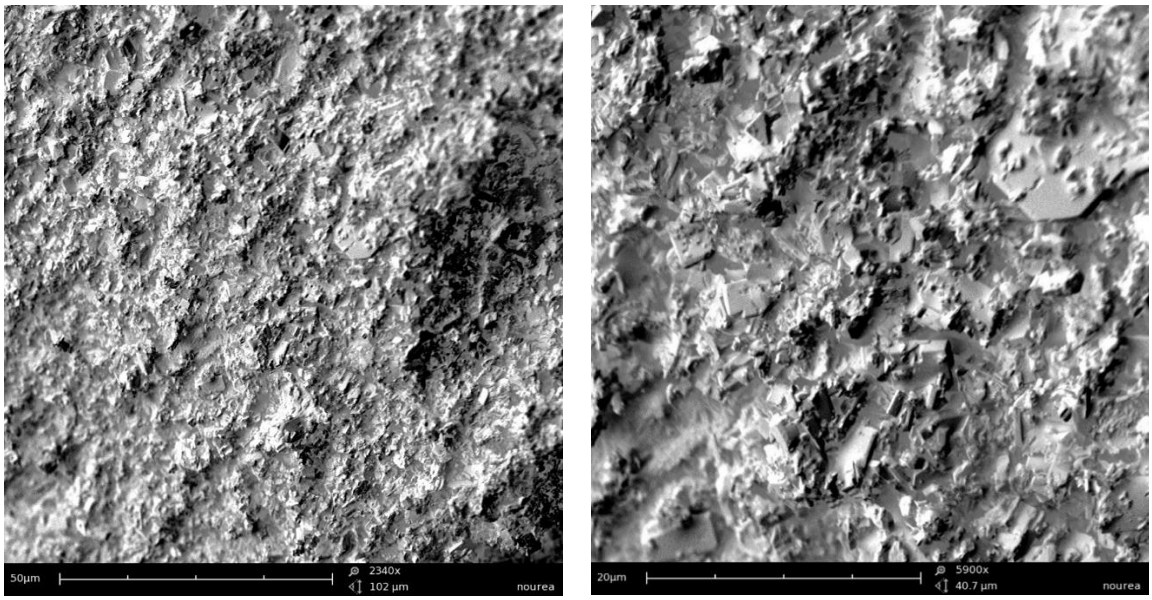

Figure 3.10 - 'HANFs' synthesised without urea created irregular structured crystals. Scale bars are 50 µm (left) and 20 µm (right). The surface appearred homogenous and it is unknown whether HA or another calcium phosphate was formed.

Figure 3.10 showed no areas of the SEM stub presented any fibrous material. Further chemical analysis on the stub would be required to determine if this was HA.

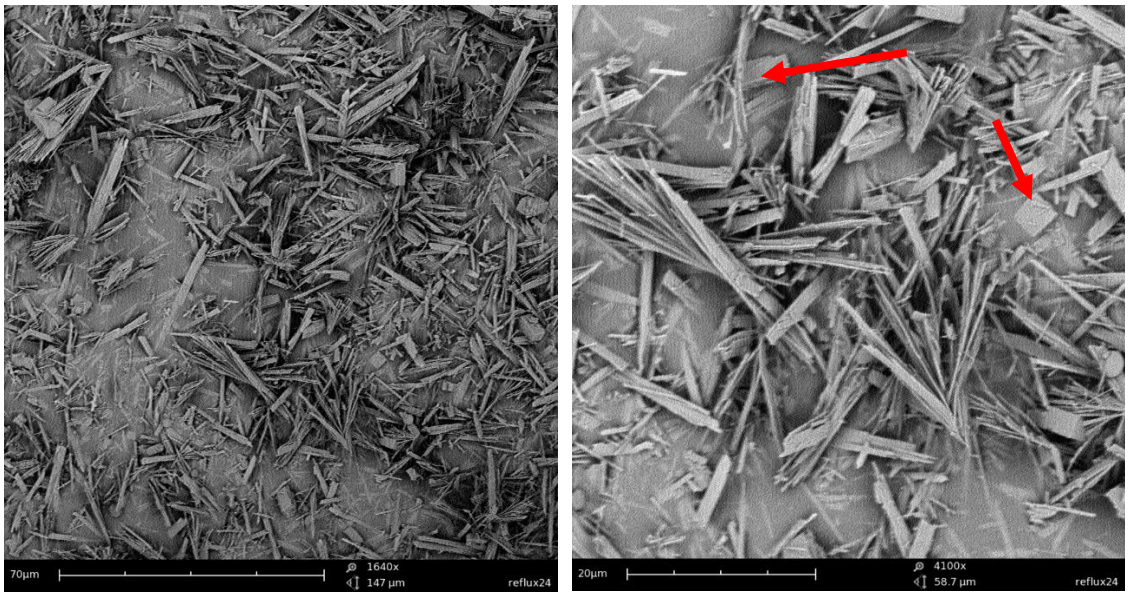

Figure 3.11 - HANFs synthesised for 24 h highlighting stunted fibrous material. Scale bars are 70 µm (left) and 20 µm (right). Some structures seen were square or rectangular, these are highlighted in the right image

Figure 3.11 showed the fibrous material was irregularly shaped with evidence of poor uniformity. Some structures seen were square or rectangular.

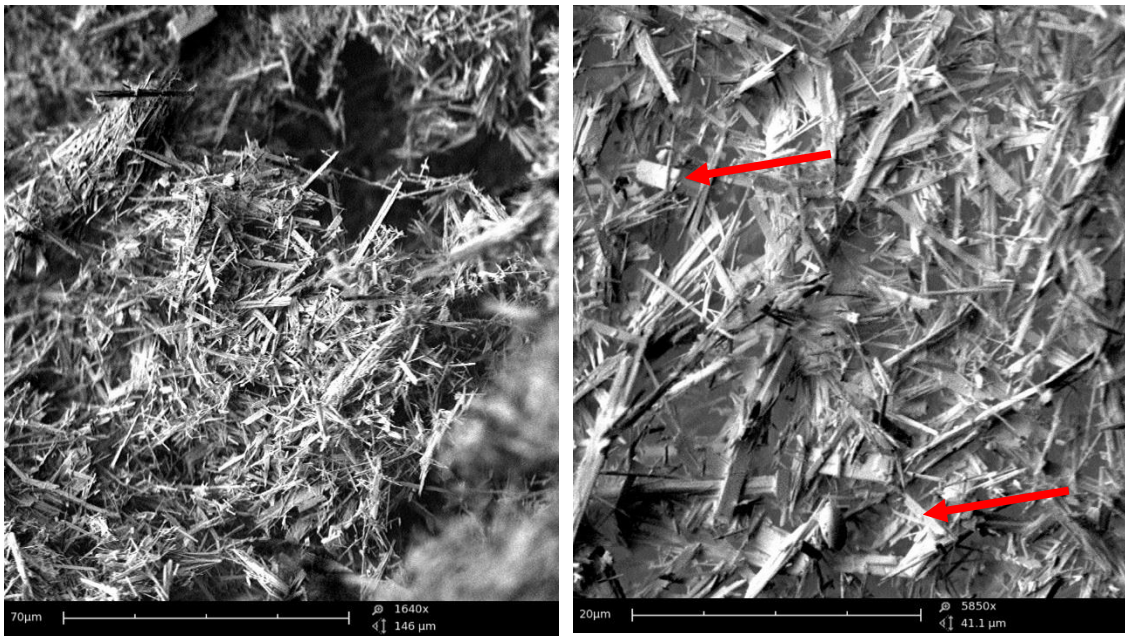

Figure 3.12 - HANFs synthesised for 48 h gave a mixture of stunted fibrous material and fibres with high aspect ratios. The material began to resemble the completed 72 h HANFs. Some irregular shaped HANFs have been highlighted. Scale bars are 70 µm (left) and 20 µm (right).

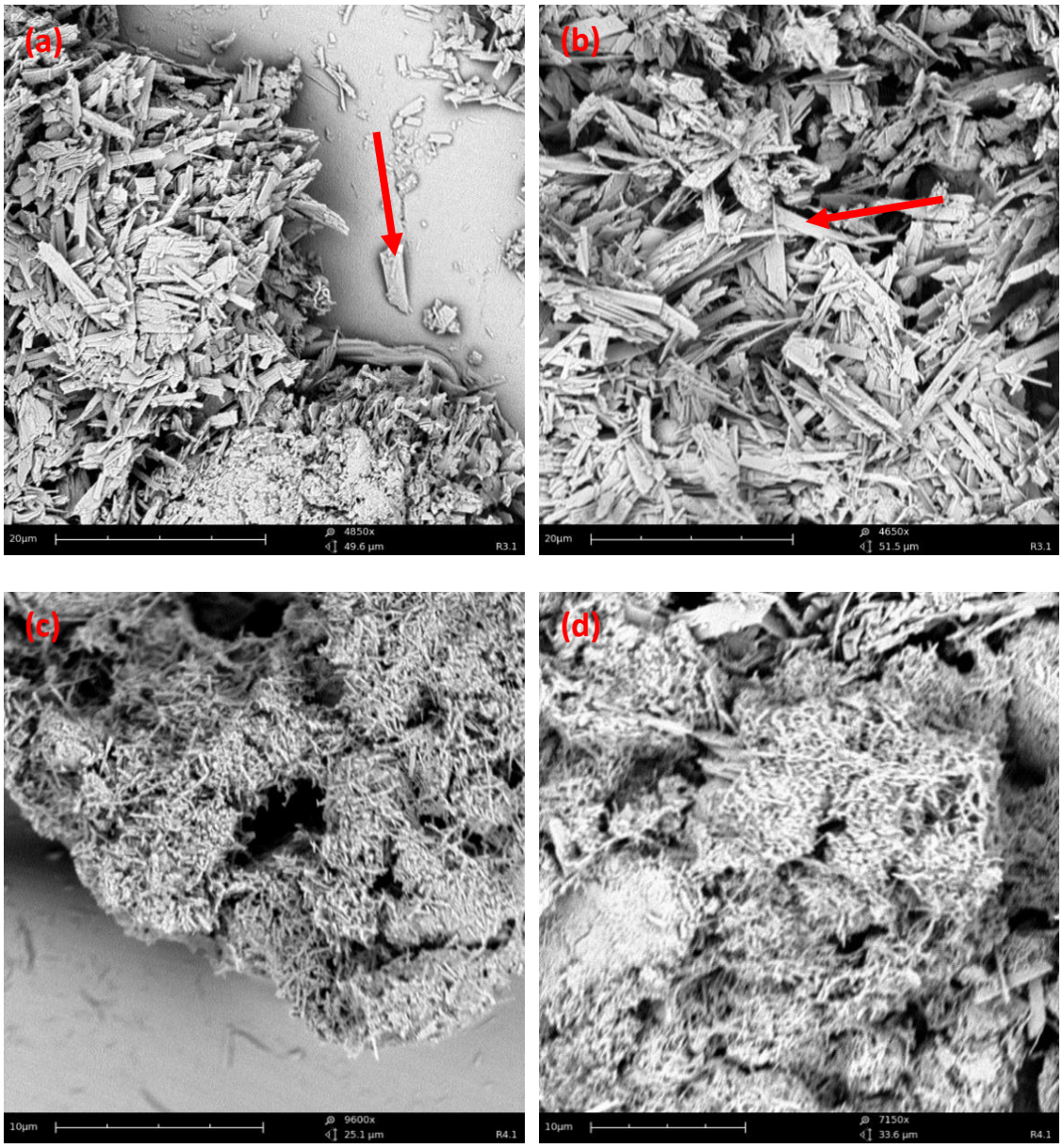

Figure 3.13 - Resultant fibres from the addition of PEG300 (a and b scale bars 20 µm) and PEG600 (c and d scale bars 10 µm). PEG300 created shard-like crystals with a lower aspect ratio (highlighted) while the addition of PEG600 created smaller nanofibres in large bundles

Figure 3.13 shows agglomeration from both PEG 300 and PEG 600 fibres, however this was more pronounced in the smaller fibres produced using PEG 600.

3.3.2 Analysis of GICs incorporating HANFs

CS values calculated from specimens (n = 40) with various substitutions of HANFs are summarised in Table 3.1.

Table 3.1 - CS of HANF substituted GIC with p value and standard deviations shown in the parenthesis. Groups marked with * are statistically different from the control (commercial Diamond Carve™ lot 24623)

% Substitution of HANFs	0 (control)	1	2	3	5	10	15
CS (MPa)	156.6 (25.9)	129.8 (21.3)*	130.9 (16.8)*	150.4 (23.2)	126.0 (19.0)*	117.5 (14.8)*	107.8 (15.0)*
p-value vs control	-	< 0.01	< 0.01	0.28	< 0.01	< 0.01	< 0.01

Table 3.2 – CS of HANF substituted GIC with and without PEG with p value and standard deviation shown in the parenthesis. Groups marked with * are statistically different from the control (Diamond Carve™ A3 lot 24623)

% Substitution of HANFs	0 (control)	5% without PEG	5% PEG 300	5% PEG 600
CS (MPa)	156.6 (25.9)	126.0 (19.0)*	124.7 (20.0)*	134.2 (17.1)*
p-value vs control	-	< 0.01	< 0.01	< 0.01

DTS values calculated from specimens (n = 40) with various substitutions of HANFs are summarised in Table 3.3

Table 3.3 - DTS of HANF substituted GIC with standard deviations (shown in the parenthesis) and p value. Groups marked with * are statistically different from the control (Diamond Carve™ A3 lot 24623)

% Substitution of HANFs	0 (control)	1	2	3	5	10	15
DTS (MPa)	6.7 (1.6)	6.1 (1.3)	6.3 (1.8)	6.8 (2.0)	6.9 (1.9)	6.3 (1.5)	8.4 (2.1)*
p-value vs control		0.062	0.30	0.74	0.73	0.24	< 0.01

3.3.3 Acid Stability of HANFs

Images of the SEM stub immersed in the HCl solution are showing in Figure 3.14.

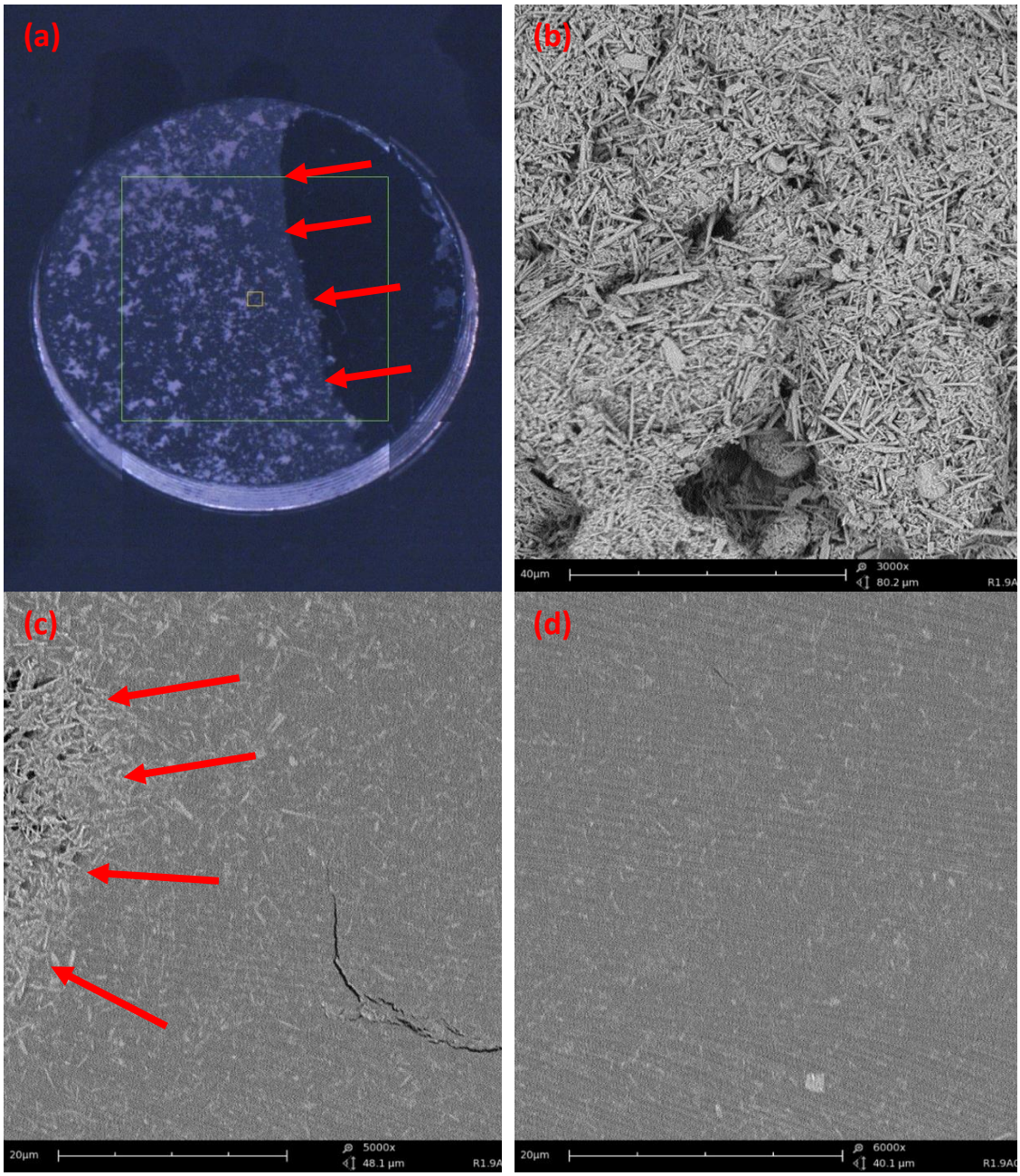

Figure 3.14 - Optical microscope (a) and SEM images of HANFs immersed into pH 2 solution showing the control (not immersed) edge saturated with HANFs (b), the mid-point showing faint signs of fibre presence (highlighted) (c) and the immersed section with little presence of any HANFs (d). Scale bars indicate 20 µm in (c, d) and 40 µm in (b). Optical microscopy magnification was x 2

There was a clear boundary present where the stub was immersed when viewed under optical microscopy, this has been highlighted by the arrows.

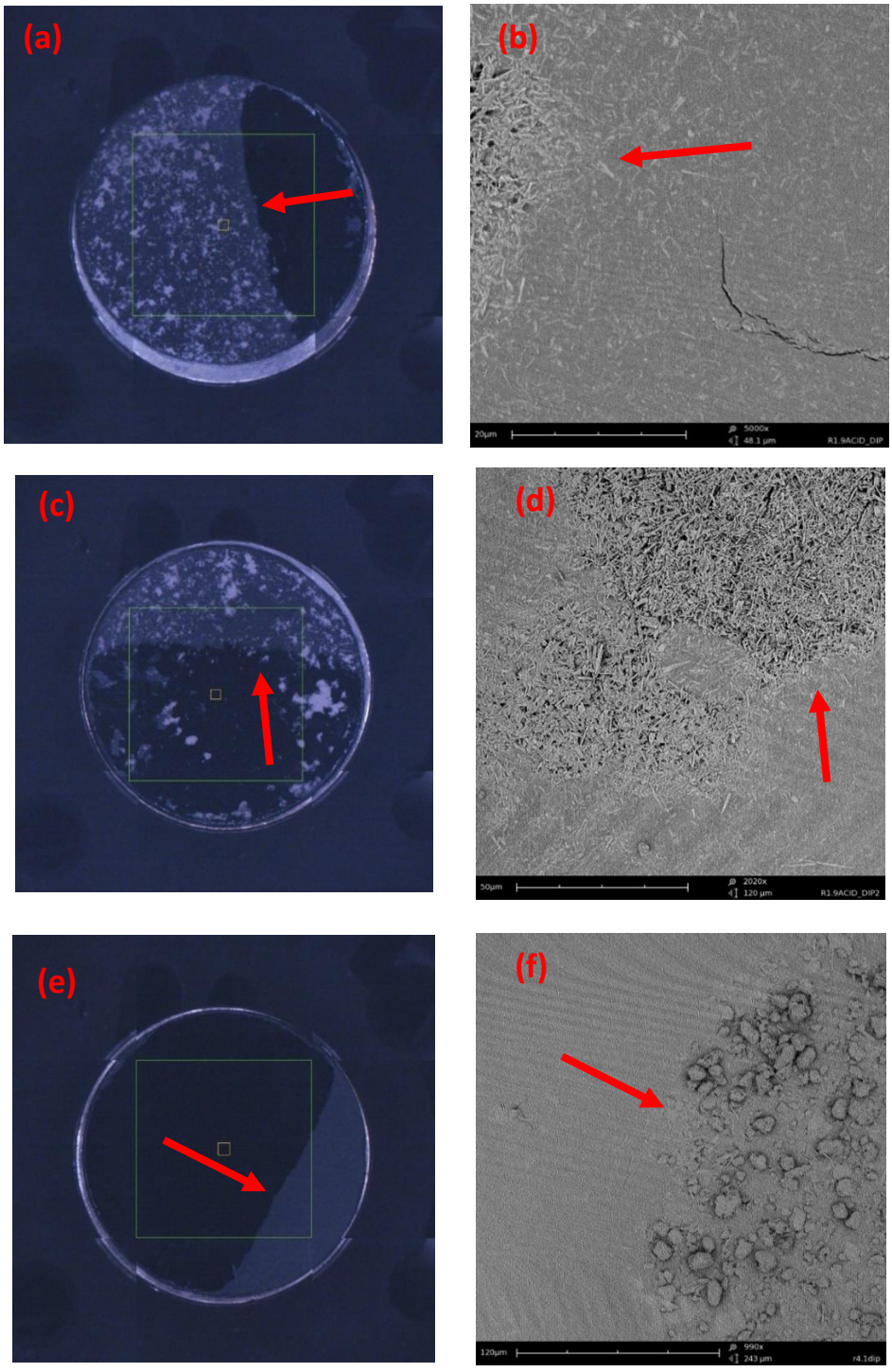

Figure 3.15 - Optical microscope (x 2 magnification) (Left) and scanning electron microscope images (right) of the materials immersed into pH 2 solution. Images a) and b) (scale bar

20µm) are standard hydroxyapatite nanofibres, c) and d) (scale bar 50µm) using PEG 300 and e) and f) (scale bar 120µm) using PEG 600. All substituted HANFs were still removed when immersed into pH 2 HCl solution. Arrows show the clear boundary between immersed and non-immersed HANFs

The boundary where the stubs were immersed was present visibly and under optical and electron microscopy.

3.4 Discussion

3.4.1 Analysis of HANFs

The peak in Figure 3.3 around 1000 cm^{-1} indicates the presence of PO_4^{3-} in the material analysed thus indicating the sodium dihydrogen phosphate reagent in the reflux synthesis has reacted to form the fibre material. This would suggest that a calcium phosphate has likely been formed due to the presence of the phosphate group and the observation that calcium phosphates are less soluble than sodium (hydrogen) phosphates. Any remaining ions are filtered out during the separation process of the HANFs and the solvent which are additionally washed, leaving only the stable covalently bonded calcium phosphate[511].

The XRD data showed a good library match for HA (HA reference PDF#01-086-0740) at the same scan readings and a good correlation to the library peak intensities (see Figure 3.5), indicating HA had been synthesised using the reflux condensation method.

Peaks identified at 2theta values of at 26, 32, 32.5, 33 and 40 are characteristic at these locations and intensities for HA. It was at these peaks where it was inherently distinguishable from other potentially viable products such as dicalcium phosphate, tricalcium phosphate or octa calcium phosphate. The sharp peaks indicate a good level of crystallinity to the HA particularly at key characteristic areas such as 30 – 35 degrees of 2theta. It has been reported to calculate the crystal size using the measurements gained from XRD[512] however due to the inclusion of TEM and SEM data which gave good measurements of the fibres this was not undertaken. Background noise was relatively high, but this did not interfere with the characteristic peaks as much as expected. This noise may be reduced by a different selection of detector or higher exposure time; however, it is not required and the characteristic peaks for HA can be clearly seen. The HA powder was washed and filtered as described in the method section 2.6. The materials are fully miscible in the washing solvent (water) and the filter pore size low enough to retain the fibres but remove any smaller calcium phosphates, therefore it is unlikely to contain any contaminants or by-products. It is important for the HANFs to have a good crystalline structure to efficiently reinforce the cement matrix, irregular or distorted crystals may take up further space within the matrix and weaken the structure.

The microscopy images showed a needle or whisker like structure with a high aspect ratio of around 10 µm long but only around 10 nm wide. The fibres were in abundance and exhibit high levels of agglomeration which was likely due to the electrostatic charge between the high surface area material.

Changes made to the reagents and timing of the reflux created misshapen and stunted shards or fibres (see Figure 3.9, Figure 3.10, Figure 3.11 and Figure 3.12). The shards created when gelatine was omitted indicates that gelatine plays an important role in directing the crystal growth in one plane, when it is no longer present, the HA grows in both x and y directional planar axis as previously suggested in a recent study using HA[513], calcium carbonate[375] and spherical HA particles[514]. Without urea, the resultant crystalline powder becomes amorphous and unstructured showing no fibrous qualities, however, it cannot be concluded these were or were not HA without chemical analysis. It is clear the urea is vital in creating the structure of the HANFs and as urea is important in maintaining the pH of the solution but is unknown if the result powder was HA. As the reflux time decreases, smaller fibres are seen with a lower aspect ratio. This further points to a crystal growth along one axis as the HA is formed, however 72 h is required to achieve the large aspect ratio seen and less time produces these same fibres which have not grown to their full extent. The use of PEG equally distorted the crystal growth, although the mechanism is unclear and not well studied, it may be sterically hindering the growth or calcium phosphate formation, thus delaying the reaction[508]. Additionally, the PEG failed to protect the HA against protonation within the cement mix.

3.4.2 Fracture Surface Analysis

SEM images of the fractured surface of the GIC specimens gave no obvious signs of fibres present. However, in Figure 3.8 image c, a potential sighting of a fibre has been

highlighted. The appearance matches the length and width of HANFs identified. However, no further inspection of the material was possible under SEM due to the comparatively small size compared to the glass particles. Chemical analysis of the HANFs in the matrix would be difficult to distinguish between the calcium and phosphate ions present in the matrix. Therefore, it was inconclusive whether this was a HANF or a fragment of the GIC matrix. The results in isolation are therefore largely inconclusive regarding the survival or presence of the HANFs in the GIC matrix but taken in combination with the acid lability studies these would appear to indicate that the HANFs have largely not survived the transient low pH conditions during setting of the cement.

3.4.3 Analysis of GICs Incorporating HANFs

The initial investigation indicated a statistically significant decrease in CS with 1 and 2% HANFs compared to the commercial control, but no reduction with 3% (see Table 3.1). Similar behaviour was observed with DTS, although there was no statistically significant difference between the specimens. This was interpreted that the lowest concentrations may have been insufficient to provide a large enough number or density of HANFs to reinforce the structure, and that it was possible that a greater proportion may continue the upward trend seen from 2 to 3%. However, upon using 5, 10 and 15% substitutions, DTS increased only at 15% and CS decreased with respect to control at all concentrations. It was hypothesised that some dissolution of the HANFs may have occurred meaning that the fibres were no longer available for structural

reinforcement, and exposure of the HANFs to acid at pH2 confirmed this, revealing dissolution to occur within 15 minutes. It is possible, within the fracture surface SEM, there may have been signs of HANFs, but this cannot be conclusive without further chemical analysis. PEG was trialled to establish whether it could protect the HANFs from dissolution during the brief period of low pH experienced within the GIC setting period[504], but this was insufficient to prevent dissolution or, therefore, increase strength.

With 1-3% substitutions of the HANFs an initial decrease followed by a contrasting increasing trend was seen. This indicates as higher concentrations are used, the strength reducing effect of the low concentration of HANFs is mitigated and a potential increase in strength may be seen at higher concentrations. While the 5% and 10% concentrations showed no significant change in the DTS of the cements a 15% substitution showed an increase in DTS. The DTS showed a different trend of the effects of the fibres compared to the CS data. It is likely that fibres have a more profound effect on the tensile properties than compressive, most studies discussed conclude this also in section 1.7.2. In summary, no percentage of HANFs created cements with a higher CS and would not be suitable for this purpose.

3.4.4 Acid Stability of HANFs

It was deduced that the acid susceptibility of HA due to the highly negative ionic dipole from the phosphate group may have contributed to the lack of strength seen. The acidic reaction conditions and therefore high availability of the proton ions within the

cement mixture may have led to the chemical breakdown of the HA to a more amorphous calcium phosphate or dissolved into their ions with no reinforcing structure or properties. This is not a new phenomenon and is the mechanism of action seen during demineralisation of apatite in enamel by acid producing bacteria in biofilms as previously discussed in section 1.1.1. Furthermore, the increased availability of calcium and phosphate within the cement setting matrix may therefore interfere with the setting reaction leading to reduced ion migration and a weakened structure. The addition of PEG did not protect these fibres against the acid attack when immersed into the acidic solution. This indicates the fibres, even with the addition of PEG, dissolve in the harshly acidic reaction conditions of the setting GIC. The SEM images showed a clear removal and degradation of the structure of the HANFs after pH conditions were replicated. This was likely the reason of the lack of reinforcement of the GIC despite literature evidence of HA reinforcement in other materials.

3.5 Conclusions and Future Directions

High aspect ratio whisker-like nano HA can be successfully synthesised using a reflux condensation method described. The use of HANFs as GIC reinforcing agents was unsuccessful possibly due to dissolution of the HA in the short-term low pH setting reaction within the GIC, creating cross link inhibiting excess calcium and phosphate ions as acid conjugators in the gelling matrix. The addition of PEG did not protect the fibres any further but instead distorted the fibre morphology by inhibiting the crystal growth. Further work to protect these fibres further without affecting the structure

may prove useful, many other surfactants (such as sodium dodecylsulfate, Triton X-100[506], polyethylene oxide polymers[507] and cetyl trimethyl ammonium bromide[510]) and lower molecular weight PEGs could have this desired effect but would be required to not interfere with the reaction mechanism. The use of HA would be preferred because of the high biocompatibility of the molecule and the existing of an easy, low cost and scalable synthetic method. The statistical data does not prove the hypothesis and the null hypothesis cannot be rejected.

Chapter 4 Investigation of Halloysite Nanotubes as Reinforcing Agents for Glass Ionomer Cements: Incorporation, Analysis and Testing

4.1 Introduction

The aim of this chapter was to explore the use of halloysites as reinforcing nanomaterials for GICs. HNTs have shown promise in reinforcement of other materials, as discussed in chapter 1 section 1.7.3. This, coupled with the other following favourable properties, led to the hypothesis that they might enhance the CS of GICs without adversely affecting other properties.

HNTs were considered to constitute a promising approach to enhance the mechanical properties of GICs because (listed in order of importance):

- They consist of very high aspect ratio tubes, which are favourable for reinforcing related materials (chapter 1 section 1.7.1.1)[212,374]
- They are biocompatible (chapter 1 section 1.7.3)[515,516]
- They are similar in composition to the fluoroaluminosilicate glass in the GIC and will therefore bond to the GIC matrix and not affect setting properties[385,517,518]
- They are readily available naturally and are cheap (chapter 1 section 1.7.3)[427,519]

To explore their utility in this application, HNTs were assessed for acid lability, then incorporated into the GIC by substitution by weight for the fluoroaluminosilicate component of the powder and tested for CS and DTS. The dispersion of the fibres was estimated by dying these with a fluorescent dye and qualitatively viewing the distribution within a set cement, since poorly dispersed and agglomerated nanomaterials have a negative effect on strength[520,521]. The effect of method of dispersion of the HNTs on CS and DTS was also evaluated.

4.2 Methods and Materials

4.2.1 HNTs

HNTs of grade MF4 (high purity) were provided by Durtec GmbH and consisted of 47.5% silica, 36.6% alumina and 13.9% hydroxyl water, with less than 1% impurities of iron and magnesium oxides. This data was provided through a specification for grade MF4.

HNTs were analysed using FTIR and XRD according to the method described in chapter 2 section 2.8.1 and section 2.8.2 respectively. These were compared against library data and published results of other HNTs to validate the identity of the material. The HNTs were also analysed for their morphology using SEM as described in chapter 2 section 2.9.2, both as provided and after exposure to acid to explore acid lability as described in chapter 2 section 2.7. TEM images were provided by Durtec GmbH.

HNTs were dyed using acridine orange, a fluorescent dye which could be viewed within the GIC as a means of assessing the distribution of the HNTs with or without milling. This was done using the following process:

1. 1g of HNTs mixed with 10 ml of 0.25g/L acridine orange in industrial methylated spirit (IMS) on a vortex mixer (Thermo Fischer Scientific) for 10 seconds
2. Agitated on a mini orbital shaker (Cole-Parmer, Staffordshire, UK) at 150 rpm for 24 h
3. Further vortex mixing for 10 seconds
4. Centrifuged at 3500 rpm for 5 minutes

5. The supernatant removed and a further 10 ml of IMS added
6. Steps 3 and 4 were repeated a further three times to completely wash the HNTs of any excess dye
7. Dried at 37°C for a minimum of 14 days

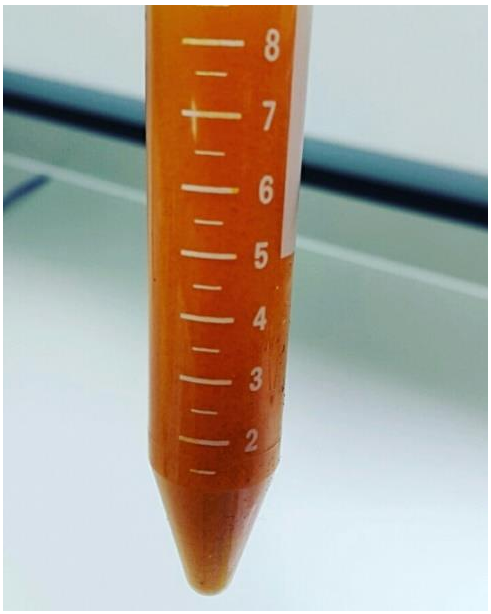

Figure 4.1 - Acridine orange dyed HNTs in suspension before centrifuge

4.2.2 Preparing and Testing GICs Incorporating HNTs

All HNTs were handled in a protective covered 'nanobox', a custom-made sealed unit used to contain any HNTs (Figure 4.2). This was put in place as an additional safety precaution due to the nano size and similar structure to that of other potentially harmful nanomaterials such as asbestos and carbon nanotubes.

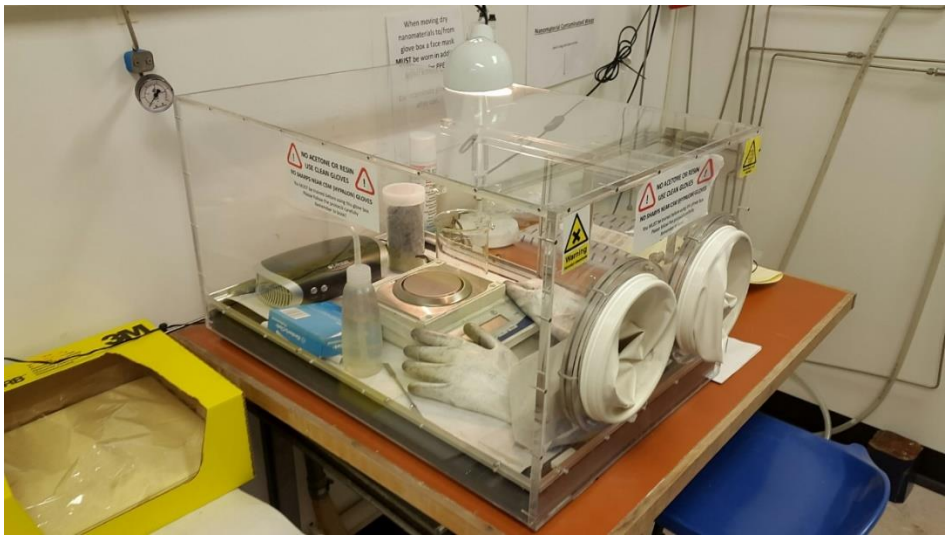

Figure 4.2 - Custom made box used for handling HNTs. A two-part door entry system on the side was used to bring materials in and out of the working chamber. All powders were handled using the arm length rubber gloves. The box was used as a precaution as some cells have shown uptake of HNTs and caution has been urged, with reference to the hazards associated with asbestos[515]

To investigate the effect of HNT doping on mechanical properties, the HNTs were substituted into the GIC powder by mass for the fluoroaluminosilicate glass component of the cement at 1, 2, 3, 5, 10 and 15%. To combine the HNTs with the glass, the two powders were mixed according to the mixing method described in chapter 2 section 2.1. The powder was then mixed with the GIC liquid at the ratio according to the manufacturer's instructions and placed into the moulds using the method described in chapter 2 section 2.3 and stored at 37°C 100% relative humidity for 24 ± 1 h before testing for CS and DTS. The methods for these are described in chapter 2 section 2.4 and section 2.5 respectively.

To explore the effect of method of combining HNTs with the GIC powder, a milling approach was compared with the simpler mixing approach described above. Samples of the powders from the steel balls were analysed for particle size distribution using the method described in chapter 2 section 2.10.6 to assess the effect of this milling on the particle size of the powder.

Figure 4.3 - IKA mills (left) and steel balls (right) used to mill the HNT-GIC powder as described in chapter 2 section 2.1

To assess dispersion of HNTs within the GIC, and identify any inhomogeneity of dispersion, HNTs dyed with acridine orange were substituted into the GIC 5% w/w and milled according to the method in chapter 2 section 2.1 for milling. Cements were mixed, and discs created measuring 20 mm in diameter and 1 mm thick, these were analysed using optical microscopy using the method described in chapter 2 section 2.9.1. Homogeneity of dyed HNTs was assessed through visual examination of the brown patterns under x 40 microscopic magnification.

To investigate the effect of powder/liquid ratio, the GIC liquid was reduced by 10, 20 and 30% w/w against a constant quantity of powder (Table 4.1). Specimens were created using this ratio for CS (Table 4.4) and DTS (Table 4.5) (n = 40 for both).

Table 4.1 – Example Quantities of Powder and Liquid used in the reduced liquid cements

	Commercial Control (Diamond Carve™)	**10% less liquid**	**20% less liquid**	**30% less liquid**
Powder Quantity	0.4 g	0.4 g	0.4 g	0.4 g
Liquid Quantity	0.1 g	0.09 g	0.08 g	0.07 g

4.2.3 Statistical Analysis

Samples were analysed for their changes in CS and DTS according to the method described in chapter 2 section 2.11. More specific hypothesis are as follows:

H_1: Substitution of HNTs into a conventional GIC increases its CS

H_0: Substitution of HNTs into a conventional GIC does not increase its CS

4.3 Results

4.3.1 Analysis of HNTs

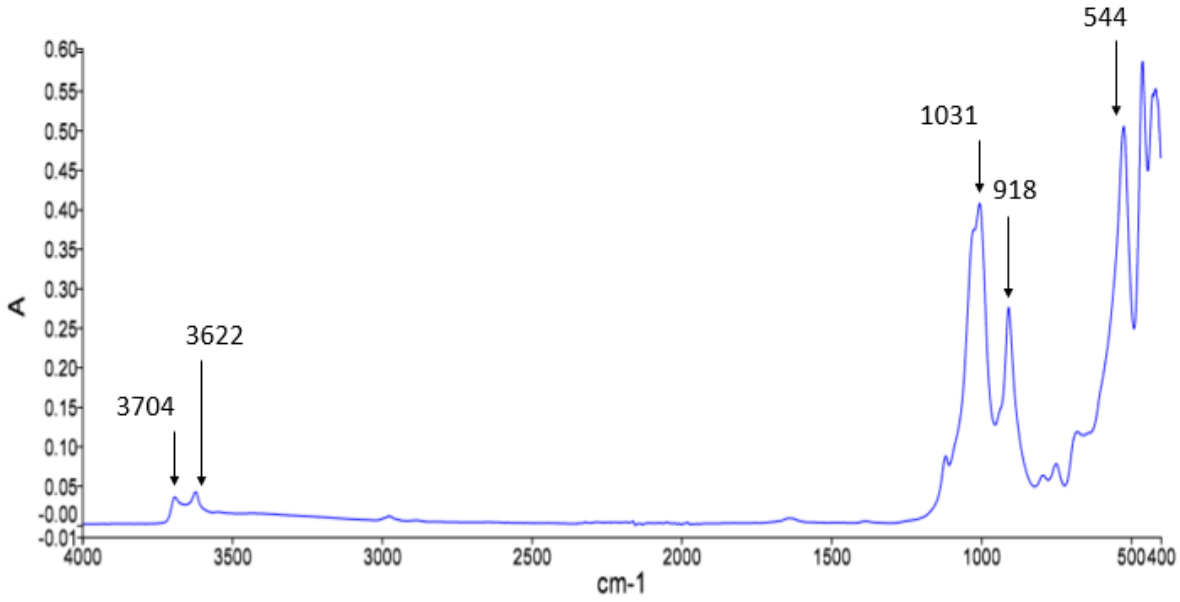

Figure 4.4 - FTIR of HNTs as provided with no further processing. Peaks at 3704, 3622, 1031, 918 and 544 were highlighted as bands of interest and discussion.

Bands at 3704 cm^{-1} and 3622 cm^{-1} in Figure 4.4 were attributed to the stretching vibration of inner surface Al_2 – OH groups and vibrational interlayered water. Bands around 1031 cm^{-1} and 918 cm^{-1} are through Si – O – Si and vibrational inner surface hydroxyl groups. Si – O bending vibrations were observed around the 544 cm^{-1} range[522].

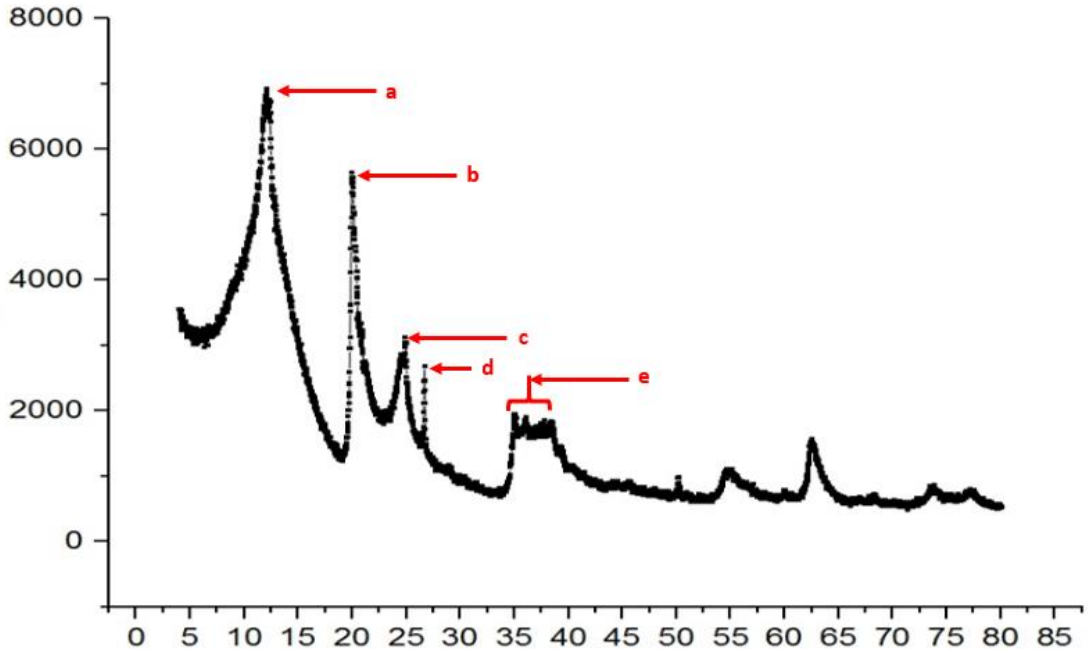

Figure 4.5 - XRD of HNTs over a 2θ scan range of 0 – 85. Areas of interest labelled at 12 (a), 20 (b), 23 (c), 25 (d) and 35-40 (e) are characteristic for HNT and identical matches for the sample and the library reference (Figure 4.6). A threshold of 500 counts was used to filter non-specific peaks against any background noise

For reference, a library spectrum was used for comparison:

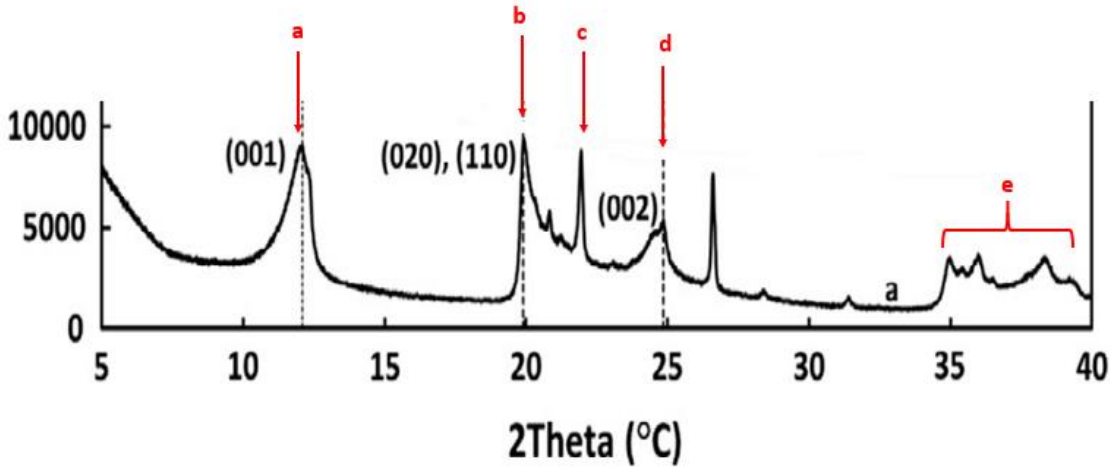

Figure 4.6 - Reference HNT XRD pattern over a scan range of 5 - 40. 2theta values identified as 12, 20, 22, 25 and 35-40 match those identified as a-e in Figure 4.5, image adapted from[523]

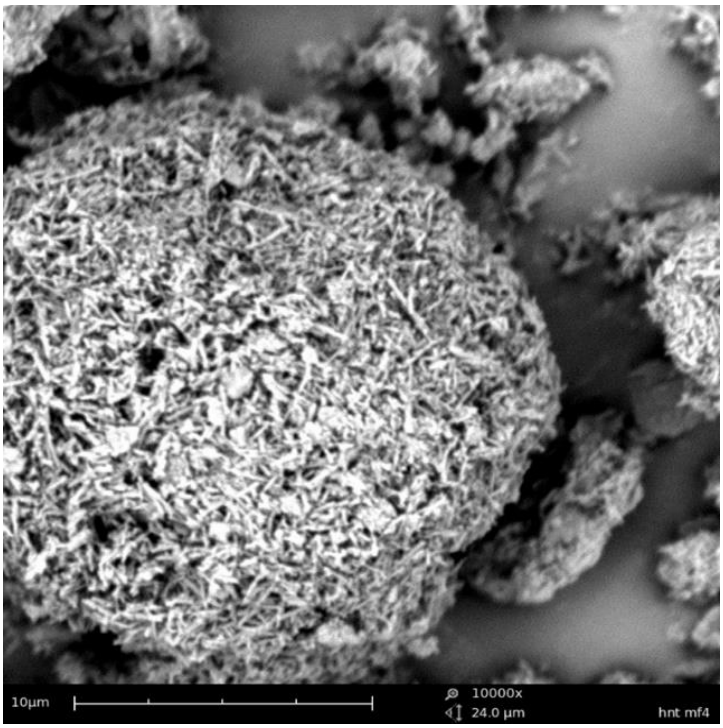

Figure 4.7 - SEM of HNTs showing agglomerated bundles of fibres. Some bundles were around 5 – 10 µm while the largest were several tens in diameter. Scale bar 10 µm.

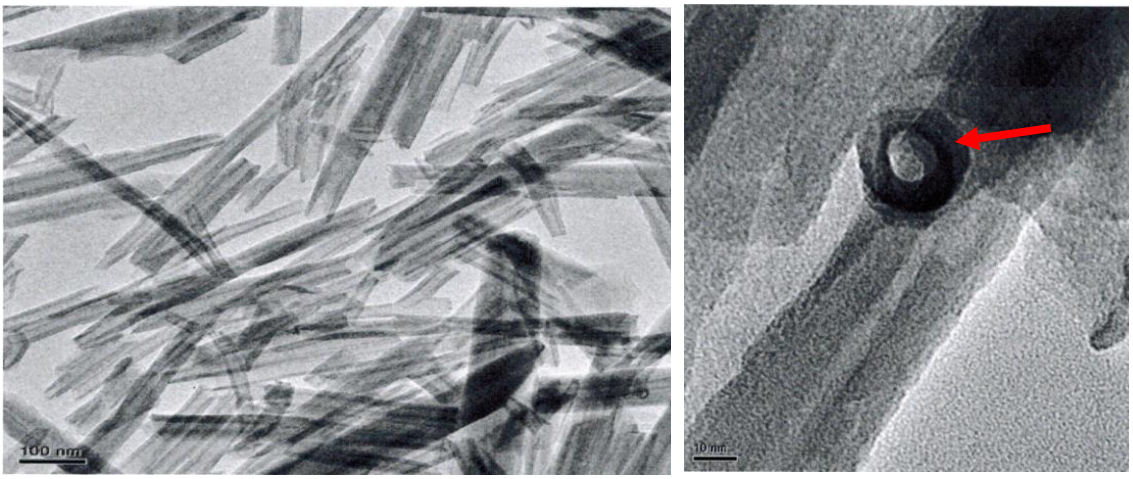

Figure 4.8 - TEM images of HNT showing rod-like hollow tubules with a high aspect ratio. Scale bars are 100 (left) and 10 nm (right). HNTs had a length of around 500 nm and a diameter of around 20 nm with an inner lumen of around 10 nm. The electron-dense tubule

wall has been highlighted in the right image. Note: these images were provided by Durtec GmbH

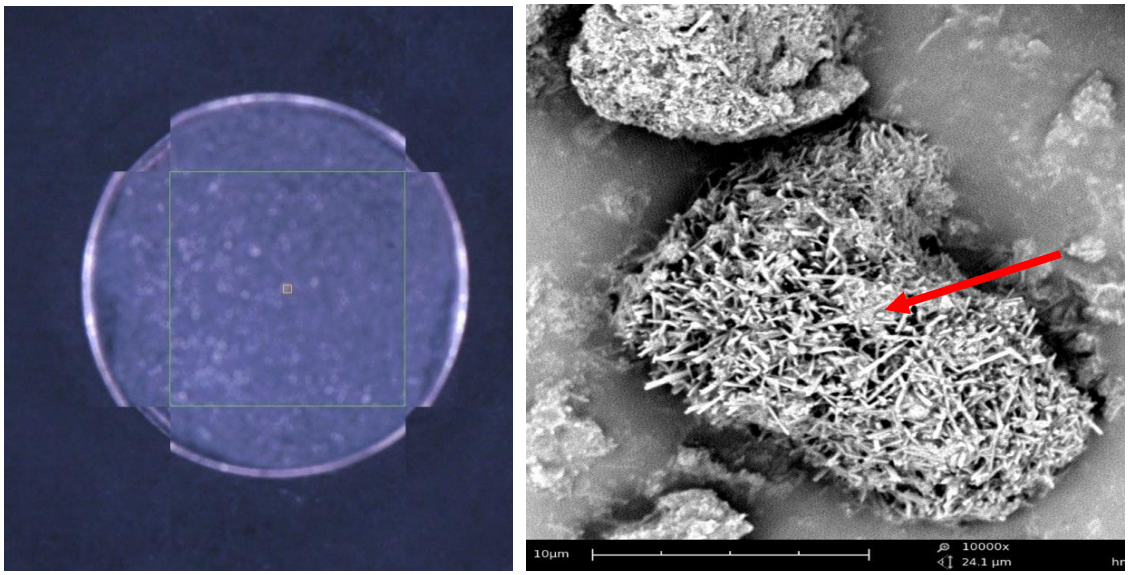

Figure 4.9 - Optical microscope (x2 magnification) (left) and SEM (right) images of HNTs immersed into a pH 2 solution. The acidic solution has not caused the fibres to dissolve, as was the case with HA, however some wetting of the HNTs of water was retained within the bundles (highlighted). SEM scale bar 10 µm

No effects of the acid were seen on the HNTs using optical microscopy or SEM as shown in Figure 4.9. The appearance of the HNTs including agglomeration was consistent before and after exposure to the pH 2 solution.

4.3.2 Analysis of GICs Incorporating HNTs

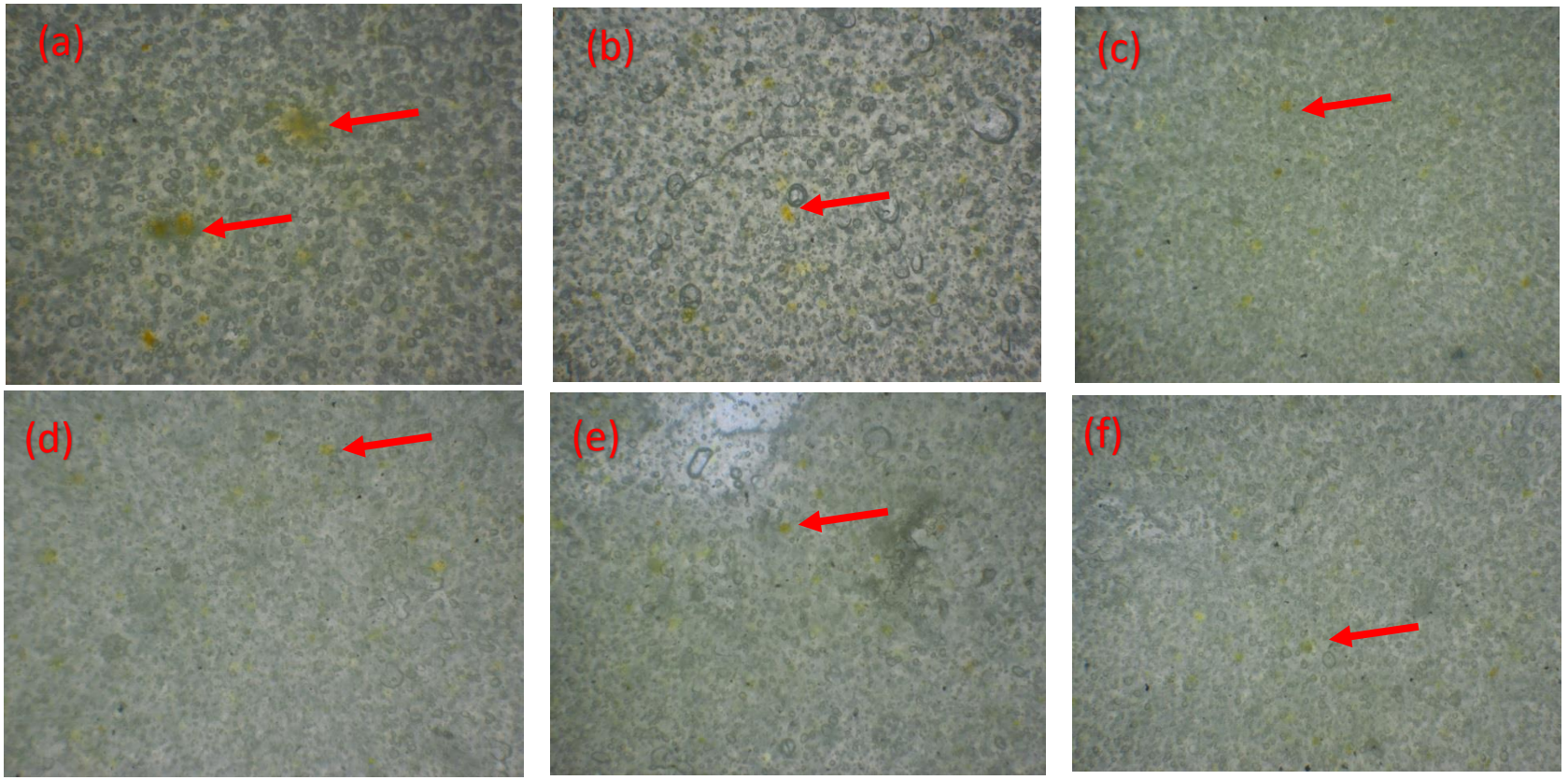

Figure 4.10 – 4 x magnification optical microscopy images of 5% acridine orange HNT substituted GICs after milling for (a) 0 mins, (b) 2 mins, (c) 4 mins, (d) 8 mins, (e) 10 mins and (f) 20 mins. Examples of dyed agglomerates seen are highlighted by arrows in each image showing smaller patches upon further milling

Figure 4.10 shows optical microscope images of GICs using acridine orange dyed HNTs which were substituted into the GIC powder for 5% of the fluoroaluminosilicate glass. Inhomogeneity in the specimens, as indicated by dark brown areas which are easily visible, was observed with the lower durations of milling of 2 – 4 minutes. Milling of 8 minutes and above gave more homogeneous specimens, and with a time of 20 minutes the darker patches were much less prominent.

Table 4.2 - Particle size distribution of 5% HNT-GIC powder after different milling times (n = 1)

Milling Time (minutes)	Range of Particle Size		
	% (2000 – 12.62 µm)	% (12.62 – 4.48 µm)	% (4.48 – 0.02 µm)
0	28.55	28.53	42.92
2	27.77	25.83	46.40
4	26.73	25.15	48.10
8	26.57	24.69	48.74
10	24.77	26.27	48.96
20	24.23	25.53	50.24

Table 4.3 – CS and standard deviation of milled and unmilled (mixed) HNT substituted GIC with p value. Groups marked with * are statistically different from their respective commercial control (Diamond Carve™ A3 lot 24623) n = 40 for all samples

% Substitution of HNTs		0 (control)	1	2	3	5	10	15
CS (MPa)	Milling	149.8 (21.2)	123.0 (22.1)*	120.3 (13.3)*	119.9 (15.8)*	157.3 (23.2)	145.1 (20.0)	136.0 (21.4)*
	p-value vs control		< 0.01	< 0.01	< 0.01	0.16	0.34	< 0.01
	Mixing	140.2 (26.1)	129.0 (35.6)	116.9 (14.2)*	119.8 (16.4)*	153.0 (27.4)*	-	-
	p-value vs control		0.099	< 0.01	< 0.01	< 0.01		
Milling v Mixing p-value		0.019*	0.29	0.30	0.79	0.34		

The powder prepared by mixing was visually unchanged, but the powder obtained after 20 minutes of milling with steel balls had discoloured, and the cement prepared with milled powder had a dark grey colour, however this effect was not seen when milled with glass balls. Milling did not have a significantly increase the CS of the GIC when compared against mixed alternative at the same HNT concentration. Only powders milled using the steel balls were used for all further tests.

Table 4.4 - CS of milled 5% HNTs substituted GIC using 10, 20 and 30% less GIC liquid in the mix with p value and standard deviations. Groups marked with * are statistically different from the commercial control (Diamond Carve™ A3 lot 24623). 30% less GIC liquid became very difficult to mix. All resultant cements were grey in colour when steel balls were used but was not found to be the case when glass balls were used. †Mixed according to the ratios in the manufacturer's instructions for use. ††5% HNT substituted GIC milled using the standard 4:1 ratio. n = 40 for all groups

% less GIC Liquid	Manufacturers GIC as supplied†	0 (control)††	10	20	30
CS (MPa)	140.2 (26.1)	157.3 (23.2)	172.6 (15.2)	187.2 (30.1)*	182.9 (29.5)*
p-value vs manufacturers GIC	-	< 0.01	< 0.01	< 0.01	< 0.01

† Mixed according to the ratios in the manufacturer's instructions for use

Cements mixed at using 30% less GIC liquid were difficult to mix and resultant in an increased number of rejected specimens due to visible flaws in the cement and poor breaking characteristics under loading.

Table 4.5 - DTS and standard deviation of milled 5% HNT substituted GIC using 20% less GIC liquid (n = 40). The control used was commercial Diamond Carve™ A3 lot 24623

Substitution of HANFs	**0 (control)**	**5**
DTS (MPa)	6.7 (1.6)	6.8 (2.1)
t-test p-value	0.795	

No significant difference in DTS was seen with the inclusion of 5% HNTs and 20% reduced GIC liquid.

4.4 Discussion

4.4.1 Analysis of HNTs

The biocompatibility of some types of nanotubes are still somewhat unknown[524]. Commonly used and researched materials such as CNTs have shown to be non-toxic[525] and both single walled and multi-walled CNTs have found uses in diabetes sensors,

cancer therapy, drug delivery carrier, bone scaffold materials etc. for more than a decade[526,527]. Other nanotubes such as silicon, titanium and boron nitride are still under investigation, but early studies show an acceptable level of biocompatibility[396]. It is thought that smaller nanomaterials have a higher risk of toxicity than larger ones and that spherical particles have fewer adverse effects than rod-like nanoparticles[528]. HNTs studied have so far shown good levels of biocompatibility and low cytotoxicity[515,516,529,530] as well as historical use in ceramics for many decades[438]. Additionally, HNTs have however the safety data sheet (SDS) provided with the material urges caution and classifies the material as potentially having a carcinogenic effect. Additionally, as previously mentioned, some cells (such as cervical and breast cancer cells tested) have shown uptake of HNTs and caution has been urged, with reference to the hazards associated with asbestos[515]. Due to this, and the quantity of material provided (1 Kg), precautions were taken to protect against any risks associated with this to the operator and surrounding personnel.

The FTIR spectrum was characteristic of HNTs and showed evidence of aluminium hydroxide bonding, silica (Si-O-Si) bonding and the presence of water which was bound in the spacing between the layers of the HNT tubules[522,531]. This is supported by the composition data provided by Durtec GmbH giving evidence of the aluminosilicate chemical structure of the material.

The XRD data showed a near identical match to the HNT studied by Dong[523] who used "premium ultrafine HNT powder" sourced from New Zealand. Peaks at 2θ values 12, 20, 25 and 35 – 37 align between the two graphs indicating a match between the two

pure HNTs. The defined and sharp peaks in the HNTs Figure 4.5 indicate a high level of crystallinity within the powder.

TEM images provided by the manufacturer (see Figure 4.8) show the HNTs have a cylindrical hollow structure which an electron dense wall, shown by the darker areas in the image. The images also show the HNTs have a high aspect ratio and are several microns in length but around 15 nm in diameter, with an inner lumen around 8 nm in diameter. The SEM image (Figure 4.7) indicates a high level of agglomeration within the HNTs forming irregular spherical structures with diameters up to 100 µm. HNTs internal and external charges are well known[391,425,437] and create a highly electrostatic tubule, prone to agglomerate like many nanomaterials[532-534]. To reduce the agglomeration and increase the homogeneity of the HNTs within the GIC matrix the powders were milled for up to 20 minutes. The dispersion of the HNTs in milled and unmilled powder samples was tracked with a fluorescent dye using optical microscopy and discussed in section 4.4.2.

Unlike the HANFs, the HNTs appeared to be unaffected by the exposure to the pH 2 solution. SEM images showed intact fibres, agglomerated and indistinguishable to those not exposed to the acid (see Figure 4.7). HNTs have been previously reported as not being susceptible to acid- or base-mediated dissolution under moderately mild conditions[535] and since the 1970s studies on the properties of the HNTs under varying pH have been studied concentrating on the change in affinity to certain molecules in the inner lumen[536,537]. This has since become a method used to etch the inner lumen to fit and transport larger molecules[538,539]. However, this occurs at a minimum 0.1 M

concentration of sulfuric acid at 333 K, conditions which would never be replicated in a setting GIC and especially the oral environment. A long-term study assessing various acids, concentrations and exposure time on HNTs concluded that even at 1 M sulfuric acid after 89 days, the external diameter of HNTs is unaffected whereas the inner lumen thickness had decreased by 35% through dissolution of the octahedral AlO_6[540]. Importantly, the authors show the HNTs retained their morphology at all pH values and time points. The SEM images support this study confirming the acid stability of the HNTs.

4.4.2 Analysis of GICs Incorporating HNTs

It has been shown that agglomerates of nanomaterials can create weakened zones in a material[520], therefore it was important to ensure a homogeneous distribution of the HNTs throughout the GIC powder and thus the GIC matrix. Mixing the powders together did not appear to have created a homogenous mix and may therefore not be effective in distributing the HNTs throughout the GIC. Optical microscopy used to evaluate the milled GIC powder showed dark brown patches from the acridine orange stained HNTs initially at low milling times after being mixed. As the milling time increased, there was a reduction in these patches and a visible difference in the dispersion of these brown spots indicates a more homogenous HNT-GIC mix. Milling has been shown to be effective in the dispersion of HNTs[541] but may also cleave kaolin-like particles creating a more dense and lower particle size[542-545] affecting the morphology of the HNTs. This may have been responsible for the colour change in the

GIC from the A3 shade to a grey appearance creating more free alumina through HNT cleaving. Similarly, milling is an effective industrial method of distributing smaller particles within a bulkier matrix. It is the primary manufacturing method of the GIC (chapter 2 section 2.1) and is an effective method of reducing the particle size of GICs[546] and a lower particle size distribution has been correlated to increased CS[242]. Milling the GIC further using the method did significantly increase the CS as expected, however there was no statistical difference between mixing and milling when various percentages of HNTs were added. It is possible that these bundles of HNTs may be protecting the grinding of the GIC powder, which is ultimately responsible for any increased CS. Assessment of the particle size found an increase in the smallest range of particles (4.48 – 0.02 μm) by nearly 7% but did not contribute towards increased CS when both milled and unmilled groups were compared against each other.

A decrease in CS was seen in HNT substitutions up to 3% in both milled and unmilled cements indicating the HNTs have an adverse effect at lower levels. This could be because they do not react with the PAA in the GIC liquid and therefore hinder the reaction in the matrix, or that they provide a reduced concentration of alumina and silica to the reaction because (while the glass was substituted for these HNTs by weight), not all the HNTs consisted of aluminosilicate and a large concentration is bound hydroxyl water between the interspacing within the layers of alumina and silica. This bound water is lost upon heating the material between 450 - 700°C changing the crystalline d-spacing which may cause the structure to collapse or distort[547-549]. Studies have shown the stability of the HNTs in acidic environments and therefore free

alumina and silica ions may be unlikely to be released in the early stages of the setting reaction. This may also account for the reason why at higher percentage substitutions, a decrease in CS is seen and that a balance between the reinforcing effect of the nanotube and the excessive ions may be required. At concentrations at 5% or above an increase was seen, significant in the unmilled powder but not the milled powder. It is possible that the HNT may have been cleaved during the aggressive milling process reducing the reinforcing effects. Additionally, a lower particle size seen in the control milled powder compared to the unmilled increased the CS by just under 7% which contributes to the increase seen in the 5% HNT milled powder. A combination of this already increased CS and potential cleavage of the HNTs may have led to the lower than expected increase in the 5% HNT. At higher concentrations the handling properties became noticeably different and the cement paste after mixing was a much lower viscosity than the control GIC. This was a surprising result, as HNTs are well known for their hydrophilic properties, there were also no changes to the viscous GIC liquid and an overall increase in the surface area of the powder could have been predicted to result in the opposite effect. Nanomaterials have reported lubricating properties[550-552] which may have contributed to the more fluid mixing when the GIC liquid was added. However, under the assumption that the HNTs do not contribute to the setting reaction of the GIC due to their stability it would eventuate in a significant reduction in the aluminosilicate glass component in the setting reaction. This deficit of reactive base will reduce the rate of reaction as it becomes limited to the reactive carboxylic acid chains accounting for a lower viscosity mix. To create handling properties more like those of the control GIC, reductions in the GIC liquid were trialled

and the CS tested for each reduction, setting properties of the final 20% reduction compared to the commercial control were assessed in chapter 5. It should be noted that as the GIC liquid was reduced, the CS standard deviations increased (Table 4.4) suggesting poor homogeneity in these mixes. However, very few 20% less GIC liquid specimens were rejected, contrary to the 30% less GIC liquid which led to a large quantity of rejects. Control samples using 10, 20 and 30% less liquid was not viable as the cement became too difficult to mix and led to a large quantity of rejected cements. The reduction in the GIC liquid led to increases in CS as expected and it is well established that a lower powder to liquid ratio increases various strength properties of GICs[193,553], this effect is further seen from the results above. Overall, compared to the manufacturer supplied GIC, a 33% increase was gained through a combination of reinforcement using HNTs and reduced GIC liquid due to a lower viscosity mix. No changes in the tensile properties, indirectly measured through DTS, were seen.

4.5 Conclusions and Future Directions

Substituting 5% HNTs w/w for the fluoroaluminosilicate glass component of the GIC powder led to a 33% increase in CS from 140.2 to 187.2 MPa when combined with a reduction in the GIC liquid of 20% (Table 4.4). It was found that the HNTs exhibited reduced levels of dispersion within the GIC powder when mixed by rolling on a tube roller, but the use of a mill improved dispersion over a 20-minute period but slightly reduced the particle size distribution of the powder by increasing the group of the lowest particle sizes by around 7% (Table 4.2). GIC-HNTs mix to a noticeably lower

viscosity to the manufacturers control. A reduction in the GIC liquid reverted the viscosity of the mix closer to the control as well as significant increases in CS. 30% less liquid became too difficult to mix and would not have been a viable product commercially as the cement would have nearly set by the time it was mixed sufficiently. The objective of increasing the CS has been achieved and therefore the null hypothesis set out in section 4.2.3 can be rejected and the hypothesis accepted. Although no changes in the tensile properties were seen, it is important clinically that other properties of the GIC have not been reduced because of the HNT inclusion or additional processing of the powder. The change is cement colour was not replicated when the steel balls were replaced with glass ones therefore this increase in CS was still achieved without jeopardising the cement shade or aesthetics of the final restoration. Future opportunities exist in quantifying the handling characteristics of the cements to track the changes in clinical working time and setting time of the cement. Other properties of conventional GICs may also have been affected from the substitution of the fluoroaluminosilicate glass for the HNTs such as fluoride release. Other properties used to measure strength may also have been affected such as wear resistance and hardness. The results of these tests are found and discussed in chapter 5

Chapter 5 Other Properties of Halloysite Nanotube Modified Glass Ionomer Cements

5.1 Introduction

GICs augmented with for 5% w/w HNT substituted for the same mass of the fluoroaluminosilicate glass component of the powder provided significant increases in CS as discussed in chapter 4. To disperse the HNTs effectively, milling was used which was shown to visually disperse the HNTs after 20 minutes. Milling with steel balls created a grey cement, however milling using equivalent sized glass balls had no effect on the colour. Substitution of the glass noticeably decreased the viscosity of the cement during mixing which would likely prolong the setting time and handling properties of the GIC in clinics. To counteract this, 20% less GIC liquid appeared to create a cement which handled in a similar way to the commercial control, this final cement is described as HNT-GIC throughout the chapter. However, these substitutions, processing and changes to the cement mix may have a detrimental effect on other properties of the GIC such as wear, hardness and its fluoride release which could represent a clinical and/or marketing disadvantage. These and other properties are explored in this chapter.

5.2 Methods and Materials

5.2.1 Cement Preparation

All cements were mixed according to the method in chapter 2 section 2.3, using HNT-GIC powder which had been milled for 20 minutes using glass balls and with 20% less GIC liquid than the usual formulation as described in chapter 4 section 4.2.2.

5.2.2 Working and Setting Time

Cements placed onto a Wilson's Oscillating Rheometer using the method in chapter 2 section 2.10.1 within 60 seconds of first mixing. All cement powders, liquids, mixing equipment and rheometer were kept at 23 ± 2°C for a minimum of 1 h before testing to ensure changes in temperature could not affect the working or setting time of the cements. Each group was tested 7 times for their working and setting times.

5.2.3 Wear

Cement samples were created and tested for wear using the method described in chapter 2 section 2.10.3. Samples were brushed for 10000 cycles at a rate of 1 cycle/second in a 19.1 mM citric acid pH 3.3 solution that had been prepared within 1 h before use. The solution was prepared by mixing the citric acid powder (Sigma) and water under constant stirring for a minimum of 30 minutes. Deionised water and artificial saliva were also trialled but did not product enough wear in the GICs, therefore a harsher acidic environment was chosen (Table 5.2). A total of 7 samples for each group were successfully tested and analysed. All samples were made on different days.

5.2.4 Hardness

Cement samples were created and tested for hardness using the method described in chapter 2 section 2.10.5 randomly testing across the surface of the cement. A total of

10 indentations were made on 6 samples of each cement. All samples were made on different days and all testing and analysis was done by the same individual.

5.2.5 Fluoride Release

Fluoride release from the control and HNT-GIC was tested according to the method described in chapter 2 section 2.10.2. Four samples of each group were tested, and all samples were made on the same day using the same batch of powder. All testing and analysis, including calibration was done on the same day after all equipment and solutions had been allowed to dwell to room temperature (20 - 25°C) for a minimum of 24 h.

5.2.6 Statistical Analysis

Working and setting times, wear and hardness were analysed using a student t-test. Fluoride release was calculated using the calibration curve which was linearized by plotting against the log of the fluoride ion concentration. Fluoride data was then plotted cumulatively as a function of time. The individual time point data from the control and HNT-GIC was compared against each other for significance using a student t-test using the method described in chapter 2 section 2.11.

5.3 Results

5.3.1 Working and Setting Time

All cements appeared identical to the commercial control by eye, no discolouration was seen when glass balls were substituted for the steel balls. Working and setting times of the GICs are presented in Table 5.1. Similar mixing viscosities and characteristics were seen across both cements during the cement mixing.

Table 5.1 - Working and setting times of the commercial control GIC and the HNT-GIC with p-values. The standard deviations are shown in parenthesis.

	Working Time (seconds)	Setting Time (seconds)
Control	132.9 (9.9)	232.7 (7.4)
HNT - GIC	157.4 (12.1)	320.6 (7.6)
t-test p-value	0.000767	8.97×10^{-7}

Table 5.1 showed the inclusion of the HNTs had a negative impact on the handling properties of the GIC, even with the reduction of the GIC liquid. Working time increased by 24.5 seconds and setting time increased 87.9 seconds, both increases were statistically significant.

5.3.2 Wear Resistance

Table 5.2 - Wear values of control GIC (Diamond Carve™ A3 lot 24623) using different solutions of media during brushing. Very little wear was achieved with large amounts of error; therefore, a more aggressive citric acid media was used. Standard deviations are shown in the parenthesis

Media	Wear (µm)
Deionised water	1.53 (0.80)
Artificial saliva	3.23 (1.50)

Table 5.3 - Reduction in height (wear) of cement sections brushed against cement sections protected from brushing with p-value. The control is commercial Diamond Carve™ A3 lot 24623. The standard deviations are shown in parenthesis

	Wear (µm)
Control	27.8 (3.2)
HNT-GIC	21.6 (5.8)
t-test p-value	0.0139

Table 5.3 showed that HNTs in the GICs created a 22.3% lower value when brushed in pH 3.3 citric acid which was statistically significant.

One sample from each group was discarded due to the PVC tape being partially removed during brushing.

5.3.3 Hardness

Over all samples tested, an average 2.66 measurements per cement sample required retesting due to either the cement slipping during indentations or the indenter meeting a pore on the cement surface, making the measurement inconclusive.

Table 5.4 - VHN values for the commercial control GIC (Diamond Carve™ A3 lot 24623_ and the HNT substituted GIC with p-value. The standard deviations are shown in parenthesis. For reference, VHN of dentine and enamel have also been included[121]

	VHN (Kg/mm^2)
Control	52.2 (7.9)
HNT-GIC	57.7 (6.2)
t-test p-value	0.000611
Dentine	62.3
Enamel	313.0

Table 5.4 demonstrated hardness significantly increased by 9.5% with HNT substituted GIC. The data had similar standard deviations suggesting homogeneity throughout the cement. No differences in porosity were observed during general testing, however this was not specifically measured. For comparison, hardness values of dentine and enamel have also been included.

5.3.4 Fluoride Release

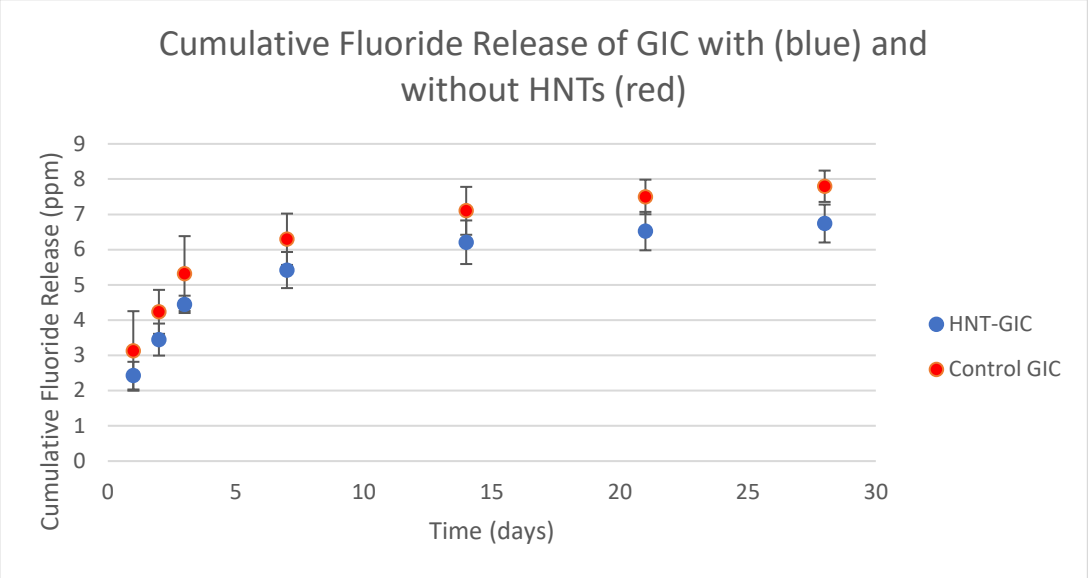

Figure 5.1 - Cumulative fluoride release from GICs with (blue) and without (red) HNTS. Error bars represent standard error. HNT-GIC fluoride release was found to be significantly lower at early time points days 1 and 2 as well as later in the setting reaction (21 and 28 days) when compared against the commercial control (Diamond Carve™ A3 lot 24623) at that time point

Table 5.5 - p-values using a student t-test of the differences between the fluoride release at each time point measured

Time (hours)	1	2	3	7	14	21	28
t-test p-value	0.00130	0.0390	0.104	0.986	0.562	0.000338	2.23×10^{-5}

Fluoride released from both GICs was initially rapid over the first 100 h and slowed over the remaining time measured (Figure 5.1). HNTs reduced the initial release of fluoride by 22.4% over the first 24 h and decreased the overall amount of fluoride released by 13.6% over the period measured. The reduction in cumulative release of fluoride was statistically different in the early and late stages of setting (Table 5.5).

5.4 Discussion

5.4.1 Working and Setting Time

The handling characteristics of the GIC were affected with the substitution of the HNTs and therefore a reduced quantity of GIC liquid was used until it was qualitatively assessed the handling properties were like that of the control, as described in chapter 4. It was not possible to create an equivalent control to these reduced concentrations of GIC liquid as reduction in the liquid with unsubstituted GIC become difficult to mix and formed many rejected cements. To quantify the setting and working times of a GIC, a Wilsons Oscillating Rheometer is often used[49,469,470] which creates a setting profile in a graphical form and a standardised approach to calculate the handling characteristics. GICs are very sensitive to changes in composition[518], temperature[470]

and mixing technique[242] which may affect its handling characteristics. Usually, an increase in the working or setting time of a GIC is directly related to a deterioration in the mechanical properties[241]. Drier high viscosity cements are well documented to have better mechanical properties to other conventional GICs, while being rapid setting[554] but a fine balance exists between strength and a long enough working time to be able to handle and place the cement correctly. With the inclusion of HNTs, the working and setting times increased, this would become a clinical disadvantage to faster setting GICs because a longer setting time would mean longer 'chair time' which would be particularly difficult for anxious patients. The change in handling properties supports the conclusions in chapter 4 that the HNTs were unlikely to be contributing to the setting reaction to the same extent that the fluoroaluminosilicate glass component was.

5.4.2 Wear Resistance

Tooth brushing simulations are useful in determining the level of wear in a GIC as an accurate simulated test to a real-life situation in the form of toothbrushing and complex masticatory motions and abrasion from food[555], thus it is generally accepted as the standard[556,557]. Brushing modifies the surface roughness of the cement through abrasion, wearing away the surface and it was noted that surfaces uncovered and exposed to the brushing in these tests were highly abraded compared to the covered sections. Wear testing was originally undertaken using deionised water and artificial saliva as the media the cements were immersed in during brushing, however the wear

using these conditions was negligible with large errors and difficult to quantify using the light profilometer. This however indicated the GICs are wear resistant under neutral conditions. Citric acid is well established to erode of the dental hard tissues, so this was used to provide a greater challenge since GICs are acid labile.

With the addition of HNTs, there was a significant reduction in wear suggesting the HNTs reinforcing properties protect the cement against wear measured using tooth brushing. This will likely help to increase the longevity of the cement in clinical use.

5.4.3 Hardness

HNTs have been shown to increase surface hardness in many other materials[558,559] and this was also seen here. As previously discussed, hardness is a simple method which probes the mechanical properties of the surface in a microscopic scale. The similarities of the standard deviations of the control and the HNG-GIC suggests both have similar levels of homogeneity. It had been discussed previously that pockets or undispersed fillers or additives can cause localised weakened patches[520], but this does not appear to have occurred in this instance and significant increases in hardness were seen across the GIC with the inclusion of HNTs uniformly. A uniform dispersion and potentially significant levels of interaction between the HNTs and the GIC matrix through hydrogen bonding maybe responsible for these increased mechanical properties[558]. It was noted that no visual difference in the porosity of the samples under indentation testing was observed, as it was previously cited that NFs may reinforce by filling mesoporous gaps in the structure[350].

5.4.4 Fluoride Release

Fluoride release profiles were similar for both cements with a higher concentration in the first few days compared to the remaining few weeks studied. This initial burst followed by a slower sustained release is a widely seen trend amongst GICs and can be described using Equation 5. Fluoride release was compared using student t-test comparing each time point against the other group in a similar method to other studies comparing fluoride release (or ANOVA when comparing more than two samples)[320,560-562]. The reduction in fluoride released from the HNT was likely due to the reduced fluoroaluminosilicate content in this cement. The HNTs were substituted for 5% of the fluoroaluminosilicate component per weight which therefore creates approximately 5% less fluoride that could be available in this powder. However, a 13.6% reduction in fluoride was seen, which proved to be statistically significant in some parts of the GIC maturation. The carboxylate in the PAA is required for the release of free fluoride during the setting reaction[563] and this concentration was reduced by 20% in the final HNT-GIC which may have also contributed to the reduction in released fluoride. The concentration of fluoride release from the cement is not necessarily determined solely from the level of fluoride in the glass, as these ions are released alongside cations of calcium and sodium in a balance between them and are therefore dependant on the release of these counterions[564]. Increasing the concentration of calcium fluoride in the glass may counter this reduction, however, the addition of fluoride does have other adverse effects on the properties of the GIC[565].

Due to the low levels of fluoride released, it is unlikely this would have any clinical relevance.

Equation 5 - Equation to describe the rate of cumulative fluoride release $[F]_c$ from a GIC in deionised water. $[F]_I$= Maximum value of fluoride released during short term reaction; t= time; $t_{1/2}$= half-life of short-term release i.e. the time required for the fluoride released by short term reaction to reach half of its maximum value; β= a constant which is a measure for the driving force of the long-term release[566]

$$[F]_c = \frac{([F]_I\, t)}{t + t_{1/2}} + \beta \sqrt{t}$$

5.5 Conclusions and Future Directions

The aim of the work presented in this chapter was to investigate whether the substitution of 5% HNTs for the glass component of the GIC, which coupled with a reduction in liquid content increased the CS by 33%, influenced other important properties of the GIC. The handling properties were affected with a significantly increased working and setting time as assessed by rheology. Handling properties can be modified by further milling of the GIC and there is a good degree of control available during manufacture, so this is not considered an unresolvable issue. Fluoride release is a much more difficult and complex mechanism to influence, however the reduction seen may not be clinically relevant in such low concentrations. The

mechanical properties of wear resistance and hardness significantly increased, reflecting the increased CS seen previously further supporting the conclusion of a stronger GIC.

Chapter 6 Conclusions and Future Work

6.1 Project Conclusions

A commercially available GIC used was augmented with HANFs and HNTs. HANF did not positively affect mechanical properties; this was attributed to the likely dissolution of the HANF during the acidic conditions of the setting GIC, it appears this has not been adequately explored by other groups investigating HA in GICs as acid lability studies are rarely carried out.

HNTs significantly increased the CS of the GIC, with the optimal formulation (5% HNTs with 20% less GIC liquid) reported here achieving a 33% increase in CS. This had a somewhat adverse effect on the handling properties by increasing setting and working times and slight reduction in the fluoride release of the cement, but no other property such as wear and hardness, was adversely influenced by the inclusion of the HNTs. In addition, significant increases in wear resistance and hardness were observed. Based on the data obtained, the null hypothesis can be rejected, and the hypothesis accepted that HNTs did significantly increase the CS of the GIC.

6.2 Strengths and Weaknesses of the Project

The project utilised a commercially available GIC with the added value of having access to exact compositions, manufacturing methods, testing procedures and other commercially sensitive technical information held by the manufacturer due to the researcher's employment under the manufacturer since 2010. This also opened the project to manipulation of these parameters if required or replication during the progression of the project. For example, the use of milling as a method of dispersing

additives within a material is well established on site, therefore preparation of the materials required such as the GIC powder and liquid could easily be achieved. The project also benefited from being able to substitute HANFs and HNTs for the glass component of the GIC powder. This could not have been achieved using a commercially available 'off the shelf' GIC with all components pre-mixed. The method of using oscillating rheology to measure the handling properties of a setting GIC is not a new one[49]. The method was used to give quantitative information regarding the working and setting times of the GIC, although this differs to the ISO method, it was preferred here in order to assess any differences giving more reproducible and measurable data.

The project used a novel method of synthesising HANFs using an economical and commercially viable process, adapted from the original publication. These HANFs were shown to be sensitive to the low pH present in the GIC setting reaction, despite evidence of strength increases in other materials such as composites. This phenomenon had not been discussed in other studies involving HA nanomaterials and no such procedure existed to assess this effect.

As previously discussed in section 1.7.3, HNTs have shown some success in strengthening other materials, such as composites. However, to date, no publication exists of HNTs being used as a method of increasing CS in a conventional GIC.

SEM analysis of the HANFs and HNTs produced images with highly agglomerated bundles of fibres. It is unknown if the processing of the powders for SEM analysis, as described in section 2.9.2, had a significant or contributing effect on this. Before

imaging, the powder coated SEM stub is subjected to a high vacuum which may have forced individual fibres to bind together and form larger bundles. Other methods such as environmental SEM may be useful to negate any effect this may have caused. Environmental SEM examines the specimen or material under a gaseous environment and can even be used to examine liquid phase materials[567].

6.3 Future Work

As previously discussed in section 3.5, further work could be undertaken to explore the use of other various surfactants described on the effect of HANFs to protect these against proton attack. Other surfactants mentioned included polymers, ionic and non-ionic variations which may have further success.

HANFs were incorporated into the GIC through a method of mixing and was unsuccessful in reinforcing the GIC, probably due to the acid lability of the high surface area fibres. Milling or utilising a dye to assess the dispersion was not explored with HANFs and was used retrospectively in the development of HNTs because of the data available linking the dispersion of HNTs to the level of reinforcement. The effect of milling has been shown to not have a direct significant impact on the CS of the GIC, therefore it is a useful method of dispersing the additives without being responsible for any CS increases. Further work may be required to assess the effect of milling of the HANFs as this biocompatible material presents an excellent option for strength reinforcement as discussed in section 1.7.2.

HNTs are not new materials but are relatively new in the reinforcement of materials. Further development is required to assess the effect of the milling on the HNTs and whether these are cleaved during the process and potentially reducing the reinforcing potential of the HNTs in their current morphology. HNTs of various grades and types are available commercially, further development to assess these different grades such as various alumina: silica ratios would be useful to determine the effect on strength reinforcement.

As previously discussed, these GICs are manufactured through a process of milling the glass frit to a powder with an optimal particle size before milling the various components of the cement together. Milling used to disperse the HNTs throughout the GIC powder was like that employed during manufacturing and can be scaled up and incorporated into existing manufacturing processes. It was found that the use of stainless-steel milling balls changed the final appearance of the cement and turned it grey, these were ultimately replaced by glass balls which rectified this problem. Under current manufacturing processes, ceramic balls are used, and further work would be required to investigate if this would have a similar effect as the steel media. As previously mentioned, optimisation of the cement to counter the changes in working and setting time would be required by further milling the powder but without having a detrimental effect on existing strength increases found by potentially cleaving the HNTs. As previously mentioned, HNTs are relatively cheap compared to the cost of the components in the GIC powder, such as the fluoroaluminosilicate glass, which also requires processing prior to being included in the final powder. Therefore, costs

associated with the addition of HNTs to the material would be minimal and highly advantageous in commercialisation.

While the project covered important characteristics of GICs such as fluoride release and wear, some such as bond strength and flexural strength were not measured. The ability to chemically bond to dentine and enamel are sought after properties of GICs distinguishing them from other materials such as composites and amalgam. It is not known what effect the nanomaterials may have on bond strength, but studies discussed in section 1.6.4 how indicated additives such as HA can penetrate deeper into dentine tubules during GIC placement, thus increasing bond strength. While this was not measured, it would likely have been a clinically significant advantage to increase the bond strength further, however this was outside of the scope of the project. Strength was measured through testing the CS and indirectly measuring the tensile properties through DTS testing. However, as discussed in section 1.4.1, many other methods of testing strength are available, including flexural strength through either three-point bending methods or BFS, often used in testing of dental materials, mainly composites. Due to the brittle nature of the GICs, test methods often used on ductile materials may not perform well and create many errors or failed specimens. The effect of the HNTs on the flexural strength and thus ductility of the GIC may have increased, as nanofibres with long aspect ratios have shown to have this effect, even when CS has been unaffected[294]. The testing of wear resistance is often undertaken using toothbrush simulation, however, to create a harsher environment and initiate some wear in the GICs, acidic conditions were used. To fully assess wear resistance, repeating the experiment under various conditions GICs would be exposed to, such as

food simulations, prophylaxis pastes or further brushing under artificial saliva until wear has been initiated may be beneficial to create a more extensive wear profile. After a device is manufactured, usually it goes through one or more quality control (QC) checks to ensure conformity to its design specifications and regulatory requirements. Currently, GICs undergo QC checks on every batch manufactured, it includes working and setting time, colour and a periodic CS test which must meet predefined specifications and tolerances set out according to the company's quality management system (QMS). Currently, these types of GIC are tested against ISO 9917-1:2007 for water-based cements which defines test methodologies and acceptance criteria for a range of tests, including CS. This ISOs test method for CS differs to that used in this project, these main differences are highlighted in Table 6.1[446].

Table 6.1 - Differences in methodology used compared to the ISO method. It is unlikely these differences would have a substantial effect on the result, however, in order to claim ISO conformance, it is likely these methods would need to be accommodated.

ISO 9917-1:2007 method	Project method used	Rationale
Set cement for 1 h at 37°C	Set cement for 15 minutes at 37°C	These cements set within 15 minutes from start of mixing, therefore an hour under no increased humidity in an oven is not what would occur clinically
Store set cement in deionised water for 23 ± 0.5 h	Store set cement at 100% relative humidity for 24 ± 1 h	Clinically, cements are not fully immersed in water/saliva after placement but a high humidity environment in the mouth therefore this was modified to replicate the clinical conditions of use
Stored in grade 3 deionised water to the standard defined ISO 3696:1987	Stored in lab deionised water	Grade 3 water is standard water purified through distillation, reverse osmosis or deionisation. The lab deionised water would therefore likely be equivalent, although not graded as such
Measure cement diameter four times at right angles to each other	Measure cement diameter three times randomly	Randomly was chosen in order to avoid any specimen shape distortions caused by the connecting parts of the steel moulds which may skew results and make specimens appear larger than they are
Sheet of damp filter paper on test platforms	No paper used	Paper is used to avoid friction and uneven breakage of specimens. This was easily detected by the break profile on the force-displacement graphs and was therefore not required

The creation of a stronger GIC may have a place in the market, especially due to the phasing down of dental amalgam[130]. If the modified device was to be brought to market, several obstacles pre-commercialisation of the device would need to be overcome. These GICs are a class IIa medical device as defined under the current Medical Device Directive (MDD) also known as the Council Directive 93/42/EEC and require a CE mark in order to be marketed and sold as a medical device in Europe[299]. Unlike class I medical devices, which are self-registered in the UK with the Medical Health Regulatory Authority (MHRA), class II and above devices require notified body approval and are subject to intense scrutinization by these notified bodies to meet the requirements of the MDD[568]. All CE marked devices or device families are required to have technical documentation or a file containing information regarding the components, intended use and contraindications of the device. Additionally, the MDD require the device to meet the essential requirements defined under annex I which require the device to have been evaluated for its risks including a clinical evaluation report (CER) and a biocompatibility report. The CER assesses the safety and clinical effectiveness of the device. The data obtained during the project can contribute largely towards this report and provides evidence of characteristics such as CS, wear resistance, handling properties and fluoride release.

As previously mentioned, HNTs are generally understood as being safe for use[437,516], however they have no current uses in commercially available dental restoratives meaning data regarding a pre-existing device cannot be relied upon and a significant level of testing to determine the products safety would be required. Some methods of

conformance to biocompatibility testing include the ISO 10993 series[569,570] which include investigation for cytotoxicity[571] and irritation/sensitisation[572]. For dentistry in particular, ISO 7405 studies biocompatibility against some more appropriate tissue such as dentin and pulp[569]. The recently introduced Medical Device Regulations (MDR), due to replace the MDD, incorporates requirements and regulations for devices containing nanomaterials. It is the HNTs which are the only new component of an existing and well-established medical device. Medical devices containing nanomaterials are to be reviewed to assess if the nanomaterial is bound or can be released from the device in addition to which parts of the body will likely encounter the nanomaterial. In 2011, the European Commission issued their definition of a nanomaterial in respect to uses in medical devices as having 50% or more of the particles with internal or external dimensions in the nanoscale, then defining nanoscale as between 1 – 100 nm[573] which has since been adopted by the MDR. Additionally, requirements on labelling and packaging to state the device contains nanomaterials when there is a possibility of it being released from the device must now be added. If this is the case, and the device does not encapsulate or bind the nanomaterial, the device must be classified as a class III medical device under rule 19 of the MDR, the highest classification and therefore subjected to the most severe testing and conformance routes[574]. It is therefore important, going forward, to deduce if these HNTs are bound by the cement matrix or these HNTs may leach from the GIC and enter the body.

6.4 Publications

Publications presented in the appendix were published based on a separate project the researcher was involved in, relating to a new antimicrobial NP incorporated into the same material used in this project. That project was sponsored by the same manufacturer the researcher is currently employed by and therefore acted as industrial supervisor and advisor to the project, occasionally providing technical data or manufacturing information when required. None of the data gathering, analysis or conclusions were contributed towards by the researcher and author of this thesis. To date of this thesis, one publication based on this work has been submitted for this project to the journal *Dental Materials* and is pending peer-review.

References

1 Selwitz, R. H., Ismail, A. I. & Pitts, N. B. Dental caries. *The Lancet* **369**, 51-59 (2007).

2 Marcenes, W. *et al.* Global burden of oral conditions in 1990-2010: a systematic analysis. *J Dent Res* **92**, 592-597, (2013).

3 Steele, J. G., Treasure, E. T., O'Sullivan, I., Morris, J. & Murray, J. J. Adult Dental Health Survey 2009: transformations in British oral health 1968-2009. *Br Dent J* **213**, 523-527, (2012).

4 Eaton, K. A. The adult dental health survey 2009. *Prim Dent Care* **18**, 99-100 (2011).

5 Public Health England, *Southampton water fluoridation scheme*, https://www.gov.uk/government/news/southampton-water-fluoridation-scheme, (2014).

6 World Dental Federation, The Oral Health Atlas. (FDI, 2015).

7 Dunsky, J. L. Alfred Einhorn: the discoverer of procaine. *J Mass Dent Soc* **46**, 25-26 (1997).

8 Loesche, W. J., Hockett, R. N. & Syed, S. A. The predominant cultivable flora of tooth surface plaque removed from institutionalized subjects. *Arch Oral Biol* **17**, 1311-1325 (1972).

9 Featherstone, J. D. Prevention and reversal of dental caries: role of low level fluoride. Community Dent Oral Epidemiol 27, 31-40 (1999).

10 Ritter, A. V., Edison, R. S. and Donovan T. E., Dental Caries: Etiology, Clinical Characteristics, Risk Assessment and Management, Pocket Dentistry Ch. 2, (2015).

11 Ismail, A. I. Visual and visuo-tactile detection of dental caries. *J Dent Res* **83 Spec No C**, C56-66 (2004).

12 Ismail, A. I. Clinical diagnosis of precavitated carious lesions. *Community Dent Oral Epidemiol* **25**, 13-23 (1997).

13 Pitts, N. B. Diagnostic tools and measurements--impact on appropriate care. *Community Dent Oral Epidemiol* **25**, 24-35 (1997).

14 Bader, J. D., Shugars, D. A. & Bonito, A. J. Systematic reviews of selected dental caries diagnostic and management methods. *J Dent Educ* **65**, 960-968 (2001).

15 Larsen, M. J. & Fejerskov, O. Chemical and structural challenges in remineralization of dental enamel lesions. *Scand J Dent Res* **97**, 285-296 (1989).

16 Featherstone, J. D. Caries prevention and reversal based on the caries balance. *Pediatr Dent* **28**, 128-132; discussion 192-128 (2006).

17 Cunha-Cruz, J. *et al.* Salivary characteristics and dental caries: evidence from general dental practices. *J Am Dent Assoc* **144**, e31-40 (2013).

18 Marinho, V. C., Higgins, J. P., Sheiham, A. & Logan, S. Fluoride toothpastes for preventing dental caries in children and adolescents. *Cochrane Database Syst Rev*, (2003).

19 Marinho, V. C., Higgins, J. P., Logan, S. & Sheiham, A. Topical fluoride (toothpastes, mouthrinses, gels or varnishes) for preventing dental caries in children and adolescents. *Cochrane Database Syst Rev*, (2003).

20 Marinho, V. C., Worthington, H. V., Walsh, T. & Chong, L. Y. Fluoride gels for preventing dental caries in children and adolescents. *Cochrane Database Syst Rev*, (2015).

21 Marinho, V. C., Chong, L. Y., Worthington, H. V. & Walsh, T. Fluoride mouthrinses for preventing dental caries in children and adolescents. *Cochrane Database Syst Rev* **7**, (2016).

22 Rasines, G. Fluoride toothpaste prevents caries in children and adolescents at fluoride concentrations of 1000 ppm and above. *Evid Based Dent* **11**, 6-7, (2010).

23 Axelsson P, A. *Diagnosis and risk prediction of dental caries*. Vol. 2 (Quintessence Publishing Company Inc., 2000).

24 Centres for Disease Control and Prevention. *Fluoridation Statistics*, <https://www.cdc.gov/fluoridation/statistics/2014stats.htm> (2014).

25 Centres for Disease Control and Prevention. *Recommendations for Using Fluoride to Prevent and Control Dental Caries in the United States*, <https://www.cdc.gov/mmwr/preview/mmwrhtml/rr5014a1.htm> (2001).

26 Centres for Disease Control and Prevention. Engineering and administrative recommendations for water fluoridation. Report No. RR-13, 40 (1995).

27 Water fluoridation confirmed to prevent dental decay in US children and adolescents. *Br Dent J* **225**, 10, (2018).

28 National Institue of Health Research Report. The prevalence of dental caries in United States children. Report No. 82-2245, (National Institute of Health, 1981).

29 Kelly JE, H. C. Basic dental examination findings of persons 1-74 years. Report No. 79-1662, (US Department of Health, Education, and Welfare, National Center for Health Statistics, 1979).

30 National Institue of Health Research Report. Oral health of United States children. The National Survey of Dental Caries in U.S. School Children: 1986-

1987. National and regional findings. Report No. 89-2247, (National Institute of Health, MD, 1989).

31 Kaste LM, S. R., Oldakowski RJ, Brunelle JA, Winn DM, Brown LJ. Coronal caries in the primary and permanent dentition of children and adolescents 1--17 years of age: United States, 1988-1991. *J Dent Res* **75**, 10 (1996).

32 Mullen, J. & European Association for Paediatric, D. History of water fluoridation. *Br Dent J* **199**, 1-4, (2005).

33 Meikle, J. New Fight to Stop Mass Fluoridation, *The Guardian*. (2009).

34 Unknown Author. Another step taken towards fluoride in water - despite protests. *The Yorkshire Post* (2016). <https://www.yorkshirepost.co.uk/news/health/another-step-taken-towards-fluoride-in-water-despite-protests-1-8240004>.

35 Unknown Author. *Fluoride plan goes down the drain*, <http://news.bbc.co.uk/1/hi/scotland/4022833.stm> (2004).

36 Water fluoridation safe and effective. *Br Dent J* **224**, 674, (2018).

37 Frazao, P. & Narvai, P. C. Water fluoridation in Brazilian cities at the first decade of the 21st century. *Rev Saude Publica* **51**, 47, (2017).

38 Hull and the East Riding of Yorkshire, *Br Dent J.* Vol. 222, 644 (2017).

39 Iheozor-Ejiofor, Z. *et al.* Water fluoridation for the prevention of dental caries. *Cochrane Database Syst Rev*, (2015).

40 Moore, D., Poynton, M., Broadbent, J. M. & Thomson, W. M. The costs and benefits of water fluoridation in NZ. *BMC Oral Health* **17**, 134, (2017).

41 Black GV, B. R. *Black's Operative Dentistry*. 9th edn, (Medico-Dnetal Publishing Co., 1955).

42 Shivakumar, K. M., Prasad, S. & Chandu, G. N. International Caries Detection and Assessment System: A new paradigm in detection of dental caries. *J Cons Dent : JCD* **12**, 10-16, (2009).

43 Pitts NB, I. A., Martignon S, Ekstrand K, Douglas GVA, Longbottom C. ICCMS™ Guide for Practitioners and Educators. 38 (Kings College London, 2014).

44 Schwendicke, F. *et al.* Managing Carious Lesions: Consensus Recommendations on Carious Tissue Removal. *Adv Dent Res* **28**, 58-67, (2016).

45 Frencken, J. E. *et al.* Minimal intervention dentistry for managing dental caries - a review: report of a FDI task group. *Int Dent J* **62**, 223-243, (2012).

46 ADA Council on Scientific Affairs. Direct and indirect restorative materials. *J Am Dent Assoc* **134**, 463-472 (2003).

47 Wilson, A. D. & Kent, B. E. A new translucent cement for dentistry. The glass ionomer cement. *Br Dent J* **132**, 133-135 (1972).

48 Wilson, A. D. Glass-ionomer cement--origins, development and future. *Clin Mater* **7**, 275-282 (1991).

49 Wilson, A. D., Crisp, S. & Ferner, A. J. Reactions in glass-ionomer cements: IV. Effect of chelating comonomers on setting behavior. *J Dent Res* **55**, 489-495, (1976).

50 Sidhu, S. K. Glass-ionomer cement restorative materials: a sticky subject? *Aus Dent J* **56 Suppl 1**, 23-30, (2011).

51 Sidhu, S. K. & Nicholson, J. W. A Review of Glass-Ionomer Cements for Clinical Dentistry. *J Funct Biomater* **7**, (2016).

52 Gorseta, K., Borzabadi-Farahani, A., Moshaverinia, A., Glavina, D. & Lynch, E. Effect of different thermo-light polymerization on flexural strength of two glass ionomer cements and a glass carbomer cement. *J Prosthet Dent* **118**, 102-107, (2017).

53 Kahvecioglu, F., Tosun, G. & Ulker, H. E. Intrapulpal Thermal Changes during Setting Reaction of Glass Carbomer(R) Using Thermocure Lamp. *Biomed Res Int* **2016**, (2016).

54 Gorseta, K. *et al.* One-year clinical evaluation of a Glass Carbomer fissure sealant, a preliminary study. *Eur J Prosthodont Restor Dent* **22**, 67-71 (2014).

55 Nicholson, J. W., Brookman, P. J., Lacy, O. M. & Wilson, A. D. Fourier transform infrared spectroscopic study of the role of tartaric acid in glass-ionomer dental cements. *J Dent Res* **67**, 1451-1454, (1988).

56 Ellis, J., Anstice, M. & Wilson, A. D. The glass polyphosphonate cement: a novel glass-ionomer cement based on poly(vinyl phosphonic acid). *Clin Mater* **7**, 341-346 (1991).

57 Khouw-Liu, V. H., Anstice, H. M. & Pearson, G. J. An in vitro investigation of a poly (vinyl phosphonic acid) based cement with four conventional glass-ionomer cements Part 2: Maturation in relation to surface hardness. *J Dent* **27**, 359-365 (1999).

58 Mount, G. Making the most of glass ionomer cements: 1. *Dent Update* **18**, 276-279 (1991).

59 Neelakantan, P., John, S., Anand, S., Sureshbabu, N. & Subbarao, C. Fluoride release from a new glass-ionomer cement. *Oper Dent* **36**, 80-85, (2011).

60 Nicholson, J. W. & Czarnecka, B. Review paper: Role of aluminum in glass-ionomer dental cements and its biological effects. *J Biomater Appl* **24**, 293-308, (2009).

61 Matsuya, S., Maeda, T. & Ohta, M. IR and NMR Analyses of Hardening and Maturation of Glass-ionomer Cement. *J Dent Res* **75**, 1920-1927, (1996).

62 Erickson, R. L. & Glasspoole, E. A. Bonding to tooth structure: a comparison of glass-ionomer and composite-resin systems. *J Esthet Dent* **6**, 227-244 (1994).

63 Yoshida, Y. *et al.* Evidence of chemical bonding at biomaterial-hard tissue interfaces. *J Dent Res* **79**, 709-714 (2000).

64 Gao, W. & Smales, R. J. Fluoride release/uptake of conventional and resin-modified glass ionomers, and compomers. *J Dent* **29**, 301-306 (2001).

65 Bhattacharya, A., Vaidya, S., Tomer, A. K., Mangat, P. & Raina, A. A. Evaluation and comparison of physical properties and fluoride release of newly introduced ceramic reinforced glass-ionomer restorative material with other glass ionomer cements–An in vitro study. *Int J App Dent Sci **3**, 486-492* (2017).

66 Leyhausen, G., Abtahi, M., Karbakhsch, M., Sapotnick, A. & Geurtsen, W. Biocompatibility of various light-curing and one conventional glass-ionomer cement. *Biomaterials* **19**, 559-564 (1998).

67 Tarim, B., Hafez, A. A., Suzuki, S. H., Suzuki, S. & Cox, C. F. Biocompatability of compomer restorative systems on nonexposed dental pulps of primate teeth. *Oper Dent* **22**, 149-158 (1997).

68 Cho, S. Y. & Cheng, A. C. A review of glass ionomer restorations in the primary dentition. *J Can Dent Assoc* **65**, 491-495 (1999).

69 Knibbs, P. J. Glass ionomer cement: 10 years of clinical use. *J Oral Rehabil* **15**, 103-115 (1988).

70 Smales, R. J., Lee, Y. K., Lo, F. W., Tse, C. C. & Chung, M. S. Handling and clinical performance of a glass ionomer sealant. *Am J Dent* **9**, 203-205 (1996).

71 Lee, J. J. *et al.* Physical properties of resin-reinforced glass ionomer cement modified with micro and nano-hydroxyapatite. *J Nanosci Nanotechnol* **10**, 5270-5276 (2010).

72 Noort van, R. & Michele, B. *Introduction to Dental Materials*. 4 edn, (Elsevier Mosby, 2013).

73 Rizzante, F. *et al. Indications and restorative techniques for glass ionomer cement*. Vol. 12 (2016).

74 Garg, N., Chandra, S. & Garg, A. *Textbook of operative dentistry*. Second edn, (Jaypee Medical, 2013).

75 Oldham, D. F., Swartz, M. L. & Phillips, R. W. Retentive properties of dental cements. *J Pros Dent* **14**, 760-768, (1964).

76 Queiroz, A. M. *et al.* Antibacterial activity of root canal filling materials for primary teeth: zinc oxide and eugenol cement, Calen paste thickened with zinc oxide, Sealapex and EndoREZ. *Braz Dent J* **20**, 290-296 (2009).

77 Siqueira Jr, J. F. & Lopes, H. P. Mechanisms of antimicrobial activity of calcium hydroxide: a critical review. *Int End J* **32**, 361-369 (1999).

78 Ben-Amar, A., Liberman, R., Apatowsky, U. & Pilo, R. pH changes of glass-ionomer lining materials at various time intervals. *J Oral Rehabil* **26**, 847-852 (1999).

79 Ahovuo-Saloranta, A. *et al.* Sealants for preventing dental decay in the permanent teeth. *Cochrane Database Syst Rev* (2013).

80 Consensus development conference statement on dental sealants in the prevention of tooth decay. National Institutes of Health. *J Am Dent Assoc* **108**, 233-236 (1984).

81 Ahovuo-Saloranta, A., Hiiri, A., Nordblad, A., Makela, M. & Worthington, H. V. Pit and fissure sealants for preventing dental decay in the permanent teeth of children and adolescents. *Cochrane Database Syst Rev*, (2008).

82 Wright, J. T. *et al.* Evidence-based clinical practice guideline for the use of pit-and-fissure sealants: A report of the American Dental Association and the American Academy of Pediatric Dentistry. *J Am Dent Assoc* **147**, 672-682 (2016).

83 Anusavice, K. J., Shen, C. & Rawls, H. R. *Phillips' science of dental materials*. (Elsevier Health Sciences, 2013).

84 Mickenautsch, S. & Yengopal, V. Caries-preventive effect of high-viscosity glass ionomer and resin-based fissure sealants on permanent teeth: a systematic review of clinical trials. *PloS one* **11**, (2016).

85 Beiruti, N., Frencken, J. E., van't Hof, M. A. & van Palenstein Helderman, W. H. Caries-preventive effect of resin-based and glass ionomer sealants over time: a systematic review*. Community Dent Oral Epidemiol* (2017).

86 Perondi, P. R., Oliveira, P. H. C., Cassoni, A., Reis, A. F. & Rodrigues, J. A. Ultimate tensile strength and microhardness of glass ionomer materials. *Braz Dent Sci* **17**, 16-22 (2014).

87 Yengopal, V., Mickenautsch, S., Bezerra, A. C. & Leal, S. C. Caries-preventive effect of glass ionomer and resin-based fissure sealants on permanent teeth: a meta analysis. *J Oral Sci* **51**, 373-382 (2009).

88 Kumar, G. & Shivrayan, A. Comparative study of mechanical properties of direct core build-up materials. *Contemp Clin Dent* **6**, 16-20, (2015).

89 Laske, M., Opdam, N. J., Bronkhorst, E. M., Braspenning, J. C. & Huysmans, M. C. Longevity of direct restorations in Dutch dental practices. Descriptive study out of a practice based research network. *J Dent* **46**, 12-17, (2016).

90 Chisini, L. A. *et al.* Restorations in primary teeth: a systematic review on survival and reasons for failures. *Int J Paediatr Dent* **28**, 123-139, (2018).

91 Gao, S. S. The longevity of posterior restorations in primary teeth. *Evid Based Dent* **19**, 44, (2018).

92 Wiegand, A., Buchalla, W. & Attin, T. Review on fluoride-releasing restorative materials--fluoride release and uptake characteristics, antibacterial activity and influence on caries formation. *Dent Mater* **23**, 343-362, (2007).

93 Forsten, L. Fluoride release and uptake by glass-ionomers and related materials and its clinical effect. *Biomaterials* **19**, 503-508 (1998).

94 Kirsten, M. *et al.* Hygroscopic expansion of self-adhesive resin cements and the integrity of all-ceramic crowns. *Dent Mater* **34**, 1102-1111, (2018).

95 Bolhuis, H. P. [Endodontically treated teeth: use of adhesive core build-up procedures]. *Ned Tijdschr Tandheelkd* **112**, 491-496 (2005).

96 Banerjee, A., Kidd, E. A. & Watson, T. F. In vitro evaluation of five alternative methods of carious dentine excavation. *Caries Res* **34**, 144-150, (2000).

97 Frencken, J. E. Atraumatic restorative treatment and minimal intervention dentistry. *Br Dent J* **223**, (2017).

98 Leal, S. C., Abreu, D. M. & Frencken, J. E. Dental anxiety and pain related to ART. *J Appl Oral Sci* **17 Suppl**, 84-88 (2009).

99 Frencken, J. E., Pilot, T., Songpaisan, Y. & Phantumvanit, P. Atraumatic restorative treatment (ART): rationale, technique, and development. *J Public Health Dent* **56**, 135-140; discussion 161-133 (1996).

100 Fleming, G. J. & Zala, D. M. An assessment of encapsulated versus hand-mixed glass ionomer restoratives. *Oper Dent* **28**, 168-177 (2003).

101 Nomoto, R., Komoriyama, M., McCabe, J. F. & Hirano, S. Effect of mixing method on the porosity of encapsulated glass ionomer cement. *Dent Mater* **20**, 972-978, (2004).

102 Rodrigues, D. S. *et al.* Mechanical Strength and Wear of Dental Glass-Ionomer and Resin Composites Affected by Porosity and Chemical Composition. *J Bio- and Tribo-Corrosion* **1**, 24, (2015).

103 Lohbauer, U. Dental glass ionomer cements as permanent filling materials?–Properties, limitations and future trends. *Materials* **3**, 76-96 (2009).

104 Nicholson, J. W. Maturation processes in glass-ionomer dental cements. *Acta biomaterialia odontologica Scandinavica* **4**, 63-71 (2018).

105 Duminis, T., Shahid, S., Karpukhina, N. G. & Hill, R. G. Predicting refractive index of fluoride containing glasses for aesthetic dental restorations. *Dent Mat* **34**, e83-e88 (2018).

106 Freitas, M. C. C. A., Fagundes, T. C., Modena, K. C. D. S., Cardia, G. S. & Navarro, M. F. L. Randomized clinical trial of encapsulated and hand-mixed glass-ionomer ART restorations: one-year follow-up. *J Appl Oral Sci* **26**, (2018).

107 Burke, F. J. T. & Lucarotti, P. S. K. The ultimate guide to restoration longevity in England and Wales. Part 3: Glass ionomer restorations - time to next intervention and to extraction of the restored tooth. *Br Dent J* **224**, 865-874, (2018).

108 Mjör, I. A. Glass-ionomer cement restorations and secondary caries: A preliminary report. *Quintessence Int* **27** (1996).

109 Randall, R. C. & Wilson, N. H. F. Glass-ionomer restoratives: a systematic review of a secondary caries treatment effect. *J Dent Res* **78**, 628-637 (1999).

110 Wilson, N. H. F., Burke, F. J. & Mjör, I. A. Reasons for placement and replacement of restorations of direct restorative materials by a selected group of practitioners in the United Kingdom. *Quintessence Int* **28** (1997).

111 Hyson, J. M. Amalgam: Its history and perils. *J Calif Dent Assoc* **34**, 215-229 (2006).

112 Hoffmann-Axthelm, W. [W.D. Miller - a pioneer of scientific dentistry]. *Quintessenz J* **13**, 927-930 (1983).

113 Hoffmann-Axthelm, W. The writing of dental history: a commentary. *J Am Dent Assoc* **88**, 1355-1357 (1974).

114 CRAWFORD, W. H. & LARSON, J. H. Dental restorative materials: amalgams, acrylics. *J Dent Res* **33**, 414-424, (1954).

115 Yong, J. B., Sivarajan, S. & Abbott, P. V. An analysis of the timing and materials associated with pulp disease following restorative dental treatment. *Int Endod J*, (2018).

116 American Dental Association statement on dental amalgam. *ASDC J Dent Child* **58**, 88-89 (1991).

117 WHO/FDI consensus statement on dental amalgam. *J Dent Assoc S Afr* **50**, 371 (1995).

118 Bharti, R., Wadhwani, K. K., Tikku, A. P. & Chandra, A. Dental amalgam: An update. *J Conserv Dent* **13**, 204-208, (2010).

119 Suchatlampong, C., Goto, S. & Ogura, H. Early compressive strength and phase-formation of dental amalgam. *Dent Mater J* **14**, 143-151 (1995).

120 Cho, G. C., Kaneko, L. M., Donovan, T. E. & White, S. N. Diametral and compressive strength of dental core materials. *J Prosthet Dent* **82**, 272-276 (1999).

121 Ilie, N. *et al.* Academy of Dental Materials guidance-Resin composites: Part I-Mechanical properties. *Dent Mater* **33**, 880-894, (2017).

122 Opdam, N. J., Bronkhorst, E. M., Loomans, B. A. & Huysmans, M. C. 12-year survival of composite vs. amalgam restorations. *J Dent Res* **89**, 1063-1067, (2010).

123 Wahl, M. J. & Swift, E. J., Jr. Critical appraisal: dental amalgam update-part I: clinical efficacy. *J Esthet Restor Dent* **25**, 360-364, (2013).

124 Rasines Alcaraz, M. G. *et al.* Direct composite resin fillings versus amalgam fillings for permanent or adult posterior teeth. *Cochrane Database Syst Rev*, (2014).

125 Chun, K. J. & Lee, J. Y. Comparative study of mechanical properties of dental restorative materials and dental hard tissues in compressive loads. *J Dent Biomech* **5**, (2014).

126 Espevik, S. Flow and creep of dental amalgam. *Acta Odontol Scand* **33**, 239-242 (1975).

127 Paganelli, C. *et al.* [In vitro study of amalgam corrosion]. *Med Lav* **93**, 286-289 (2002).

128 Yang, L. W. & Kong, D. G. [Comparative study of grind-resistance,corrosion,and adhesion of dental plaque on gallium and amalgam alloy's filling]. *Shanghai Kou Qiang Yi Xue* **6**, 198-201 (1997).

129 Mackey, T. K., Contreras, J. T. & Liang, B. A. The Minamata Convention on Mercury: attempting to address the global controversy of dental amalgam use and mercury waste disposal. *Sci Total Environ* **472**, 125-129, (2014).

130 Fisher, J., Varenne, B., Narvaez, D. & Vickers, C. The Minamata Convention and the phase down of dental amalgam. *Bull World Health Organ* **96**, 436-438, (2018).

131 United Nations Environment Programme, Minamata Convention on Mercury, Annex A Section II (2017).

132 Bakhurji, E., Scott, T., Mangione, T. & Sohn, W. Dentists' perspective about dental amalgam: current use and future direction. *J Public Health Dent* **77**, 207-215, (2017).

133 Bowen, R. L. Properties of a silica-reinforced polymer for dental restorations. *J Am Dent Assoc* **66**, 57-64 (1963).

134 Blum, I. R. Composite restorations in anterior teeth: fundamentals and possibilities. *Br Dent J* **201**, 313, (2006).

135 Ferracane, J. L. Resin composite-State of the art. *Dent. Mater.* **27**, 29-38, (2011).

136 Drummond, J. L. Degradation, fatigue, and failure of resin dental composite materials. *J Dent Res* **87**, 710-719, (2008).

137 Lutz, F. & Phillips, R. W. A classification and evaluation of composite resin systems. *J Prosthet Dent* **50**, 480-488 (1983).

138 Alexander, G., Hopcraft, Tyas, M. J. & Wong, R. H. K. Dentists' restorative decision-making and implications for an 'amalgamless' profession. Part 4: clinical factors. *Aus Dent J*, (2017).

139 Loomans, B. A. C. *et al.* Clinical performance of full rehabilitations with direct composite in severe tooth wear patients: 3.5 Years results. *J Dent* **70**, 97-103, (2018).

140 Collares, K. *et al.* Longevity of Anterior Composite Restorations in a General Dental Practice-Based Network. *J Dent Res* **96**, 1092-1099, (2017).

141 Palotie, U., Eronen, A. K., Vehkalahti, K. & Vehkalahti, M. M. Longevity of 2- and 3-surface restorations in posterior teeth of 25- to 30-year-olds attending Public Dental Service—A 13-year observation. *J Dent* **62**, 13-17, (2017).

142 Tyas, M. J. Adhesive dental restorative materials and systems. *Ann R Australas Coll Dent Surg* **10**, 101-107 (1989).

143 Nesbit, S. P. *et al.* in *Diagnosis and Treatment Planning in Dentistry (Third Edition)* (2017).

144 Ferracane, J. L. *et al.* Academy of Dental Materials guidance-Resin composites: Part II-Technique sensitivity (handling, polymerization, dimensional changes). *Dent Mater* **33**, 1171-1191, (2017).

145 Unemori, M., Matsuya, Y., Akashi, A., Goto, Y. & Akamine, A. Composite resin restoration and postoperative sensitivity: clinical follow-up in an undergraduate program. *J Dent* **29**, 7-13 (2001).

146 Moosavi, H., Maleknejad, F., Sharifi, M. & Ahrari, F. A randomized clinical trial of the effect of low-level laser therapy before composite placement on postoperative sensitivity in class V restorations. *Lasers Med Sci* **30**, 1245-1249, (2015).

147 Cakir, N. N., Demirbuga, S., Balkaya, H. & Karadas, M. Bonding performance of universal adhesives on composite repairs, with or without silane application. *J Conserv Dent* **21**, 263-268, (2018).

148 Taubock, T. T., Bortolotto, T., Buchalla, W., Attin, T. & Krejci, I. Influence of light-curing protocols on polymerization shrinkage and shrinkage force of a dual-cured core build-up resin composite. *Eur J Oral Sci* **118**, 423-429, (2010).

149 Rohr, N., Muller, J. A. & Fischer, J. Influence of Ambient Temperature and Light-curing Moment on Polymerization Shrinkage and Strength of Resin Composite Cements. *Oper Dent*, (2018).

150 Davidson, C. L. & Feilzer, A. J. Polymerization shrinkage and polymerization shrinkage stress in polymer-based restoratives. *J Dent* **25**, 435-440, (1997).

151 Moberg, M., Brewster, J., Nicholson, J. & Roberts, H. Physical property investigation of contemporary glass ionomer and resin-modified glass ionomer restorative materials. *Clin Oral Investig*, (2018).

152 Attin, T., Vataschki, M. & Hellwig, E. Properties of resin-modified glass-ionomer restorative materials and two polyacid-modified resin composite materials. *Quintessence Int* **27**, 203-209 (1996).

153 Bresciani, E. *et al.* Compressive and diametral tensile strength of glass ionomer cements. *J Appl Oral Sci* **12**, 344-348 (2004).

154 Baig, M. S. & Fleming, G. J. Conventional glass-ionomer materials: A review of the developments in glass powder, polyacid liquid and the strategies of reinforcement. *J Dent* **43**, 897-912, (2015).

155 Khoroushi, M. & Keshani, F. A review of glass-ionomers: From conventional glass-ionomer to bioactive glass-ionomer. *Dent Res J (Isfahan)* **10**, 411-420 (2013).

156 Savarino, L. *et al.* In vitro investigation of aluminum and fluoride release from compomers, conventional and resin-modified glass-ionomer cements: a standardized approach. *J Biomater Sci Polym Ed* **11**, 289-300 (2000).

157 Cabral, M. F. *et al.* Do conventional glass ionomer cements release more fluoride than resin-modified glass ionomer cements? *Restor Dent Endod* **40**, 209-215, (2015).

158 Garoushi, S., Vallittu, P. K. & Lassila, L. Characterization of fluoride releasing restorative dental materials. *Dent Mater J* **37**, 293-300, (2018).

159 Guo, J. *et al.* Determining the temporal development of dentin-composite bond strength during curing. *Dent Mater* **32**, 1007-1018, (2016).

160 Sulaiman, T. A., Abdulmajeed, A. A., Altitinchi, A., Ahmed, S. N. & Donovan, T. E. Physical Properties, Film Thickness, and Bond Strengths of Resin-Modified Glass Ionomer Cements According to Their Delivery Method. *J Prosthodont*, (2018).

161 Paschoal, M. A. *et al.* Fluoride release profile of a nanofilled resin-modified glass ionomer cement. *Braz Dent J* **22**, 275-279 (2011).

162 Iqbal, A., Fishan, M. & Sahar, R. Evaluating the Efficacy of Resin Modified Glass Ionomer Cement versus Conventional Glass Ionomer Cement in Terms of Success Rate: A Clinical Assessment Exploring the best in between. *Pak J Med Health Sci* **11**, 336-338 (2017).

163 McLean, J. W., Nicholson, J. W. & Wilson, A. D. Proposed nomenclature for glass-ionomer dental cements and related materials. *Quintessence Int* **25**, 587-589 (1994).

164 Luong, E. & Shayegan, A. Assessment of microleakage of class V restored by resin composite and resin-modified glass ionomer and pit and fissure resin-based sealants following Er:YAG laser conditioning and acid etching: in vitro study. *Clin Cosmet Investig Dent* **10**, 83-92, (2018).

165 Yan, Z., Sidhu, S. K., Carrick, T. E. & McCabe, J. F. Response to thermal stimuli of glass ionomer cements. *Dent Mater* **23**, 597-600, (2007).

166 Bullard, R. H., Leinfelder, K. F. & Russell, C. M. Effect of coefficient of thermal expansion on microleakage. *J Am Dent Assoc* **116**, 871-874 (1988).

167 Krejci, I., Gebauer, L., Häusler, T. & Lutz, F. [Composite polymers--an amalgam substitute for deciduous tooth cavities?]. *Schweizer Monatsschrift fur*

Zahnmedizin = Revue mensuelle suisse d'odonto-stomatologie = Rivista mensile svizzera di odontologia e stomatologia **104**, 724-730 (1994).

168 Zimmerli, B., Strub, M., Jeger, F., Stadler, O. & Lussi, A. Composite materials: composition, properties and clinical applications. A literature review. *Schweiz Monatsschr Zahnmed* **120**, 972-986 (2010).

169 Nicholson, J. W. Polyacid-modified composite resins ("compomers") and their use in clinical dentistry. *Dent Mater* **23**, 615-622, (2007).

170 Ruse, N. D. What is a "compomer"? *J Can Dent Assoc* **65**, 500-504 (1999).

171 Hammouda, I. M. & Al-Wakeel, E. E. Effect of water storage on fluoride release and mechanical properties of a polyacid-modified composite resin (compomer). *J Biomed Res* **25**, 254-258, (2011).

172 Herrera, M., Castillo, A., Bravo, M., Liébana, J. & Carrión, P. Antibacterial activity of resin adhesives, glass ionomer and resin-modified glass ionomer cements and a compomer in contact with dentin caries samples. *Oper Dent* **25**, 265-269 (2000).

173 Olegário, I. C., Hesse, D., Mendes, F. M., Bonifácio, C. C. & Raggio, D. P. Glass carbomer and compomer for ART restorations: 3-year results of a randomized clinical trial. *Clin Oral Investig* 1-10 (2018).

174 Puppin-Rontani, R. M., Baglioni-Gouvea, M. E., deGoes, M. F. & Garcia-Godoy, F. Compomer as a pit and fissure sealant: effectiveness and retention after 24 months. *J Dent Child (Chic)* **73**, 31-36 (2006).

175 Krämer, N., García-Godoy, F., Reinelt, C. & Frankenberger, R. Clinical performance of posterior compomer restorations over 4 years. *Am J Dent* **19**, 61-66 (2006).

176 Williams, P. H., Sherriff, M. & Ireland, A. J. An investigation into the use of two polyacid-modified composite resins (compomers) and a resin-modified glass poly(alkenoate) cement used to retain orthodontic bands. *Eur J Orthod* **27**, 245-251, (2005).

177 Croll, T. P., Helpin, M. L. & Donly, K. J. Multi-colored dual-cured compomer. *Pediatr Dent* **26**, 273-276 (2004).

178 Demirci, M., Ersev, H., Topcubasi, M. & Ucok, M. Clinical evaluation of a polyacid-modified resin composite in class V carious lesions: 3-year results. *Dent Mater J* **24**, 321-327 (2005).

179 Mandall, N. A. *et al.* Adhesives for fixed orthodontic brackets. *Cochrane Database Syst Rev* **4,** (2018).

180 Premović, M., Ramić, B., Stojanac, I., Drobac, M. & Petrović, L. [One-year clinical evaluation of compomer restorations in cervical lesions of different aetiology]. *Med Pregl* **65**, 115-121 (2012).

181 Pascon, F. M. *et al.* Clinical evaluation of composite and compomer restorations in primary teeth: 24-month results. *J Dent* **34**, 381-388, (2006).

182 Kramer, N. & Frankenberger, R. Compomers in restorative therapy of children: a literature review. *Int J Paediatr Dent* **17**, 2-9, (2007).

183 Cvikl, B. *et al.* Immediate shear bond strengths of a composite, a compomer and a glass ionomer to a ceramic substrate. *J Adhes Dent* **15**, 385-391, (2013).

184 Münchow, E. A., Meereis, C. T. W., de Oliveira da Rosa, W. L., da Silva, A. F. & Piva, E. Polymerization shrinkage stress of resin-based dental materials: A systematic review and meta-analyses of technique protocol and photo-activation strategies. *J Mech Behav Biomed Mater* **82**, 77-86, (2018).

185 Kumar, T., Bhargava, K., Sanap, A. & Aggarwal, S. *Advances in Reinforced Restorations: A Review*. Vol. 1 (2015).

186 Buergers, R., Schneider-Brachert, W., Hahnel, S., Rosentritt, M. & Handel, G. Streptococcal adhesion to novel low-shrink silorane-based restorative. *Dent Mater* **25**, 269-275, (2009).

187 Burgers, R., Schneider-Brachert, W., Rosentritt, M., Handel, G. & Hahnel, S. Candida albicans adhesion to composite resin materials. *Clin Oral Investig* **13**, 293-299, (2009).

188 Kelly, P. G. & Smales, R. J. Long-term cost-effectiveness of single indirect restorations in selected dental practices. *Br Dent J* **196**, 639-643; discussion 627, (2004).

189 Wren, A., Boyd, D. & Towler, M. R. The processing, mechanical properties and bioactivity of strontium based glass polyalkenoate cements. *J Mater Sci Mater Med* **19**, 1737-1743, (2008).

190 Towler, M. R., Bushby, A. J., Billington, R. W. & Hill, R. G. A preliminary comparison of the mechanical properties of chemically cured and ultrasonically cured glass ionomer cements, using nano-indentation techniques. *Biomaterials* **22**, 1401-1406 (2001).

191 Burke, F. J., Shortall, A. C., Combe, E. C. & Aitchison, T. C. Assessing restorative dental materials: I. Test methods and assessment of results. *Dent Update* **29**, 188-194, (2002).

192 Whitehead, S. A., Wilson, N. H. & Watts, D. C. Demonstration of "vertical barrelling" using profilometry. *Eur J Prosthodont Restor Dent* **7**, 131-134 (1999).

193 Crisp, S., Lewis, B. G. & Wilson, A. D. Characterization of glass-ionomer cements. 1. Long term hardness and compressive strength. *J Dent* **4**, 162-166 (1976).

194 Williams, J. A. & Billington, R. W. Increase in compressive strength of glass ionomer restorative materials with respect to time: a guide to their suitability for use in posterior primary dentition. *J Oral Rehabil* **16**, 475-479 (1989).

195 Takaki, P., Vieira, M. & Bommarito, S. Maximum bite force analysis in different age groups. *Int Arch Otorhinolaryngol* **18**, 272-276, (2014).

196 Lundgren, D. & Laurell, L. Occlusal force pattern during chewing and biting in dentitions restored with fixed bridges of cross-arch extension. I. Bilateral end abutments. *J Oral Rehabil* **13**, 57-71 (1986).

197 Gu, Y. W., Yap, A. U., Cheang, P. & Khor, K. A. Effects of incorporation of HA/ZrO(2) into glass ionomer cement (GIC). *Biomaterials* **26**, 713-720, (2005).

198 Moshaverinia, A. *et al.* Effects of incorporation of hydroxyapatite and fluoroapatite nanobioceramics into conventional glass ionomer cements (GIC). *Acta Biomater* **4**, 432-440, (2008).

199 Pereira, L. C. *et al.* Mechanical properties and bond strength of glass-ionomer cements. *J Adhes Dent* **4**, 73-80 (2002).

200 Elsaka, S. E., Hamouda, I. M. & Swain, M. V. Titanium dioxide nanoparticles addition to a conventional glass-ionomer restorative: influence on physical and antibacterial properties. *J Dent* **39**, 589-598, (2011).

201 Piwowarczyk, A., Ottl, P., Lauer, H. C. & Büchler, A. Laboratory strength of glass ionomer cement, compomers, and resin composites. *J Pros* **11**, 86-91 (2002).

202 Combe, E. C., Shaglouf, A. M., Watts, D. C. & Wilson, N. H. Mechanical properties of direct core build-up materials. *Dent Mat*, **15**, 158-165 (1999).

203 Millstein, P. L. & Naguib, G. H. Effects of two resin adhesives on mechanical properties of set amalgam. *J Pros Dent* **74**, 106-109 (1995).

204 Ender, A. *et al.* Marginal adaptation, fracture load and macroscopic failure mode of adhesively luted PMMA-based CAD/CAM inlays. *Dent Mat* **32**, e22-e29 (2016).

205 Chrysanthakopoulos, N. A. Placement, replacement and longevity of composite resin-based restorations in permanent teeth in Greece. *Int Dent J* **62**, 161-166, (2012).

206 Rankine, W. J. M. II. On the stability of loose earth. *Philos Trans Royal Soc* **147**, 9-27 (1857).

207 Memorial University, Faculty of Engineering and Applied Science, *Theories of Failure*, <http://www.engr.mun.ca/~katna/5931/Theories%20of%20Failure2.pdf> (2011).

208 Mahest, W. Maximum Principle Stress Theory – Theories of Elastic Failure – Strength of Materials, Recorded Lecture, 2016

209 Hosford, W. F. *Mechanical Behavior of Materials / William F. Hosford*. 2nd ed., (Cambridge : Cambridge University Press, 2010).

210 Li, Y., Lin, H., Zheng, G., Zhang, X. & Xu, Y. A comparison study on the flexural strength and compressive strength of four resin-modified luting glass ionomer cements. *Biomed Mater Eng* **26 Suppl 1**, S9-17, (2015).

211 Moshaverinia, A. *et al.* Measure of microhardness, fracture toughness and flexural strength of N-vinylcaprolactam (NVC)-containing glass-ionomer dental cements. *Dent Mater* **26**, 1137-1143, (2010).

212 Shouha, P., Swain, M. & Ellakwa, A. The effect of fiber aspect ratio and volume loading on the flexural properties of flowable dental composite. *Dent Mater* **30**, 1234-1244, (2014).

213 Kelly, J. R. *et al.* ADM guidance-ceramics: Fatigue principles and testing. *Dent Mater* **33**, 1192-1204, (2017).

214 Piao, J. *et al.* Correlation between cyclic fatigue and the bending properties of nickel titanium endodontic instruments. *Dent Mater J* **33**, 539-544 (2014).

215 Chen, S. *et al.* Compressive fatigue limit of four types of dental restorative materials. *J Mech Behav Biomed Mater* **61**, 283-289, (2016).

216 Hibbeler, R. C. *Mechanics of materials*. 7th ed., (Singapore : Prentice Hall, 2008).

217 Hedayati, R., Amin Yavari, S. & Zadpoor, A. A. Fatigue crack propagation in additively manufactured porous biomaterials. *Mater Sci Eng C Mater Biol Appl* **76**, 457-463, (2017).

218 Griffin, A., The phenomena of rupture and flow in solids VI. *Philos. Trans. Royal Soc. A,* **221**, 163 (1921).

219 Li, H. F., Wang, S. G., Zhang, P., Qu, R. T. & Zhang, Z. F. Crack propagation mechanisms of AISI 4340 steels with different strength and toughness. *Mater Sci Eng A* **729**, 130-140, (2018).

220 Goldman, M. Fracture properties of composite and glass ionomer dental restorative materials. *J Biomed Mater Res* **19**, 771-783 (1985).

221 Chiu, C.-K., Ueda, T., Chi, K.-N. & Chen, S.-Q. Shear Crack Control for High Strength Reinforced Concrete Beams Considering the Effect of Shear-Span to Depth Ratio of Member. *Int J Concr Struct M* **10**, 407-424, (2016).

222 International Organisation for Standardisation, BS EN ISO 20795-1:2013 Dentistry – Base Polymers. Part 1: Denture base polymers, *Section 8.6 Fracture Toughness with a Modified Bending Test* (British Standards Institute, 2013).

223 Marti, L. M. *et al.* Incorporation of chlorhexidine gluconate or diacetate into a glass-ionomer cement: porosity, surface roughness, and anti-biofilm activity. *Am J Dent* **27**, 318-322 (2014).

224 Higg, W. A., Lucksanasombool, P., Higgs, R. J. & Swain, M. V. Evaluating acrylic and glass-ionomer cement strength using the biaxial flexure test. *Biomaterials* **22**, 1583-1590 (2001).

225 Darvell, B. W. *A glossary of terms for dental materials science*. (BW Darvell Pokfulam, 2006).

226 Sabbagh, J., Vreven, J. & Leloup, G. Dynamic and static moduli of elasticity of resin-based materials. *Dent Mater* **18**, 64-71 (2002).

227 Broz, M. E., Cook, R. F. & Whitney, D. L. Microhardness, toughness, and modulus of Mohs scale minerals. *Am Min* **91**, 135-142 (2006).

228 Giannakopoulos, A. E., Larsson, P. L. & Vestergaard, R. Analysis of Vickers indentation. *Int J Solids Struct* **31**, 2679-2708, (1994).

229 Palmqvist, S. Method att bestamma segheten hos sproda material, sarskilt hardmetaller. *Jernkontorets Ann* **141**, 300-307 (1957).

230 Bishop, R. F., Hill, R. & Mott, N. F. The theory of indentation and hardness tests. *Proc Phys Soc* **57**, 147 (1945).

231 Callister, W. D. & Rethwisch, D. G. *Materials science and engineering*. 8th ed., (Wiley, 2011).

232 Nujella, B. P., Choudary, M. T., Reddy, S. P., Kumar, M. K. & Gopal, T. Comparison of shear bond strength of aesthetic restorative materials. *Contemp Clin Dent* **3**, 22-26, (2012).

233 Porenczuk, A., Firlej, P., Szczepańska, G., Kolenda, A. & Olczak-Kowalczyk, D. The laboratory comparison of shear bond strength and microscopic assessment of failure modes for a glass-ionomer cement and dentin bonding systems combined with silver nanoparticles. *Acta Bioeng Biomech* **18**, 59-70 (2016).

234 Murthy, S. S. & Murthy, G. S. Comparative Evaluation of Shear Bond Strength of Three Commercially Available Glass Ionomer Cements in Primary Teeth. *J Int Oral Health* **7**, 103-107 (2015).

235 Hoshika, S., De Munck, J., Sano, H., Sidhu, S. K. & Van Meerbeek, B. Effect of conditioning and aging on the bond strength and interfacial morphology of glass-ionomer cement bounded to dentin. *J Adhes Dent* **17**, 141-146 (2015).

236 Kaup, M., Dammann, C. H., Schäfer, E. & Dammaschke, T. Shear bond strength of Biodentine, ProRoot MTA, glass ionomer cement and composite resin on human dentine ex vivo. *Head Face Med* **11**, 14 (2015).

237 Scherrer, S. S., Cesar, P. F. & Swain, M. V. Direct comparison of the bond strength results of the different test methods: A critical literature review. *Dent Mater* **26**, e78-e93, (2010).

238 Inoue, S. *et al.* Effect of remaining dentin thickness and the use of conditioner on micro-tensile bond strength of a glass-ionomer adhesive. *Dent Mater* **17**, 445-455 (2001).

239 Powis, D. R., Follerås, T., Merson, S. A. & Wilson, A. D. Materials science: Improved adhesion of a glass ionomer cement to dentin and enamel. *J Dent Res* **61**, 1416-1422 (1982).

240 Nujella, B. P. S., Choudary, M. T., Reddy, S. P., Kumar, M. K. & Gopal, T. Comparison of shear bond strength of aesthetic restorative materials. *Contemp Clin Dent* **3**, 22-26, (2012).

241 Crisp, S., Lewis, B. G. & Wilson, A. D. Characterization of glass-ionomer cements: 2. Effect of the powder: liquid ratio on the physical properties. *J Dent* **4**, 287-290, (1976).

242 Prentice, L. H., Tyas, M. J. & Burrow, M. F. The effect of mixing time on the handling and compressive strength of an encapsulated glass-ionomer cement. *Dent Mater* **21**, 704-708, (2005).

243 Singh, J. B., Chakravartty, J. K. & Sundararaman, M. Work hardening behaviour of service aged Alloy 625. *Mater Sci Eng A* **576**, 239-242, (2013).

244 Younes, A. *et al.* Structural and magnetic properties of FeCuNi nanostructured produced by mechanical alloying. *Appl Surf Sci* **446**, 258-265, (2018).

245 Xie, D., Park, J. G., Faddah, M., Zhao, J. & Khanijoun, H. K. Novel amino acid-constructed polyalkenoates for dental glass-ionomer restoratives. *J Biomater Appl* **21**, 147-165, (2006).

246 Moshaverinia, A., Roohpour, N. & Rehman, I. U. Synthesis and characterization of a novel fast-set proline-derivative-containing glass ionomer cement with enhanced mechanical properties. *Acta Biomater* **5**, 498-507, (2009).

247 Holst, A. A 3-year clinical evaluation of Ketac-Silver restorations in primary molars. *Swed Dent J* **20**, 209-214 (1996).

248 Kilpatrick, N. M., Murray, J. J. & McCabe, J. F. The use of a reinforced glass-ionomer cermet for the restoration of primary molars: a clinical trial. *Br Dent J* **179**, 175-179 (1995).

249 Shetty, R. & Munshi, A. K. Tunnel restorations using glass ionomer or glass cermet: in vitro marginal ridge fracture and microleakage. *J Clin Pediatr Dent* **21**, 77-84 (1996).

250 Kerby, R. E. & Bleiholder, R. F. Physical properties of stainless-steel and silver-reinforced glass-ionomer cements. *J Dent Res* **70**, 1358-1361 (1991).

251 Paiva, L. *et al.* Antibacterial properties and compressive strength of new one-step preparation silver nanoparticles in glass ionomer cements (NanoAg-GIC). *J Dent* **69**, 102-109, (2018).

252 Garcia-Contreras, R. *et al.* Mechanical, antibacterial and bond strength properties of nano-titanium-enriched glass ionomer cement. *J Appl Oral Sci* **23**, 321-328 (2015).

253 Hamid, N. *et al.* Titanium Dioxide Nanoparticles and Cetylpyridinium Chloride Enriched Glass-Ionomer Restorative Cement: A Comparative Study Assessing Compressive Strength and Antibacterial Activity. *J Clin Pediatr Dent*, (2018).

254 Sun, J. *et al.* Synergistic effects of titanium dioxide and cellulose on the properties of glassionomer cement. *Dent Mater J*, (2018).

255 Weir, A., Westerhoff, P., Fabricius, L., Hristovski, K. & Von Goetz, N. Titanium dioxide nanoparticles in food and personal care products. *Environ Sci Tech* **46**, 2242-2250 (2012).

256 Czajka, M. *et al.* Toxicity of titanium dioxide nanoparticles in central nervous system. *Toxicol in Vitro* **29**, 1042-1052, (2015).

257 Coccini, T., Grandi, S., Lonati, D., Locatelli, C. & De Simone, U. Comparative cellular toxicity of titanium dioxide nanoparticles on human astrocyte and neuronal cells after acute and prolonged exposure. *Neurotoxicology* **48**, 77-89 (2015).

258 Sukwong, P., Somkid, K., Kongseng, S., Pissuwan, D. & Yoovathaworn, K. Respiratory tract toxicity of titanium dioxide nanoparticles and multi-walled carbon nanotubes on mice after intranasal exposure. *Micro Nano Lett* **11**, 183-187 (2016).

259 Younes, N. R. B. *et al.* Subacute toxicity of titanium dioxide (TiO 2) nanoparticles in male rats: emotional behavior and pathophysiological examination. *Environ Sci Pol Res* **22**, 8728-8737 (2015).

260 Heringa, M. B. *et al.* Risk assessment of titanium dioxide nanoparticles via oral exposure, including toxicokinetic considerations. *Nanotoxicology* **10**, 1515-1525 (2016).

261 Advanced Healthcare Ltd. *Amalgomer - an introduction*, Online, <http://www.ahl.uk.com/index.php/products/amalgomer/141-amalgomer-intro> (2018).

262 Gu, Y. W., Yap, A. U. J., Cheang, P. & Khor, K. *Zirconia-glass ionomer cement - A potential substitute for Miracle Mix*. Vol. 52 (2005).

263 Deepa, G. & Shobha, T. A clinical evaluation of two glass ionomer cements in primary molars using atraumatic restorative treatment technique in India: 1 year follow up. *Int J Paediatr Dent* **20**, 410-418 (2010).

264 Bahadure, R. N., Pandey, R. K., Kumar, R., Gopal, K. & Singh, R. K. An estimation of fluoride release from various dental restorative materials at different pH: In vitro study. *J Indian Soc Pedod Prev Dent* **30**, 122-126, (2012).

265 Wang, Y. & Darvell, B. W. Hertzian load-bearing capacity of a ceramic-reinforced glass ionomer cement stored wet and dry. *Dent Mater* **25**, 952-955, (2009).

266 Zoergiebel, J. & Ilie, N. Evaluation of a conventional glass ionomer cement with new zinc formulation: effect of coating, aging and storage agents. *Clin Oral Investig* **17**, 619-626, (2013).

267 Boyd, D., Clarkin, O. M., Wren, A. W. & Towler, M. R. Zinc-based glass polyalkenoate cements with improved setting times and mechanical properties. *Acta Biomater* **4**, 425-431, (2008).

268 Molina, G. F., Cabral, R. J., Mazzola, I., Lascano, L. B. & Frencken, J. E. Mechanical performance of encapsulated restorative glass-ionomer cements for use with Atraumatic Restorative Treatment (ART). *J Appl Oral Sci* **21**, 243-249, (2013).

269 Al-Angari, S. S. *et al.* Physicomechanical properties of a zinc-reinforced glass ionomer restorative material. *J Oral Sci* **56**, 11-16 (2014).

270 Chen, S. *et al.* Compressive fatigue limit of four types of dental restorative materials. *J Mech Behav Biomed Mater* **61**, 283-289, (2016).

271 Panahandeh, N., Torabzadeh, H., Aghaee, M., Hasani, E. & Safa, S. Effect of incorporation of zinc oxide nanoparticles on mechanical properties of conventional glass ionomer cements. *J Conserv Dent* **21**, 130-135, (2018).

272 Kim, D. A. *et al.* Biological and mechanical properties of an experimental glass-ionomer cement modified by partial replacement of CaO with MgO or ZnO. *J Appl Oral Sci* **23**, 369-375, (2015).

273 Hammouda, I. M. Reinforcement of conventional glass-ionomer restorative material with short glass fibers. *J Mech Behav Biomed Mater* **2**, 73-81, (2009).

274 Lohbauer, U. *et al.* Reactive fibre reinforced glass ionomer cements. *Biomaterials* **24**, 2901-2907 (2003).

275 Lohbauer, U., Frankenberger, R., Clare, A., Petschelt, A. & Greil, P. Toughening of dental glass ionomer cements with reactive glass fibres. *Biomaterials* **25**, 5217-5225, (2004).

276 Garoushi, S., Vallittu, P. & Lassila, L. Hollow glass fibers in reinforcing glass ionomer cements. *Dentl Mater* **33**, e86-e93, (2017).

277 Kobayashi, M., Kon, M., Miyai, K. & Asaoka, K. Strengthening of glass-ionomer cement by compounding short fibres with CaO-P2O5-SiO2-Al2O3 glass. *Biomaterials* **21**, 2051-2058 (2000).

278 Garoushi, S. K., He, J., Vallittu, P. K. & Lassila, L. V. J. Effect of discontinuous glass fibers on mechanical properties of glass ionomer cement. *Acta Biomater Odontol Scand* **4**, 72-80, (2018).

279 Yli-Urpo, H., Lassila, L. V., Närhi, T. & Vallittu, P. K. Compressive strength and surface characterization of glass ionomer cements modified by particles of bioactive glass. *Dent Mater* **21**, 201-209, (2005).

280 Yli-Urpo, H., Närhi, M. & Närhi, T. Compound changes and tooth mineralization effects of glass ionomer cements containing bioactive glass (S53P4), an in vivo study. *Biomaterials* **26**, 5934-5941, (2005).

281 Allam, G. & Abd El-Geleel, O. Evaluating the Mechanical Properties, and Calcium and Fluoride Release of Glass-Ionomer Cement Modified with Chicken Eggshell Powder. *Dent J (Basel)* **6**, (2018).

282 Lubis, M., H S Ginting, M., F Dalimunthe, N., M T Hasibuan, D. & Sastrodihardjo, S. *The Influence of Chicken Egg Shell as Fillers on Biocomposite Acrylic Resin for Denture Base*. Vol. 180 (2017).

283 Toro, P., Quijada, R., Yazdani-Pedram, M. & Arias, J. L. Eggshell, a new bio-filler for polypropylene composites. *Mater Lett* **61**, 4347-4350, (2007).

284 Mohamad, M., Mahmood, A., Yik Yee Min, A. & Abd Khalid, N. H. *A Review of the Mechanical Properties of Concrete Containing Biofillers*. Vol. 160 (2016).

285 Neunzehn, J., Szuwart, T. & Wiesmann, H. P. Eggshells as natural calcium carbonate source in combination with hyaluronan as beneficial additives for bone graft materials, an in vitro study. *Head Face Med* **11**, 12, (2015).

286 Suzuki, F. K., Wang, P.-Y., Weatherspoon, J. B. & Mead, L. C. (Google Patents, 2014).

287 M, K., S, A. & A, D. Influence of Incorporating Fluoroapatite Nanobioceramic on the Compressive Strength and Bioactivity of Glass Ionomer Cement. *J Dent Biomater* **3**, 276-283 (2016).

288 Aoki, H. Science and medical applications of hydroxyapatite. *JAAS* **1991**, 123-134 (1991).

289 Sharafeddin, F., Shoale, S. & Kowkabi, M. Effects of Different Percentages of Microhydroxyapatite on Microhardness of Resin-modified Glass-ionomer and Zirconomer. *J Clin Exp Dent* **9**, e805-e811, (2017).

290 Rasheed, M. & Mohammed, R. A. Assessment of diametral tensile strength and microhardness of Glass ionomer reinforced by different amounts of Hydroxyapatite. *J* Baghdad *Coll Dent* **18**, 17-20 (2006).

291 Moreno, E. C., Kresak, M. & Zahradnik, R. T. Fluoridated hydroxyapatite solubility and caries formation. *Nature* **247**, 64 (1974).

292 Chen, Z. F., Darvell, B. W. & Leung, V.-H. Hydroxyapatite solubility in simple inorganic solutions. *Arch Oral Biol* **49**, 359-367 (2004).

293 Larsen, M. J. & Jensen, S. J. The hydroxyapatite solubility product of human dental enamel as a function of pH in the range 4.6–7.6 at 20° C. *Arch Oral Biol* **34**, 957-961 (1989).

294 Arita, K. *et al.* Hydroxyapatite particle characteristics influence the enhancement of the mechanical and chemical properties of conventional restorative glassionomer cement. *Dent Mater J* **30**, 672-683 (2011).

295 Bell, L. C., Mika, H. & Kruger, B. J. Synthetic hydroxyapatite-solubility product and stoichiometry of dissolution. *Arch Oral Biol* **23**, 329-336, (1978).

296 Zhang, H. & Darvell, B. W. Mechanical properties of hydroxyapatite whisker-reinforced bis-GMA-based resin composites. *Dent Mater* **28**, 824-830, (2012).

297 Poorzandpoush, K., Omrani, L. R., Jafarnia, S. H., Golkar, P. & Atai, M. Effect of addition of Nano hydroxyapatite particles on wear of resin modified glass ionomer by tooth brushing simulation. *J Clin Exp Dent* **9**, e372-e376, (2017).

298 Williams, D. F. On the mechanisms of biocompatibility. *Biomaterials* **29**, 2941-2953, (2008).

299 Robertson, C. W. The medical device directive. *Health Estate* **52**, 26-27 (1998).

300 BS EN ISO. 14971: 2009. *Medical devices-Application of risk management to medical devices (ISO 14971: 2007, Corrected version 2007-10-01)." Brussels: CEN/CENELEC* (2009).

301 Kramer, D. B., Xu, S. & Kesselheim, A. S. Regulation of medical devices in the United States and European Union, (Mass Medical Soc, 2012).

302 Carraway, J. & Ghosh, C. The challenge to global acceptance of Part 3 of ISO 10993. *Med Device Technol* **17**, 16-18 (2006).

303 Miller, F. *et al.* Validation of eGFP fluorescence intensity for testing in vitro cytotoxicity according to ISO 10993-5. *J Biomed Mater Res B* **105**, 715-722, (2015).

304 Kavitha Sankar, P. C., Rajmohan, G. & Rosemary, M. J. Physico-chemical characterisation and biological evaluation of freeze dried chitosan sponge for wound care. *Mater Lett* **208**, 130-132, (2017).

305 Jiang, R. D. *et al.* In vitro dentin barrier cytotoxicity testing of some dental restorative materials. *J Dent* **58**, 28-33, (2017).

306 Soares, D. G. *et al.* Biocompatibility of a restorative resin-modified glass ionomer cement applied in very deep cavities prepared in human teeth. *Gen Dent* **64**, 33-40 (2016).

307 Marvin, J. C., Gallegos, S. I., Parsaei, S. & Rodrigues, D. C. In Vitro Evaluation of Cell Compatibility of Dental Cements Used with Titanium Implant Components. *J Prosthodont*, (2018).

308 Angelieri, F., da Silva, Y. S. & Ribeiro, D. A. Genotoxicity and cytotoxicity induced by eluates from orthodontic glass ionomer cements in vitro. *Saudi Dent J* **30**, 38-42, (2018).

309 Costa, C. A., Ribeiro, A. P., Giro, E. M., Randall, R. C. & Hebling, J. Pulp response after application of two resin modified glass ionomer cements (RMGICs) in deep cavities of prepared human teeth. *Dent Mater* **27**, e158-170, (2011).

310 Ansari, S. *et al.* Properties of a proline-containing glass ionomer dental cement. *J Prosthet Dent* **110**, 408-413, (2013).

311 Cibim, D. D. *et al.* Novel Nanotechnology of TiO2 Improves Physical-Chemical and Biological Properties of Glass Ionomer Cement. *Int J Biomater* **2017**, (2017).

312 Silva, R. M. *et al.* Dental glass ionomer cement reinforced by cellulose microfibers and cellulose nanocrystals. *Mater Sci Eng C Mater Biol Appl* **58**, 389-395, (2016).

313 Forsten, L. Fluoride release from a glass ionomer cement. *Scand J Dent Res* **85**, 503-504 (1977).

314 el Mallakh, B. F. & Sarkar, N. K. Fluoride release from glass-ionomer cements in de-ionized water and artificial saliva. *Dental Mater* **6**, 118-122 (1990).

315 Shaw, A. J., Carrick, T. & McCabe, J. F. Fluoride release from glass-ionomer and compomer restorative materials: 6-month data. *J Dent* **26**, 355-359 (1998).

316 Czarencka, B. & Nicholson, J. W. Uptake of fluoride by Glass-ionomer dental cements from a commercial fluoridated mouthwash, *Ceramics–Silikáty* **62**, 158-162 (2018).

317 Nicholson, J. W. & Czarnecka, B. Maturation affects fluoride uptake by glass-ionomer dental cements. *Dent Mater* **28**, e1-5, (2012).

318 Fan, C. *et al.* Development of an antimicrobial resin—A pilot study. *Dent Mater* **27**, 322-328, (2011).

319 Chau, N. P. T., Pandit, S., Cai, J.-N., Lee, M.-H. & Jeon, J.-G. Relationship between fluoride release rate and anti-cariogenic biofilm activity of glass ionomer cements. *Dent Mater* **31**, e100-e108 (2015).

320 Tiwari, S. *et al.* Antibacterial Activity and Fluoride Release of Glass-Ionomer Cement, Compomer and Zirconia Reinforced Glass-Ionomer Cement. *J Clin Diagn Res* **10**, (2016).

321 Simmons, J. O. *et al.* Effect of surface treatments on the mechanical properties and antimicrobial activity of desiccated glass ionomers. *Dent Mater* **32**, 1343-1351, (2016).

322 Zhao, I. S., Mei, M. L., Burrow, M. F., Lo, E. C.-M. & Chu, C.-H. Prevention of secondary caries using silver diamine fluoride treatment and casein

phosphopeptide-amorphous calcium phosphate modified glass-ionomer cement. *J Dent* **57**, 38-44 (2017).

323 Alhilou, A. *et al. Physicochemical and Antibacterial Characterization of a Novel Fluorapatite Coating*. Vol. 1 (2016).

324 Yesilyurt, C., Er, K., Tasdemir, T., Buruk, K. & Celik, D. Antibacterial activity and physical properties of glass-ionomer cements containing antibiotics. *Oper Dent* **34**, 18-23, (2009).

325 DeSchepper, E. J., White, R. R. & von der Lehr, W. Antibacterial effects of glass ionomers. *Am J Dent* **2**, 51-56 (1989).

326 Pouralibaba, F. *et al.* Clinical evaluation of reasons for replacement of amalgam restorations in patients referring to a dental school in iran. *J Dent Res Dent Clin Dent Prospects* **4**, 56-59, (2010).

327 Scholtanus, J. & Huysmans, M. *Clinical failure of class-II restorations of a highly viscous glass-ionomer material over a 6-year period: A retrospective study*. Vol. 35 (2007).

328 Dias, A. G. A. *et al.* Clinical performance of glass ionomer cement and composite resin in Class II restorations in primary teeth: A systematic review and meta-analysis. *J Dent* **73**, 1-13, (2018).

329 Kramer, N., Schmidt, M., Lucker, S., Domann, E. & Frankenberger, R. Glass ionomer cement inhibits secondary caries in an in vitro biofilm model. *Clin Oral Investig* **22**, 1019-1031, (2018).

330 Hegde, N. N., Attavar, S. H., Hegde, M. N. & Priya, G. Antibacterial activity of dental restorative material: An. *J Conserv Dent* **21**, 42-46, (2018).

331 Cury, J. A., de Oliveira, B. H., dos Santos, A. P. P. & Tenuta, L. M. A. Are fluoride releasing dental materials clinically effective on caries control? *Dent Mater* **32**, 323-333, (2016).

332 Parkinson, C. R., Hara, A. T., Nehme, M., Lippert, F. & Zero, D. T. A randomised clinical evaluation of a fluoride mouthrinse and dentifrice in an in situ caries model. *J Dent* **70**, 59-66, (2018).

333 de Moraes, M. D. R. *et al.* Clinical study of the caries-preventive effect of resin-modified glass ionomer restorations: aging versus the influence of fluoride dentifrice. *J Investig Clin Dent* **7**, 180-186 (2016).

334 Creeth, J. E., Karwal, R., Hara, A. T. & Zero, D. T. A Randomized in situ clinical study of fluoride dentifrices on enamel remineralization and resistance to demineralization: Effects of zinc. *Caries Res* **52**, 129-138 (2018).

335 Farrugia, C. & Camilleri, J. Antimicrobial properties of conventional restorative filling materials and advances in antimicrobial properties of composite resins

and glass ionomer cements—A literature review. *Dent Mater* **31**, e89-e99, (2015).

336 Bansal, R. & Bansal, T. A comparative evaluation of the amount of fluoride release and re-release after recharging from aesthetic restorative materials: an in vitro study. *J Clin Diagn Res* **9**, (2015).

337 Alexander, G., Hopcraft, M. S., Tyas, M. J. & Wong, R. H. K. Dentists' restorative decision-making and implications for an 'amalgamless' profession. Part 4: clinical factor. *Aust Dent J* **62**, 363-371, (2017).

338 Singla, M. *et al.* Comparison of Push-Out Bond Strength of Furcation Perforation Repair Materials - Glass Ionomer Cement Type II, Hydroxyapatite, Mineral Trioxide Aggregate, and Biodentine: An in vitro Study. *Contemp Clin Dent* **9**, 410-414, (2018).

339 El-Deeb, H. A. & Mobarak, E. H. Microshear Bond Strength of High-viscosity Glass-ionomer to Normal and Caries-affected Dentin Under Simulated Intrapulpal Pressure. *Oper Dent*, (2018).

340 Aljdaimi, A., Devlin, H. & Dickinson, M. Effect of the Er: YAG laser on the shear bond strength of conventional glass ionomer and Biodentine to dentine. *Eur J Dent* **12**, 380-385, (2018).

341 Ogata, M. *et al.* Effects of different burs on dentin bond strengths of self-etching primer bonding systems. *Oper Dent* **26**, 375-382 (2001).

342 Kanca, J., 3rd. Wet bonding: effect of drying time and distance. *Am J Dent* **9**, 273-276 (1996).

343 Wilson, A. D. Alumino-silicate polyacrylic acid and related cements. *Br Polym J* **6**, 165-179, (1974).

344 Yoshida, Y. *et al.* Adhesion to and decalcification of hydroxyapatite by carboxylic acids. *J Dent Res* **80**, 1565-1569 (2001).

345 Bleeker, E. A. *et al.* Considerations on the EU definition of a nanomaterial: science to support policy making. *Regul Toxicol Pharmacol* **65**, 119-125, (2013).

346 Rauscher, H., Sokull-Klüttgen, B. & Stamm, H. The European Commission's recommendation on the definition of nanomaterial makes an impact. *Nanotoxicology* **7**, 1195-1197, (2013).

347 Gad, M., ArRejaie, A. S., Abdel-Halim, M. S. & Rahoma, A. The Reinforcement Effect of Nano-Zirconia on the Transverse Strength of Repaired Acrylic Denture Base. *Int J Dent* (2016).

348 Nochaiya, T. & Chaipanich, A. Behavior of multi-walled carbon nanotubes on the porosity and microstructure of cement-based materials. *Appl Surf Sci* **257**, 1941-1945, (2011).

349 Sanchez, F., Zhang, L. & Ince, C. in *Nanotechnology in Construction 3.* (eds Zdeněk Bittnar *et al.*) 345-350 (Springer Berlin Heidelberg).

350 Konsta-Gdoutos, M. S., Metaxa, Z. S. & Shah, S. P. Highly dispersed carbon nanotube reinforced cement based materials. *Cement Concrete Res* **40**, 1052-1059, (2010).

351 Soares, R., de Ataide, I. e. N., Fernandes, M. & Lambor, R. Fibre reinforcement in a structurally compromised endodontically treated molar: a case report. *Restor Dent Endod* **41**, 143-147, (2016).

352 Faltermeier, A., Rosentritt, M., Faltermeier, R. & Müssig, D. Influence of fibre and filler reinforcement of plastic brackets: an in vitro study. *Eur J Orthod* **29**, 304-309 (2007).

353 Mutluay, M. M., Tezvergil-Mutluay, A., Vallittu, P. & Lassila, L. Flexural strength,water sorption and solubility of a methylmethacrylate-free denture base polymer reinforced with glass fibre reinforcement. *Eur J Prosthodont Restor Dent* **21**, 146-151 (2013).

354 Singh, M. P., Singh, S. P. & Singh, A. P. Experimental Study on the Strength Characteristics and Water Permeability of Hybrid Steel Fibre Reinforced Concrete. *Int Sch Res Notices* **2014**, (2014).

355 Maensiri, S., Nuansing, W., Klinkaewnarong, J., Laokul, P. & Khemprasit, J. Nanofibers of barium strontium titanate (BST) by sol–gel processing and electrospinning. *J Colloid Interface Sci* **297**, 578-583, (2006).

356 Manesh, K. M., Santhosh, P., Gopalan, A. & Lee, K. P. Electrospun poly(vinylidene fluoride)/poly(aminophenylboronic acid) composite nanofibrous membrane as a novel glucose sensor. *Anal Biochem* **360**, 189-195, (2007).

357 Shi, W., Lu, W. & Jiang, L. The fabrication of photosensitive self-assembly Au nanoparticles embedded in silica nanofibers by electrospinning. *J Colloid Interface Sci* **340**, 291-297, (2009).

358 Wang, H. *et al.* Fabrication of continuous highly ordered mesoporous silica nanofibre with core/sheath structure and its application as catalyst carrier. *Nanoscale* **3**, 3601-3604 (2011).

359 Horzum, N. *et al.* Hierarchically structured metal oxide/silica nanofibers by colloid electrospinning. *ACS Appl Mater Interfaces* **4**, 6338-6345, (2012).

360 Moshaverinia, A. *et al.* Modification of conventional glass-ionomer cements with N-vinylpyrrolidone containing polyacids, nano-hydroxy and fluoroapatite to improve mechanical properties. *Dent Mater,* **24**, 1381-1390, (2008).

361 Goenka, S., Balu, R. & Sampath Kumar, T. S. Effects of nanocrystalline calcium deficient hydroxyapatite incorporation in glass ionomer cements. *J Mech Behav Biomed Mater* **7**, 69-76, (2012).

362 Wang, H. *et al.* Biocompatibility and osteogenesis of biomimetic nano-hydroxyapatite/polyamide composite scaffolds for bone tissue engineering. *Biomaterials* **28**, 3338-3348, (2007).

363 David, L., Argenta, L. & Fisher, D. Hydroxyapatite cement in pediatric craniofacial reconstruction. *J Craniofac Surg* **16**, 129-133 (2005).

364 Deb, S., Braden, M. & Bonfield, W. Water absorption characteristics of modified hydroxyapatite bone cements. *Biomaterials* **16**, 1095-1100, (1995).

365 Alfotawi, R. *et al.* A novel surgical approach for the reconstruction of critical-size mandibular defects using calcium sulphate/hydroxyapatite cement, BMP-7 and mesenchymal stem cells-histological assessment. *J Biomater Tissue Eng* **6**, 1-11 (2016).

366 Volsky, P. G. *et al.* Hydroxyapatite cement cranioplasty following translabyrinthine approach: Long-term study of 369 cases. *Laryngoscope* **127**, 2120-2125 (2017).

367 Aldahak, N. *et al.* Hydroxyapatite bone cement application for the reconstruction of retrosigmoid craniectomy in the treatment of cranial nerves disorders. *Surg Neurol Int* **8** (2017).

368 Fearon, J. A., Griner, D., Ditthakasem, K. & Herbert, M. Autogenous bone reconstruction of large secondary skull defects. *Plast Reconstr Surg* **139**, 427-438 (2017).

369 Delrue, S., van Dinther, J., Zarowski, A., Somers, T. & Offeciers, E. Hydoroxyapatite cement for hearing reconstruction. *Cholesteatoma and Ear Surgery: An Update 2017*, 89 (2017).

370 House, J. W., Lupo, J. E. & Goddard, J. C. Management of incus necrosis in revision stapedectomy using hydroxyapatite bone cement. *Otol Neurotol* **35**, 1312-1316 (2014).

371 Kanazawa, S., Kiya, K., Kubo, T. & Hosokawa, K. Hydroxyapatite implantation for the repair of a congenital nasal anomaly: 10 years follow-up. *J Surg Case Reports* **2018**, (2018).

372 Murugan, R. & Ramakrishna, S. Bioresorbable composite bone paste using polysaccharide based nano hydroxyapatite. *Biomaterials* **25**, 3829-3835, (2004).

373 Shiozawa, M., Takahashi, H., Iwasaki, N., Wada, T. & Uo, M. Effect of immersion time of restorative glass ionomer cements and immersion duration in calcium chloride solution on surface hardness. *Dent Mater* **30**, e377-383, (2014).

374 Chen, L., Yu, Q., Wang, Y. & Li, H. BisGMA/TEGDMA dental composite containing high aspect-ratio hydroxyapatite nanofibers. *Dent Mater* **27**, 1187-1195, (2011).

375 J, Z., P, L. H. & Y, M. C. Biomimetic Formation of Porous Single-Crystalline CaCO3 via Nanocrystal Aggregation. *Adv Mater* **15**, 3 (2003).

376 Dowling, A. H. & Fleming, G. J. P. The impact of montmorillonite clay addition on the in vitro wear resistance of a glass-ionomer restorative. *J Dent* **35**, 309-317, (2007).

377 Dowling, A. H., Stamboulis, A. & Fleming, G. J. The influence of montmorillonite clay reinforcement on the performance of a glass ionomer restorative. *J Dent* **34**, 802-810, (2006).

378 Kojima, Y. *et al.* Synthesis of nylon 6–clay hybrid by montmorillonite intercalated with ϵ-caprolactam. *J Polym Sci A* **31**, 983-986, (1993).

379 Kojima, Y. *et al.* Mechanical properties of nylon 6-clay hybrid. *J Mater Res* **8**, 1185-1189 (1993).

380 Biasci, L., Aglietto, M., Ruggeri, G. & Ciardelli, F. Functionalization of montmorillonite by methyl methacrylate polymers containing side-chain ammonium cations. *Polymer* **35**, 3296-3304, (1994).

381 Fareed, M. A. & Stamboulis, A. Effect of nanoclay dispersion on the properties of a commercial glass ionomer cement. *Int J Biomater* **2014**, 685389, (2014).

382 Fareed, M. A. & Stamboulis, A. Nanoclays reinforced glass ionomer cements: dispersion and interaction of polymer grade (PG) montmorillonite with poly(acrylic acid). *J Mater Sci Mater Med* **25**, 91-99, (2014).

383 Solhi, L. *et al.* Poly(acrylic acid) grafted montmorillonite as novel fillers for dental adhesives: synthesis, characterization and properties of the adhesive. *Dent Mater* **28**, 369-377, (2012).

384 Fareed, M. A. & Stamboulis, A. Nanoclay addition to a conventional glass ionomer cements: Influence on physical properties. *Eur J Dent* **8**, 456-463, (2014).

385 Abdullayev, E., Joshi, A., Wei, W., Zhao, Y. & Lvov, Y. Enlargement of halloysite clay nanotube lumen by selective etching of aluminum oxide. *ACS Nano* **6**, (2012).

386 Yah, W. O. *et al.* Biomimetic dopamine derivative for selective polymer modification of halloysite nanotube lumen. *J Am Chem Soc* **134**, 12134-12137, (2012).

387 Barr, M. & Arnista, E. S. Adsorption studies on clays. I. The adsorption of two alkaloids by activated attapulgite, halloysite, and kaolin. *J Am Pharm Assoc Am Pharm Assoc* **46**, 486-489 (1957).

388 Barr, M. Adsorption studies on clays. II. The adsorption of bacteria by activated attapulgite, halloysite, and kaolin. *J Am Pharm Assoc Am Pharm Assoc* **46**, 490-492 (1957).

389 Barr, M. & Arnista, E. S. Adsorption studies on clays. III. The adsorption of diphtheria toxin by activated attapulgites, halloysite, and kaolin. *J Am Pharm Assoc Am Pharm Assoc* **46**, 493-497 (1957).

390 Coyne, L., Mariner, R. & Rice, A. Air oxidation of hydrazine. 1. Reaction kinetics on natural kaolinites, halloysites, and model substituent layers with varying iron and titanium oxide and O- center contents. *Langmuir* **7**, 1660-1674 (1991).

391 Tarì, G., Bobos, I., Gomes, C. S. F. & Ferreira, J. M. F. Modification of Surface Charge Properties during Kaolinite to Halloysite-7Å Transformation. *J Colloid Interface Sci* **210**, 360-366, (1999).

392 Lvov, Y. M., Shchukin, D. G., Möhwald, H. & Price, R. R. Halloysite clay nanotubes for controlled release of protective agents. *ACS Nano* **2**, 814-820, (2008).

393 Levis, S. R. & Deasy, P. B. Characterisation of halloysite for use as a microtubular drug delivery system. *Int J Pharm* **243**, 125-134 (2002).

394 Levis, S. R. & Deasy, P. B. Use of coated microtubular halloysite for the sustained release of diltiazem hydrochloride and propranolol hydrochloride. *Int J Pharm* **253**, 145-157 (2003).

395 Wang, Y., Zhang, X., Wang, Q., Zhang, B. & Liu, J. Continuous fixed bed adsorption of Cu(II) by halloysite nanotube-alginate hybrid beads: an experimental and modelling study. *Water Sci Technol* **70**, 192-199, (2014).

396 Li, R. *et al.* Highly selective solid-phase extraction of trace Pd(II) by murexide functionalized halloysite nanotubes. *Anal Chim Acta* **713**, 136-144, (2012).

397 Zhao, Y. *et al.* Ammonium removal from aqueous solution by zeolite X synthesized from halloysite mineral. *Water Sci Technol* **62**, 937-946, (2010).

398 Zhao, Y. *et al.* Preparation of highly ordered cubic NaA zeolite from halloysite mineral for adsorption of ammonium ions. *J Hazard Mater* **178**, 658-664, (2010).

399 Abdullayev, E., Price, R., Shchukin, D. & Lvov, Y. Halloysite tubes as nanocontainers for anticorrosion coating with benzotriazole. *ACS Appl Mater Interfaces* **1**, 1437-1443, (2009).

400 Luo, P., Zhao, Y., Zhang, B., Liu, J. & Yang, Y. Study on the adsorption of Neutral Red from aqueous solution onto halloysite nanotubes. *Water Res* **44**, 1489-1497, (2010).

401 Cai, H. *et al.* Preparation and characterization of novel carbon dioxide adsorbents based on polyethylenimine-modified Halloysite nanotubes. *Environ Technol* **36**, 1273-1280, (2015).

402 Jana, S., Das, S., Ghosh, C., Maity, A. & Pradhan, M. Halloysite nanotubes capturing isotope selective atmospheric CO2. *Sci Rep* **5**, 8711, (2015).

403 Lvov, Y., Aerov, A. & Fakhrullin, R. Clay nanotube encapsulation for functional biocomposites. *Adv Colloid Interface Sci* **207**, 189-198, (2014).

404 Naumenko, E. A., Guryanov, I. D., Yendluri, R., Lvov, Y. M. & Fakhrullin, R. F. Clay nanotube-biopolymer composite scaffolds for tissue engineering. *Nanoscale* **8**, 7257-7271, (2016).

405 Song, K. *et al.* Spray-Coated Halloysite-Epoxy Composites: A Means To Create Mechanically Robust, Vertically Aligned Nanotube Composites. *ACS Appl Mater Interfaces* **8**, 20396-20406, (2016).

406 Riedlinger, M. & Corkery, R. Cosmetic skincare applications employing mineral-derived tubules for controlled release (Google Patents, 2007).

407 Wei, W. *et al. Enhanced efficiency of antiseptics with sustained release from clay nanotubes*. Vol. 4 (2014).

408 Kurczewska, J., Pecyna, P., Ratajczak, M., Gajęcka, M. & Schroeder, G. Halloysite nanotubes as carriers of vancomycin in alginate-based wound dressing. *Saudi Pharm J : SPJ* **25**, 911-920, (2017).

409 Yendluri, R. *et al.* Paclitaxel Encapsulated in Halloysite Clay Nanotubes for Intestinal and Intracellular Delivery. *J Pharm Sci* **106**, 3131-3139, (2017).

410 Yendluri, R., Otto, D. P., De Villiers, M. M., Vinokurov, V. & Lvov, Y. M. Application of halloysite clay nanotubes as a pharmaceutical excipient. *Int J Pharm* **521**, 267-273, (2017).

411 Alkatheeri, M. S., Palasuk, J., Eckert, G. J., Platt, J. A. & Bottino, M. C. Halloysite nanotube incorporation into adhesive systems—effect on bond strength to human dentin. *Clin Oral Investig* **19**, 1905-1912, (2015).

412 Kemp-Scholte, C. M. & Davidson, C. L. Complete marginal seal of Class V resin composite restorations effected by increased flexibility. *J Dent Res* **69**, 1240-1243, (1990).

413 Bottino, M. C. *et al.* Nanotube-modified dentin adhesive--physicochemical and dentin bonding characterizations. *Dent Mater* **29**, 1158-1165, (2013).

414 Liu, M., Guo, B., Zou, Q., Du, M. & Jia, D. Interactions between halloysite nanotubes and 2,5-bis(2-benzoxazolyl) thiophene and their effects on reinforcement of polypropylene/halloysite nanocomposites. *Nanotechnology* **19**, (2008).

415 Chen, Q.-Z., Liang, S.-L., Wang, J. & Simon, G. P. Manipulation of mechanical compliance of elastomeric PGS by incorporation of halloysite nanotubes for soft tissue engineering applications. *J Mech Behav Biomed Mater* **4**, 1805-1818, (2011).

416 Lin, Y., Ng, K. M., Chan, C.-M., Sun, G. & Wu, J. High-impact polystyrene/halloysite nanocomposites prepared by emulsion polymerization using sodium dodecyl sulfate as surfactant. *J Colloid Interface Sci* **58**, 423-429, (2011).

417 Liu, M., Zhang, Y., Wu, C., Xiong, S. & Zhou, C. Chitosan/halloysite nanotubes bionanocomposites: Structure, mechanical properties and biocompatibility. *Int J Biol Macromol* **51**, 566-575, (2012).

418 Chen, Q., Zhao, Y., Wu, W., Xu, T. & Fong, H. *Fabrication and evaluation of Bis-GMA/TEGDMA dental resins/composites containing halloysite nanotubes*. Vol. 28 (2012).

419 Joo, Y., Sim, J. H., Jeon, Y., Lee, S. U. & Sohn, D. Opening and blocking the inner-pores of halloysite. *Chem Commun (Camb)* **49**, 4519-4521, (2013).

420 Lecouvet, B., Horion, J., D'Haese, C., Bailly, C. & Nysten, B. Elastic modulus of halloysite nanotubes. *Nanotechnology* **24**, 105704, (2013).

421 Lu, D., Chen, H., Wu, J. & Chan, C. M. Direct measurements of the Young's modulus of a single halloysite nanotube using a transmission electron microscope with a bending stage. *J Nanosci Nanotechnol* **11**, 7789-7793 (2011).

422 Ismail, H., Salleh, S. Z. & Ahmad, Z. Properties of halloysite nanotubes-filled natural rubber prepared using different mixing methods. *Materials & Design* **50**, 790-797, (2013).

423 Lecouvet, B., Sclavons, M., Bourbigot, S. & Bailly, C. Thermal and flammability properties of polyethersulfone/halloysite nanocomposites prepared by melt compounding. *Polym Degrad Stab* **98**, 1993-2004, (2013).

424 Thakur, P., Kool, A., Bagchi, B., Das, S. & Nandy, P. Enhancement of β phase crystallization and dielectric behavior of kaolinite/halloysite modified poly(vinylidene fluoride) thin films. *Appl Clay Sci* **99**, 149-159, (2014).

425 Shankar, S., Kasapis, S. & Rhim, J. W. Alginate-based nanocomposite films reinforced with halloysite nanotubes functionalized by alkali treatment and zinc oxide nanoparticles. *Int J Biol Macromol* **118**, 1824-1832, (2018).

426 Kim, S., Kim, M. I., Shon, M., Seo, B. & Lim, C. Mechanical and Thermal Properties of Epoxy Composites Containing Zirconia-Impregnated Halloysite Nanotubes with Different Loadings. *J Nanosci Nanotechnol* **18**, 6152-6156, (2018).

427 Du, M., Guo, B. & Jia, D. Newly emerging applications of halloysite nanotubes: a review. *Polym Int* **59**, 574-582, (2010).

428 Liu, M., Jia, Z., Jia, D. & Zhou, C. Recent advance in research on halloysite nanotubes-polymer nanocomposite. *Prog Polym Sci* **39**, 1498-1525, (2014).

429 Vergaro, V. *et al. Cytocompatibility and Uptake of Halloysite Clay Nanotubes*. Vol. 11 (2010).

430 Zhou, W. *et al. Poly(vinyl alcohol)/Halloysite nanotubes bionanocomposite films: Properties and in vitro osteoblasts and fibroblasts response*. Vol. 93 (2009).

431 Qi, R. *et al. Biocompatibility of Electrospun Halloysite Nanotube-Doped Poly(Lactic-co-Glycolic Acid) Composite Nanofibers*. Vol. 23 (2011).

432 H. Murray, H., Harvey, C. & M. Smithr, J. *Mineralogy and Geology of the Maungaparerua Halloysite Deposit in New Zealand*. Vol. 25 (1977).

433 Bobos, I., Duplay, J., Rocha, J. o. & Gomes, C. Kaolinite to Halloysite-7 Å transformation in the kaolin deposit of Sao Vicente de Pereira, Portugal. *Clays Clay Miner* **49**, 596-607 (2001).

434 Kamble, R., Ghag, M., Gaikawad, S. & Panda, B. *Halloysite nanotubes and applications: A review*. Vol. 3 (2012).

435 Bugatti, V., Viscusi, G., Naddeo, C. & Gorrasi, G. Nanocomposites Based on PCL and Halloysite Nanotubes Filled with Lysozyme: Effect of Draw Ratio on the Physical Properties and Release Analysis. *Nanomaterials* **7**, 213, (2017).

436 Kryuchkova, M., Danilushkina, A., Lvov, Y. & Fakhrullin, R. *Evaluation of toxicity of nanoclays and graphene oxide: in vivo A Paramecium caudatum study*. Vol. 3 (2016).

437 Yuan, P., Tan, D. & Annabi-Bergaya, F. Properties and applications of halloysite nanotubes: recent research advances and future prospects. *Appl Clay Sci* **112-113**, 75-93, (2015).

438 Pasbakhsh, P., Churchman, G. J. & Keeling, J. L. Characterisation of properties of various halloysites relevant to their use as nanotubes and microfibre fillers. *Appl Clay Sci* **74**, 47-57, (2013).

439 Yuan, P. *et al. Functionalization of Halloysite Clay Nanotubes by Grafting with 1,2-Aminopropyltriethoxysilane*. Vol. 112 (2008).

440 van de Sande, F. H. *et al.* 18-year survival of posterior composite resin restorations with and without glass ionomer cement as base. *Dent Mater* **31**, 669-675, (2015).

441 Burke, F. J. T. *et al.* Clinical performance of reinforced glass ionomer restorations placed in UK dental practices. *Br Dent J,* **203**, E2, (2007).

442 Lynch AJ, R. C. *The History of Grinding*. (Society for Mining, Metallurgy, and Exploration Inc., 2005).

443 Li, H. *et al.* Investigation on the potential of waste cooking oil as a grinding aid in Portland cement. *J Environ Manage* **184**, 545-551, (2016).

444 Diamond Carve/90 Instructions for Use, F038, Kemdent. Swindon UK.

445 Newton, I. *Philosophiae Naturalis Principia Mathematica*. (Londini: Jussu Societatis Regiae ac Typis Josephi Streater, 1687).

446 ISO 9917-1 Dentistry--Water-based cements--Part 1: Powder/liquid acid based cements. *Geneva. Switzerland: International Organization for Standardization* (2003).

447 Radleys and Co., *Findenser™ Super Air Condenser*, <https://www.radleys.com/products/our-products/benchtop-and-hotplate-tools/findenser-air-condenser> (2017).

448 Chen, H., Clarkson, B. H., Sun, K. & Mansfield, J. F. Self-assembly of synthetic hydroxyapatite nanorods into an enamel prism-like structure. *J Colloid Interface Sci* **288**, 97-103, (2005).

449 Shellis, R. P. & Wilson, R. M. Apparent solubility distributions of hydroxyapatite and enamel apatite. *J Colloid Interface Sci* **278**, 325-332, (2004).

450 Kaufman, H. W. & Kleinberg, I. Studies on the incongruent solubility of hydroxyapatite. *Calcif Tissue Int* **27**, 143-151 (1979).

451 Mäkinen, K. K. & Söderling, E. Solubility of calcium salts, enamel, and hydroxyapatite in aqueous solutions of simple carbohydrates. *Calcif Tissue Int* **36**, 64-71 (1984).

452 Wasson, E. A. & Nicholson, J. W. Change in pH during setting of polyelectrolyte dental cements. *J Dent* **21**, 122-126 (1993).

453 Issa, M., Brunton, P., Silikas, N. & Watts, D. C. Expulsion force, surface pH, and porosity of encapsulated glass-ionomer cements mixed with a Rotomix device. *Eur J Prosthodont Restor Dent* **10**, 119-123 (2002).

454 Newport Industries. Introduction to FTIR, online, www.newport.com/n/introduction-to-ftir-spectroscopy, (2018).

455 Stuart, B. in *Analytical Techniques in Science* Ch. 1, 223 (John Wiley & Sons Ltd., 2004).

456 Derrick, M., Stulik D, Landry JM. *Infrared Spectroscopy in Conservation Science*. (The Getty Conservation Institute, 1999).

457 Collins, A. M. in *Nanotechnology Cookbook* Ch. 3, 19-20 (Elsevier, 2012).

458 Rühl, H. *Optical Microscopes – Some Basics*, <https://www.leica-microsystems.com/science-lab/optical-microscopes-some-basics/> (2012).

459 McMaster, G. K. & Carmichael, G. G. Analysis of single-and double-stranded nucleic acids on polyacrylamide and agarose gels by using glyoxal and acridine orange. *Proceedings of the National Academy of Sciences* **74**, 4835-4838 (1977).

460 Hayashi, M., Sofuni, T. & Ishidate Jr, M. An application of acridine orange fluorescent staining to the micronucleus test. *Mutation Res Lett* **120**, 241-247 (1983).

461 Ji, H., Johnson, N. P., von Hippel, P. H. & Marcus, A. H. Monitoring the Intercalation of Acridine Orange (AO) Molecules into 6-Methyl isoxanthopterin (6-MI)-Labeled DNA by Circular Dichroism and Single-Molecule FRET. *Biophys J* **112**, 288a (2017).

462 Osman, H. *et al.* Acridine Orange as a Novel Photosensitizer for Photodynamic Therapy in Glioblastoma. *World Neurosurg* **114**, e1310-e1315 (2018).

463 Kwizera, R. *et al.* Acridine orange fluorescent microscopy is more sensitive than India ink light microscopy in the rapid detection of cryptococcosis among CrAg positive HIV patients. *PloS one* **12**, e0182108 (2017).

464 Neeraja, M., Lakshmi, V., Padmasri, C. & Padmaja, K. Utility of Acridine Orange staining for detection of bacteria from positive blood cultures. *J Microbio Methods* **139**, 215-217 (2017).

465 Lametschwandtner, S. H. A. a. A. in *Microvascular Corrosion Casting in Scanning Electron Microscopy* 44-51 (Springer, 1992).

466 Vernon-Parry, K. D. Scanning electron microscopy: an introduction. *III-Vs Review* **13**, 40-44, (2000).

467 S. Amelinckx, D. v. D., J. van Landuyt, G. van Tendeloo. *Electron Microscopy Principles and Fundamentals*. (Wiley-VCH, 1997).

468 Niranjan, P. *et al.* Injectable glass polyalkenoate cements: evaluation of their rheological and mechanical properties with and without the incorporation of lidocaine hydrochloride. *Biomed Phys Eng Express* **4**, (2018).

469 Prosser, H. J., Powis, D. R., Brant, P. & Wilson, A. D. Characterization of glass-ionomer cements 7. The physical properties of current materials. *J Dent* **12**, 231-240 (1984).

470 Pearson, G. J. & Atkinson, A. S. Effects of temperature change on the working and setting characteristics of water-based dental cements. *Dent Mater* **3**, 275-279, (1987).

471 Forsten, L. Fluoride release and uptake by glass ionomers. *Scand J Dent Res* **99**, 241-245 (1991).

472 Forsten, L. Fluoride release of glass ionomers. *J Esthet Dent* **6**, 216-222 (1994).

473 Forsten, L. Resin-modified glass ionomer cements: fluoride release and uptake. *Acta Odontol Scand* **53**, 222-225 (1995).

474 Kaur, K. *Basics of an Ion-Selective Electrode*, <https://www.azosensors.com/article.aspx?ArticleID=244> (2013).

475 Khruschov, M. M. Principles of abrasive wear. *Wear* **28** (1974).

476 Kurtz, S. M., Muhlstein, C. L. & Edidin, A. A. Surface morphology and wear mechanisms of four clinically relevant biomaterials after hip simulator testing. *J Biomed Mater Res* **52**, 447-459 (2000).

477 Kaddick, C. & Wimmer, M. A. Hip simulator wear testing according to the newly introduced standard ISO 14242. *Proc Inst Mech Eng H* **215**, 429-442, (2001).

478 Walker, P. S. *et al.* Methodology for long-term wear testing of total knee replacements. *Clin Orthop Relat Res*, 290-301 (2000).

479 Hu, X., Shortall, A. C. & Marquis, P. M. Wear of three dental composites under different testing conditions. *J Oral Rehabil* **29**, 756-764 (2002).

480 Joyce, T. J. Wear testing of a DJOA finger prosthesis in vitro. *J Mater Sci Mater Med* **21**, 2337-2343, (2010).

481 Li, L. *et al.* Computational wear simulation of patellofemoral articular cartilage during in vitro testing. *J Biomech* **44**, 1507-1513, (2011).

482 Harrison, A. Wear of combinations of acrylic resin and porcelain, on an abrasion testing machine. *J Oral Rehabil* **5**, 111-115 (1978).

483 Wulfman, C., Koenig, V. & Mainjot, A. K. Wear measurement of dental tissues and materials in clinical studies: A systematic review. *Dent Mater* **34**, 825-850, (2018).

484 Nayyer, M. *et al.* Comparative abrasive wear resistance and surface analysis of dental resin-based materials. *Eur J Dent* **12**, 57-66, (2018).

485 D'Arcangelo, C., Vanini, L., Rondoni, G. D. & De Angelis, F. Wear properties of dental ceramics and porcelains compared with human enamel. *J Prosthet Dent* **115**, 350-355, (2016).

486 Barbour, M. E., Parker, D. M., Allen, G. C. & Jandt, K. D. Human enamel erosion in constant composition citric acid solutions as a function of degree of saturation with respect to hydroxyapatite. *J Oral Rehabil* **32**, 16-21, (2005).

487 Whitefield, R. J. Noncontact optical profilometer. *Appl Opt* **14**, 2480-2485, (1975).

488 Westbrook, J. H. & Conrad, H. *The science of hardness testing and its research applications*. (American society for metals, 1973).

489 Guy, H. Laboratory theory and methods for sediment analysis. (1969).

490 Konert, M. & Vandenberghe, J. E. F. Comparison of laser grain size analysis with pipette and sieve analysis: a solution for the underestimation of the clay fraction. *Sedimentology* **44**, 523-535, (2008).

491 Washington, C. *Particle Size Analysis In Pharmaceutics And Other Industries: Theory And Practice: Theory And Practice*. (CRC Press, 2005).

492 Allen, T. *Particle size measurement*. (Springer, 2013).

493 Hassan, P. A., Rana, S. & Verma, G. Making sense of Brownian motion: colloid characterization by dynamic light scattering. *Langmuir* **31**, 3-12 (2014).

494 Edwards, M. A., German, S. R., Dick, J. E., Bard, A. J. & White, H. S. High-speed multipass coulter counter with ultrahigh resolution. *ACS nano* **9**, 12274-12282 (2015).

495 Cornillault, J. Particle Size Analyzer. *Applied Optics* **11**, 265-268, (1972).

496 Swithenbank, J., M. Beer, J., S. Taylor, D., S. Abbot, D. & C. McCreath, G. *A Laser Diagnostic Technique for the Measurement of Droplet and Particle Size Distribution*. Vol. -1 (1975).

497 Ma, Z., Merkus, H. G., de Smet, J. G. A. E., Heffels, C. & Scarlett, B. New developments in particle characterization by laser diffraction: size and shape. *Powder Technology* **111**, 66-78 (2000).

498 Mount, G. J. & Makinson, O. F. Glass-ionomer restorative cements: clinical implications of the setting reaction. *Oper Dent* **7**, 134-141 (1982).

499 Tay, W. M. & Lynch, E. Glass-ionomer (Polyalkenoate) cements. Part 1. Development, setting reaction, structure and types. *J Ir Dent Assoc* **35**, 53-57 (1989).

500 Williamson, R. T. Protection of glass ionomer cements during the setting reaction. *J Prosthet Dent* **73**, 400-401 (1995).

501 Nurrohman, H. *et al.* Apatite crystal protection against acid-attack beneath resin-dentin interface with four adhesives: TEM and crystallography evidence. *Dent Mater* **28**, e89-98, (2012).

502 Fu, S. Z. *et al.* Preparation and properties of nano-hydroxyapatite/PCL-PEG-PCL composite membranes for tissue engineering applications. *J Biomed Mater Res B Appl Biomater* **97**, 74-83, (2011).

503 Ragaseema, V. M., Unnikrishnan, S., Kalliyana Krishnan, V. & Krishnan, L. K. The antithrombotic and antimicrobial properties of PEG-protected silver nanoparticle coated surfaces. *Biomaterials* **33**, 3083-3092, (2012).

504 Simpson, C. A., Agrawal, A. C., Balinski, A., Harkness, K. M. & Cliffel, D. E. Short-chain PEG mixed monolayer protected gold clusters increase clearance and red blood cell counts. *ACS Nano* **5**, 3577-3584, (2011).

505 Zawrah, M. F., Khattab, R. M., Saad, E. M. & Gado, R. A. Effect of surfactant types and their concentration on the structural characteristics of nanoclay. *Spectrochim Acta A Mol Biomol Spectrosc* **122**, 616-623, (2014).

506 Bricha, M., Belmamouni, Y., Essassi, e. M., Ferreira, J. M. & El Mabrouk, K. Surfactant-assisted hydrothermal synthesis of hydroxyapatite nanopowders. *J Nanosci Nanotechnol* **12**, 8042-8049 (2012).

507 Nga, N. K., Giang, L. T., Huy, T. Q., Viet, P. H. & Migliaresi, C. Surfactant-assisted size control of hydroxyapatite nanorods for bone tissue engineering. *Colloids Surf B Biointerfaces* **116**, 666-673, (2014).

508 Qiu, C., Xiao, X. & Liu, R. Biomimetic synthesis of spherical nano-hydroxyapatite in the presence of polyethylene glycol. *Ceramics Int* **34**, 1747-1751, (2008).

509 Fujishiro, Y., Yabuki, H., Kawamura, K., Sato, T. & Okuwaki, A. Preparation of needle-like hydroxyapatite by homogeneous precipitation under hydrothermal conditions. *J Chem Technol Biotechnol* **57**, 349-353 (1993).

510 Mujahid, M., Sarfraz, S. & Amin, S. *On the Formation of Hydroxyapatite Nano Crystals Prepared Using Cationic Surfactant*. Vol. 18 (2015).

511 Duckworth, P. Personal Communication, University of Bristol (2018).

512 Collins, A. M. in *Nanotechnology Cookbook* Ch. 3, 27-28 (Elsevier, 2012).

513 M, A. & M, M. In Situ Biomimetic Synthesis of Gelatin-Carbon Nanotube-Hydroxyapatite Biocomposites as Bone Filler. *Orient J Chem* **33** (2017).

514 Brundavanam, R. K. *et al.* Effect of dilute gelatine on the ultrasonic thermally assisted synthesis of nano hydroxyapatite. *Ultrason Sonochem* **18**, 697-703, (2011).

515 Vergaro, V. *et al. Halloysite Clay Nanotubes: Characterization, Biocompatibility and Use as Drug Carriers*. Vol. 11 (2010).

516 Chiriacò, F. *et al.* in *2014 IEEE International Symposium on Medical Measurements and Applications (MeMeA).* 1-4.

517 Hill, R. G. & Griffin, S. G. Influence of Glass Composition on the Properties of Glass Polyalkenoate Cements. Part I: Influence of Aluminium to Silicon Ratio. *Biomaterials* **20**, 1579 - 1586.

518 Griffin, S. G. & Hill, R. G. Influence of glass composition on the properties of glass polyalkenoate cements. Part I: influence of aluminium to silicon ratio. *Biomaterials* **20**, 1579-1586 (1999).

519 Song, K., Rubner, M. F., Cohen, R. E. & Askar, K. A. Polymer/Halloysite Nanotubes Composites: Mechanical Robustness and Optical Transmittance. *MRS Advances* **2**, 27-32 (2017).

520 Kong, D. *et al.* Influence of nano-silica agglomeration on microstructure and properties of the hardened cement-based materials. *Constr Build Mater* **37**, 707-715, (2012).

521 Gojny, F. H., Wichmann, M. H. G., Fiedler, B., Bauhofer, W. & Schulte, K. Influence of nano-modification on the mechanical and electrical properties of conventional fibre-reinforced composites. *Compos Part A Appl Sci Manuf* **36**, 1525-1535, (2005).

522 Fizir, M. *et al.* Halloysite nanotubes in analytical sciences and in drug delivery: A review. *Mikrochim Acta* **185**, 389, (2018).

523 Dong, Y. *et al.* Polylactic acid (PLA)/halloysite nanotube (HNT) composite mats: Influence of HNT content and modification. *Compos Part A Appl Sci Manuf* **76**, 28-36, (2015).

524 Hu, X., Sun, A., Kang, W. & Zhou, Q. Strategies and knowledge gaps for improving nanomaterial biocompatibility. *Environ Int* **102**, 177-189, (2017).

525 d' Amora, M. *et al.* Biocompatibility and biodistribution of functionalized carbon nano-onions (f-CNOs) in a vertebrate model. *Sci Reports* **6**, https://www.nature.com/articles/srep33923#supplementary-information (2016).

526 Liopo, A. V., Stewart, M. P., Hudson, J., Tour, J. M. & Pappas, T. C. Biocompatibility of native and functionalized single-walled carbon nanotubes for neuronal interface. *J Nanosci Nanotechnol* **6**, 1365-1374 (2006).

527 Yang, W., Thordarson, P., Gooding, J. J., Ringer, S. P. & Braet, F. Carbon nanotubes for biological and biomedical applications. *Nanotechnology* **18**, 412001 (2007).

528 Adabi, M. *et al.* Biocompatibility and nanostructured materials: applications in nanomedicine. *Artif Cells Nanomed Biotechnol* **45**, 833-842, (2017).

529 Cavallaro, G. *et al.* Biocompatible Poly(N-isopropylacrylamide)-halloysite Nanotubes for Thermoresponsive Curcumin Release. *J Phys Chem C* **119**, 8944-8951, (2015).

530 Zhang, J., Liu, T. & Liu, M. Hydrothermal synthesis of halloysite nanotubes @carbon nanocomposites with good biocompatibility. *Microporous and Mesoporous Mater* **266**, 155-163, (2018).

531 Abdullayev, E., Abbasov, V. & Lvov, Y. Halloysite clay nanotubes: structural study and technological applications. *J. Petrochem. Oil Ref* **23**, 234-246 (2010).

532 Bahr, J. L., Mickelson, E. T., Bronikowski, M. J., Smalley, R. E. & Tour, J. M. Dissolution of small diameter single-wall carbon nanotubes in organic solvents? *Chem Comm*, 193-194 (2001).

533 Hudson, J. L., Casavant, M. J. & Tour, J. M. Water-Soluble, Exfoliated, Nonroping Single-Wall Carbon Nanotubes. *J Am Chem Soc* **126**, 11158-11159, (2004).

534 Cui, H. M., Liu, H., Wang, J. Y., Li, X. & Han, F. Agglomeration and dispersion of nano-scale powders. *Mater. Mech. Eng.(China)* **28**, 38-41 (2004).

535 Gaaz, T. S., Sulong, A. B., Kadhum, A. A. H., Nassir, M. H. & Al-Amiery, A. A. Impact of Sulfuric Acid Treatment of Halloysite on Physico-Chemic Property Modification. *Mater (Basel)* **9**, (2016).

536 Carr, R. M., Chaikum, N. & Patterson, N. Intercalation of salts in halloysite. *Clays Clay Miner* **26**, 144-152 (1978).

537 Theng, B. K. G., Russell, M., Churchman, G. J. & Parfitt, R. L. Surface properties of allophane, halloysite, and imogolite. *Clays Clay Miner* **30**, 143-149 (1982).

538 Yu, L., Wang, H., Zhang, Y., Zhang, B. & Liu, J. Recent advances in halloysite nanotube derived composites for water treatment. *Environ Sci Nano* **3**, 28-44 (2016).

539 Bediako, E. G. *et al.* Modified halloysite nanoclay as a vehicle for sustained drug delivery. *Heliyon* **4**, e00689, (2018).

540 White, R. D., Bavykin, D. V. & Walsh, F. C. The stability of halloysite nanotubes in acidic and alkaline aqueous suspensions. *Nanotechnology* **23**, 065705, (2012).

541 Tomiczek, B., Dobrzański, L. A., Adamiak, M. & Labisz, K. Effect of Milling Conditions on Microstructure and Properties of AA6061/halloysite Composites. *Procedia Manuf* **2**, 402-407, (2015).

542 Takahashi, H. Effects of dry grinding on kaolin minerals. I. kaolinite. *Bull Chem Soc Jpn* **32**, 235-245 (1959).

543 Takahashi, H. Effects of dry grinding on kaolin minerals. II. Kibushi-clay. *Bull Chem Soc Jpn* **32**, 245-251 (1959).

544 Takahashi, H. Effects of Dry Grinding on Kaolin Minerals. III. Halloysite. *Bull Chem Soc Jpn* **32**, 252-263 (1959).

545 Sánchez-Soto, P. J., del Carmen Jiménez de Haro, M., Pérez-Maqueda, L. A., Varona, I. & Pérez-Rodríguez, J. L. Effects of dry grinding on the structural changes of kaolinite powders. *J Am Ceram Soc* **83**, 1649-1657 (2000).

546 Randklev, R. M. Glass Ionomer Cement Powder (Google Patents, 1989).

547 Grim, R. E. & Bradley, W. F. Rehydration and dehydration of the clay minerals. *Am Min* **33**, 50-59 (1948).

548 Presti, D. *et al.* Insights into structural and dynamical features of water at halloysite interfaces probed by DFT and classical molecular dynamics simulations. *Phys Chem Chem Phys* **18**, 2164-2174 (2016).

549 Schomburg, J. Personal Communication, HNT hydroxyl water (2018).

550 Ali, M. K. A. *et al.* Improving the tribological characteristics of piston ring assembly in automotive engines using Al2O3 and TiO2 nanomaterials as nano-lubricant additives. *Trib Int* **103**, 540-554 (2016).

551 Sayuti, M., Sarhan, A. A. D. & Salem, F. Novel uses of SiO2 nano-lubrication system in hard turning process of hardened steel AISI4140 for less tool wear, surface roughness and oil consumption. *J Clean Prod* **67**, 265-276, (2014).

552 Rebis, J., Frydrych, J., Skibinski, J. & Rozniatowski, K. Cheap nano-clay additive as a lubricating enhancer. *J Power Tech* **97** (2017).

553 Fonseca, R. B. *et al.* Influence of powder/liquid ratio on the radiodensity and diametral tensile strength of glass ionomer cements. *J Appl Oral Sci* **18**, 577-584 (2010).

554 van Duinen, R. N., Kleverlaan, C. J., de Gee, A. J., Werner, A. & Feilzer, A. J. Early and long-term wear of 'fast-set' conventional glass-ionomer cements. *Dent Mater* **21**, 716-720, (2005).

555 Esquivel-Upshaw, J. F. *et al.* Three years in vivo wear: core-ceramic, veneers, and enamel antagonists. *Dent Mater* **28**, 615-621, (2012).

556 Heintze, S., Forjanic, M., Ohmiti, K. & Rousson, V. Surface deterioration of dental materials after simulated toothbrushing in relation to brushing time and load. *Dent Mater* **26**, 306-319 (2010).

557 Wakamatsu, Y., Kakuta, K. & Ogura, H. Wear test combining simulated occlusal wear and toothbrush wear. *Dent Mat J* **22**, 383-396 (2003).

558 Du, M., Guo, B., Lei, Y., Liu, M. & Jia, D. Carboxylated butadiene–styrene rubber/halloysite nanotube nanocomposites: interfacial interaction and performance. *Polymer* **49**, 4871-4876 (2008).

559 Albdiry, M. T. & Yousif, B. F. Morphological structures and tribological performance of unsaturated polyester based untreated/silane-treated halloysite nanotubes. *Mater Des* **48**, 68-76 (2013).

560 Ei, T. Z. *et al.* Comparison of resin-based and glass ionomer sealants with regard to fluoride-release and anti-demineralization efficacy on adjacent unsealed enamel. *Dent Mater J* **37**, 104-112, (2018).

561 Prabhakar, A. R., Balehosur, D. V. & Basappa, N. Comparative Evaluation of Shear Bond Strength and Fluoride Release of Conventional Glass Ionomer with 1% Ethanolic Extract of Propolis Incorporated Glass Ionomer Cement -Invitro Study. *J Clin Diagn Res* **10**, ZC88-91, (2016).

562 Tolidis, K., Dionysopoulos, D., Gerasimou, P. & Sfeikos, T. Effect of radiant heat and ultrasound on fluoride release and surface hardness of glass ionomer cements. *J Appl Biomater Funct Mater* **14**, e463-e469, (2016).

563 Shahid, S., Hassan, U., Billington, R. W., Hill, R. G. & Anderson, P. Glass ionomer cements: effect of strontium substitution on esthetics, radiopacity and fluoride release. *Dent Mater* **30**, 308-313, (2014).

564 Thevadass, K. P., Pearson, G. J., Anstice, H. M. & Davies, E. H. Method for enhancing the fluoride release of a glass-ionomer cement. *Biomaterials* **17**, 425-429 (1996).

565 Kent, B. E., Lewis, B. G. & Wilson, A. D. Glass ionomer cement formulations: I. The preparation of novel fluoroaluminosilicate glasses high in fluorine. *J Dent Res* **58**, 1607-1619 (1979).

566 De Moor, R. J., Martens, L. C. & Verbeeck, R. M. Effect of a neutral citrate solution on the fluoride release of conventional restorative glass ionomer cements. *Dent Mater* **21**, 318-323, (2005).

567 Vesseur, E. J. R. Latest Developments in Environmental SEM Systems. *Microsc Microanal* **24**, 1136-1137 (2018).

568 Frumento, C. Classification of medical devices. *Medical Devices*, 84 (2011).

569 Schmalz, G. Concepts in biocompatibility testing of dental restorative materials. *Clin Oral Invest* **1**, 154-162 (1998).

570 Murray, P. E., García Godoy, C. & García Godoy, F. How is the biocompatibilty of dental biomaterials evaluated? *Medicina Oral, Patología Oral y Cirugía Bucal (Internet)* **12**, 258-266 (2007).

571 Wallin, R. F. & Arscott, E. F. A practical guide to ISO 10993-5: Cytotoxicity. *Medical Device and Diagnostic Industry* **20**, 96-98 (1998).

572 Rogero, S. O. *et al.* Biocompatibility study of polymeric biomaterials. *Artif Organs* **27**, 424-427 (2003).

573 Commission, E. U. Commission Recommendation of 18 October 2011 on the definition of nanomaterial (2011/696/EU). *Official Journal of the European Communities: Legis* (2011).

574 EU Commission, Regulation of the European Parliament and of the Council on medical devices, and amending Directive 2001/83/EC, Regulation (EC) No 178/2002 and Regulation (EC) No 1223/2009 (2012).

Appendix

Presented at the United Kingdom Society for Biomaterials Conference

Loughborough University

Tuesday 20th June 2017 and Wednesday 21st June 2017

Abstract

Glass ionomer cements (GICs) are one of many restorative materials available to dental clinicians. These are widely used due to their fluoride release, biocompatibility, ease of use and ability to adhere to dentine/enamel without bonding agents. However, the poor strength compared to materials such as composites and amalgams, limit their applications. Hydroxyapatite nanofibers (HANFs) and Halloysite Nanotubes (HNTs) were synthesised and purchased respectively, substituted by various methods into a commercial GIC and the diametral tensile strength (DTS) and compressive strength (CS) assessed. HANF show no significant increase in CS and are unlikely to survive the acidic GIC conditions. HNTs appear more acid resistant but still show some enhancement of mechanical properties at higher percentage substitutions. In addition, the dispersion of the HNTs within the GIC matrix appears to be increased by a simple milling process.

Presented at the United Kingdom Society for Biomaterials Conference

Loughborough University

Tuesday 20th June 2017 and Wednesday 21st June 2017

Abstract

Glass ionomer cements (GICs) are one of many restorative materials available to dental clinicians. These are widely used due to their fluoride release, biocompatibility, ease of use and ability to adhere to dentine/enamel without bonding agents. However, the poor strength compared to materials such as composites and amalgams, limit their applications. Hydroxyapatite nanofibers (HANFs) and Halloysite Nanotubes (HNTs) were synthesised and purchased respectively, substituted by various methods into a commercial GIC and the diametral tensile strength (DTS) and compressive strength (CS) assessed. HANF show no significant increase in CS and are unlikely to survive the acidic GIC conditions. HNTs appear more acid resistant but still show some enhancement of mechanical properties at higher percentage substitutions. In addition, the dispersion of the HNTs within the GIC matrix appears to be increased by a simple milling process.

The Effect of Nanofibers and Nanotubes on the Strength of Glass Ionomer Cements

James Holder[1,2], Michele Barbour[2]

1. School of Oral and Dental Sciences, University of Bristol, BS1 2LY
2. Associated Dental Products Ltd., Swindon, SN5 4HT

Introduction

Conventional glass ionomer cements (GICs) are one of many restorative materials available to dental clinicians. These are widely used due to their fluoride release, biocompatibility, ease of use and ability to adhere to dentine/enamel without bonding agents. However, they lack strength compared to materials such as composites and amalgams, limiting their applications. Hydroxyapatite Nanofibers (HANF) and Halloysite Nanotubes (HNT) were substituted into a GIC and the effect on diametral and compressive strength assessed.

Methods and Materials

HANF were created using a reflux condensation described modified from Chen[1] and analysed using scanning electron microscopy (SEM), transmission electron microscopy (TEM) and x-ray diffraction (XRD). HANFs were substituted into a GIC (Diamond Carve, Kemdent, Swindon) in 1, 2, 3, 5, 10 and 15% and tested for compressive strength (CS) (6 mm height, 4 mm diameter, n = 40) and diametral tensile strength (DTS) (4 mm height, 6 mm diameter, n = 40). After 24 hours samples were loaded to failure using a Zwick/Roell Z020 Testing Machine (Zwick, Leominster) with a crosshead speed of 0.5 mm/min and force at fracture used to calculate CS or DTS. HANF acid lability was assessed by fixing fibers onto an adhesive and immersing into a pH 2 solution for 10 minutes to mimic the GIC neutralisation reaction. HNT (Durtec GmbH, Germany) were also investigated for acid stability using the same method. HNTs were imaged using SEM and TEM and substituted into GICs at 1, 2 and 3% by two approaches: adding HNTs to the GIC powder and mixing on a tube roller (Denley Instruments Ltd, Cambridge) for 15 minutes or milling the powders using a tube mill (IKA, Oxford) for 120s and CS tested.

Results

Hydroxyapatite

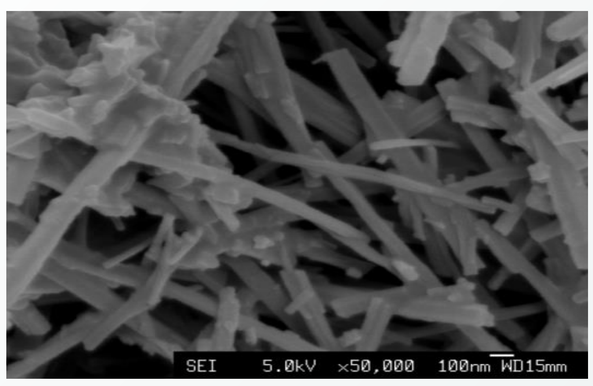

Figure 1: SEM of HANFs (scale x 50,000)

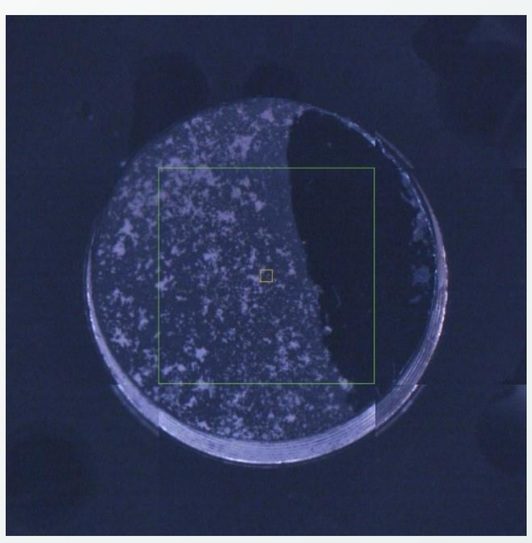

Figure 2: Optical microscope image of HANFs half Immersed into pH 2 solution

% substitution	HANF		HNT	
	CS (MPa)	DTS (MPa)	CS (MPa)	
			Mixed (15 mins)	Milled (120 s)
0 (Control)	156.62 (±25.86)	6.70 (±1.64)	140.25 (±26.14)	149.78 (±21.21)
1	129.84 (±21.26)	6.11 (±1.33)	128.96 (±35.59)	122.97 (±22.12) *
2	130.92 (±16.83)	6.26 (±1.84)	116.89 (±14.16) *	120.29 (±13.30) *
3	150.44 (±23.18)	6.84 (±2.00)	119.79 (±16.36) *	119.90 (±15.81) *
5	126.01 (±18.96) *	6.85 (±1.87)		
10	117.53 (±14.83) *	6.25 (±1.54)		
15	107.77 (±14.95) *	8.39 (±2.10) *		

Table 1: CS and DTS of HANF and HNT substituted into GIC powder (*significant difference)

Halloysites

Figure 3: TEM of HNTs (Image provided by Durtec GmbH)

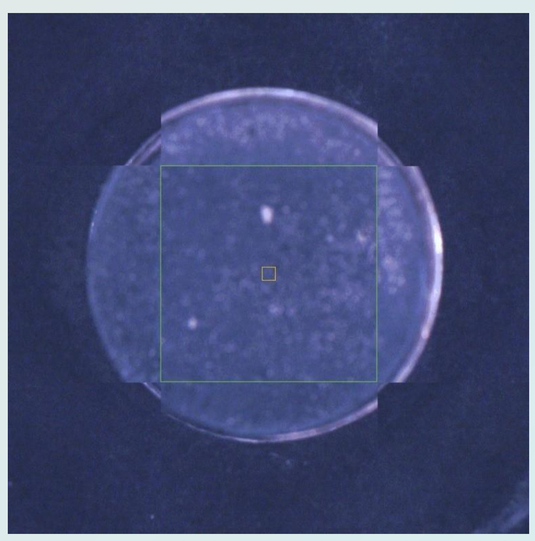

Figure 4: Optical microscope image of HNTs half Immersed into pH 2 solution

Discussion

HANF SEM/TEM showed rod morphologies with 10–50 nm diameters and lengths of 5–10 µm. No increases in CS was seen with up to 15% substitutions of HANFs. However, a significant increase was seen in DTS with a 15% substitution. HANF dissolved when immersed into pH 2 solution and likely the reason of reduced CS as the HANF left voids or reaction inhibiting calcium phosphate upon dissolution. HNT SEM/TEM images showed irregular, hollow, tubular structures with a diameter of 10–30 nm and lengths of 1–5 µm. Acid dipping HNTs showed no dissolution or change in morphology. Milling the fibers with the GIC has not shown any effect on the CS up to a 3% substitution.

Conclusions

- At 1, 2, 3, 5, 10 and 15% HANF showed no significant increase in CS
- Only at a 15% HANF subsitution was a significant increase seen in the DTS, the fibers had little effect below this concentration.
- HANFs were unlikely to have survived the acidic setting reaction

- HNTs appear to be more acid resistant
- No increase in CS has been seen with substitutions of up to 3%
- No differences were seen between milling and mixing the HNTs as a means of dispersion

Acknowledgements

The authors acknowledge Associated Dental Products Ltd. for funding the project and Durtec GmbH for providing HNT TEM images.

References
1. Chen Q *et al.* Dent Mater. 28(10): 1071-1079, 2012.. 2. Sidhu S K and Nicholson J W. J Funct Biomater. 7(3), 2016

JOURNAL OF NANOBIOTECHNOLOGY

RESEARCH Open Access

Development of a novel antimicrobial-releasing glass ionomer cement functionalized with chlorhexidine hexametaphosphate nanoparticles

Edward R Hook[1], Olivia J Owen[1], Candice A Bellis[1], James A Holder[1,2], Dominic J O'Sullivan[1] and Michele E Barbour[1*]

Abstract

Background: Glass ionomer cements (GICs) are a class of dental biomaterials. They have a wide range of uses including permanent restorations (fillings), cavity linings, fissure sealants and adhesives. One of the most common reasons for replacing a dental restoration is recurrent bacterial tooth decay around the margins of the biomaterial. Therefore, a dental biomaterial which creates a sustained antimicrobial environment around the restoration would be of considerable clinical benefit. In this manuscript, the formulation of a GIC containing novel antimicrobial nanoparticles composed of chlorhexidine hexametaphosphate at 1, 2, 5, 10 and 20% powder substitution by mass is reported. The aim is to create GICs which contain chlorhexidine-hexametaphosphate nanoparticles and characterize the nanoparticle size, morphology and charge and the release of chlorhexidine and fluoride, tensile strength and morphology of the GICs.

Results: The GICs released chlorhexidine, which is a broad spectrum antimicrobial agent effective against a wide range of oral bacteria, over the duration of the experiment in a dose-dependent manner. This was not at the expense of other properties; fluoride release was not significantly affected by the substitution of antimicrobial nanoparticles in most formulations and internal structure appeared unaffected up to and including 10% substitution. Diametral tensile strength decreased numerically with substitutions of 10 and 20% nanoparticles but this difference was not statistically significant.

Conclusion: A series of GICs functionalized with chlorhexidine-hexametaphosphate nanoparticles were created for the first time. These released chlorhexidine in a dose-dependent manner. These materials may find application in the development of a new generation of antimicrobial dental nanomaterials.

Keywords: Nanoparticles, Nanobiomaterials, Antimicrobial, Dentistry

Background

Glass ionomer cements (GICs) are a class of biomaterial in widespread use in modern dentistry [1]. They are used for a multitude of applications including for filling cavities caused by tooth decay or wear, as cavity liners, as fissure sealants, and as cements to form an adhesive bond between the tooth and a prosthetic dental restoration such as a crown or bridge. GICs have several favorable properties which make them suitable for these applications: They are tooth colored and available in a range of shades to allow matching to a patient's natural dentition, they have a good biocompatibility profile, and they have an inherent adhesion to enamel and dentine and thus require minimal preparation of the tooth surface prior to application. In comparison to the other main clinical material used for direct tooth-coloured restorations, methacrylate resin-based silica-filled composites, GICs are less compromised by moisture contamination. This means that the clinician does not have to comply with such stringent requirements to thoroughly dry the tooth and surrounding area, which is a significant benefit over the less forgiving resin-based materials, although of course moisture control and careful

* Correspondence: m.e.barbour@bristol.ac.uk
[1]Oral Nanoscience, School of Oral and Dental Sciences, University of Bristol, Lower Maudlin St, Bristol, BS1 2LY, UK
Full list of author information is available at the end of the article

preparation of the field is important with GICs and indeed all restorative materials. Aesthetically GICs are generally considered good, although the opacity and thus the "life-like" appearance are inferior to that of the resin-based materials. As well as for the applications described above, GICs also find application in Atraumatic Restorative Treatment (ART), whereby a dental filling is placed rapidly and without the use of drills or anesthetics [2]. This is particularly beneficial for pediatric and elderly patients as well as those with dental anxiety or learning difficulties.

GICs are acid–base cements composed of glass filler particles and polyacid molecules. The setting of the material is initiated by mixing with water, whereupon the polyacid molecules dissociate and cause dissolution of the glass, resulting in the release of ions which allow cross-linking of the polyacids. The transition from viscous liquid to rigid solid takes place typically over around 2 minutes, although the reaction does not reach completion until several days have elapsed. Even after setting the GICs can still participate in ion exchange with the oral fluids [3]. This has the outcome that GICs can release and absorb fluoride; the glasses in GICs contain calcium fluoride which leaches soluble fluoride into the mouth during normal function. The fluoride in the glass can be replenished by exposure to fluoride-containing oral care products such as dentifrice and mouth rinse, thus creating a rechargeable fluoride "reservoir" and allowing for sustained release of fluoride in the vicinity of a GIC restoration. The intention, when GICs were first developed, was that this fluoride release would protect the surrounding tooth tissue from further decay. While there is no doubt that fluoride in drinking water and oral care products serves to protect the teeth and improve oral health at an individual and community level [4], clinical data is not supportive of an anti-caries effect of GICs [5], and a recent Cochrane Database Systematic Review could find no evidence to support any beneficial result of fluoride-releasing restorative materials [6].

A GIC which offers a genuinely antimicrobial and antibiofilm efficacy would be of considerable clinical benefit [7]. Such a material could reduce recurrent decay in the vicinity of a restoration and could provide an antibacterial seal under other materials, protecting the pulp from bacterial ingress. It could be useful in ART, and as a fissure sealant, providing a protective seal over the occlusal surfaces of caries-vulnerable teeth. The fact that ions can readily travel in and out of the material offers the opportunity to dope the cement with other soluble antimicrobials. New advances in nanotechnology may provide the means to developing such a material [8].

In this manuscript the development of a GIC which contains novel antimicrobial nanoparticles composed of chlorhexidine hexametaphosphate (CHX-HMP nanoparticles) is reported. A recent publication describes surface functionalization of other materials using CHX-HMP nanoparticles prepared using a similar technique, and it was found that they acted as slow release devices for soluble chlorhexidine (CHX) [9] which is a potent antimicrobial agent in widespread use in medicine and dentistry. The CHX-HMP nanoparticles are formed by a precipitation reaction on mixing of aqueous CHX and HMP solutions with HMP in excess. The aim of this study was to establish whether it was possible to create viable GICs containing CHX-HMP nanoparticles and to investigate the properties of those GICs. The ultimate aim of this work is to create a GIC which exhibits a lasting antimicrobial effect *in vivo* without compromising other useful properties of the material.

Results and discussion

Overview

GIC specimens with substitutions of 1, 2, 5, 10 and 20% CHX-HMP nanoparticles for GIC powder were successfully created and compared with unmodified GICs (0% substitution). Those with 30% substitution of CHX-HMP nanoparticles were difficult to handle and the set material was crumbly so these were discarded without further analysis.

Chlorhexidine release

CHX release over 791 h (33 days) normalized to surface area and CHX-free controls is shown in Figure 1. CHX release persisted for the duration of the study with a rate of release which decreased with time. A dose–response was evident in that specimens with a higher substitution of CHX-NPs exhibited a larger CHX release, although the relationship was not directly proportional.

Cumulative CHX release at 1 and 24 h and 8, 15 and 33 days for the 6 specimen groups and the outcome of the statistical analyses are shown in Table 1. In this table,

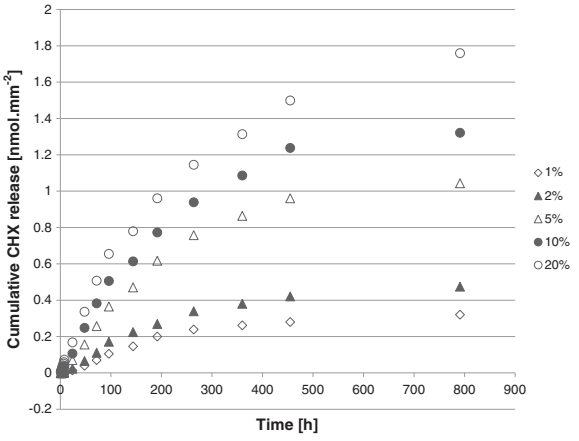

Figure 1 Cumulative CHX release from experimental GIC specimens with varying substitutions of CHX-HMP nanoparticles.

Table 1 Cumulative CHX release for specimens with differing levels of nanoparticle substitution at each of 5 time points

	Cumulative CHX release [nmol.mm^{-2}] (standard deviation in parentheses)				
NP substitution [%]	**1 h**	**24 h**	**8 days**	**15 days**	**33 days**
0	0.01 (0.003)^{a}	0.01 (0.02)^{a}	0.11 (0.06)^{a}	0.12 (0.07)^{a}	0.16 (0.08)^{a}
1	0.16 (0.08)$^{a, b}$	0.20 (0.09)$^{a, b}$	0.48 (0.15)$^{a, b}$	0.56 (0.16)$^{a, b}$	0.65 (0.17)$^{a, b}$
2	0.66 (0.18)^{b}	0.70 (0.19)^{b}	1.04 (0.21)^{b}	1.17 (0.22)^{b}	1.30 (0.24)^{b}
5	1.30 (0.24)^{c}	1.39 (0.25)^{c}	2.03 (0.34)^{c}	2.30 (0.36)^{c}	2.51 (0.38)^{c}
10	2.52 (0.38)^{d}	2.65 (0.40)^{d}	3.40 (0.43)^{d}	3.73 (0.44)^{d}	4.01 (0.45)^{d}
20	4.02 (0.48)^{e}	4.20 (0.50)^{e}	5.09 (0.55)^{e}	5.46 (0.59)^{e}	5.94 (0.67)^{e}

Within each time point, superscript letters indicate statistically homogeneous groups, so figures with different superscript letters are statistically significantly different to a 95% confidence level at that time.

values for the 0% (unsubstituted) GICs are also shown; it can be seen that these readings were small compared to the actual CHX concentration readings, but these are included in the statistical analysis nevertheless so as not to manipulate the data unnecessarily and to allow a figure for comparison. The outcome was the same for each time point in that 0% and 1% were not statistically significantly different from one another, and 1% and 2% were not statistically significantly different from one another, but all other pairings were significantly different indicating a clear increase in chlorhexidine release correlated with an increase in nanoparticle substitution at all measured times.

Since CHX is efficacious against a wide range of bacteria and yeasts, this may confer antimicrobial and thus anti-caries properties on these nanofunctionalized dental filling materials. CHX disrupts the bacterial cell membrane [10] and results in the loss of intracellular components; this has the outcome that the evolution of bacterial resistance to CHX is considered unlikely [11].

Since CHX is an appealing option for the development of a dental cement which reduces the incidence of recurrent tooth decay, is it not surprising that there have been other attempts to incorporate CHX into GICs. CHX diacetate was added to a resin-modified GIC and this resulted in CHX release, but this was only sustained at significant levels for one week [12] and thus offered limited scope for lasting anti-caries effects. Incorporating CHX diacetate into a conventional (not resin-modified) GIC also yielded a CHX-releasing material, but again the CHX release was sustained for only around a week with all except the highest substitutions, and these high substitutions resulted in a deterioration of the mechanical properties of the material [13]. Dental composite resins supplemented with pulverized CHX diacetate also showed CHX release which reached a plateau after around 7 days [14]. The CHX release observed in the study reported here was more prolonged, and it is thought that this ie because the nanoparticlces themselves exhibit a gradual release of soluble CHX [9] rather than the already soluble and thus readily lost CHX in the studies described above.

Another report describes a longer-term effect of incorporating CHX – as ground CHX diacetate powder or as CHX digluconate solution – into GICs [15]. The CHX release per se was not measured but it was shown that an antimicrobial effect persisted for between 40 and 90 days. The peak of efficacy was the first 24 h for all GIC specimens, suggesting that most CHX may have been released during this initial period, and most specimens showed no antimicrobial behavior after 60–90 days. For some formulations, a limited deterioration in mechanical properties was observed. CHX digluconate solution has also been incorporated into GICs in combination with another antimicrobial agent, cetrimide, and this too had an antimicrobial effect on oral bacteria [16]. The authors indicate that this effect persisted for up to 180 days, but whether this was due to antimicrobial still leaching at the 180 day point, or that which had earlier leached and was still present in the agar plate, is not clear.

Fluoride release

Fluoride release over 791 h (33 days) normalized to surface area can be seen in Figure 2. All of the GIC specimens released fluoride continually over the duration of the experiment. The initial release rate was the most rapid and this gradually slowed over the experimental period, as has been observed for conventional GICs by other researchers [17].

Cumulative fluoride release at 1 and 24 h and 8, 15 and 33 days for the 6 specimen groups and the outcome of the statistical analysis are shown in Table 2. At 1 h, the unmodified GIC released significantly more fluoride than nanoparticle-substituted cements but there were no statistically significant differences between the different substitutions. At later times, in numerical terms fluoride release displayed a pattern of 20% > 5, 10% > 1, 2% with a complex relationship with 0%. However, there were few statistically significant differences; the only ones observed were at 24 h, 2% nanoparticle-substituted GICs released

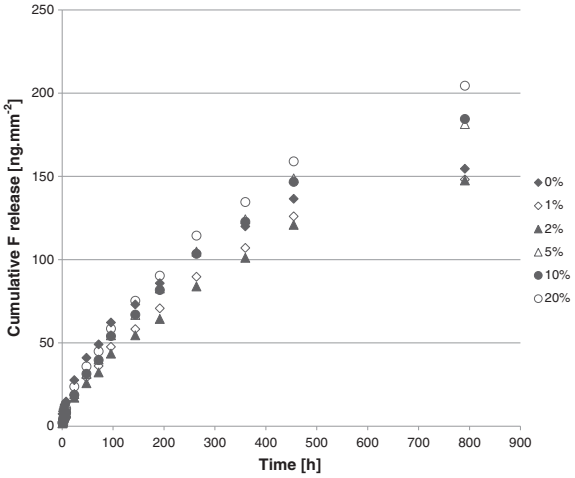

Figure 2 Cumulative fluoride release from experimental GIC specimens with varying substitutions of CHX-HMP nanoparticles.

less fluoride than the 0% control, and at the longest time point, 33 days, the 20% nanoparticle-substituted GICs released more fluoride than the 2% nanoparticle-substituted GICs. It is not clear why the most highly substituted GIC released the most fluoride, especially as the greater the proportion of CHX-HMP nanoparticles, the smaller the total mass of fluoride-containing filler present. It is possible that the presence of the CHX-HMP nanoparticles alters the setting reaction and this renders fluoride more mobile in the cement lattice, but this is a hypothesis that has yet to be tested, and should be considered in the context that only the 2%-20% comparison showed significant differences. Although the impact of fluoride release from restorative materials is still a source of some controversy [1], it is not of concern in this study since the nanofunctionalized GICs showed similar fluoride release profiles to the unmodified cements. This is in contrast to an earlier report in which GICs supplemented with CHX digluconate solution exhibited a reduction in fluoride release [18].

Tensile strength

Diametral tensile strength of the 6 specimen groups are shown in Table 3. The ANOVA gave a p value of 0.054 indicating that, although there was a numerical trend towards lower tensile strength for 10 and 20% substitution cements, there was no statistically significant difference between these values and those of the other GICs. The fact that substitutions up to 5% appeared to have no significant deleterious effect on the tensile strength of the cements is encouraging.

Nanoparticle characterization

Dynamic light scattering (DLS) indicated that there were structures of mean diameter 196 nm, but it was observed that there was substantial polydispersity and the standard deviation was large (76 nm). The correlation functions observed during some DLS measurements suggested the presence of some much larger particles. This may be explained by observations made by atomic force microscopy (AFM) (Figure 3) which indicated that nanoparticles sometimes formed aggregates which could be as large as several micrometres. The individual nanoparticles which compose these aggregates were regularly shaped, globular and had typical diameters of 80–90 nm (Figure 3). This would not be observed in DLS since the signal is proportional to diameter to the 6th power, so the signal from these small nanoparticles would be masked by that from the larger aggregates.

Zeta potential measurements indicated that the nanoparticles had a mean surface charge of −55 mV (standard deviation 1.4 mV), indicating a net negative charge.

Morphology and structure

Scanning electron micrographs of representative GIC specimens are shown in Figure 4. The appearances of the GIC specimens with different substitutions of nanoparticles were similar, with the glass filler particles and surrounding matrix clearly visible. Only the 20% nanoparticle substitution exhibited a slightly different appearance (Figure 4f), with textured areas depleted in glass

Table 2 Cumulative fluoride release for specimens with differing levels of nanoparticle substitution at each of 5 time points

	Cumulative fluoride release [ng.mm^{-2}] (standard deviation in parentheses)				
NP substitution [%]	**1 h**	**24 h**	**8 days**	**15 days**	**33 days**
0	7.38 (1.69)^{a}	27.65 (0.85)^{a}	85.82 (5.68)^{a}	119.9 (11.0)^{a}	154.5 (14.3)$^{a, b}$
1	2.61 (1.11)^{b}	18.59 (3.12)$^{a, b}$	70.72 (8.40)^{a}	106.9 (14.1)^{a}	148.1 (16.6)^{a}
2	1.68 (0.73)^{b}	17.10 (2.33)^{b}	64.30 (7.68)^{a}	101.1 (12.2)^{a}	147.5 (15.7)^{a}
5	1.74 (0.70)^{b}	19.31 (4.32)$^{a, b}$	82.67 (7.49)^{a}	124.2 (9.2)^{a}	181.4 (14.0)$^{a, b}$
10	1.83 (0.96)^{b}	18.73 (9.50)$^{a, b}$	81.73 (30.22)^{a}	122.8 (39.3)^{a}	184.4 (49.8)$^{a, b}$
20	2.09 (0.34)^{b}	23.74 (5.89)$^{a, b}$	81.73 (13.15)^{a}	134.6 (19.2)^{a}	204.4 (23.4)^{b}

Within each time point, superscript letters indicate statistically homogeneous groups, so figures with different superscript letters are statistically significantly different to a 95% confidence level at that time.

Table 3 Diametral tensile strength of GIC specimens

NP substitution [%]	Diametral tensile strength [MPa] (standard deviation in parentheses)
0	14.1 (3.7)
1	14.3 (4.9)
2	15.7 (4.3)
5	15.5 (1.1)
10	11.5 (2.8)
20	9.4 (2.6)

The ANOVA gave $p = 0.054$ indicating that there were no statistically significantly differences between tensile strengths of the different GICs to a 95% confidence level.

particles and a smoother fracture plane which are suggestive of nanoparticle aggregates. It is possible that these could lead to a reduction in strength since they cannot be presumed to interact with the polyacid in the same way as the glass filler particles, and future studies will address this important question.

Overview

By adding CHX-HMP nanoparticles to a commercial GIC it has proven possible to create a material which releases CHX for in a dose-dependent manner for longer than has been observed using some other approaches to CHX functionalization. The results of this study would suggest that substitutions of up to 20% nanoparticles for glass by mass using this approach may be suitable for further development as clinical materials. 10% and 20% substitutions showed a numerical reduction in strength but not a statistically significant one; subsequent follow-on studies will allow for further investigation of this observation. Higher substitutions, of 30% or more, are unlikely to find application without other changes to the cement as this resulted in a dry, crumbly cement with unacceptable handling properties. Options to use more dispersed nanoparticles, rather than the ground aggregates discussed here, are under investigation. Possibilities for CHX recharging and the microbiological impact of the CHX release are the subject of ongoing experiments, as well as larger studies to investigate the effect on different kinds of strength. Interestingly, it has recently been shown that resin-modified GICs can act as a short-term in vivo reservoir for topically applied CHX [19].

In this study, nanoparticles were substituted for powder by weight. An alternative approach is to substitute like-for-like by surface area, and this would account for the fact that the specific surface area of the nanoparticles is higher than that of the glass filler particles.

Conclusions

Novel GICs have been created which contain antimicrobial CHX-HMP nanoparticles at a range of dopings. These GICs released soluble CHX over a period of at least 33 days, and the quantity of CHX released was dependent on the doping of nanoparticles in the cement. All cements released fluoride with a similar profile to the control, unmodified cement and moderate substitutions did not detrimentally affect the tensile strength of the material. These cements may find clinical application as dental biomaterials which prevent or reduce the incidence of secondary caries and protect the tooth and soft tissues from bacterial infection.

Methods

Synthesis and preparation of CHX-HMP nanoparticles

Aqueous stock solutions of chlorhexidine digluconate and sodium hexametaphosphate (Sigma Aldrich, Gillingham, UK) were mixed in deionized water such that the final concentration was 4 mM CHX and 5 mM HMP. The resulting colloidal suspension of CHX-HMP nanoparticles was mixed thoroughly and then centrifuged at 21000 g for 60 min. The supernatant was removed and discarded and the nanoparticle pellet dried for at least 48 h at 40°C. The pellet was then removed from the centrifuge tubes and ground to a fine white powder composed of nanoparticle aggregates using an agate mortar and pestle. Further details regarding the properties of CHX-HMP nanoparticles and their antimicrobial efficacy can be found elsewhere [9].

Prototype nanofunctionalized glass ionomer cements

A commercially available GIC (Diamond Carve (TM), Kemdent, Purton, UK) was used as the starting material. This commercially available GIC comprises a powder, which consists of alumina-silica based glass filler particles containing calcium fluoride and other minor salts and freeze-dried poly (vinyl) phosphonic acid, and a liquid which contains polyacrylic and tartaric acids. It is mixed in a ratio of 1:4 liquid:powder by mass. Cylindrical GIC specimens with nominal dimensions of 6 mm diameter and 3 mm height were formed by mixing the GIC according to the manufacturers' instructions and packing into Perspex molds coated with a thin layer of petroleum jelly to aid removal. The mixing was carried out by one individual (OJO) with extensive experience of GIC mixing and handling. The precise dimensions of each specimen were measured using calipers and recorded. The nanoparticle powder created by grinding the nanoparticle pellet and thus yielding compacted clusters of nanoparticles was used to substitute for the GIC powder at fractions of 0, 1, 2, 5, 10, 20 and 30% by mass. Ten specimens of each substitution were created giving a total of 70 specimens. They were removed from the mold within 60 minutes and placed in individual small, sealed plastic vessels that contained wet tissue paper not in direct contact with the specimen, to achieve

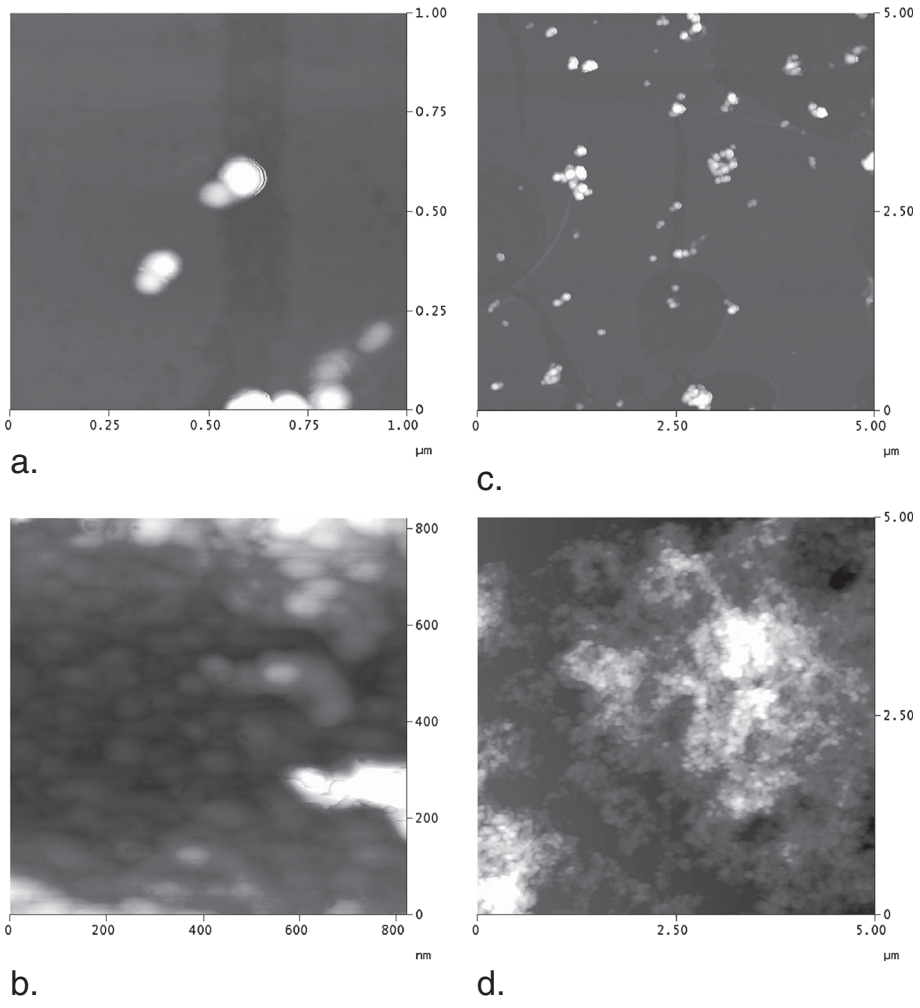

Figure 3 Atomic force microscopy images showing CHX-HMP nanoparticles deposited on a glass coverslip. a: 1 × 1 μm image with vertical scale 50 nm showing individual globular nanoparticles. **b**: 0.8 × 0.8 μm image with vertical scale 20 nm showing individual nanoparticles of similar shape and morphology as in **(a)** but in an aggregate. **c**: 5 × 5 μm image with vertical scale 100 nm showing individual nanoparticles and small aggregates. **d**: 5 × 5 μm image with vertical scale 500 nm showing nanoparticles in a large aggregate.

an atmosphere of 100% humidity but prevent the specimen being in contact with liquid water which could result in dissolution during the critical early phases of setting. These were stored at 37°C for 7 days.

After this the specimens were divided into two sets of 5 specimens each. One set of each substitution was set aside for tensile strength and fracture surface morphology analysis and the other set was used to investigate the CHX and fluoride leaching from the cement.

For the investigations of CHX and fluoride release, each specimen was immersed in 1 mL artificial saliva in individually labeled vials at 37°C. The artificial saliva was composed of $CaCl_2 \cdot 2H_2O$ 0.103 gL^{-1}, $MgCl_2$ 0.019 gL^{-1}, KH_2PO_4 0.544 gL^{-1}, $C_8H_{18}N_2O_4S$ (HEPES buffer acidic form) 4.77 gL^{-1}, KCl 2.24 gL^{-1}, 1.80 mL 1 M HCl, KOH titrated to obtain a pH of 6.8. Specimens were periodically removed and placed in duplicate tubes containing fresh artificial saliva so that the artificial saliva the specimen had been incubated in could be sampled for CHX and fluoride concentrations. A pilot study was conducted to establish the saturation limit of fluoride concentration within the vessels to ensure that the sampling periods were selected appropriately and erroneous readings owing to saturation of the eluent by a fluoride salt were not obtained by leaving too large a gap between readings. Using the findings from this pilot study, the sampling occurred at hourly intervals during the first day, followed by intervals of 4 hours, then daily and then weekly. Controls containing only artificial saliva without a GIC specimen were sampled in the same way.

Chlorhexidine measurements

CHX concentration in the artificial saliva was measured using ultraviolet spectrophotometry. The 1 mL artificial

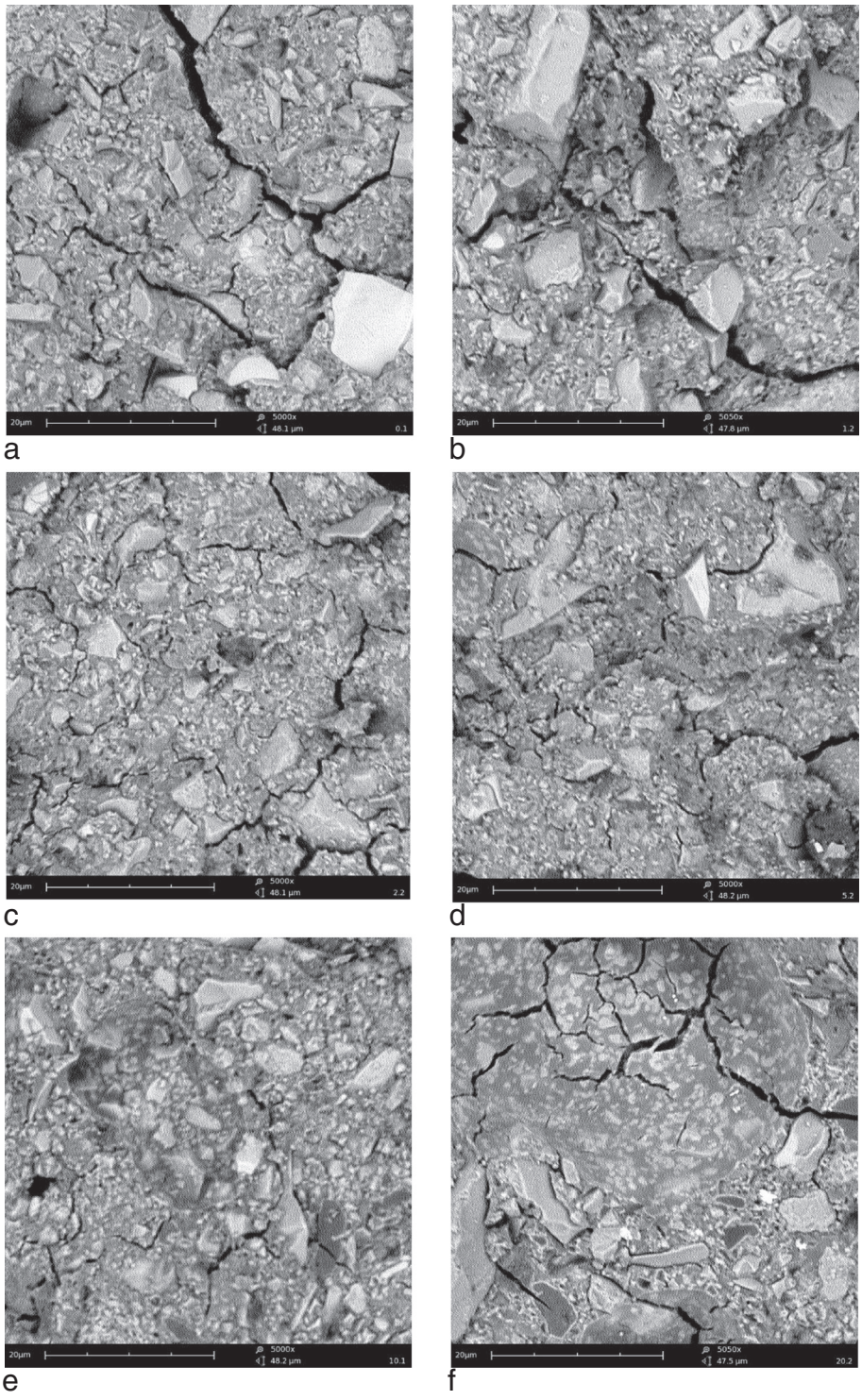

Figure 4 Scanning electron micrographs showing fracture surfaces of GIC specimens. a: unmodified GIC; **b**: 1% nanoparticles; **c**: 2% nanoparticles; **d**: 5% nanoparticles; **e**: 10% nanoparticles; **f**: 20% nanoparticles. The scale bar is 20 μm in each image.

saliva was placed into a semi-micro cuvette transparent under ultraviolet wavelengths and absorption was measured at 255 nm using a spectrophotometer (Hitachi U1900, Tokyo, Japan). The reading was converted to CHX concentration with reference to calibration standards at 5–50 $\mu mol.l^{-1}$. The concentration was converted to moles of CHX released per unit surface area of the GIC specimen with reference to the individual dimension measurements

for each specimen and was normalized by subtracting the reading for 0% substitution to correct for any other molecules present in the system which absorbed at 255 nm such as the polyacrylic acid which is another component of the GIC.

Fluoride measurements

Fluoride concentration in the artificial saliva was measured using an ion-selective electrode (9609BNWP, Thermo Fisher Scientific, Waltham, MA, USA) by mixing 0.5 mL artificial saliva with 0.5 mL TISAB solution (Thermo Fisher Scientific, Waltham, MA, USA). The data output was converted to mg/L fluoride ion with reference to calibration standards of 0.1, 0.5, 1, 2 and 5 mg/L F^-, also diluted with equal quantities of TISAB.

Tensile strength measurements

Indirect tensile strength (S_T) was measured by applying a compressive diametric force to the curved sides of the cylindrical specimen (n = 5 per group) until fracture occurred, using a universal testing machine (LR5K, Lloyd Instruments, Ametek, FL, USA) recording the load at fracture (L) and using this with the specimen dimensions of height (h) and diameter (d) to calculate tensile strength according to the relationship:

$$Sr = \frac{2L}{\pi dt}$$

Statistical analysis

Cumulative CHX and fluoride release at time points of 1 h, 24 h, 8 days, 15 days and 33 days, and indirect tensile strength, were compared using one-way ANOVAs with a Tukey honestly significant difference post-hoc test.

Characterization of CHX-HMP nanoparticles

The size and zeta potential of the nanoparticles as prepared in colloidal suspension were measured using a Malvern Zetasizer (Malvern, UK). The size, morphology and aggregation of the nanoparticles were investigated when immobilized on glass coverslips. Coverslips were cleaned by ultrasonicating for 10 minutes in acetone followed by ultrasonicating for 10 minutes in ethanol then coated by dipping into a freshly prepared colloid of the nanoparticles for 30 seconds, then rinsing in running deionized water for 10 seconds, then allowing to dry in air. The nanoparticle-coated coverslips were imaged using AFM (Nanoscope IIIa, Digital Instruments, CA, USA).

Morphology and structure

Specimens which had been tested for tensile strength were coated with a thin layer of gold-palladium (SC7620, Emitech, Taiwan) and examined using SEM (Phenom, Eindhoven, Netherlands). Images were obtained at nominal magnifications of 400, 1000 and 5000×.

Abbreviations

CHX: Chlorhexidine; CHX-HMP: Chlorhexidine hexametaphosphate; GIC: Glass ionomer cement.

Competing interests

The University of Bristol filed a patent application relating to the work presented in this manuscript in 2013.

Authors' contributions

ERH, OJO and CAB were the students who carried out the laboratory work and statistical analysis. JAH was the industry supervisor of the study, providing guidance and input on study design from the industrial perspective. DJOS was the clinical supervisor of the study, providing a clinician's perspective on important material properties and helping to develop the study parameters and design. MEB was the principal, scientific supervisor of the study. She conceived the study, supervised the students in the laboratory, directed the analysis and wrote the manuscript. All authors read and approved the final draft of the manuscript.

Author details

[1]Oral Nanoscience, School of Oral and Dental Sciences, University of Bristol, Lower Maudlin St, Bristol, BS1 2LY, UK. [2]Kemdent, Associated Dental Products Ltd, Cricklade Road, Purton, Wiltshire, SN5 4HT, UK.

Received: 5 November 2013 Accepted: 21 January 2014
Published: 23 January 2014

References

1. Sidhu SK: **Glass-ionomer cement restorative materials: a sticky subject?** *Aust Dent J* 2011, **56**(1):23–30.
2. Holmgren CJ, Roux D, Domejean S: **Minimal intervention dentistry: part 5. Atraumatic restorative treatment (ART)–a minimum intervention and minimally invasive approach for the management of dental caries.** *Br Dent J* 2013, **214:**11–18.
3. Billington RW, Williams JA, Pearson GJ: **Ion processes in glass ionomer cements.** *J Dent* 2006, **34:**544–555.
4. Griffen AL, Goepferd SJ: **Preventive oral health care for the infant, child, and adolescent.** *Pediatr Clin North Am* 1991, **38:**1209–1226.
5. Randall RC, Wilson NH: **Glass-ionomer restoratives: a systematic review of a secondary caries treatment effect.** *J Dent Res* 1999, **78:**628–637.
6. Yengopal V, Harneker SY, Patel N, Siegfried N: **Dental fillings for the treatment of caries in the primary dentition.** *Cochrane Database Syst Rev* 2009:CD004483.
7. Wang Z, Shen Y, Haapasalo M: **Dental materials with antibiofilm properties.** *Dent Mater* 2013, **30:**e1–e16.
8. Melo MA, Guedes SF, Xu HH, Rodrigues LK: **Nanotechnology-based restorative materials for dental caries management.** *Trends Biotechnol* 2013, **31:**459–467.
9. Barbour ME, Maddocks SE, Wood NJ, Collins AM: **Synthesis, characterization, and efficacy of antimicrobial chlorhexidine hexametaphosphate nanoparticles for applications in biomedical materials and consumer products.** *Int J Nanomedicine* 2013, **8:**3507–3519.
10. Gilbert P, Moore LE: **Cationic antiseptics: diversity of action under a common epithet.** *J Appl Microbiol* 2005, **99:**703–715.
11. Meyer B, Cookson B: **Does microbial resistance or adaptation to biocides create a hazard in infection prevention and control?** *J Hosp Infect* 2010, **76:**200–205.
12. Sanders BJ, Gregory RL, Moore K, Avery DR: **Antibacterial and physical properties of resin modified glass-ionomers combined with chlorhexidine.** *J Oral Rehabil* 2002, **29:**553–558.
13. Palmer G, Jones FH, Billington RW, Pearson GJ: **Chlorhexidine release from an experimental glass ionomer cement.** *Biomaterials* 2004, **25:**5423–5431.
14. Cheng L, Weir MD, Xu HH, Kraigsley AM, Lin NJ, Lin-Gibson S, Zhou X: **Antibacterial and physical properties of calcium-phosphate and calcium-fluoride nanocomposites with chlorhexidine.** *Dent Mater* 2012, **28:**573–583.

15. Turkun LS, Turkun M, Ertugrul F, Ates M, Brugger S: **Long-term antibacterial effects and physical properties of a chlorhexidine-containing glass ionomer cement.** *J Esthet Restor Dent* 2008, **20:**29–44. discussion 45.
16. Korkmaz FM, Tuzuner T, Baygin O, Buruk CK, Durkan R, Bagis B: **Antibacterial activity, surface roughness, flexural strength, and solubility of conventional luting cements containing chlorhexidine diacetate/ cetrimide mixtures.** *J Prosthet Dent* 2013, **110:**107–115.
17. Yip HK, Smales RJ: **Fluoride release from a polyacid-modified resin composite and 3 resin-modified glass-ionomer materials.** *Quintessence Int* 2000, **31:**261–266.
18. Hoszek A, Ericson D: **In vitro fluoride release and the antibacterial effect of glass ionomers containing chlorhexidine gluconate.** *Oper Dent* 2008, **33:**696–701.
19. Lim BS, Cheng Y, Lee SP, Ahn SJ: **Chlorhexidine release from orthodontic adhesives after topical chlorhexidine treatment.** *Eur J Oral Sci* 2013, **121:**211–217.

doi:10.1186/1477-3155-12-3
Cite this article as: Hook *et al.*: Development of a novel antimicrobial-releasing glass ionomer cement functionalized with chlorhexidine hexametaphosphate nanoparticles. *Journal of Nanobiotechnology* 2014 **12**:3.

Journal of Dentistry 45 (2016) 53–58

Contents lists available at ScienceDirect

Journal of Dentistry

journal homepage: www.intl.elsevierhealth.com/journals/jden

Glass ionomer cements functionalised with a concentrated paste of chlorhexidine hexametaphosphate provides dose-dependent chlorhexidine release over at least 14 months

Candice A. Bellis[a], Angela H. Nobbs[b], Dominic J. O'Sullivan[a], James A. Holder[a,c], Michele E. Barbour[a,*]

[a] Oral Nanoscience, School of Oral and Dental Sciences, University of Bristol, Lower Maudlin St BS1 2LY, UK
[b] Oral Microbiology, School of Oral and Dental Sciences, University of Bristol, Lower Maudlin St BS1 2LY, UK
[c] Kemdent, Associated Dental Products Ltd., Purton, Swindon SN5 4HT, UK

ARTICLE INFO

Article history:
Received 11 September 2015
Received in revised form 7 December 2015
Accepted 30 December 2015

Keywords:
Glass ionomer
Restorative
Antimicrobial
Chlorhexidine
Biomaterials

ABSTRACT

Objectives: The aim of this study was to create prototype glass ionomer cements (GICs) incorporating a concentrated paste of chlorhexidine–hexametaphosphate (CHX–HMP), and to investigate the long-term release of soluble chlorhexidine and the mechanical properties of the cements. The purpose is the design of a glass ionomer with sustained anticaries efficacy.
Methods: CHX–HMP paste was prepared by mixing equimolar solutions of chlorhexidine digluconate and sodium hexametaphosphate, adjusting ionic strength, decanting and centrifuging. CHX–HMP paste was incorporated into a commercial GIC in substitution for glass powder at 0.00, 0.17, 0.34, 0.85 and 1.70% by mass CHX–HMP. Soluble chlorhexidine release into artificial saliva was observed over 436 days using absorbance at 255 nm. Diametral tensile and compressive strength were measured after 7 days' setting (37 °C, 100% humidity) and tensile strength after 436 days' aging in artificial saliva. 0.34% CHX–HMP GICs were tested for their ability to inhibit growth of *Streptococcus mutans in vitro.*
Results: GICs supplemented with CHX–HMP exhibited a sustained dose-dependent release of soluble chlorhexidine. Diametral tensile strength of new specimens was unaffected up to and including 0.85% CHX–HMP, and individual values of tensile strength were unaffected by aging, but the proportion of CHX–HMP required to adversely affect tensile strength was lower after aging, at 0.34%. Compressive strength was adversely affected by CHX–HMP at substitutions of 0.85% CHX–HMP and above.
Conclusions: Supplementing a GIC with CHX–HMP paste resulted in a cement which released soluble chlorhexidine for over 14 months in a dose dependent manner. 0.17% and 0.34% CHX–HMP did not adversely affect strength at baseline, and 0.17% CHX–HMP did not affect strength after aging. 0.34% CHX–HMP GICs inhibited growth of *S. mutans* at a mean distance of 2.34 mm from the specimen, whereas control (0%) GICs did not inhibit bacterial growth.
Clinical Significance: Although GICs release fluoride *in vivo,* there is inconclusive evidence regarding any clinical anticaries effect. In this study, GICs supplemented with a paste of chlorhexidine-hexametaphosphate (CHX–HMP) exhibited a sustained release of chlorhexidine over at least 14 months, and small additions of CHX–HMP did not adversely affect strength.

1. Introduction

Glass ionomer cements (GICs) are used for a number of purposes, including as direct restorative materials, lining and luting materials, adhesives, and in atraumatic restorative therapy. GIC restorations typically have shorter lifetimes than composites or amalgams [1–3], although the reasons for this are complex and, of course, the materials are not selected at random but are chosen by the clinician according to clinical need. When a GIC does fail, there are a number of potential reasons, one of which is secondary caries; this is responsible for 25% of failures of GIC-lined restorations after 18 years of clinical service [4] and around 18% of GIC failures over a range of 0.1–23 years [5].

GICs leach fluoride into the oral environment. This results in elevated fluoride concentrations close to the restoration, and thus there is an hypothesis that this may reduce dental caries in the

* Corresponding author.
E-mail address: m.e.barbour@bristol.ac.uk (M.E. Barbour).

http://dx.doi.org/10.1016/j.jdent.2015.12.009
0300-5712/

local area owing to the interaction of the fluoride ion with the hydroxyapatite in the enamel and dentine. This hypothesis is broadly supported by *in vitro* data, but *in situ* and clinical studies of caries incidence in the vicinity of fluoride-releasing restoratives do not show consistent results [6]. At the current time it is not possible to conclude whether fluoride release from GICs provides lasting protection against dental caries [6,7].

Chlorhexidine (CHX) is a biocide with broad spectrum efficacy against a wide range of microbes. Its main application in dentistry is as a topical agent, usually in oral care products, products for treatment of periodontal disease, and varnishes. CHX is efficacious against the microbes implicated in dental caries, and is used in a number of products designed to protect the dentition against decay. However, the CHX salts in currently available commercial form have poor retention *in situ*, providing typically a few hours of antimicrobial function. One commercial material used for treatment of periodontal disease provides some sustained CHX release, but this is a short-term effect with 80% of the CHX released within the first 2 days, and a very slow release over the following 3–4 weeks [8].

There have been a number of attempts to incorporate CHX into GICs, with the aim of creating a restorative material that offers lasting protection against caries. GICs doped with CHX diacetate and CHX digluconate have been reported, and these inhibited growth of *Streptococcus mutans* and *Lactobacillus acidophilus*, but there was also some deterioration of mechanical properties and the antimicrobial effects were limited to the first 40–90 days of the study, with no bactericidal effect observed after this time [9]. There are also reports of an increase in porosity and setting time and a reduction in hardness and tensile bond strength when GICs are doped with CHX digluconate [10,11]. CHX diacetate and CHX hydrochloride have also been incorporated into GICs, and these too inhibited growth of caries-causing organisms, but CHX release was only observed for 24 h so it is not clear how long this effect would be sustained [12]. CHX diacetate doped resin modified GICs exhibited some sustained release of CHX, although this reached completion in 14–21 days [13]. The release profiles of soluble CHX from GICs doped with these conventional salts of CHX exhibit a high initial release followed by little or no sustained release, and this perhaps explains the cytotoxic effects observed against fibroblasts when GICs were doped with 1% CHX diacetate [14]. However, supplementation of a resin-modified GIC with CHX digluconate at modest concentrations (1.25%) had no adverse effects on osteoblasts *in vitro* and resulted in an elimination of *S. mutans* populations following indirect pulp treatment *in vivo* [15], suggesting a potential clinical benefit of a CHX-functionalised restorative material.

We have previously reported the use of a novel salt of CHX: CHX–hexametaphosphate (CHX–HMP) [16]. CHX–HMP has a lower solubility than CHX digluconate or CHX diacetate and, when used as a coating or dopant, can confer a sustained release of CHX that persists for at least three months [17]. We have described the use of CHX–HMP as a filler for GICs [18]. In that study, large clusters of CHX–HMP particles were used, and the size of these large particles, which were formed due to the production process, is likely to account for the adverse effects on the mechanical properties observed. The aim of the study described here was to investigate the use of CHX–HMP particles as GIC fillers but using a new preparation method which omits the drying process which creates the large aggregates and instead uses a process of ionic strength adjustment and centrifugation to sequester the particles. CHX release was probed over a clinically relevant timescale of over one year, and both compressive and tensile strength were investigated; the latter was measured also after 14 months' aging to determine if the modification of the cement adversely affects long-term mechanical properties.

The hypothesis was that the prototype cements incorporating a concentrated paste of CHX–HMP particles would confer a more sustained CHX release, sufficient to inhibit growth of cariogenic microbes, coupled with less adverse effects on mechanical properties in comparison to large, dry aggregates of CHX–HMP or conventional salts of CHX such as digluconate or diacetate.

2. Methods

2.1. Preparation of CHX–HMP paste

Aqueous 10 mM solutions of CHX digluconate and sodium HMP were prepared. 100 mL of each solution were combined in a glass beaker under ambient laboratory conditions. The suspension created was stirred vigorously for approximately 1 min, then 30 mL 1 M potassium chloride was added. Stirring continued for a further 1 min before the preparation was allowed to settle for 24 h. The precipitate settled at the bottom of the flask and the supernatant was gently discarded leaving a concentrated suspension of the precipitate. This suspension was then centrifuged at $4760 \times g$ for 30 min. The supernatant was again discarded and the pellet of paste was removed from the centrifuge tubes using a spatula and used immediately.

2.2. Preparation of specimens

A commercially available GIC, Diamond Carve™ (Kemdent Ltd., Purton, UK), was used as the base material to create the experimental cements. This GIC comprises a powder, consisting of alumina–silica based glass filler particles which contain calcium fluoride and other minor salt components and freeze dried poly (vinyl) phosphonic acid, and a liquid, which contains polyacrylic and tartaric acids. The manufacturers' instructions indicate that the powder and liquid should be mixed in a 4:1 ratio by mass to create the finished cement.

The water content of the paste was established to allow the concentration of the liquid component of the GIC to be adjusted to account for the additional water in the CHX–HMP paste. CHX–HMP paste was weighed as freshly prepared, then stored at 37 °C and weighed periodically until the mass of the powder was constant, indicating that the available water had evaporated (24 h). This revealed a composition of 83% water and 17% CHX–HMP particles. The GIC liquid component was thus prepared at a concentration that resulted in the standard final concentration when diluted by the paste. The paste was substituted for the overall mass at 0, 0.17, 0.34, 0.85 and 1.70% by mass of CHX–HMP (0, 1, 2, 5 and 10% by mass of the paste). The paste was mixed into the liquid first and then the powder was added to the paste–liquid combination. Mixing of the specimens was completed in 40–50 s and packing into the moulds took a further 10 s, such that all manipulation of the cement was completed within 1 min.

GICs were packed, using a stainless steel spatula, into stainless steel moulds with dimensions of 6 mm height and 4 mm diameter (for compressive strength determination) or 4 mm height and 6 mm diameter (for measurement of diametral tensile strength and elution of CHX). The moulds were lined with a thin layer of petroleum jelly to aid removal of the set cement. Immediately after packing, the moulds were placed between two sheets of acetate and a 2 kg weight placed on top of the specimens on a flat surface in order to ensure even distribution of the cement. After 5 min the specimens were sanded using a P120 grit sanding disc (Hermes, Hamburg, Germany) to remove excess material and were then placed into small, sealed plastic vessels containing wet tissue paper packed into the lid to achieve 100% humidity without direct contact with water. Specimens were stored at 37 °C for 7 days prior

to any further testing to ensure the setting process had reached completion.

2.3. Compressive strength (CS) testing

CS was measured by applying a compressive force to the flat surface of the cylindrical specimens using a universal testing machine (Zwick/Roell Universal Testing Machine, Zwick/Roell, Leominster, Herefordshire, UK) and recording the load at fracture. Specimens were examined after fracture for evidence of flaws on the internal or external surfaces and data from flawed specimens were rejected. Load at fracture L_F was used with diameter D to calculate CS according to the relationship $CS = 4L/\pi D^2$. The load was used in conjunction with the average diameter of the specimen. Specimen dimensions were measured three times using a digital micrometer. $N = 24$ specimens per group were used. Data were analysed using a one-way ANOVA followed by a Tukey Honestly Significant Difference *post-hoc* test.

2.4. Diametral tensile strength (DTS) testing

DTS was measured by applying a compressive force to the curved sides of the cylindrical specimen using a universal testing machine and recording the load at fracture. Specimens were examined after fracture for evidence of flaws on the internal or external surfaces and data from specimens found to be flawed were rejected. The load at fracture L_F was used in conjunction with the average diameter D and height h of the specimens to calculate DTS according to the relationship $DTS = 2L/\pi Dh$. Specimen dimensions were measured three times using a digital micrometer.

$N = 24$ specimens per group were used for the "new" specimens; these were prepared, allowed to set for 7 days then tested immediately. Specimens were also tested after 436 days' elution, to establish the diametral tensile strength of "aged" specimens. $N = 15$ specimens were used for this test. Data were analysed using one-way ANOVA followed by Tukey Honestly Significant Difference *post-hoc* tests.

2.5. Characterisation of CHX release

GIC specimens were weighed using a precision balance then placed in individual cuvettes (Z637157-100EA, Sigma–Aldrich, Gillingham, UK) transparent to ultraviolet (UV) light. 1.5 mL artificial saliva was added to each cuvette. The artificial saliva was composed of 0.9 mM CaCl2, 0.2 mM MgCl2, 4.0 mM KH2PO4, 30.0 mM KCl, 20.0 mM HEPES buffer, titrated to pH of 6.8. The cuvettes were sealed with tightly-fitting lids (SEMA2533, VWR, Lutterworth, UK) and then placed onto an orbital shaker (SSM1, Stuart, Staffordshire, UK) at 150 rpm and readings taken initially once a day, and less frequently as CHX release decelerated. Artificial saliva was refreshed at two-week intervals to avoid any decrease in CHX release that could be attributed to saturation of the artificial saliva with respect to CHX salts. Adsorption of light at wavelength 255 nm was measured at regular intervals using a spectrophotometer (Hitachi U-1900, Hitachi, Japan) and calibration standards of 5–50 μM CHX used as references to establish CHX release from the GICs into the artificial saliva [19]. This was converted to μmoles CHX released per unit surface area for each specimen and normalised by subtracting the mean reading for the 0% substitution, correcting for other eluents of the GIC such as the polyacrylic acid [18]. $N = 15$ specimens per group were used.

2.6. Microbiological testing

S. mutans GS-5 was cultivated anaerobically at 37 °C on BHYN agar (per litre: 37 g Brain Heart Infusion, 5 g yeast extract, 5 g Neopeptone, 15 g agar). Suspension cultures were grown in BHY medium (per litre: 37 g Brain Heart Infusion, 5 g yeast extract) in sealed bottles and incubated stationary at 37 °C for 16 h. Bacterial cells were washed once with phosphate-buffered saline (PBS) by alternate centrifugation ($5000 \times g$, 7 min) and suspension, and suspended in PBS at OD_{600} 1.0 (approximately 2×10^8 cells/ml). A lawn of bacterial growth was generated by spreading 100 μl of adjusted *S. mutans* suspension onto a BHYN agar plate, which was then incubated anaerobically at 37 °C for 16 h.

The GIC specimens were made using the method described above in a 0% (control) and a 0.34% substitution. These specimens were prepared using a sterile spatula and moulds in a biological safety cabinet (ESCO airstream, ESCO Micro Pte Ltd., Singapore). The specimens were left to mature in a moist environment for 7 days at 37 °C, then placed onto the bacterial lawn plates (with minimal force to ensure no movement once in the incubator). Lawn plates were incubated for 16 h at 37 °C under anaerobic conditions and the zones of inhibition (clearance) measured by diameter.

3. Results

3.1. Compressive strength

Rejection of specimens with internal voids, imperfections or non-linear force-distance curves resulted in final n per specimen group of 16–21 (mean $n = 19$). CS data are shown in Fig. 1. There was no statistically significant difference between CS of control, 0.17 or 0.34% CHX–HMP specimens. 0.85CHX–HMP had significantly lower CS than control, 0.17 or 0.34% specimens, and 1.70% CHX–HMP had statistically significantly lower CS than all other groups.

3.2. Diametral tensile strength

Rejection of specimens with internal voids, imperfections or non-linear force-distance curves resulted in final n per specimen group of 18–24 (mean $n = 21$). DTS data are shown in Fig. 2. The only group that was statistically significantly different from the control was the 1.70% CHX–HMP, which had a reduced DTS ($p < 0.0001$). 0.17 and 0.34% CHX–HMP had a numerically higher DTS than control specimens but this was not statistically significant ($p = 0.981$ and 0.638 respectively).

3.3. Diametral tensile strength of aged specimens

Rejection of specimens with internal voids, imperfections or non-linear force-distance curves resulted in final n per specimen group of 10–13 (mean $n = 11.6$) for specimens aged for 436 days. DTS data are shown in Fig. 3. It can be seen that there were numerical changes in DTS compared to baseline values, but these

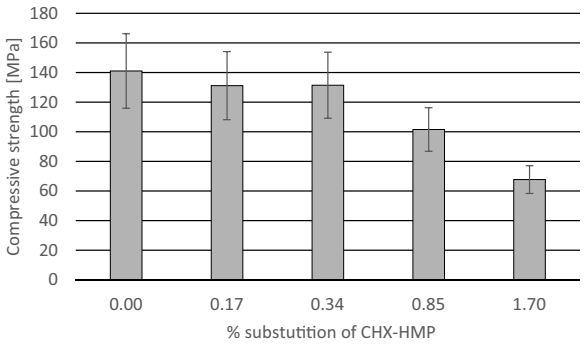

Fig. 1. CS of GIC specimens as a function of CHX–HMP substitution. Error bars represent standard deviations.

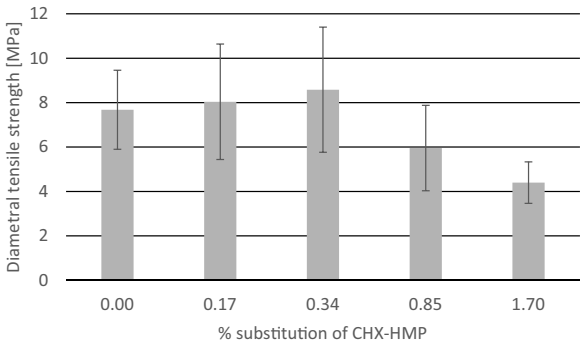

Fig. 2. DTS of GIC specimens as a function of CHX–HMP substitution. Error bars represent standard deviations.

were not statistically significant. For the aged specimens, 0% and 0.17% formed a homogeneous group, 0.34% was significantly lower than 0 and 0.17%, and 0.85% and 1.70% were significantly lower still.

3.4. Characterisation of CHX release

Elution of soluble CHX from CHX–HMP doped GICs normalised to control specimens are shown in Fig. 3 and Fig. 4. Fig. 3 shows mean cumulative CHX elution for specimens with 1.70% CHX–HMP at all time points measured. The purpose of displaying the data in this way is to illustrate the smooth curve, indicating that the practice of refreshing the artificial saliva elution medium at 14 day intervals was sufficient to prevent saturation with respect to CHX salts from inhibiting the release of further CHX. There is a slight suggestion that there is a step in CHX concentration between day 28 and day 29 (*i.e.* before and after a saliva change) but no other such step changes or accelerations of CHX elution are observed.

In Fig. 5, data from day 14x is shown illustrating CHX release as a function of time and dose of CHX–HMP. A dose response is observed, with greater CHX–HMP substitution in the GIC resulting in a greater, and faster, release of CHX–HMP throughout the experimental period. All specimens groups were still releasing CHX at the conclusion of the experiment, with the greatest release observed for the higher CHX–HMP substitutions (Fig. 5).

The mean cumulative CHX release at each 14x day time was compared to the lowest substitution, to establish the relationship between CHX–HMP dose and CHX release. There was a non-linear

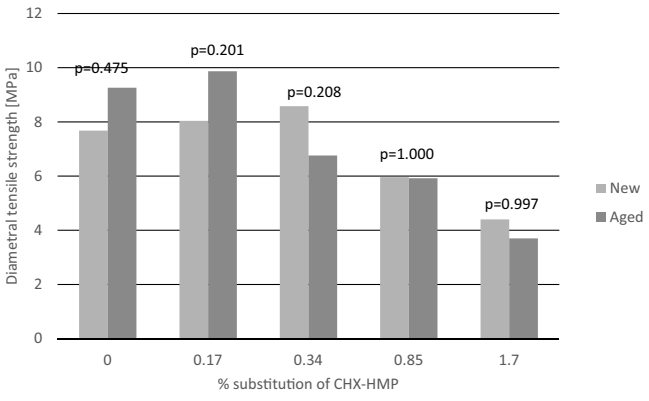

Fig. 3. Diametral tensile strength of newly prepared GIC specimens ("new") and specimens immersed in artificial saliva, refreshed fortnightly, for 436 days ("aged"). *p* values refer to comparisons of new and aged specimens for a given % substitution of CHX–HMP; although numerical differences were observed these were not statistically significant.

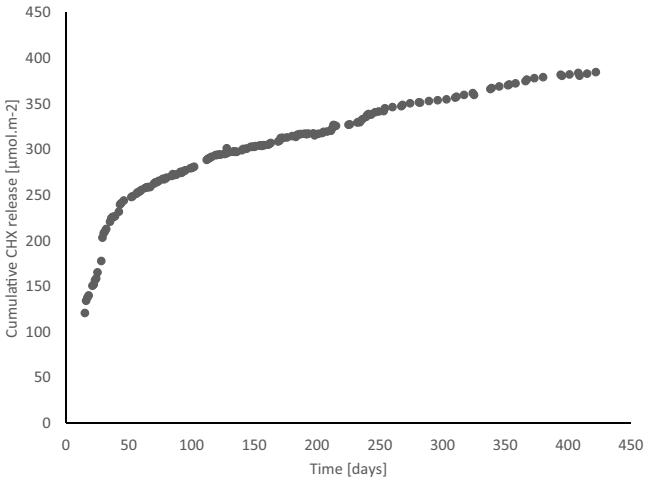

Fig. 4. Cumulative CHX release from GIC specimens containing 1.70% CHX–HMP in substitution for the powder component. This figure shows data points from all sampling days, indicating the smooth transition between the 14 day periods, and no local saturation existing prior to artificial saliva change, with one possible exception where there is a step change from day 28 (before saliva change) to day 29 (after saliva change) indicating the possibility of some minor inhibition of CHX release at this single time point.

relationship between CHX–HMP dose and CHX release; while the ratio of CHX–HMP concentration for 0.17, 0.34, 0.85 and 1.70% CHX-HMP was 1:2:5:10, the ratio of CHX release was 1:4.6:12.3:30.6.

3.5. Microbiological testing

0.34% CHX–HMP GICs exhibited zones of inhibition on the lawn of *S. mutans*. The mean zone of inhibition was 2.34 mm (standard deviation 1.19 mm) from the periphery of the specimen. The control GICs displayed no zones of inhibition.

4. Discussion

CHX–HMP particles in a concentrated aqueous paste were prepared and incorporated into a commercial GIC, using a bespoke polyacid formulation to correct for the water fraction of the CHX–HMP paste. The experimental GICs exhibited a sustained release of aqueous CHX into artificial saliva. This CHX release continued for

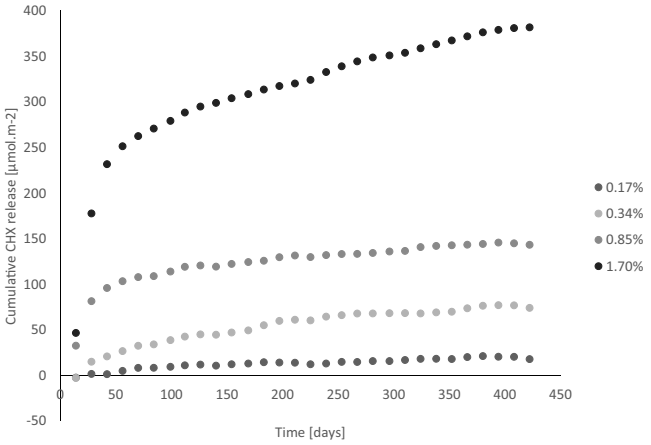

Fig. 5. Cumulative CHX release from GIC specimens as a function of CHX–HMP substitution for the powder component of the cement. Data is presented at 14 day intervals.

the duration of the experiment (436 days), and although all decelerated over the course of the experiment, even the lowest substitution (0.17%) had a gradient >0 at the conclusion of the experiment. For the higher substitutions there was still a steady and substantial release of CHX when the experiment concluded.

The CHX release observed from GICs supplemented with CHX–HMP was sustained for much longer than that achieved using CHX digluconate or CHX diacetate as the dopant [9]. This is likely to be owing to the low solubility of CHX–HMP; the CHX salt is added as a solid filler which is incorporated into the GIC structure, only releasing its soluble CHX payload as some of the particles gradually dissociate. This is in contrast to the approach of supplementing a GIC with CHX digluconate or diacetate; in this case the CHX is added either already in solution (digluconate) or as a solid, but highly soluble, filler. It is not surprising that these approaches lead to a rapid release of CHX in contrast to CHX–HMP.

CHX release was dose-dependent, with a non-linear relationship; the greater the CHX–HMP in the GIC, the more the CHX release, but CHX release increased faster than CHX–HMP dose. This may reflect a less stable structure for the higher substitutions; with the higher dopings of CHX–HMP, the particles disrupt the setting process of the GIC, meaning that the GIC is more porous and the CHX–HMP particles embedded deep within the cement structure are "accessible" to the artificial saliva and contribute to the CHX release. In contrast, those with lower dopings of CHX–HMP have an effective setting process and the particles that contribute to the CHX release are only those close to the GIC's external surface. This is supported by the mechanical property data (discussed below) which indicates that the higher dopings of CHX–HMP adversely affect the material's strength.

The presence of soluble CHX in the elution medium was insufficient during the experiments to restrict any further CHX release owing to the large solution: surface area ratio, the agitation of the reaction vessels (cuvettes) and the regular changes of artificial saliva. It should be noted that the conditions used in this study are not an accurate representation of the clinical scenario; much higher shear conditions and larger volumes of saliva were used in this study than would be in contact with the GIC at the margins of a restoration. As such it is likely that the rate of CHX release would be slower *in vivo*, because local low shear forces and small fluid volumes would result in a local saturation with respect to CHX. That is to say, it is likely that CHX concentrations at the restoration-tooth interface would be higher than reported here, as there is little shear or diffusion to remove the CHX, and that these locally high CHX concentrations would likely slow the subsequent release of CHX owing to saturation effects. Thus the true duration of CHX release from these cements could only be determined from a study with a more accurate depiction of the clinical conditions, but it is hypothesised to be longer than that observed here.

DTS of the GICs was not statistically significantly affected by addition of CHX–HMP, compared to the unmodified cement, up to and including 0.85% CHX–HMP (Fig. 2). There was a numerical rise in DTS up to 0.34% CHX–HMP and then a fall with the lowest value recorded for 1.70% CHX–HMP, but only the 1.70% CHX–HMP group differed from the control to a statistically significant degree. DTS of specimens aged for 436 days indicated no statistically significant changes compared to the baseline values. This is consistent with previously published data, indicating that while flexural strength of GICs typically decreases after laboratory aging, by as much as 55% [20], compressive and tensile strengths tend to remain similar or increase [21], as was observed here. Although there were increases in DTS for control and 0.17% CHX–HMP and a decrease in DTS for 0.34% CHX–HMP, these were not statistically significant (Fig. 3). One outcome of this was that the substitution of CHX–HMP required to affect a reduction in DTS was lower with aged specimens; 0.34% CHX–HMP specimens had a statistically significantly lower DTS than control specimens after 436 days' aging, as compared to 1.70% for new specimens. This development can be attributed to the increase in DTS for control specimens, as well as the decrease in DTS for specimens with 0.34% CHX–HMP, associated with aging.

CS of GICs was affected by addition of CHX–HMP; cements with 0.84 and 1.70% CHX–HMP had statistically significantly reduced CS compared with control, but those with 0.17 and 0.34% were equivalent to the unmodified cement. CS is acknowledged as one of the more sensitive properties as regards modifications to GIC formulations [22] and thus it is not surprising that this parameter was affected by CHX-HMP addition more than DTS.

The lower strengths of the GICs with the higher substitutions of CHX–HMP can be explained by observing that, in increasing the doping of CHX–HMP, the ratio of polyacid to glass is altered, with less glass to account for the greater proportion of CHX–HMP. This will disrupt the GIC setting process as fewer glass particles and thus fewer bi- and trivalent ions are available to cross-link the polyacid matrix. Thus those specimens with more CHX–HMP are likely to have a less complete setting reaction, and this is likely to explain the reduced strength for these specimens.

The 0.34% CHX–HMP GIC was tested for its ability to inhibit the growth of oral pathogen *S. mutans in vitro*. This GIC formulation was selected on the basis that it was the highest substitution of CHX–HMP that did not have an adverse effect on initial mechanical properties. It was observed that these GICs inhibited growth of the microorganism to a mean distance of 2.34 mm from the periphery of the specimen, whereas control GICs displayed no zone of inhibition. This indicates that, *in vitro* and utilising a simple, single species model, the concentration of CHX released by the 0.34% CHX–HMP GIC was sufficient to inhibit growth of this cariogenic organism.

The strength data, particularly the DTS of the aged specimens combined with the CS data, suggests that if such a GIC were to find clinical application, the lower substitutions of CHX–HMP paste would be more suitable, as these have no negative impact on mechanical properties. The 0.34% CHX–HMP GIC, which was the highest concentration of CHX–HMP while not adversely affecting mechanical properties at baseline, inhibited growth of *S. mutans* in an *in vitro* zone of inhibition model. Noting the comments above regarding the experimental conditions, the next step should be to determine whether this cement can inhibit the growth of caries-causing microorganisms under flow conditions more representative of the clinical environment of a GIC.

5. Conclusions

CHX–HMP particles in a concentrated paste were incorporated into a commercial GIC, with adjustment of the acid concentration in the commercial GIC to account for the water in the paste. Higher substitutions of CHX–HMP paste (0.85 and 1.70% CHX–HMP by mass, or 5 and 10% paste by mass) had a negative impact on compressive strength, but lower substitutions had no significant impact on compressive strength. None of the prototype cements displayed a reduction in diametral tensile strength at baseline; DTS after 436 days aging was not statistically significantly different when comparing specimens with and without aging, although the substitutions of 0.34% and higher were significantly weaker than the control cement after aging. All of the prototype cements exhibited a sustained release of soluble CHX over the 436 day experimental period.

Acknowledgements

CAB is grateful to the Medical Research Council and Kemdent for supporting her PhD CASE studentship.

References

[1] S. Pinto Gdos, L.J. Oliveira, A.R. Romano, L.R. Schardosim, M.L. Bonow, M. Pacce, M.B. Correa, F.F. Demarco, D.D. Torriani, Longevity of posterior restorations in primary teeth: results from a paediatric dental clinic, J. Dent. 42 (2014) 1248–1254.

[2] F.J. Burke, P.S. Lucarotti, How long do direct restorations placed within the general dental services in England and Wales survive? Br. Dent. J. 206 (2009) E2 discussion 26-7.

[3] E. Hurley, C. Da Mata, C. Stewart, M. Kinirons, A study of primary teeth restored by intracoronal restorations in children participating in an undergraduate teaching programme at Cork University Dental School and Hospital, Ireland, Eur. J. Paediatr. Dent. 16 (2015) 78–82.

[4] F.H. van de Sande, P.A. Rodolpho, G.R. Basso, R. Patias, Q.F. da Rosa, F.F. Demarco, N.J. Opdam, M.S. Cenci, 18-year survival of posterior composite resin restorations with and without glass ionomer cement as base, Dent. Mater. 31 (2015) 669–675.

[5] C. Namgung, Y.J. Rho, B.H. Jin, B.S. Lim, B.H. Cho, A retrospective clinical study of cervical restorations: longevity and failure-prognostic variables, Oper. Dent. 38 (2013) 376–385.

[6] A. Wiegand, W. Buchalla, T. Attin, Review on fluoride-releasing restorative materials-fluoride release and uptake characteristics, antibacterial activity and influence on caries formation, Dent. Mater. 23 (2007) 343–362.

[7] V. Yengopal, S.Y. Harneker, N. Patel, N. Siegfried, Dental fillings for the treatment of caries in the primary dentition, Cochrane Database Syst. Rev. (2009) CD004483.

[8] N. Tabary, F. Chai, N. Blanchemain, C. Neut, L. Pauchet, S. Bertini, E. Delcourt-Debruyne, H.F. Hildeband, B. Martel, A chlorhexidine-loaded biodegradable cellulosic device for periodontal pockets treatment, Acta Biomater. 10 (2014) 318–329.

[9] L.S. Turkun, M. Turkun, F. Ertugrul, M. Ates, S. Brugger, Long-term antibacterial effects and physical properties of a chlorhexidine-containing glass ionomer cement, J. Esthet. Restor. Dent. 20 (2008) 29–44 discussion 45.

[10] L.M. Marti, M.D. Mata, B. Ferraz-Santos, E.R. Azevado, E.M. Giro, A.C. Zuanon, Addition of chlorhexidine gluconate to a glass ionomer cement: a study on mechanical, physical and antibacterial properties, Braz. Dent. J. 25 (2014) 33–37.

[11] L.M. Marti, A.C. Becci, D.M. Spolidorio, F.L. Brighenti, E.M. Giro, A.C. Zuanon, Incorporation of chlorhexidine gluconate or diacetate into a glass-ionomer cement: porosity, surface roughness, and anti-biofilm activity, Am. J. Dent. 27 (2014) 318–322.

[12] Y. Takahashi, S. Imazato, A.V. Kaneshiro, S. Ebisu, J.E. Frencken, F.R. Tay, Antibacterial effects and physical properties of glass-ionomer cements containing chlorhexidine for the ART approach, Dent. Mater. 22 (2006) 647–652.

[13] L. Cheng, M.D. Weir, H.H. Xu, A.M. Kraigsley, N.J. Lin, S. Lin-Gibson, X. Zhou, Antibacterial and physical properties of calcium-phosphate and calcium-fluoride nanocomposites with chlorhexidine, Dent. Mater. 28 (2012) 573–583.

[14] S.G. Iz, F. Ertugrul, E. Eden, S.I. Gurhan, Biocompatibility of glass ionomer cements with and without chlorhexidine, Eur. J. Dent. 7 (2013) S89–S93.

[15] A.R. de Castilho, C. Duque, C. Negrini Tde, N.T. Sacono, A.B. de Paula, C.A. de Souza Costa, D.M. Spolidorio, R.M. Puppin-Rontani, In vitro and *in vivo* investigation of the biological and mechanical behaviour of resin-modified glass-ionomer cement containing chlorhexidine, J. Dent. 41 (2013) 155–163.

[16] M.E. Barbour, S.E. Maddocks, N.J. Wood, A.M. Collins, Synthesis, characterization, and efficacy of antimicrobial chlorhexidine hexametaphosphate nanoparticles for applications in biomedical materials and consumer products, Int. J. Nanomed. 8 (2013) 3507–3519.

[17] N.J. Wood, H.F. Jenkinson, S.A. Davis, S. Mann, D.J. O'Sullivan, M.E. Barbour, Chlorhexidine hexametaphosphate nanoparticles as a novel antimicrobial coating for dental implants, J. Mater. Sci.: Mater. Med. 26 (2015) 201.

[18] E.R. Hook, O.J. Owen, C.A. Bellis, J.A. Holder, D.J. O'Sullivan, M.E. Barbour, Development of a novel antimicrobial-releasing glass ionomer cement functionalized with chlorhexidine hexametaphosphate nanoparticles, J. Nanobiotechnol. 12 (2014) 3.

[19] M.E. Barbour, D.J. O'Sullivan, D.C. Jagger, Chlorhexidine adsorption to anatase and rutile titanium dioxide, Colloids Surf. A 307 (2007) 116–120.

[20] M.S. Bapna, C.M. Gadia, J.L. Drummond, Effects of aging and cyclic loading on the mechanical properties of glass ionomer cements, Eur. J. Oral Sci. 110 (2002) 330–334.

[21] S.B. Mitra, B.L. Kedrowski, Long-term mechanical properties of glass ionomers, Dent. Mater. 10 (1994) 78–82.

[22] M.S. Baig, A.H. Dowling, X. Cao, G.J. Fleming, A discriminatory mechanical testing performance indicator protocol for hand-mixed glass-ionomer restoratives, Dent. Mater. 31 (2015) 273–283.

DENTAL MATERIALS 34 (2018) 1717–1726

Available online at www.sciencedirect.com

ScienceDirect

journal homepage: www.intl.elsevierhealth.com/journals/dema

Glass ionomer cements with milled, dry chlorhexidine hexametaphosphate filler particles to provide long-term antimicrobial properties with recharge capacity

Candice A. Bellis[a], *Owen Addison*[b], *Angela H. Nobbs*[c], *Peter F. Duckworth*[a,d], *James A. Holder*[a,e], *Michele E. Barbour*[a,f,*]

[a] *Oral Nanoscience, Bristol Dental School, University of Bristol, UK*
[b] *School of Dentistry, University of Birmingham, UK*
[c] *Oral Microbiology, Bristol Dental School, University of Bristol, UK*
[d] *ACCIS, University of Bristol, UK*
[e] *Kemdent, Purton, UK*
[f] *Pertinax Pharma Ltd., Bristol, UK*

ARTICLE INFO

Article history:
Received 26 April 2018
Received in revised form
10 September 2018
Accepted 10 September 2018

Keywords:
Glass ionomer cement
Restorative materials
Caries
Antimicrobials
Chlorhexidine

ABSTRACT

Objective. Glass ionomer cements (GICs) are a versatile material, offering the opportunity for ion exchange with the oral environment. The aim of this study was to develop a GIC that delivers a controlled, rechargeable dose of chlorhexidine (CHX) over an extended period without compromising mechanical properties.

Methods. GICs were supplemented with finely milled particles of chlorhexidine hexametaphosphate (CHX-HMP). CHX release into artificial saliva was measured over 660 days, and recharge with CHX and CHX-HMP was investigated. Mechanical properties were investigated, and an agar diffusion test was carried out to assess antimicrobial properties using *Streptococcus mutans* and *Scardovia wiggsiae*.

Results. Dose-dependent CHX release was observed, and this was ongoing at 660 days. Compared with related studies of GICs containing CHX-HMP, the fine, dry particles resulted in fewer adverse effects on mechanical properties, including tensile, compressive and biaxial flexural strength, with 1% CHX-HMP GICs indistinguishable from control specimens. The GICs could be recharged with CHX using both a conventional CHX digluconate solution comparable to commercial mouthrinses, and a suspension of CHX-HMP of equivalent concentration. Recharging with CHX digluconate increased subsequent CHX release by 50% compared with no recharge, and recharging with CHX-HMP increased subsequent CHX release by 100% compared with no recharge. The GICs inhibited growth of *St. mutans* and *Sc. wiggsiae* in a simple agar diffusion model.

Abbreviations: BFS, biaxial flexural strength; CHX, chlorhexidine; CS, compressive strength; DTS, diametral tensile strength; GIC, glass ionomer cement; HMP, hexametaphosphate.

* *Corresponding author at*: Bristol Dental School, University of Bristol, Lower Maudlin St, Bristol BS1 2LY, UK.
E-mail address: m.e.barbour@bristol.ac.uk (M.E. Barbour).

https://doi.org/10.1016/j.dental.2018.09.003

Significance. These materials, which provide sustained CHX release over clinically relevant timescales, may find application as a restorative material intended to inhibit secondary caries as well as in temporary restorations and fissure sealants.

1. Introduction

Glass ionomer cements (GICs) are a mainstay of modern dentistry. Their uses include temporary and permanent restorations, lining and luting materials, fissure sealants and in atraumatic restorative therapy. Although GICs exhibit fluoride release, and antimicrobial effects of this can be demonstrated *in vitro*, the data in support of an anticariogenic effect *in vivo* is inconclusive [1–3]. Nevertheless, a bioactive material that participates in ion exchange with its local environment offers an adaptable vehicle for delivery of other useful molecules to the locale of a restoration.

Chlorhexidine (CHX) is a broad-spectrum antimicrobial in widespread use as a topical agent. It owes its antimicrobial properties to membrane disruption and is efficacious against a wide range of microbes including those implicated in caries. CHX in commercial products is typically present as the CHX digluconate salt which is highly soluble and thus has poor substantivity, usually providing only short term antimicrobial function before it is depleted. CHX concentrations in saliva fall rapidly after an oral rinse, with 90% of the initially retained CHX cleared from the mouth within 6 h and 98% cleared within 12 h [4]. One product used for treatment of periodontal disease provides sustained CHX release, but 80% of the CHX is released within the first 2 days, with a much lower release over the following 3–4 weeks [5].

Owing to the useful antimicrobial functionality of CHX, coupled with its low cost and well-understood pharmacological properties, there have been attempts to incorporate CHX into dental materials, including GICs. GICs supplemented with CHX diacetate and CHX digluconate inhibited growth of oral microbes *Streptococcus mutans* and *Lactobacillus acidophilus*, but the antimicrobial effects were sustained for only 40–90 days, with no bactericidal effect observed after this time [6]. In another study where GIC was doped with CHX digluconate and antimicrobial efficacy again assessed using *St. mutans* and *L. acidophilus*, there was an exponential decay of the zone of inhibition over the first 30 days [7]. These short-term antimicrobial effects may be explained by the release profiles of soluble CHX from GICs doped with these conventional salts, which show a high initial release which rapidly diminishes leaving little or no sustained release [8]. A recent report of core–shell microparticles containing CHX chloride salts reveals potential for graduate release of CHX, although this study only probed CHX release to a maximum of 430 h (18 days) [9]. Supplementation with these CHX salts has also been found to be associated with a negative impact on mechanical properties [6,10–12]. More recently, some attempts have been made to incorporate CHX when loaded into particles that may facilitate gradual rather than rapid release, and there has been some success in this, but still the CHX release was heavily front loaded and decayed rapidly after the first 1–3 days [13].

Although *in vivo* studies of these experimental materials are rare, there are a few small studies of note. Supplementation of a resin-modified GIC with 1.25% CHX digluconate resulted in elimination of *St. mutans* populations following indirect pulp treatment *in vivo* [14], and incorporation of CHX digluconate into a GIC reduced microbial counts in cavities in first primary molars in 6–9 year olds, although the CHX digluconate GICs also exhibited a higher failure rate than the controls [15]; similar results were observed in a study of CHX digluconate doped GICs in children receiving atraumatic restorative therapy, where the CHX GICs resulted in reduced *St. mutans* counts at 7 days but not 3 or 12 months after placement [16]. These tentative findings highlight the potential benefit of CHX-functionalised restorative materials as well as the challenges, in that the other properties of the GIC are often compromised by the new component.

We have recently reported a novel salt of CHX: CHX-hexametaphosphate (CHX-HMP) [17]. CHX-HMP has a much lower solubility than CHX digluconate or CHX diacetate, and when in or on biomaterials, can confer a sustained release of CHX [18]. We have described a pilot study demonstrating the use of manually ground CHX-HMP as a filler for GICs [19], and another where the CHX-HMP was incorporated into a GIC as a viscous paste formulation [20]. In the first study [19], large clusters of CHX-HMP particles were used, and this had adverse effects on the mechanical properties; furthermore, another limitation of that study was the short time over which CHX release from the prototype cements was recorded, and the large particle size would have had a detrimental effect on this CHX release. In the second report [20], the incorporation of the particles in a wet aqueous paste resulted in deterioration of the mechanical properties when the substitution of CHX-HMP was at 0.34% by mass or greater, although the CHX release was improved on the earlier approach, being sustained for at least 14 months. The aim of the study described here was to investigate the use of CHX-HMP particles as GIC fillers but incorporating a mechanical milling process resulting in much smaller CHX-HMP filler particles. The hypothesis was that the smaller particle size and thus larger specific surface area would create a more sustained CHX release coupled with fewer adverse effects on mechanical properties. Furthermore, given that any antimicrobial incorporated into a biomaterial has a finite duration of release, the capacity of these materials to be "recharged" with CHX, in analogy to the well-known fluoride recharge phenomenon, was investigated. A simple microbiological test was incorporated into the study to determine whether CHX release from the prototype GICs had an effect on two cariogenic bacteria in an agar diffusion test. The conventional and well-characterised *St. mutans* was selected for the

test, as well as *Scardovia wiggsiae*, a recently recognised anaerobic pathogen associated with aggressive childhood caries [21,22].

2. Methods

2.1. Preparation of CHX-HMP filler particles

100 mL 10 mM solutions of each of CHX digluconate and sodium HMP (Sigma Aldrich, Gillingham, UK) were prepared in deionised water and were combined in a glass beaker under ambient laboratory conditions. The resulting aqueous suspension of CHX-HMP was stirred vigorously for approximately 1 min, then 30 mL 1 M potassium chloride was added and stirred for a further minute. The suspension was stored without disturbing for 24 h, allowing the precipitate to sediment at the base of the container. The supernatant was gently discarded leaving a concentrated suspension of the precipitate, which was then centrifuged at 4760 g for 30 min. The supernatant was again discarded and the pellet dried at ambient temperature under air extraction for 24 h, then removed from the centrifuge tubes. 100 g total mass of dried CHX-HMP pellets prepared in this way was placed into a cylindrical ceramic mill of 80 mm diameter and 70 mm height containing ceramic balls of sizes 12.5–20.5 mm (Pascal Engineering Company Ltd., Crawley, UK), and this was placed on a rolling platform for 4 h. The mill was opened every hour and particles dislodged from the internal walls. The resulting powder was passed through a coarse sieve and examined using scanning electron microscope (SEM). The specific surface area was measured by nitrogen adsorption following outgassing for 48 h at 30 °C under vacuum. Elemental microanalysis (CHNP) was used to confirm the composition of the precipitate; CHX-HMP was prepared as described above and analysed for C, H, N and P (Microanalytical Laboratory, School of Chemistry, University of Bristol).

2.2. Preparation of specimens (elution, DTS, CS)

Diamond Carve™ GIC (Kemdent, Purton, UK) was used as the base material to create experimental cements. This commercial GIC comprises a powder consisting of alumina-silica based glass filler particles which also contain calcium fluoride and other minor salt components and freeze-dried poly(vinyl)phosphonic acid, and a liquid, which contains polyacrylic and tartaric acids.

For the prototype GICs, CHX-HMP particles were substituted for the glass component in the GIC powder at 0, 1, 2, 5 and 10% by mass. All dopings were tested for each parameter below, unless otherwise specified. The CHX-HMP particles were mixed with the GIC powder in the ball mill for 10 min as described above to ensure homogeneous incorporation of the components. This powder was then mixed at a 4:1 ratio by mass with the GIC liquid according to the manufacturers' instructions. Mixing was completed in 40–50 s and packing into the moulds took a further 10 s, such that the process of creating the specimens was complete within 60 s.

GICs were packed, using a stainless steel dental spatula, into stainless steel moulds with dimensions dependent on the purpose of the specific specimen. Dimensions were: 6 mm height and 4 mm diameter for compressive strength determination; 4 mm height and 6 mm diameter for measurement of diametral tensile strength, release of soluble CHX, and antimicrobial testing; 2 mm height and 15 mm diameter for determination of flexural strength. The moulds were lined with a thin layer of petroleum jelly to aid removal of the set cement. Immediately after packing, the moulds were placed between two sheets of acetate and a 2 kg weight placed on top of the specimens on a flat surface to ensure even distribution of the cement. After 5 min the specimens, except those for biaxial flexural strength testing, were ground on the two flat surfaces using a P120 grit SiC disc and were then placed into small, sealed plastic vessels containing wet tissue paper packed into the lid to achieve 100% humidity without direct contact with water. Specimens were stored at 37 °C for 7 days prior to testing.

2.3. Compressive strength (CS) testing

CS was measured by applying a compressive force to the flat surface of the cylindrical specimens (6 mm height, 4 mm diameter) using a universal testing machine (Instron, Buckinghamshire, UK) with cross-head speed of 1 mm/min and recording the load at fracture. Specimen dimensions were measured three times using a digital micrometer. Load at fracture L_F was used with diameter D to calculate CS according to the relationship $CS = 4L/\pi D^2$. Specimens were examined after fracture for evidence of flaws on the internal or external surfaces and flawed specimens were rejected. n = 24 specimens per group were used. Data were analysed using a one-way ANOVA followed by a Tukey Honestly Significant Difference post-hoc test at $\alpha = 0.05$.

2.4. Diametral tensile strength (DTS) testing

DTS was measured by applying a compressive force to the curved sides of the cylindrical specimen (4 mm height, 6 mm diameter) using a universal testing machine (Instron, Buckinghamshire, UK) with cross-head speed of 1 mm/min and recording the load at fracture. Specimen dimensions were measured three times using a digital micrometer. The load at fracture L_F was used in conjunction with the average diameter D and height h of the specimens to calculate DTS according to the relationship $DTS = 2L/\pi Dh$. Specimens were examined after fracture for evidence of flaws on the internal or external surfaces and data from specimens found to be flawed were rejected. Data were analysed using a one-way ANOVA followed by a Tukey Honestly Significant Difference post-hoc test at $\alpha = 0.05$. As well as freshly prepared specimens (n = 24 per group), the specimens that were subjected to the long-term CHX elution experiments were also tested for DTS to ascertain whether strength deteriorated after long-term exposure to artificial saliva (n = 15 per group).

2.5. Biaxial flexural strength (BFS) testing

BFS was measured in a ball-on-ring configuration, by applying force to the flat surfaces of the specimens (15 mm diameter, 2 mm height) using a universal testing machine with cross-

head speed of 1 mm/min (Instron, Buckinghamshire, UK) and recording the load at failure. The circular discs were positioned on a 10 mm diameter knife-edge annulus with a thin sheet of rubber between the annulus and the sample. Specimens were centrally loaded with a spherical 4 mm diameter stainless steel ball indentor. BFS (in MPa) was calculated according to the relationship,

$$BFS = \frac{L_F}{h^2}\left\{(1+\upsilon)\left[0.484ln\left(\frac{a}{h}\right)+0.52\right]+0.48\right\}$$

where L_F = measured load at fracture, a = radius of knife edge support in mm, h = specimen thickness measured at point of fracture in mm and ν = Poisson's ratio (0.30). n = 24 specimens per group were prepared, and specimens were rejected if there were any visible flaws.

2.6. Measurement of elution of soluble CHX

GIC specimens were weighed using a precision balance then placed in individual cuvettes transparent to ultraviolet light (Z637157; Sigma–Aldrich, Gillingham, UK). 1.5 mL artificial saliva was added to each cuvette. The artificial saliva was composed of 0.9 mM $CaCl_2$, 0.2 mM $MgCl_2$, 4.0 mM KH_2PO_4, 30.0 mM KCl, 20.0 mM HEPES buffer, titrated to pH of 6.8 [23]. The cuvettes were sealed with tightly-fitting lids (SEMA2533; VWR, Lutterworth, UK) and then placed onto an orbital shaker (SSM1, Stuart, Staffordshire, UK) at 150 rpm and readings taken initially once a day, and less frequently as CHX release decelerated. Artificial saliva was refreshed at two-week intervals to avoid any decrease in CHX release that could be attributed to saturation of the artificial saliva with respect to CHX salts. Adsorption of light at wavelength 255 nm was measured at regular intervals and calibration standards of 5–50 μM CHX used as references to establish CHX release from the GICs into the artificial saliva [24]. This was converted to μmoles CHX released per unit surface area for each specimen and normalised by subtracting the mean reading for the 0% substitution, correcting for any systematic error due to background readings. n = 15 specimens per group were used. Cuvettes were inspected carefully at each reading and, in the rare event that leakage occurred, the specimen was discarded. CHX elution was measured for 660 days.

2.7. Investigation of CHX recharge capacity of GICs

Specimens were prepared as described above and subjected to CHX elution measurements as described in the previous section, with modification to permit the investigation of the capacity for recharge and subsequent release of the CHX. Three sets of specimens (n = 15 each of 0, 1, 2, 5, 10% CHX-HMP for each set) were stored in artificial saliva and CHX release was assessed using UV spectrophotometry as described above. Every 4 weeks the specimens were removed from the artificial saliva and were immersed in one of three "recharge" preparations: deionised water (negative control), 2.2 mM CHX digluconate ("CHX") and a CHX-HMP suspension containing the equivalent of 2.2 mM CHX ("CHX-HMP"). CHX release of the three groups was assessed to determine whether the specimens periodically exposed to CHX or CHX-HMP had a different subsequent CHX release than those exposed only to water. Readings were converted to μmoles CHX released per unit surface area for each specimen and normalised by subtracting the mean reading for the 0% substitution. Cuvettes were inspected carefully at each reading and, in the rare event that leakage occurred, the specimen was discarded. CHX elution was measured for 315 days.

2.8. Assessment of antimicrobial efficacy

St. mutans GS-5 [25] was maintained in Brain Heart Infusion broth supplemented with 0.5% (w/v) Yeast Extract (BHY) and incubated for 16 h at 37 °C in a candle jar. *Sc. wiggsiae* C1A_55 [26] was maintained in Tryptic Soy broth supplemented with 0.5% (w/v) Yeast Extract, 25 μg/mL haemin and 5 μg/mL menadione (TSBYHM) and incubated for 5 days at 37 °C anaerobically under N_2:CO_2:H_2 (80:10:10). Bacterial cells were harvested (5000 *g*, 7 min), washed and resuspended in PBS at OD_{600} 1.0 (approximately 2×10^8 cells/mL). Adjusted cell suspensions (100 μL) were spread evenly over BHY agar plates (*St. mutans*) or fastidious anaerobe agar (FAA) plates (*Sc. wiggsiae*), before placing GIC specimens (0 and 2% CHX-HMP) (6 mm diameter, 4 mm height) onto the agar. These lawn plates were then incubated as before for 16 h (*St. mutans*) or 5 days (*Sc. wiggsiae*), before zones of inhibition around the GIC specimens were measured.

3. Results

3.1. Characterisation of CHX-HMP filler particles

SEM images of the milled CHX-HMP particles are shown in Fig. 1. The milled particles were polydisperse, with the most common sizes in the 1–20 μm range and some aggregates as large as 50–150 μm. The specific surface area of the powder as determined using BET was 1.55 $m^2\,g^{-1}$ and no micropore volume could be measured indicating a very low porosity. Elemental microanalysis indicated that the composition of the precipitate was 20% N, 40% C, 5.3% H and 8.6% P, which corresponds most closely to a composition of 3 CHX to 1 HMP (theoretical values 21% N, 40% C, 4.9% H, 9.3% P). Given the relative molecular masses of CHX and HMP this indicates that the CHX-HMP solid is approximately 76% CHX by mass.

3.2. Compressive strength of CHX-HMP functionalised cements

CS data are shown in Fig. 2 with error bars representing standard deviations. Rejection of specimens with internal voids, imperfections or non-linear force-distance curves resulted in final n per specimen group of 17–22 (mean n = 18.6; initial n = 24). According to the ANOVA and Tukey HSD test, there was no statistically significant difference between CS of control, 1% or 2% CHX-HMP specimens; 5% and 10% CHX-HMP had significantly lower CS; that is, substitutions up to and including 2% had no impact of CS compared with control specimens, whereas 5% or more CHX-HMP had a negative impact on CS.

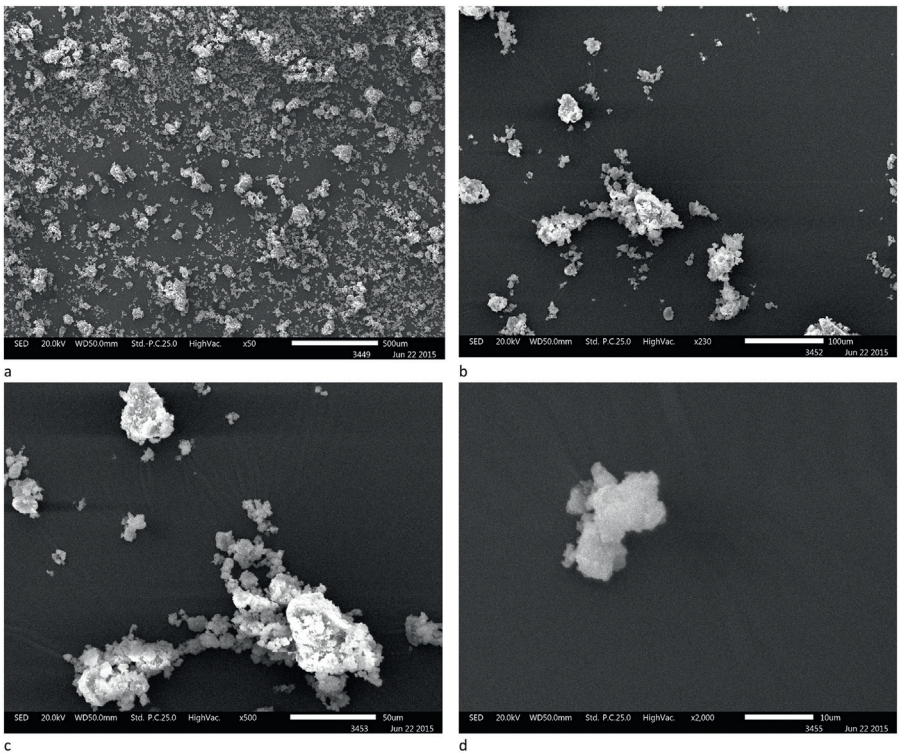

Fig. 1 – Scanning electron micrographs showing ball-milled CHX-HMP filler particles. Scale bars are a: 500 μm; b: 100 μm; c: 50 μm; d: 10 μm. The particles are polydisperse, with typical sizes ranging from 1 to 20 μm and some aggregates as large as 50–150 μm.

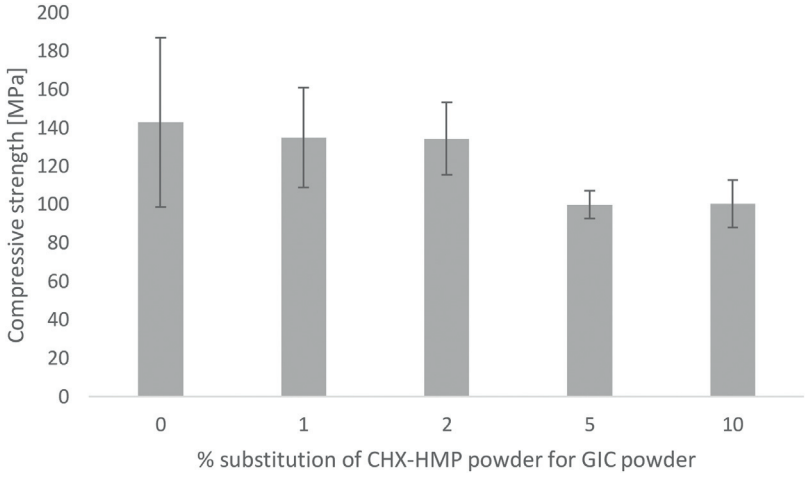

Fig. 2 – Compressive strength of GIC specimens as a function of CHX-HMP substitution. Error bars represent standard deviations. There was no statistically significant difference between CS of control, 1% or 2% CHX-HMP specimens; 5% and 10% CHX-HMP had significantly lower CS than control, 1% and 2% specimens.

3.3. *Diametral tensile strength of CHX-HMP functionalised cements*

DTS data are shown in Fig. 3 with error bars representing standard deviations. For specimens tested without aging, rejection of specimens with internal voids, imperfections or non-linear force-distance curves resulted in final n per specimen group of 19–24 (mean n = 21.2; initial n = 24). For specimens tested after immersion in artificial saliva for 660 days, rejection of specimens with internal voids, imperfections or non-linear force-distance curves resulted in final n per specimen group of 8–14 (mean n = 11.2; initial n = 15).

According to the ANOVA and Tukey HSD test, the only statistically significant differences in these data were between unaged 2% and 10% CHX-HMP specimens, where 10% CHX-HMP had lower DTS than 2%, and between unaged 2% and aged 2% CHX-HMP specimens, where the aged material had lower DTS than the unaged material. That is, for unaged

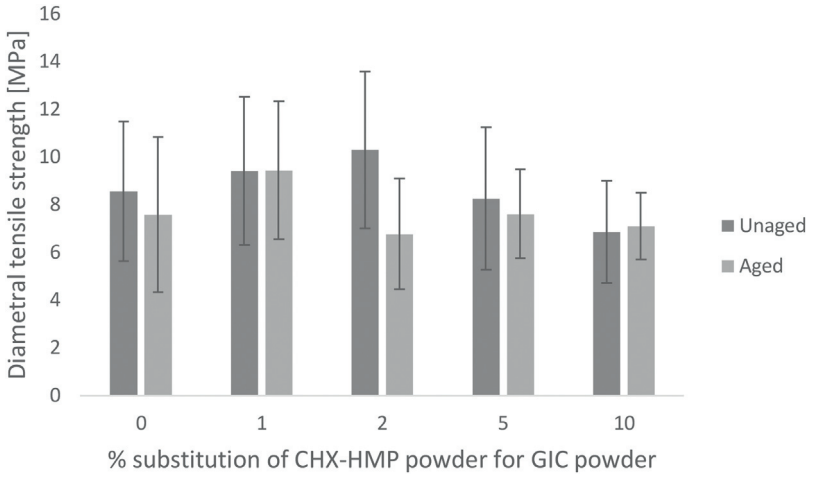

Fig. 3 – Diametral tensile strength of GIC specimens as a function of CHX-HMP substitution. Error bars represent standard deviations. Dark grey: freshly prepared specimens after storage for 7 days; light grey: aged specimens after 660 days in artificial saliva. The only statistically significant differences were between unaged 2% and 10% CHX-HMP specimens, where 10% CHX-HMP had lower DTS than 2%, and between unaged 2% and aged 2% CHX-HMP specimens, where the aged material had lower DTS than the unaged material.

specimens substitutions up to and including 10% CHX-HMP had no impact on DTS compared with control specimens, and after aging one specimen group exhibited a reduction in DTS but there were no differences among the groups of specimens comparing all aged specimens.

3.4. *Biaxial flexural strength (BFS) of CHX-HMP functionalised cements*

BFS data are shown in Fig. 4 with error bars representing standard deviations. Rejection of specimens with imperfections resulted in final n per specimen group of 22–24 (mean n = 23.0; initial n = 24). According to the ANOVA and Tukey HSD test, the 1% CHX-HMP was indistinguishable from the control group, whereas the others (2, 5 and 10% CHX-HMP) had lower BFS than the control group.

3.5. *Elution of soluble CHX from functionalised cements*

Elution of soluble CHX from CHX-HMP doped GICs is shown in Fig. 5. A dose-dependent CHX release was seen, with the total CHX released being related, although not directly proportional, to the total CHX content of the material. The CHX release had a smooth profile and did not accelerate and decelerate over the period investigated, indicating that the frequent changing of elution medium ensured that saturation was not a factor in controlling the rate of CHX release.

3.6. *Investigation of CHX recharge capacity of GICs*

Elution of soluble CHX from CHX-HMP doped GICs is shown in Fig. 6. Specimens recharged with the 2.2 mM CHX solution released more CHX than negative controls exposed to DIW;

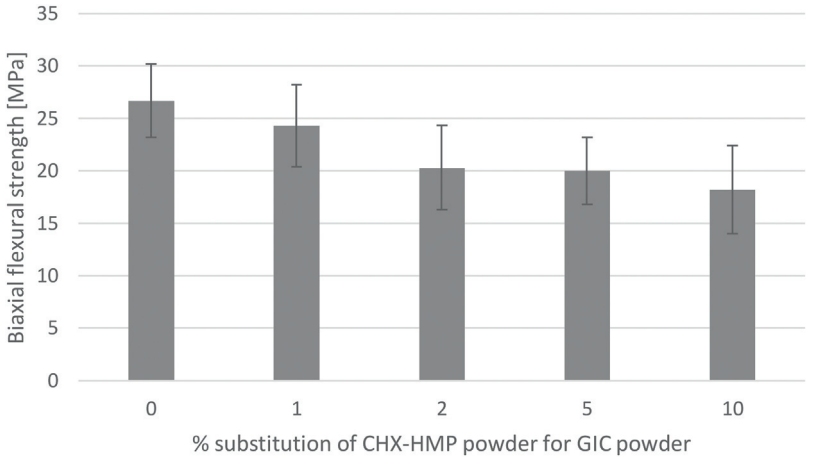

Fig. 4 – Biaxial flexural strength of GIC specimens as a function of CHX-HMP substitution. Error bars represent standard deviations. The control and 1% CHX-HMP formed one statistically homogeneous group, whereas the others (2, 5 and 10% CHX-HMP) formed a second group with significantly lower BFS than the control and 1% CHX-HMP specimens.

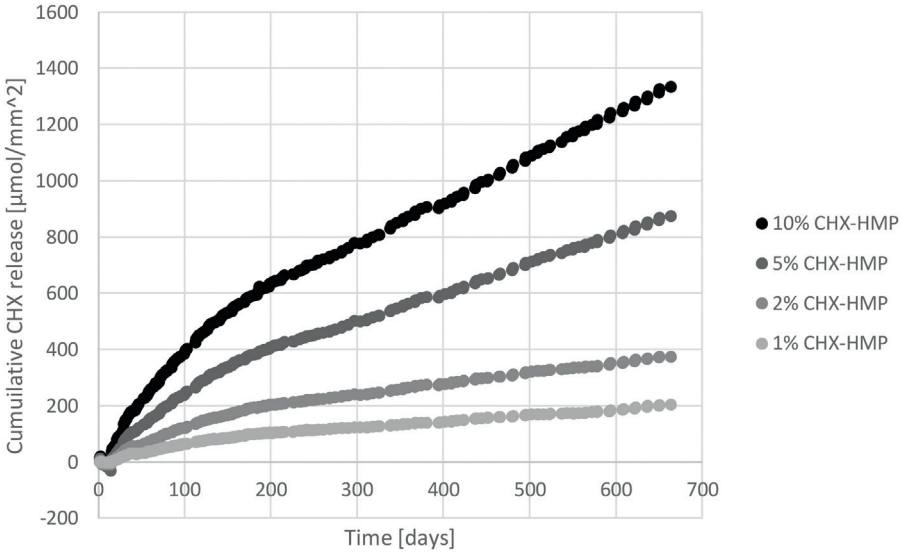

Fig. 5 – Cumulative CHX release from GIC specimens as a function of CHX-HMP substitution, normalised to control specimens (no CHX-HMP). The elution medium was changed frequently to ensure that at no time the degree of saturation approached the limit of solubility of the CHX HMP salt, ensuring sink conditions throughout.

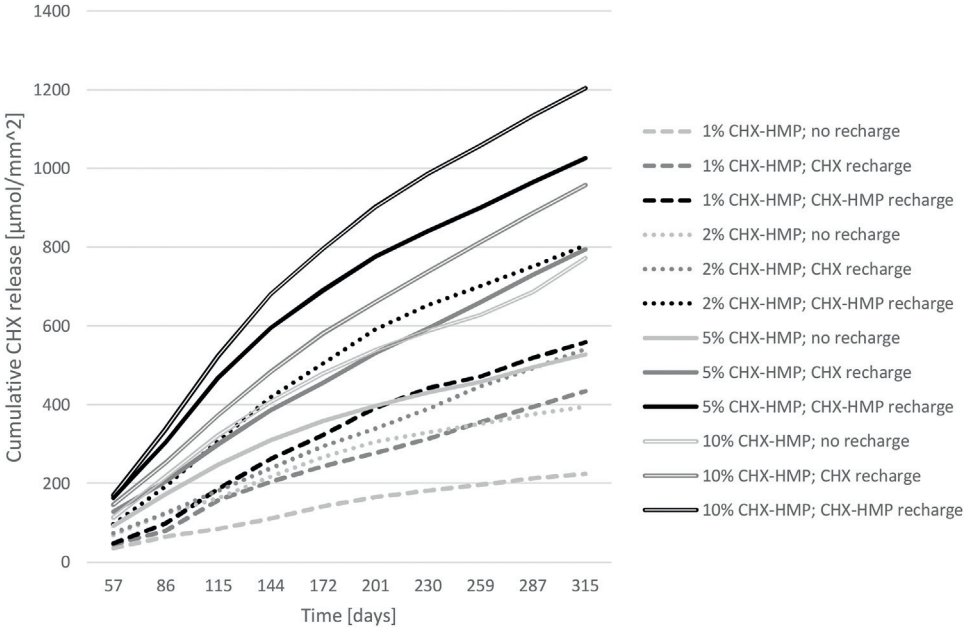

Fig. 6 – Cumulative CHX release from GIC specimens as a function of CHX-HMP substitution and recharge medium, normalised to control specimens. Specimens recharged with 2.2 mM CHX solution released on average 50% more CHX than negative controls (exposed to DIW). Specimens recharged with CHX-HMP suspension at the same equivalent total CHX concentration released on average 33% more CHX than those recharged with CHX solution and on average 100% more CHX than negative controls.

on average 50% more CHX was released by the CHX recharged specimens than the controls over the 315 day period. Specimens recharged with CHX-HMP suspension at the same equivalent total CHX concentration released more CHX again than the CHX solution recharged specimens; on average over the 315 period specimens recharged with CHX-HMP released 33% more CHX than those recharged with CHX solution and 100% more CHX than negative controls.

3.7. *Antimicrobial efficacy of functionalised cements*

Control GICs without CHX-HMP showed no remote or contact inhibition of microbial growth with either *St. mutans* or *Sc. wiggsiae*. 2% CHX-HMP GICs resulted in both contact and remote microbial inhibition of *St. mutans*, with an average 11.9 mm zone of inhibition (5.7 mm as measured from the edge of the GIC specimen). 2% CHX-HMP GICs inhibited growth of *Sc. wig-*

gsiae but did not result in remote inhibition (*i.e.* the inhibition of microbial growth was restricted to the area of agar in direct contact with the specimen).

4. Discussion

Incorporation of dry, milled CHX-HMP particles into a commercial GIC resulted in the release of aqueous CHX that was still ongoing at 660 days for all specimen groups. There was a dose response, with higher CHX-HMP dopings releasing more CHX, although this was non-linear, as the total release at 660 days for 2, 5 and 10% CHX-HMP was 1.8x, 4.3x and 6.5x that of the 1% CHX-HMP material respectively. The rate of CHX release decelerated after approximately 150 days, and from that time was close to constant until the conclusion of the study.

The kinetics of CHX release are very different from those observed in other CHX-doped GICs, where there is a rapid decay of CHX release after the first few days of measurement. The fundamental difference is that most of the studies described above utilise CHX digluconate and diacetate which, owing to their solubility, dissipate rapidly in contact with aqueous solutions. CHX-HMP has a much lower solubility than CHX digluconate or diacetate and the rate of CHX release is governed by kinetic factors (agitation of the surrounding medium) and thermodynamic factors (degree of undersaturation of the surrounding medium, which were effectively sink conditions in this study as evidenced by the smooth profile where the 14 day medium changes were not detectable by an acceleration in CHX release). Thus the release profile is not characterised by the "burst" release that has been observed in all studies of CHX digluconate and CHX diacetate GICs.

Utilising the elemental analysis data it can be concluded that the CHX-HMP solid is ~72% CHX, and this enables calculation of the total CHX contained within the GIC specimens. Given a specimen mass of 202 mg taken from the mean of 152 specimens, this equates to a total content of CHX in the specimens as 1%: 2.9 μmol CHX; 2%: 5.8 μmol CHX; 5%: 14.4 μmol CHX; 10%: 28.7 μmol CHX. At the end of the 660 day period the total CHX released by the specimens was 1%: 0.027 μmol CHX; 2%: 0.049 μmol CHX; 5%: 0.115 μmol CHX; 10%: 0.175 μmol CHX. This indicates that the total CHX release over the 660 day period for all four specimen groups was of the order of 1% of the total CHX contained within the material. It is likely that the CHX that was released was primarily from the outer region of the specimen, where ion exchange with the artificial saliva would most readily take place. It does indicate that the CHX was far from depleted at the endpoint of the study and that continued CHX release would have been likely for a substantially longer time even without recharge. Furthermore, the volume of saliva and the perpetual undersaturation reflects the conditions at the surface of the GIC that would be exposed in the oral environment, and not that interface which would be of most clinical interest, that is, the interface between GIC and tooth tissue. At this location the fluid flow would be very much less and therefore the CHX concentration would likely reach a saturation that would decelerate any further CHX release owing to the common ion effect. To the extent that these observations can be used to infer clinical behaviour it is likely that the duration of CHX release in these experiments underestimates the duration that would be observed at the material-tooth interface *in vivo*.

The capacity to recharge CHX-containing GICs has not previously been investigated. The data indicated that when exposed to either CHX digluconate solution with a concentration equivalent to that in widely used oral rinses, or a CHX-HMP suspension with the same total CHX, subsequent CHX release by the GICs was greater. This indicates that the GIC can take up CHX from its environment, and subsequently release it again in a reversible process. The aim of this part of the study was to determine whether the longevity of the CHX release could potentially be extended by periodic exposure to an oral rinse containing CHX. It appears that this could be effective, and furthermore, a rinse composed of a suspension of CHX-HMP is likely to be more effective, leading to greater CHX release than the CHX digluconate solution. However, the data must be interpreted with caution, since while GICs have long been accepted to take up fluoride from their environment, this ability is now recognised to be short-lived, and is lost after the first month of maturation [27]. Therefore, further investigations regarding the recharge of GICs with chlorhexidine will need to be carried out with more mature specimens to determine whether the same limitations apply.

A primitive assessment of antimicrobial efficacy, the zone of inhibition or agar diffusion method was adopted in this study. The method has many limitations but is commonly used as a first attempt to assess antimicrobial materials, including dental restoratives. It is commonly used in other fields to assess antimicrobial susceptibility of particular microbes. It is important to bear in mind, if comparing different antimicrobials, that the remote effect (the "zone of inhibition") is affected not only by the interaction between the microbe and the antimicrobial, but also by the ease by which the antimicrobial can diffuse through the agar. CHX, being a comparatively large molecule, diffuses through agar less readily than some antiseptics.

The aim of the disc diffusion study was to take the first steps in assessing whether the CHX release from the prototype GICs was sufficient to have an adverse effect on growth of oral cariogenic microbes, whilst it is acknowledged that more sophisticated, multi-species models would be beneficial in future in ascertaining the optimal dose of CHX-HMP for a given clinical indication. In this simple study, it was illustrated that the 2% CHX-HMP doped specimens inhibited the growth of both *St. mutans* and *Sc. wiggsiae*, with a greater effect on the former microbe.

When adding materials such as CHX salts to GICs it is important to consider the effect that the dissolution of the salts may have on mechanical properties, and the higher the concentration of material the greater the likelihood of an adverse effect on properties such as strength. When adding conventional CHX salts digluconate and diacetate, a dose response of an adverse affect on strength is indeed observed, although the threshold for a statistically significant effect varies from study to study and is likely to be affected by a number of factors including sample size and means of incorporating the CHX. Turkun et al. [6] observed that 0.5% CHX diacetate and 0.5, 1.25 and 2.5% CHX CHX had no adverse effect on CS but higher concentrations of CHX diacetate did

reduce CS. There was a numerical reduction in DTS for 2.5% CHX diacetate and digluconate of ~30% but this was not statistically significant; 0.5 or 1.25% had no effect on DTS either. Ahluwalia observed similarly that 1% CHX diacetate had no adverse effect on the CS or DTS of a GIC, but did not investigate higher or lower concentrations [28]; whereas Mittal who utilised concentrations of 1.5 and 3% CHX diacetate observed a ~30% reduction in CS compared to unmodified GIC [29], while Duque observed no decrease in CS when adding 1.25 and 2.5% CHX digluconate to a GIC [30]. While it is therefore not possible to draw a definitive conclusion as to what concentration of CHX salts has a significant (whether statistical or clinical) effect on strength, a likely explanation of the reduction in CS and DTS observed by some authors with higher concentrations may be explained Marti's observation that increased concentration of CHX diacetate or digluconate is accompanied by an increase in porosity [10] which is likely to reduce strength.

The higher the substitution of CHX-HMP, the more likely a deleterious effect on the mechanical properties, with substitutions of 5% or greater adversely affecting CS, and substitutions of 2% or above adversely affecting BFS, although none significantly affected DTS. At the higher concentrations of 5 and 10%, the CS was 100 MPa which is the minimum CS stipulated by the relevant ISO standard for restorative cements [31]; lower concentrations brought the strength more comfortably within the acceptable range at 130–150 MPa. The threshold for adverse effects on the mechanical properties of these materials appears therefore to be broadly comparable, or perhaps a little higher, than that for more soluble CHX salts, although it would be interesting to explore how these mechanical properties vary over time as the CHX is released from the various GIC materials.

It is considered encouraging that for the lower dopings of CHX-HMP the effects on the mechanical properties are moderately small; should such materials become commercially viable, it is plausible that other aspects of the formulation could be modified to compensate for this loss of strength. On the other hand, these GIC materials could be considered as prototypes for GIC-based fissure sealants, where absolute strength is of lesser importance and the local delivery of antimicrobial to the fissure areas could be considered beneficial, and as temporary materials designed to stabilise the region before the definitive restoration is placed. However, given the calculations presented above regarding the proportion of CHX released from the specimens, and the reflections on relative fluid flow rate and therefore CHX saturation at the tooth-tissue interface, it is plausible that even the lower concentrations of CHX-HMP used here may still offer sufficient CHX release to operate as long-term restoratives without compromise to mechanical properties.

5. Summary

GICs have been developed which are supplemented with fine, milled, CHX-HMP particles. CHX release was sustained for considerably longer and at a more consistent rate than with any previous published studies, and with fewer adverse effects on mechanical properties than many formulations with short lived and front-loaded CHX release. Earlier studies with CHX-HMP prepared in different ways have achieved long term CHX release, for example ongoing release after over 400 days in artificial saliva, but this was at the expense of mechanical properties even using much smaller CHX-HMP dopings. The materials presented in this manuscript may prove beneficial as technologies with the aim of inhibiting secondary caries in mainstream restorative materials, as well as related materials such as temporary restorations and GIC-based fissure sealants.

Funding

The study was funded by the Medical Research Council as part of a CASE PhD studentship awarded to Candice Bellis. Kemdent were the CASE partner and provided in-kind support but did not take an active role in the data acquisition, interpretation or analysis of data, or the decision as to whether and how to publish the data. PFD was supported by EPSRC under its ACCIS Centre for Doctoral Training grant, EP/G036772/1.

Acknowledgements

The authors gratefully acknowledge Dr. Keith Bean and Formumetrics Ltd. for BET analysis and Dr. Sean Davis and the Electron Microscopy Unit, University of Bristol, for SEM imaging. The authors are also grateful to Dr. Nick Jakubovics (University of Newcastle) and Professor William Wade (Kings College London) for provision of *St. mutans* and *Sc. wiggsiae* strains respectively.

REFERENCES

[1] Tedesco TK, Bonifacio CC, Calvo AF, Gimenez T, Braga MM, Raggio DP. Caries lesion prevention and arrestment in approximal surfaces in contact with glass ionomer cement restorations—a systematic review and meta-analysis. Int J Paediatr Dent 2015;26:161–72, http://dx.doi.org/10.1111/ipd.12174.

[2] Ahovuo-Saloranta A, Forss H, Walsh T, Hiiri A, Nordblad A, Makela M, et al. Sealants for preventing dental decay in the permanent teeth. Cochrane Database Syst Rev 2013;3:CD001830, http://dx.doi.org/10.1002/14651858.CD001830.pub4.

[3] Yengopal V, Harneker SY, Patel N, Siegfried N. Dental fillings for the treatment of caries in the primary dentition. Cochrane Database Syst Rev 2009;2:CD004483, http://dx.doi.org/10.1002/14651858.CD004483.pub2.

[4] Bonesvoll P, Gjermo P. A comparision between chlorhexidine and some quaternary ammonium compounds with regard to retention, salivary concentration and plaque-inhibiting effect in the human mouth after mouth rinses. Arch Oral Biol 1978;23:289–94.

[5] Tabary N, Chai F, Blanchemain N, Neut C, Pauchet L, Bertini S, et al. A chlorhexidine-loaded biodegradable cellulosic device for periodontal pockets treatment. Acta Biomater 2014;10:318–29, http://dx.doi.org/10.1016/j.actbio.2013.09.032.

[6] Turkun LS, Turkun M, Ertugrul F, Ates M, Brugger S. Long-term antibacterial effects and physical properties of a chlorhexidine-containing glass ionomer cement. J Esthet

Restor Dent 2008;20:29–44, http://dx.doi.org/10.1111/j.1708-8240.2008.00146.x. JERD146[pii].
[7] Shanmugaavel AK, Asokan S, John JB, Priya PG, Devi JG. Effect of one percent chlorhexidine addition on the antibacterial activity and mechanical properties of sealants: an in vitro study. Int J Clin Pediatr Dent 2015;8:196–201, http://dx.doi.org/10.5005/jp-journals-10005-1312.
[8] Palmer G, Jones FH, Billington RW, Pearson GJ. Chlorhexidine release from an experimental glass ionomer cement. Biomaterials 2004;25:5423–31, http://dx.doi.org/10.1016/j.biomaterials.2003.12.051. S0142961203012237[pii].
[9] Luo D, Shahid S, Wilson RM, Cattell MJ, Sukhorukov GB. Novel formulation of chlorhexidine spheres and sustained release with multilayered encapsulation. ACS Appl Mater Interfaces 2016;8:12652–60, http://dx.doi.org/10.1021/acsami.6b02997.
[10] Marti LM, Becci AC, Spolidorio DM, Brighenti FL, Giro EM, Zuanon AC. Incorporation of chlorhexidine gluconate or diacetate into a glass-ionomer cement: porosity, surface roughness, and anti-biofilm activity. Am J Dent 2014;27:318–22.
[11] Marti LM, Mata M, Ferraz-Santos B, Azevedo ER, Giro EM, Zuanon AC. Addition of chlorhexidine gluconate to a glass ionomer cement: a study on mechanical, physical and antibacterial properties. Braz Dent J 2014;25:33–7.
[12] Jaidka S, Somani R, Singh DJ, Shafat S. Comparative evaluation of compressive strength, diametral tensile strength and shear bond strength of GIC type IX, chlorhexidine-incorporated GIC and triclosan-incorporated GIC: an in vitro study. J Int Soc Prev Commun Dent 2016;6:S64–9, http://dx.doi.org/10.4103/2231-0762.181188.
[13] Yan H, Yang H, Li K, Yu J, Huang C. Effects of chlorhexidine-encapsulated mesoporous silica nanoparticles on the anti-biofilm and mechanical properties of glass ionomer cement. Molecules 2017;22:E1225, http://dx.doi.org/10.3390/molecules22071225.
[14] de Castilho AR, Duque C, Negrini Tde C, Sacono NT, de Paula AB, de Souza Costa CA, et al. In vitro and in vivo investigation of the biological and mechanical behaviour of resin-modified glass-ionomer cement containing chlorhexidine. J Dent 2013;41:155–63, http://dx.doi.org/10.1016/j.jdent.2012.10.014.
[15] Kabil NS, Badran AS, Wassel MO. Effect of the addition of chlorhexidine and miswak extract on the clinical performance and antibacterial properties of conventional glass ionomer: an in vivo study. Int J Paediatr Dent 2016;27:380–7, http://dx.doi.org/10.1111/ipd.12273.
[16] Duque C, Aida KL, Pereira JA, Teixeira GS, Caldo-Teixeira AS, Perrone LR, et al. In vitro and in vivo evaluations of glass-ionomer cement containing chlorhexidine for atraumatic restorative treatment. J Appl Oral Sci 2017;25:541–50, http://dx.doi.org/10.1590/1678-7757-2016-0195.
[17] Barbour ME, Maddocks SE, Wood NJ, Collins AM. Synthesis, characterization, and efficacy of antimicrobial chlorhexidine hexametaphosphate nanoparticles for applications in biomedical materials and consumer products. Int J Nanomed 2013;8:3507–19, http://dx.doi.org/10.2147/IJN.S50140.
[18] Wood NJ, Jenkinson HF, Davis SA, Mann S, O'Sullivan DJ, Barbour ME. Chlorhexidine hexametaphosphate nanoparticles as a novel antimicrobial coating for dental implants. J Mater Sci: Mater Med 2015;26:201.
[19] Hook ER, Owen OJ, Bellis CA, Holder JA, O'Sullivan DJ, Barbour ME. Development of a novel antimicrobial-releasing glass ionomer cement functionalized with chlorhexidine hexametaphosphate nanoparticles. J Nanobiotechnol 2014;12:3, http://dx.doi.org/10.1186/1477-3155-12-3.
[20] Bellis CA, Nobbs AH, O'Sullivan DJ, Holder JA, Barbour ME. Glass ionomer cements functionalised with a concentrated paste of chlorhexidine hexametaphosphate provides dose-dependent chlorhexidine release over at least 14 months. J Dent 2016;45:53–8.
[21] Kressirer CA, Smith DJ, King WF, Dobeck JM, Starr JR, Tanner ACR. *Scardovia wiggsiae* and its potential role as a caries pathogen. J Oral Biosci 2017;59:135–41, http://dx.doi.org/10.1016/j.job.2017.05.002.
[22] Tanner AC, Mathney JM, Kent RL, Chalmers NI, Hughes CV, Loo CY, et al. Cultivable anaerobic microbiota of severe early childhood caries. J Clin Microbiol 2011;49:1464–74, http://dx.doi.org/10.1128/JCM.02427-10.
[23] Eisenburger M, Addy M, Hughes JA, Shellis RP. Effect of time on the remineralisation of enamel by synthetic saliva after citric acid erosion. Caries Res 2001;35:211–5, 47458.
[24] Barbour ME, O'Sullivan DJ, Jagger DC. Chlorhexidine adsorption to anatase and rutile titanium dioxide. Colloids Surf A 2007;307:116–20.
[25] Gibbons RJ, Berman KS, Knoettner P, Kapsimalis B. Dental caries and alveolar bone loss in gnotobiotic rats infected with capsule forming streptococci of human origin. Arch Oral Biol 1966;11:549–60.
[26] Downes J, Mantzourani M, Beighton D, Hooper S, Wilson MJ, Nicholson A, et al. *Scardovia wiggsiae* sp. nov., isolated from the human oral cavity and clinical material, and emended descriptions of the genus *Scardovia* and *Scardovia inopinata*. Int J Syst Evol Microbiol 2011;61:25–9, http://dx.doi.org/10.1099/ijs.0.019752-0.
[27] Nicholson JW, Czarnecka B. Maturation affects fluoride uptake by glass-ionomer dental cements. Dent Mater 2012;28:1–5, http://dx.doi.org/10.1016/j.dental.2011.10.011.
[28] Ahluwalia P, Chopra S, Thomas AM. Strength characteristics and marginal sealing ability of chlorhexidine-modified glass ionomer cement: an in vitro study. J Indian Soc Pedod Prev Dent 2012;30:41–6, http://dx.doi.org/10.4103/0970-4388.95580.
[29] Mittal S, Soni H, Sharma DK, Mittal K, Pathania V, Sharma S. Comparative evaluation of the antibacterial and physical properties of conventional glass ionomer cement containing chlorhexidine and antibiotics. J Int Soc Prev Commun Dent 2015;5:268–75, http://dx.doi.org/10.4103/2231-0762.161754.
[30] Duque C, Aida KL, Pereira JA, Teixeira GS, Caldo-Texeira AS, Perrone LR, et al. In vitro and in vivo evaluations of glass-ionomer cement containing chlorhexidine for atraumatic restorative treatment. J Appl Oral Sci 2016;25:541–50, http://dx.doi.org/10.1590/1678-7757-2016-0195.
[31] Sidhu SK, Nicholson JW. A review of glass-ionomer cements for clinical dentistry. J Funct Biomater 2016;7, http://dx.doi.org/10.3390/jfb7030016.